IMPLICACIÓN DEL SISTEMA DE MELANOCORTINAS

EN LA REGULACIÓN DE LA PIGMENTACIÓN Y EL CRECIMIENTO DE LOS PECES:
PAPEL DE LOS ANTAGONISTAS ENDÓGENOS

Raúl Vicente Guillot Miralles

Director: José Miguel Cerdá Reverter

This Thesis has been submitted in accordance with the requirements for the degree of Doctor at the Universitat Politècnica de València.

Esta tesis ha sido presentada para optar al grado de Doctor por la Universitat Politècnica de València.

Valencia, Septiembre 2019

UNIVERSITAT POLITÈCNICA DE VALÈNCIA

IATS | CSIC — INSTITUTO DE ACUICULTURA TORRE DE LA SAL | CONSEJO SUPERIOR DE INVESTIGACIONES CIENTÍFICAS

D. **José Miguel-Cerdá-Reverter**, Investigador del Consejo Superior de Investigaciones Científicas (CSIC) en el Instittuto de Acuicultura de Torre de la Sal (IATS).

Informa que la Tesis Doctoral titulada IMPLICACIÓN DEL SISTEMA DE MELANOCORTINAS EN LA REGULACIÓN DE LA PIGMENTACIÓN Y EL CRECIMIENTO DE LOS PECES: PAPEL DE LOS ANTAGONISTAS ENDÓGENOS ha sido realizada por Don Raúl Vicente Guillot Miralles en el Instittuto de Acuicultura de Torre de la Sal (IATS) bajo su dirección y que, una vez revisado y comprobado el trabajo, considera que reúne los requisitos necesarios para la obtención del grado de Doctor, por lo que autoriza su presentación.

Para que así conste

José Miguel Cerdá Reverter

Agradecimientos

Esta Tesis comenzó a gestarse casi sin quererlo, fruto del entusiasmo y el placer que siempre he tenido al trabajar con animales, especialmente con peces y otros animales acuáticos, y el querer llevar un trabajo intelectual hasta los límites que fueran posibles sin importarme hacer ciertos sacrificios personales.

Pese a que gran parte del trabajo se realizó hace ya algunos años; la falta de recursos económicos derivados de la dura crisis económica que sufrió este país, en la que la ciencia fue uno de los sectores más afectado, impuso la necesidad de buscar prados más verdes, y puso este proyecto en letargo.

Cuando las circunstancias económicas mejoraron algo, y fue viable mi retorno, el trabajo pudo retomarse, no sin dificultades. Dificultades que jamás podrían haber sido superadas sin el interés, la insistencia y las facilidades que me dió José Miguel.

Pueda parecer que agradecer tu Tesis Doctoral a tu director es algo que hay que hacer, y que por tratarse de un convencionalismo puede perder todo su valor, pero en este caso el agradecimiento es absolutamente sincero, y la deuda contraída impagable.

La realización de una Tesis Doctoral es algo que afecta a tu entorno más próximo, por ello es justo agradecer el apoyo de mi madre y sobre todo la paciencia de Almudena Santos Bajo, la que fuera mi pareja durante muchos de los años que este proyecto ha estado vivo.

Muchas gracias a todos.

Índice

Abreviaturas frecuentes

5HIAA	Ácido 5-hidroxindolacético
5HT	5-hidroxitriptamina, también denominada Serotonina
Ac	Núcleo Arcuato
actb	Actina B (gen)
ACTH	Hormona Adenocorticotropa
AGRP	Proteína Relacionada con Agouti
agrp	Proteína Relacionada con Agouti (gen)
ANOVA	Análisis Estadístico de la Varianza
ASIP	Proteína de Señalización Agouti
asip	Proteína de Señalización Agouti (gen)
bp	Pares de bases (inglés)
BW	Peso corporal
CART	Transcrito inducido por cocaína y anfetaminas
cart	Transcrito inducido por cocaína y anfetaminas (gen)
CCK	Colcistoquinina
cDNA	DNA complementario
cfs1r	"Colony stimulating factor 1 receptor" (gen)
CNBR1	Receptor de Cannabinoides tipo 1
CREB	Elementos de respuesta a AMPc
CRH	Hormona liberadora de la Corticotropina
CSIC	Consejo Superior de Investigaciones Científicas
CTRL	Control
D2	Yodotirosina desyodinasa tipo 2
dio2	Yodotirosina desyodinasa tipo 2 (gen)

DA	Dopamina
DCT	Dopacroma Tautomerasa
dct	Dopacroma Tautomerasa (gen)
DEG	Genes Diferencialmente Expresados
DMSO	Dimetilsulfóxido
dpf	Días post-fertilización
DHICA	Ácido 5,6-Dihidroxiendol-2-carboxílico
DNA	Ácido Desoxiribonucleico
DOPAC	Ácido 5-hidroxifenilacético
EDTA	Ácido etilendiaminotetraacético
EF-1	Factor de Elongación 1
FAME	Ésteres Metílicos de Ácidos Grasos
FCE	Eficiencia en la conversión de alimento
FGD	Síndrome hereditario de deficiencia de glucorticoides
FoxD3	Factor de transcripción perteneciente a la familia "Forkhead"
foxd3	Factor de transcripción perteneciente a la familia "Forkhead" (gen)
GABA	Ácido gamma-aminobutírico
GFP	Proteína Fluorescente Verde
GH	Hormona del Crecimiento
GRE	Grelina
HE	Hematoxilana-Eosina
HEK-293	Línea Celular de Células embrionarias de riñón humano
KISS	Kisspeptina
kit	Receptores de la Tisona-kinasa (gen)
hpf	Horas post-fertilización
HPLC	Cromatografía líquida de alta eficiencia
IATS	Instituto de Acuicultura de Torre la Sal
icv	Intracerebroventricular
IEO	Instituto Español de Oceanografía

igf1	factor de crecimiento similar a la insulina (gen)
L	Longitud
LPH	Lipotrofina
ltk	Leucocito tirosina-kinasa
MCR	Receptor de las Melanocortinas
MIF	Factor Inhibidor de la Melanización
MSH	Hormona Estimuladora de los Melanocitos
MRAP	Proteína Accesoria del Receptor de Melanocortinas
mRNA	RNA mensajero
MS-222	Metasulfonato de Tricaína
MSCs	"Melanocyte Stem Cells"
MTII	Receptor 2 de la melatonina
MTIF	Factor de transcripción microftalmia
NA	Noradrenalina
NCCs	"Neural Crestal Cells"
NTS	Tracto solitario
PAF	Paraformaldehido
PB	Tampón Fosfato
PBS	Tampón Fosfato
PC1	Prohormona Convertasa 1
PC2	Prohormona Convertasa 2
pcer	Reductasa del coenzima A perixosomal (gen)
PCR	Reacción en Cadena de la Polimerasa
PFA	Paraformaldehido
POC	Variante del POMC identificada en las lampreas
POM	Variante del POMC identificada en las lampreas
POMC	Propopiomelanocortína
pomc	Propopiomelanocortína (gen)

PTU	Feniltiourea
PVN	Núcleo Paraventricular
PYY	Péptido tirosina-tirosina
qPCR	Reacción en Cadena de la Polimerasa cuantitativa en tiempo real
qRT-PCR	Reacción en Cadena de la Polimerasa cuantitativa en tiempo real
R1	Primer evento de Duplicación Génica en la evolución de los cordados.
R2	Segundo evento de Duplicación Génica en la evolución de los cordados
R3	Tercer evento de Duplicación Génica, Teleósteos.
RACE	"Rapid Amplification cDNA Ends" (técnica genómica)
RNA	Ácido Ribonucleico
RT	"Room Temperature"
RT-PCR	Reaccion de Retrotranscripción seguida de una PCR
SEM	Error Estándar de la Media
Slc24a5	Carrier 5 de la familia 24 (gen)
SNC	Sistema Nervioso Central
sox10	Factor de transcripción sox10 (gen)
T3	Triyodotironina
T4	Tiroxina
TESPA	3-aminopropiltrietoxisilano
TSGG	Evento de Duplicación Génica exclusivo de los Teleósteos, ver R3
TU	"Tübingen", cepa de peces cebra con fenotipo salvaje
TYR	Tirosinasa
TYRP	Proteína Relacionada con la Enzima Tirosinasa
tyrp	Proteína relacionada con la enzima tirosina (gen)
WT	"Wild-Type", peces cebra con fenotipo salvaje
xdh	Xantina deshidrogenasa (gen)

Preámbulo

Los patrones de coloración que lucen los seres vivos son uno de los espectáculos más impresionantes que nos ofrece la naturaleza. Este despliegue ha fascinado tanto a la humanidad desde la antigüedad que ha intentado atesorar su belleza, ya sea *in vivo* o mediante expresiones artísticas. Se sabe que las primeras civilizaciones ya creaban jardines en los que el colorido de las flores era uno de los elementos más importantes, y mantenían en cautividad animales de colores exóticos para poder contemplarlos a placer. A lo largo de toda la historia, son innumerables las obras artísticas en las que se plasman flores y animales como elementos principales de la obra.

Con el nacimiento de la ciencia moderna se publican gran cantidad de trabajos sobre botánica y zoología, algunos con ilustraciones de gran belleza artística, en los que las flores y las libreas de los animales se representan con gran detalle. En algunas de estas obras se intenta dar explicación a la gran variedad de patrones de coloración. Las libreas discretas se asocian con el camuflaje. Las libreas disruptivas, como las rayas de los tigres y de las cebras, con la ruptura de patrones para evitar que sean detectados o aislados como individuos. Para explicar las espectaculares explosiones de color que despliegan los machos de ciertas especies de aves, Darwin desarrolló en su obra *The Descent of Man, and Selection in Relation to Sex* (1871) el concepto de selección sexual poniendo al pavo real como ejemplo.

La mayoría de los colores que vemos en los seres vivos se deben a la presencia de uno o más pigmentos, pero en algunos casos también a la reflexión de la luz sobre estructuras extra o intracelulares. Los reflejos metálicos que vemos en el plumaje de algunas aves tropicales son un ejemplo de estos fenómenos de reflexión.

Los pigmentos, pueden ser producidos por el propio organismo o ser adquiridos en la dieta. En el grupo de las aves, los tonos rosados y rojizos dependen de su alimentación. El color rosa de los flamencos se debe a los carotenoides presentes en los invertebrados que constituyen su dieta. La intensidad de colores rojos brillantes en las gallináceas son reflejo de la salud y fortaleza del individuo y demuestran la capacidad de procesar metabolitos tóxicos en pigmentos inertes.

Independientemente de que el origen de los pigmentos sea externo o interno, la forma en que entran a formar parte del patrón de coloración varía en los diferentes grupos de animales.

En los insectos, los pigmentos son generados por células epidérmicas y luego traspasados a las cutículas externas. En otros invertebrados, y en los vertebrados poiquilotermos la mayor parte de los pigmentos permanecen en el interior de las células. En el caso de los peces teleósteos, parte de los pigmentos se transfieren a las escamas, que también son estructuras vivas. En todos estos grupos el patrón de coloración resulta, en gran medida, de la distribución de los diferentes tipos de células pigmentarias, y de los pigmentos dentro de ellas. La contención de los pigmentos en estructuras vivas permite controlar los patrones de coloración mediante mecanismos fisiológicos, siendo los cefalópodos y los camaleones los ejemplos más significativos.

En las aves y en los mamíferos parte de los pigmentos permanecen en las células dérmicas dando color a las partes expuestas, y parte son transferidos a las estructuras de recubrimiento: plumas y pelos, respectivamente; y otras extensiones corporales no vivas, como, por ejemplo, el pico de las aves.

Desentrañar las relaciones funcionales que hacen posible la organización del patrón de coloración a nivel celular es una tarea compleja que sólo se ha podido empezar a acometer en las últimas décadas gracias al desarrollo de potentes herramientas bioquímicas, moleculares y celulares.

Una de las grandes sorpresas fue constatar que el sistema hormonal que controla la adquisición del patrón de coloración en los vertebrados, participa también en el control de la ingesta y parte de la respuesta hormonal al estrés. Y que, en muchas ocasiones, este sistema participa en estas funciones, a priori poco relacionadas, gracias a diferencias espaciales de expresión que por diferencias estructurales de sus elementos constituyentes. El sistema de melanocortinas es exclusivo de los vertebrados. En invertebrados se han identificado moléculas que guardan relación con elementos de este sistema, pero no se han hallado indicios de que formen parte de un sistema hormonal organizado. En los invertebrados, las funciones asociadas con el sistema de melanocortinas están controladas por otros mecanismos que no están relacionados entre sí. El sistema de melanocortinas comienza a organizarse en algún punto entre la aparición de la notocorda y el desarrollo de las vértebras, y con cada duplicación génica se hace más complejo, sin que se produzcan cambios estructurales drásticos. Cómo se produjo la diversificación de funciones, es todavía un misterio.

Debido a todas las peculiaridades, los conocimientos derivados del estudio del sistema de las melanocortinas sirven a evolucionistas, a etólogos, a nutricionistas e incluso al estudio de la salud humana, ya que el defecto de funcionamiento de alguno de sus mecanismos es la causa de diversos trastornos alimenticios.

Resumen

El sistema de melanocortinas es un complejo sistema hormonal implicado en la regulación de diversas funciones fisiológicas.

Todas las melanocortinas derivan de un mismo precursor peptídico denominado proopiomelanocortina (POMC), en el que están integradas las diferentes hormonas estimuladoras de los melanocitos (MSHs), la hormona adrenocorticotropa (ACTH), y el péptido opioide β-endorfina. Las melanocortinas señalizan a través de 5 receptores (MC1R-MC5R), con diferentes grados de especificidad hormona-receptor, lo que supone un buen ejemplo de su coevolución. El sistema de melanocortinas es el único sistema hormonal que presenta antagonistas endógenos: la proteína de señalización agouti (ASIP) y la proteína relacionada con agouti (AGRP).

En mamíferos, ASIP actúa como un antagonista de MC1R. La modificación de la señalización del MC1R desequilibra la síntesis de pigmentos en el folículo piloso, potenciando la síntesis de feomelanina (pigmento amarillo-naranja) en lugar de eumelanina (pigmento negro-marrón). La expresión tegumentaria de ASIP es responsable del patrón de pigmentación dorso-ventral polarizado que tienen muchas especies de mamíferos. Esta polaridad puede observarse incluso cuando la especie presenta patrones más complejos. AGRP actúa como antagonista de MC4R, uno de los receptores de sistema nervioso central implicados en el control del metabolismo energético; a través de la regulación de la saciedad.

Se ha demostrado que ASIP es capaz de antagonizar la actividad del MC4R, lo que no ocurre en condiciones normales, ya que ASIP sólo se expresa de forma local en el tegumento, y nunca alcanza el MC4R cerebral. En la cepa de ratones mutantes "*yellow*" [A(vy)/a], la expresión de ASIP queda bajo el control de un promotor de expresión ubicua que permite su síntesis en todos los tejidos incluyendo el cerebro, accediendo al MC4R central. El bloqueo/disminución de la actividad constitutiva del MC4R en esta cepa de ratones, disminuye la sensación de saciedad, aumentando los niveles de ingesta que conllevan una tasa de crecimiento mayor, pero también el desarrollo de obesidad. En los peces teleósteos los antagonistas endógenos del sistema de melanocortinas están duplicados debido a una tercera duplicación genómica (R3) específica de su rama evolutiva. Los cuatro péptidos antagonistas se identificaron inicialmente como ASIP1, ASIP2, AGRP1, y AGRP2. El principio de parsimonia asocia la expresión polarizada de ASIP1 en el tegumento de estos peces con el desarrollo del patrón de pigmentación dorsoventral que se puede observar en muchas especies y la expresión hipotalámica de AGRP1 con el control de la ingesta.

El objetivo de esta tesis doctoral es demostrar la implicación del sistema de melanocortinas en la regulación de la pigmentación y el balance energético de peces mediante relaciones causas-efecto de sus antagonistas endógenos.

Para alcanzar este objetivo, en primer lugar, caractericé los genes ASIP1 en dos especies de peces planos: el rodaballo (*Scophthalmus maximus*) y el lenguado senegalés (*Solea senegalensis*). La elección de este grupo de teleósteos se debe a la extrema polaridad pigmentaria dorsoventral que presentan los peces planos, las numerosas malformaciones pigmentarias que aparecen en cultivo, y a la carencia de secuencias génicas caracterizadas de ASIP1 en pleuronectiformes. Los experimentos demostraron que ASIP1 se expresa masivamente en la región ventral y apenas es detectable en la región dorsal. Además, los resultados sugieren que la expresión ectópica de ASIP1 podría ser la responsable del pseudoalbinismo observado en los peces planos de cultivo.

En segundo lugar, desarrollamos una nueva línea transgénica de peces cebra (*Danio rerio*) (tgASIP1) que expresa el gen ASIP1 de pez dorado *(Carassius auratus)* de forma constitutiva. Esta expresión ubicua rompía la polaridad de la expresión de ASIP1 en el tegumento y, permitía que este antagonista accediera al MC4R cerebral. El antagonismo competitivo de ASIP sobre MC1R y MC4R permite estudiar al mismo tiempo la implicación del sistema de melanocortinas en el control de la pigmentación y de la ingesta/crecimiento.

Los experimentos llevados a cabo revelaron que la sobreexpresión de ASIP1 produce una "ventralización" de la piel dorsal mediante inhibición de la diferenciación de los melanóforos y desvelan la existencia de dos patrones de pigmentación superpuestos en el pez cebra. Un patrón de pigmentación dorsoventral básico, que se puede considerar como el ancestral, sobre el que se superpone el patrón bandeado característico de la especie, más moderno desde el punto de vista evolutivo. Estos dos patrones de coloración tienen un mecanismo de regulación diferente, como demuestra el hecho de que ASIP1 sea capaz de desorganizar el patrón dorsoventral sin afectar el patrón bandeado.

La expresión ubicua de ASIP también muestra la implicación del sistema de melanocortinas en la regulación del balance energético y el crecimiento de los peces. Los experimentos de ingesta llevados a cabo demostraron que los peces tgASIP1 tienen tasas de ingesta mayores. Los análisis transcriptómicos del cerebro de estos peces revelaron alteraciones en diversos sistemas neurales capaces de modificar la saciedad. Los experimentos de ingesta también demostraron que con tasas de ingesta restringidas los peces tgASIP1 son capaces de crecer hasta un 15% más en longitud, con incrementos asociados de peso de hasta el 50%, sugiriendo una mejora en la conversión de alimento.

Finalmente, la exploración de posibles mecanismos de regulación de la expresión de ASIP, puso de manifiesto que la administración oral de triyodotironina (T3) produce una inhibición reversible de la melanogénesis que conlleva una evidente palidez pigmentaria. Estos resultados sugieren que la presencia demostrada de componentes tirogénicos en los piensos de cultivo podría inducir problemas pigmentarios en los peces cultivados.

RESUM

El sistema de melanocortines és un complex sistema hormonal implicat en la regulació de diverses funcions fisiològiques.

Totes les hormones melanocortines deriven d'un mateix pèptid precursor denominat propiomelanocortina (POMC), al qual estan integrades les diferents hormones estimuladores dels melanocits (MSHs), la hormona adrenocorticotropa (ACTH), i el pèptid opioide β-endorfina. Les melanocortines senyalitzen a través de 5 receptors (MC1R-MC5R), amb diferents graus d'especificitat hormona-receptor, la qual cosa suposa un bon exemple de coevolució. El sistema de melanocortines és l'únic sistema hormonal que presenta antagonistes endògens: la proteïna de senyalització agouti (ASIP) i la proteïna relacionada con agouti (AGRP).

En mamífers, ASIP actua com antagonista de MC1R: La modificasió de la senyalització de MC1R desequilibra la síntesi de pigments en el fol·licle pilós potenciant la síntesi de feomelanina (pigment groc-taronja) en lloc de eumelanina (pigment negre-marró). L'expressió tegumentària de ASIP és la responsable del patró de pigmentació dors-ventral polaritzat que tenen moltes espècies de mamífers. Aquesta polaritat és observable fins i tot quan l'espècia presenta patrons més complexos. AGRP actua com antagonista de MC4R, un dels receptors del sistema nerviós central implicats en el control del metabolisme energètic; en concret a través de la regularització de la sacietat.

S'ha demostrat que ASIP és capaç d'antagonitzar l'activitat del MC4R, la qual cosa no succeeixen condicions normals a causa de que ASIP sols s'expressa en el tegument, i mai arriba al MC4R cerebral. En la soca de ratolins mutants yellow A(yy)/a a l'expressió d'ASIP resta baix el control d'un promotor d'expressió ubiqua que permet la síntesi en tots els teixits incloent el cervell, accedint MC4R central. El bloqueig/disminució de l'activitat constitutiva del MC4R en aquesta soca de ratolins, disminueix la sensació de sacietat, augmentant els nivells d'ingesta, produint un major taxa de creixement, però també obesitat. Als peixos teleostis els antagonistes endògens del sistema de melacortines estan duplicats a causa d'una tercera duplicació genòmica (R 3) específica de la seua branca evolutiva. Els quatre pèptids antagonistes en els teleostis foren identificats inicialment com a ASIP1, ASIP2, AGRP1 y AGRP2. El principi de parsimònia associa l'expressió polaritzada de ASIP1 en el tegument d'aquests peixos amb el desenvolupament del patró de pigmentació dors-ventral que es pot observar en moltes espècies; i l'expressió d'AGRP1 al hipotàlem amb el control de la ingesta.

L'objectiu d'aquesta tesis doctoral és demostrar l'implicació del sistema de melanocortines en la regulació de la pigmentació i el balanç energètic de peixos mitjançant relacions causa-efecte dels seus antagonistes endògens.

Per assolir aquest objectiu, en primer lloc, caracteritzaré ASIP1 en dues espècies de peixos plans: rèmol (Scophthalmus maximus) i el llenguado (Solea senegalensis). L'elecció d'aquest grup de teleostis es deu a l'extrema polaritat de pigmentació dors-ventral presenten els peixos plans, les nombroses malformacions pigmentàries que apareixen en en cultiu, i a la manca de seqüències gèniques caracteritzades d'ASIP1 de Pleuronectiforme. Els experiments demostraren que ASIP1 s'expressa massivament en la regió ventral i a penes és detectable en la regió dorsal. A més a més, els resultats demostren que l'expressió ectòpica d'ASIP1 podria ser la responsable del pseudealbinisme observat en els peixos en cultiu.

En segon lloc, vaig desenvolupar una nova línia estratègica de peixos zebra (Danio rerio) (tgASIP1) que expressa el gen ASIP1 de carpa daurada (Carassius auratus) de forma constitutiva. Aquesta expressió ubícua trencava la polaritat de l'expressió d'ASIP1 en el tegument i, permetia que aquest antagonista accedira al MC4R cerebral. L'antagonisme competitiu d'ASIP sobre MC1R i MC4R permet estudiar al mateix temps l'implicació del sistema de melacortines en el control de la pigmentació i de l'ingesta/creixement.

Els experiments duts a terme van rellevar que la sobreexpressió d'ASIP1 produeix una «ventralització» de la pell dorsal mitjançant inhibició de la diferenciació dels melanòfors i desvetllen l'existència de dos patrons de pigmentació superposats en el peix zebra. Un patró de pigmentació dors-ventral bàsic, que es pot considerar com l'ancestral, sobre el que es superposa el patró bandejat característic de l'espècie, més modern des del punt de vista evolutiu. Aquests dos patrons de coloració tindrien un mecanisme de regulació diferent, com demostra el fet de que ASIP1 siga capaç de desorganitzar el patró dors-ventral però afecte al patró bandejat.

L'expressió ubiqua de ASIP demostra la implicació del sistema de melanocortines en la regulació del balanç energètic i el creixement dels peixos. Els experiments d'ingesta duts a terme van demostrar que els peixos tgASIP1 tenen taxes d'ingesta majors. Les anàlisis transcriptòmics del cervell d'aquests peixos van revelar alteracions en diversos sistemes neurals capaços de modificar la sacietat. Els experiments d'ingesta també van demostrar que amb taxes d'ingesta restringides els peixos tgASIP1 són capaços de créixer fins a un 15% més en longitud, amb increments associats de pes de fins al 50%, suggerint una millora en la conversió del aliment.

Finalment l'exploració de possibles mecanismes de regulació de l'expressió d'ASIP, va posar de manifest que l'administració oral de triiodotironina (T3) produeix una inhibició reversible de la melanogénesis que comporta una evident pal·lidesa pigmentària. Aquests resultats suggereixen que la presència demostrada de components tirogènics en els pinsos de cultiu podria induir problemes pigmentaris en els peixos cultivats.

ABSTRACT

Melanocortin system is a complex hormonal system involved in the regulation of several physiological functions. All melanocortin peptides are encoded by the same precursor called proopiomelanocortin (POMC) that integrates the different melanocyte-stimulating hormones (MSHs), the adrenocorticotropic hormones (ACTH) and the opioid peptide b-endorphin. Melanocortin signals through five different receptors (MC1R-MC5R) with different specificity showing a good example of co-evolutiorary processes. The melanocortin system is unique because the presence of endogenous antagonist the so-called: agouti-signalling protein (ASIP) and agouti–related protein (AGRP).

In mammal species, ASIP works as an antagonist of MC1R thus unbalancing the pigment synthesis in the hair follicle from eumelanin (brown-black pigment) to pheomelanin (a yellow-red pigment). ASIP is responsible of the polarized dorsoventral pigment pattern present in most mammalian species. This polarity can be observed even when some other colour patterns are present. On the other hand, AGRP works as an antagonist of MC4R, a central receptor involved in the regulation of energy balance, throughout the regulation of satiety

ASIP1 is also able to antagonize MC4R. This interaction does not occur in the regular situation since ASIP is exclusively expressed in the tegument as a local protein and never reach the central MC4R. In the yellow mutant mouse strain [A(vy)/a], ASIP expression remains under the control of the Rely promotor that allow ubicuosly ASIP expression, including the brain, thus acting on MC4R. Disruption of MC4R signalling decrease satiety sensing thus promoting food intake, obesity and increased linear growth. In teleost fish endogenous antagonist are duplicated thanks to specific extra genome duplication (R3). The four antagonists are initially identified as AGRP1, AGRP2, ASIP1 and ASIP2. Parsimony principle associated the skin expression of ASIP1 with the ventral pigmentary polarity of many species and the hypothalamic expression of AGRP with the control of food intake.

The main goal of this doctoral thesis in to demonstrate the involvement of the melanocortin system in the regulation of pigment patterns and energy balance in fish by means of cause-effect relationships of this endogenous antagonist. To reach this objective, firstly I characterized ASIP1 in two different flatfish species, i.e. turbot (Scophthalmus maximus) and sole (Solea senegalensis). The selection of this teleost group is due to the extreme pigment dorsoventral polarity, the numerous pigment malformations in culture and the absence of characterized ASIP sequences in pleuronectiforms. The experiments demonstrate that ASIP1 is massively expressed in the ventral region and basically undetectable in the dorsal skin. Results also suggest that ectopic ASIP1 expression could be responsible of the flatfish pseudoalbinism.

14

Subsequently, we developed a new transgenic zebrafish (Danio rerio) strain constitutively and ubicuosly overexpressing goldfish (Carassius auratus) ASIP1. The ubicuosly expression would break the dorsoventral polarity of ASIP expression in the tegumentum but also would allow reaching central MC4R. It would me allow to study at the same time the competitive antagonism on MC1R and MC4R and by extension the involvement of the melanocortin system in the regulation of pigmentation and energy balance.

The experiments revealed that ASIP1 overexpression induces a ventralization of the dorsal skin by inhibiting the melanophore differentiation thus showing the existence of two differnnt pigment patterns. An ancestral dorsoventral pigment pattern on that the new stripped pattern is overimposed. Both pigment patterns are regulated in a different way since we can modify the dorsoventral pigment pattern without affecting the stripped pattern.

In addition, the ubicuosly ASIP expression demonstrate the involvement of melanocortin system in the regulation of food intake and growth in fish. Food intake experiments demonstrated that transgenic fish exhibit higher food intake rates. The brain transcriptomic analysis revealed disruptions in several neuronal systems, which are able to regulate satiety. The experiments also demonstrate that ASIP fish are able to growth 15% longer under restrictive food intake rates with associate weight increases close to 50%, thus suggesting improvements in the food conversion rate.

Finally, the exploration of possible mechanisms related to the regulation of ASIP expression revealed that oral triiodothyronine administration induce a reversible inhibition of melanogenesis that brings fish paling. This result suggests that the proven presence of thyrogenic compounds in the fish diets could be responsible for pigmentary disruptions in reared fish.

Introducción

General

1. El sistema de melanocortinas

Las hormonas estimuladoras de los melanocitos: α, β, γ, δ-MSH, y la hormona adrenocorticotropa (ACTH) constituyen la familia de las melanocortinas. Estas hormonas, de naturaleza peptídica, se caracterizan por la presencia de la secuencia aminoacídica HFRW. Todas ellas se producen a partir del procesado de un mismo péptido precursor denominado proopiomelanocortina (POMC), que está codificado por un gen, de igual nombre, perteneciente a la familia opioide/orfanina. Esta familia génica se caracteriza por la presencia de una secuencia opioide u orfanina, y tiene su origen en la segunda ronda (2R) de duplicaciones génicas que sufrieron los vertebrados durante su proceso evolutivo (*Sundström et al., 2009*).

1.1. El gen POMC

1.1.1. Estructura

En los tetrápodos y en sus antecesores filogenéticos, los peces con aletas lobuladas (sarcopterigios), el POMC presenta tres dominios estructurales, con la secuencia tetrapeptídica HFRW en cada uno de ellos (Fig.1).

El dominio amino-(N)-terminal contiene la secuencia de la hormona γ-MSH. El dominio central contiene la secuencia de la ACTH, que integra en su porción Amino-(N)-terminal la secuencia de la α-MSH. Finalmente, el dominio C-terminal contiene la secuencia β-lipotrofina (β-LPH), dentro de la cual están integradas las secuencias de la β-MSH (N-terminal) y de la β-endorfina (C-terminal), característica de la familia génica (*Nakanishi et al., 1979*).

En el resto de los vertebrados mandibulados (gnatóstomos), el número de dominios varía. En los peces cartilaginosos (condrictios), aparece un dominio adicional entre el N-terminal y el central, que contiene la secuencia de una hormona exclusiva de este grupo: la δ-MSH. En los peces con aletas con radios (actinopterigios), se observa la desaparición paulatina del dominio N-terminal. La secuencia está prácticamente inalterada en el grupo más basal (condrósteos), pero está ausente en el grupo más moderno (teleósteos).

En el grupo más antiguo de vertebrados, los peces sin mandíbulas (agnatos), se han identificado dos formas independientes del gen POMC, denominados POC y POM. Ambos genes tienen en común la ausencia de una secuencia completa para la γ-MSH en el dominio N-terminal, pero se diferencian en los otros dos dominios. El POC conserva la secuencia completa de la ACTH en el dominio central, pero ha perdido la secuencia de la β-MSH en el C-terminal. Por el contrario, el POM sólo conserva la secuencia de la α-MSH en el dominio central, y sí que conserva la secuencia de la β-MSH en el dominio terminal (*Takahashi and Kawauchi, 2006*).

En las aves y en los mamíferos sólo se ha identificado una copia del gen POMC, pero en los teleósteos, debido a la tercera duplicación génica (3R), y a eventos

particulares, el número de copias está aumentado. En la mayoría de teleósteos se identifican dos copias del gen POMC (a o α y b o β) (*Gonzalez-Nuñez et al., 2003; Sundström et al., 2009*), pero en el "barfin flounder" (*Verasper moseri*) se han identificado tres copias (a1, a2 y b) (*Takahashi et al., 2005*). Los estudios llevados al respecto en pez cebra indican que las dos copias del gen POMC han sufrido un proceso de subfuncionalización que ha llevado a la compartimentación de funciones (*de Souza et al., 2005*).

1.1.2. Expresión

En los tetrápodos, el mayor índice de expresión del POMC tiene lugar en la región anterior de la hipófisis. En las células corticotropas de la *pars* anterior, el POMC se procesa hacia la liberación de ACTH y β-LPH por acción de la prohormona proconvertasa 1 (PC1). Mientras que las células de la *pars intermedia*, se libera mayoritariamente α-MSH y β-endorfina por acción combinada de PC1 y PC2. (*Castro and Morrison, 1997*).

En los teleósteos, la hipófisis también es el principal lugar de síntesis de POMC; y pese a las diferencias anatómicas la producción de melanocortinas es equivalente (*Takahashi et al., 2006*). Las células corticotropas se localizan en la *pars distalis*, mientras que las melanotropas se distribuyen por la *pars intermedia* (*Cerdá-Reverter and Canosa, 2009*). Los extractos hipofisarios muestran que las células corticotropas además de producir ACTH son capaces de producir una forma des-acetilada de la α-MSH, lo que indica que estas células son capaces de procesar el péptido ACTH, pero que carecen del aparato enzimático necesario para inducir esta modificación postransduccional (*Takahashi et al., 2008*).

En mamíferos el POMC también se expresa en el sistema nervioso central (SNC), donde se procesa mayoritariamente hacia la síntesis de α-MSH y β-endorfina (*Castro and Morrison, 1997*). En ratón, esta expresión se ha observado en el núcleo arqueado o arcuato, situado en el hipotálamo, y en el núcleo del tracto solitario (*Bangol et al., 1999*). La expresión hipotalámica se ha podido comprobar en anfibios (*Tuinhof et al., 1998*), aves (*Gerets et al., 2000*) y en los teleósteos (*Cerdá-Reverter et al., 2003a*), pero no existen datos de expresión caudal en vertebrados no mamíferos.
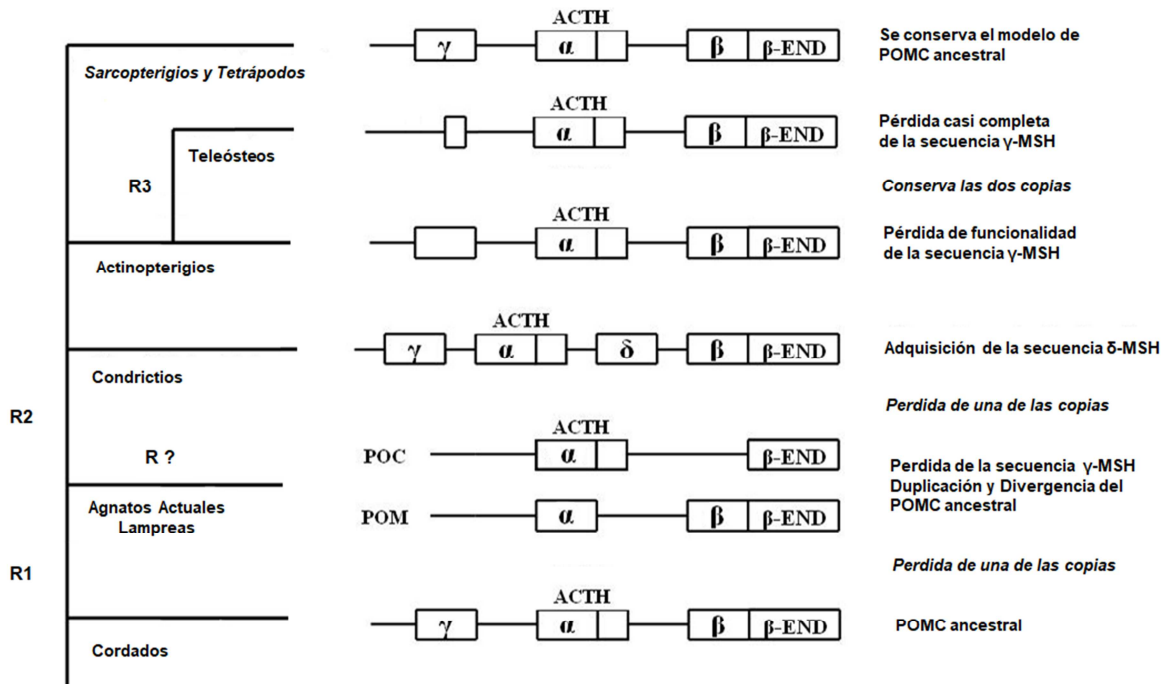
Figura 1. *Arquetipos del gen POMC en las diferentes clases de vertebrados y su posible secuencia evolutiva. Existe un consenso bastante amplio entre los expertos que el modelo de gen POMC ancestral que estaría presente en los ancestros de los vertebrados ya tendría las tres regiones que hoy encontramos en los tetrápodos. Las variantes de POMC en los diferentes grupos estarían resultarían de ganancias o pérdidas de regiones que habrían tenido lugar durante la evolución particular de cada grupo. La parte más controvertida es la presencia de dos variantes de POMC en las lampreas actuales (agnatos). Inicialmente se planteó la posibilidad de que ambas copias fueran el resultado de la primera duplicación génica (R1), y una divergencia posterior; pero la ausencia γ-MSH en las dos variantes del gen, y el hecho de que esta secuencia se conserve en los condrictios juega en contra de esta hipótesis. Actualmente muchos expertos opinan que ambos genes son el resultado de una duplicación génica propia que tuvo lugar durante la evolución de los agnatos, y que habría tenido lugar después de una pérdida de la secuencia γ-MSH, justamente como está ocurriendo actualmente en los actinopterigios. Sin embargo si la secuencia de γ-MSH hubiera aparecido más tarde, en grupos de agnatos no relacionados con las lampreas actuales, la primera hipótesis volvería a coger fuerza. Desgraciadamente hasta nuestros días sólo han llegado unas pocas especies de agnatos separadas en dos grupos (mixinoideos y petromizóntidos), por lo que establecer una cadena de sucesos es realmente complicado. Tal vez la caracterización del gen POMC en los anfioxos, un puñado de especies pertenecientes al grupo de los cephalocordados, único grupo de cordados no vertebrado actual, podría arrojar algo de luz sobre la filogenia de este gen en particular*

1.2. Los receptores de melanocortinas

Las melanocortinas realizan sus funciones biológicas mediante la activación de 5 receptores específicos denominados receptores de las melanocortinas (MC1R-MC5R). Esta diversidad es resultado de las dos duplicaciones génicas (1R y 2R) y una duplicación local (*Dores, 2013*).

El MC2R es activado por ACTH, pero no por las diferentes formas de MSH. El resto de receptores responden con diferente afinidad a las MSHs, mostrando baja afinidad por la ACTH (*Schiöth et al., 2005*). El MC1R es el que mayor afinidad muestra por α-MSH. Mientras que el MC3R parece ser el receptor de γ-MSH, la única melanocortina lineal en mamíferos. En los teleósteos, el número de receptores varía (*Logan et al., 2003*). En el pez cebra (*Danio rerio*) se identifican seis MCRs debido a la duplicación del MC5R. En el pez globo (*Takifugu rubripes*) solo cuatro, ya que carece del MC3R. La ausencia de MC3R en uno de los grupos de teleósteos más modernos parece ser un fenómeno de evolución concomitante con la progresiva desaparición del dominio N-terminal en el grupo de los actinopterigios.

Los receptores de melanocortinas tienen diferentes dominios de expresión. El MC1R se expresa mayoritariamente en el tegumento. El MC2R exhibe sus mayores niveles de expresión en las glándulas suprarrenales. Los receptores MC3R y MC4R se expresan principalmente en el sistema nervioso central (SNC), aunque su expresión periférica también es importante. Por último, el MC5R presenta una distribución poco específica, pudiendo ser detectado en diversos tejidos, pero sin una predominancia clara en ninguno de ellos.

1.3. Los antagonistas endógenos

Una característica diferencial del sistema de melanocortinas es la existencia de dos antagonistas endógenos de los receptores de melanocortinas denominados proteína de señalización agutí (ASP o ASIP) y proteína relacionada con agutí (AGRP). En ratón, ASIP es un antagonista fuerte de MC1R y MC4R, y más débil, de MC3R. En cambio, AGRP actúa como antagonista de MC3R y MC4R, pero no tiene efecto sobre MC1R.

Aunque ambos péptidos antagonistas pueden actuar sobre MC4R, los dominios de expresión de los receptores y de los propios antagonistas segregan las funciones. ASIP se expresa en el folículo piloso, donde ejerce su acción antagónica sobre MC1R. AGRP se expresa en el núcleo arqueado hipotálamico, donde ejerce su acción sobre MC3R y MC4R (*Cone, 2005*).

En los teleósteos se han identificado ortólogos de ASIP y AGRP (*Cerdá-Reverter and Peter, 2003; Song et al., 2003; Cerdá-Reverter et al., 2005; Kurokawa et al., 2006; Murashita et al., 2009*). En un principio se pensó que ambos genes estaban duplicados en los teleósteos debido a la 3R (*Kurokawa et al., 2006; Murashita et al., 2009*). Sin embargo, los estudios filogenéticos y sinténicos más recientes, han

sugerido que la supuesta duplicación de AGRP es, en realidad, una segunda copia de ASIP2 (*Braasch and Postlethwait 2011*). Estos estudios consideran que en teleósteos sólo hay una copia de AGRP y tres copias de ASIP (1, 2a y 2b) (Fig. 2). Como resultado de las dos primeras duplicaciones del genoma de vertebrados (1R y 2R) se obtuvieron 2 pares de copias génicas (AGRP1/AGRP2 y ASIP1/ASIP2). Tras la 2R, AGRP2 se perdió rápidamente, lo que explica la presencia de una sola copia génica de AGRP en tetrápodos. Durante la 3R, específica de teleósteos, AGRP1 se duplicó (AGRP1a y AGRP1b), pero la segunda copia volvió a perderse. Simultáneamente, se duplicaron las dos copias de ASIP, dando lugar a ASIP1a/ASIP1b y ASIP2a/ASIP2b; e inmediatamente tuvo lugar la concomitante desaparición de ASIP1b.

Los resultados en diferentes especies de peces indican que ASIP1 exhibe elevados niveles de expresión en tejidos periféricos, especialmente en la región ventral de la piel, y niveles reducidos en el SNC (*Cerdá-Reverter et al., 2005*). Por el contrario, AGRP se expresa fundamentalmente en el núcleo lateral tuberal, homólogo del núcleo arqueado de mamíferos (*Cerdá-Reverter et al., 2003a; 2003b 2003c; Forlano and Cone, 2003*). A diferencia de lo que ocurre en mamíferos, en teleósteos AGRP también es capaz de antagonizar MC1R (*Sánchez et al., 2010*).
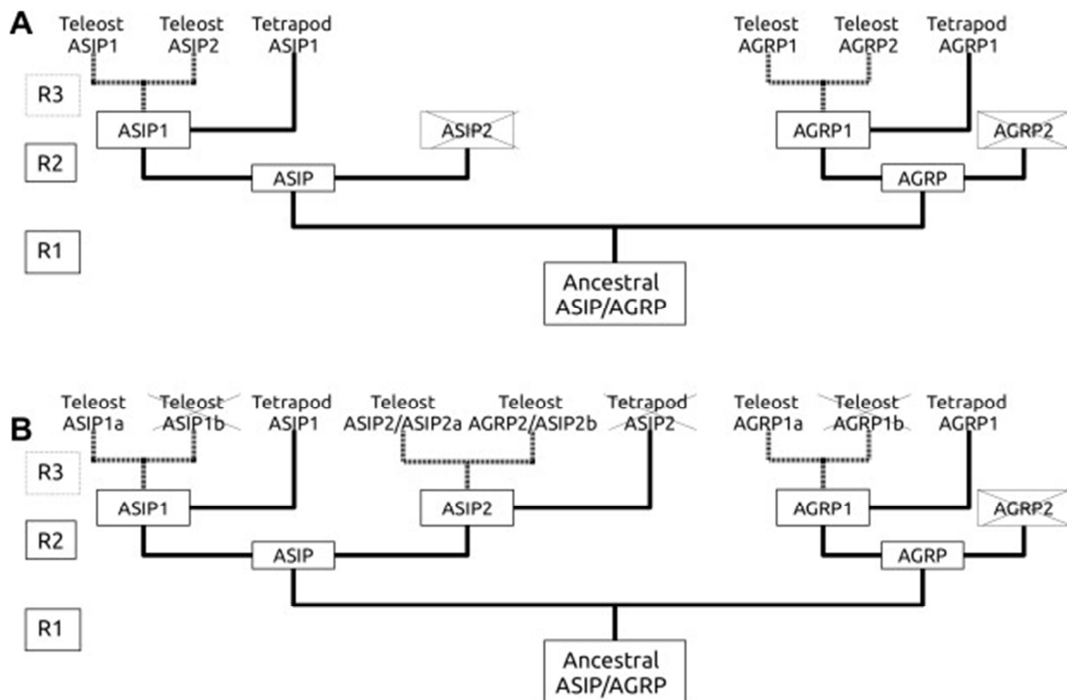

Figura 2. *Representación de las dos teorías evolutivas de la familia de genes ASIP/AGRP. La figura A representa la hipótesis de Kurokawa (2006) y la figura B la hipótesis de Braasch and Postlethwait (2011).*

2. Las melanocortinas en la pigmentación

2.1. Regulación en mamíferos

En los mamíferos, el patrón de pigmentación se adquiere gracias a un único tipo de célula pigmentaria, los melanocitos. Estos cromatóforos producen dos tipos de pigmentos a partir de la dopaquinona: la eumelanina (negro/marrón) y la feomelanina (rojo/amarillo). La producción de estos pigmentos está controlada por dos *loci*, identificados como *locus extensión* y *locus agouti*. Gracias a la caracterización de diferentes cepas de ratones mutantes con alteraciones pigmentarias se pudieron identificar los genes que ocupaban estos loci (*Cone, 2006*). Las cepas de ratones que presentaban un pelaje amarillo (*e/e*) se debían a mutaciones que inactivaban el MC1R; y algunas cepas con pelaje negro (E^{so}/E^{so}) a mutaciones que conferían actividad constitutiva al MC1R (*Robbins et al., 1993*). De manera inversa, una cepa de ratones con patrón de coloración amarillento y notables alteraciones tróficas, cuya homozigosis resultaba mortal (a/A^y), era debida a una mutación que hace que la expresión de ASIP sea ubicua (*Bultman et al., 1992; Miller et al., 1993; Michaud et al., 1993*). Por último, también se caracterizó otra cepa de ratones mutantes de coloración negra homogénea que son incapaces de producir una proteína ASIP funcional (*Bultman et al., 1992*).

En los melanocitos de los mamíferos, la estimulación del MC1R inicia una cadena de reacciones que induce el aumento de los niveles de expresión del factor de transcripción microftalmia (MTIF), y cuyo resultado final es un aumento de los niveles de expresión de la enzima tirosinasa (TYR) (*Lin and Fisher, 2007*). Este enzima cataliza la oxidación de dopaquinona produciendo dopacromo, que a su vez sirve de sustrato para que la proteína relacionada con la tirosinasa 2 (TYRP2) catalice la producción de ácido 5,6-dihidroxindol-2-carboxílico (DHICA). Finalmente, la proteína relacionada con la tirosinasa 1 (TYRP1) cataliza la oxidación del DHICA a eumelanina (Fig. 3).

En presencia de ASIP, la activación de MC1R queda bloqueada o atenuada, lo que disminuye los niveles de expresión de MITF que, a su vez, disminuye los niveles de TYR. De forma espontánea, la dopaquinona reacciona con un residuo de cisteína dando lugar a cisteinil-dopa. Mientras que se mantenga el consumo de dopaquinona en la producción de dopacromo, los niveles de cisteinil-dopa permanecen bajos. Pero ante una caída de la expresión de TYR los niveles de cisteinil-dopa aumentan desequilibrando la producción de eumelanina en favor de la de feomelanina (*Le Pape et al., 2008*).

Las altas concentraciones de TYR favorecen la síntesis de eumelanina (*Sakai et al., 1997*), mientras que bajas concentraciones favorecen la síntesis de feomelanina (*Matsunaga et al., 2000*). Un control fino de la expresión de ASIP en cada región permite establecer el patrón de coloración de la especie. Las variaciones de coloración intermedias entre los patrones homogéneos amarillento y negro se explican debidas a diferentes polimorfismos y modificaciones epigenéticas de ASIP (*Miltenberger et al., 2002; Cropley et al., 2006*). En condiciones naturales, el patrón de coloración dorsoventral se debe a la expresión regional y temporal de diferentes isoformas de ASIP, las cuales están reguladas por la activación de diferentes promotores (Vrieling et al., 1994).
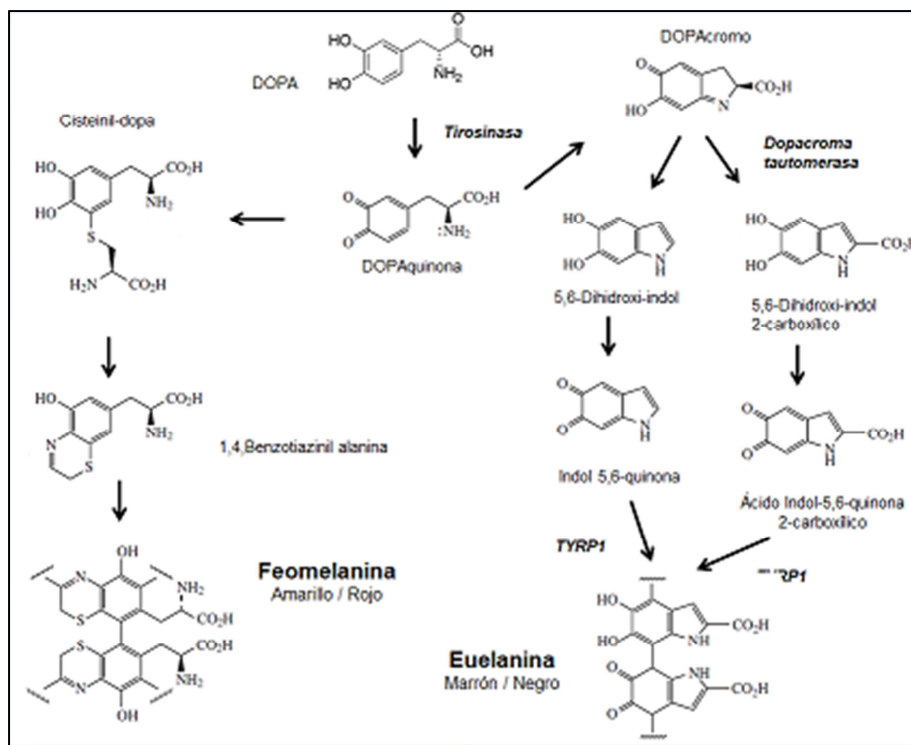
Figura 3. *Ruta simplificada de síntesis de eumelanina y felomelania a partir de la DOPA*

ASIP también participa en la regulación de la población de las células pigmentarias a través de la inhibición la diferenciación de los melanocitos (*Aberdam et al., 1998; Sviderskaya et al., 2001; Le Pape et al., 2008*).

2.2. Regulación en teleósteos

En los teleósteos, el patrón de coloración es el resultado de la combinación y distribución de diferentes células pigmentarias que se dividen en cromatóforos que reflejan sólo una parte del espectro visible (melanóforos, xantóforos, eritróforos y cianóforos), y cromatóforos que actúan como reflectores y reflejan la luz (iridóforos y leucóforos) (*Fuji, 1993*). Los melanóforos de los teleósteos solamente producen eumelanina, con una ruta de síntesis similar a la de los mamíferos. Los xantóforos y los eritróforos contienen carotenoides y pteridinas (rojo/naranja), respectivamente. Los iridóforos reflejan la luz gracias a la presencia de plaquetas de purinas cristalizadas, especialmente de guanina; y son los responsables de los colores plateados e irisados.

Figura 4. *Imagen ampliada de la interbanda clara ventral y las dos bandas oscuras que la flaquean de un pez cebra adulto de fenotipo salvaje. En las bandas oscuras se pueden apreciar los melanocitos de color negro. En la interbanda es más fácil apreciar los xantóforos y los iridóforos. Los xantóforos se aprecian como punto dorados, y los iridóforos, como puntos blancos iridiscentes. Imagen obtenida de Dae Seok Eom y David Parichy, University of Washington*

Al igual que en los mamíferos el sistema de melanocortinas juega un papel crítico en la adquisición del patrón de coloración de los teleósteo. En el pez tetra ciego (*Astyanax mexicanum*), la despigmentación se debe a una mutación que introduce un codón de parada en la secuencia del MC1R que provoca su inactivación (*Gross et al., 2009*). Esta ausencia de actividad reduce el número de melanóforos y el contenido de melanina en los que sí se desarrollan. Este mismo fenotipo puede reproducirse en pez cebra anulando el MC1R (*Gross et al., 2009*). Experimentos con lubina han demostrado que MC1R presenta una actividad constitutiva (*Sánchez et al., 2010*). Esto supondría un problema a la hora de establecer el patrón de coloración dorsoventral, por lo que la actividad de MC1R deber estar permanente inhibida en la región ventral.

Experimentos con anfibios y peces sugerían la existencia de un factor de inhibición de la melanización (MIF), que se produciría mayormente en las células de la región ventral y que difundiría hacia la zona dorsal creando un gradiente de concentración descendente. Este factor, además de reducir la melanización, inhibiría la diferenciación de melanóforos y estimularía la de iridóforos (*Fukuzawa and Ide, 1988; Fukuzawa and Bagnara, 1989; Bagnara and Fukuzawa, 1990, Zuasti et al., 1992; Zuasti 2002*).

Una vez se comprobó la presencia en teleósteos de un péptido homólogo a la ASIP de mamíferos (*Cerdá-Reverter and Peter, 2003*), cuya expresión es mayoritaria en la región ventral (*Cerdá-Reverter et al., 2005; Kurokawa et al., 2006*), y que, al igual que en mamíferos, antagonizaba a la α-MSH en su unión con MC1R y MC4R (*Cerdá-Reverter et al., 2005*); fue lógico plantearse la hipótesis de que ASIP fuera el MIF.

En teleósteos, ASIP también puede estar regulando de manera directa a otros cromatóforos diferentes de los melanóforos. En cepas de pez dorado, que carece de melanóforos, la distribución de los xantóforos e iridóforos también sigue este patrón dorsoventral (*Cerdá-Reverter et al., 2005*). Los peces cebras mutantes con fenotipo "*nacre*" tienen una mutación en el gen MITFa cuyo resultado es una total ausencia de melanóforos en el cuerpo del adulto y un incremento del 40 % en el número de iridóforos respecto a la cepa salvaje (*Lister et al., 1999*).

Dada la expresión en el tegumento de los teleósteos de otros elementos del sistema de melanocortinas diferentes de MC1R y ASIP se debe tener en cuenta su posible participación en la adquisición del patrón de pigmentación. En lo que respecta a otros receptores, MC5R se expresa por todo el tegumento de pez dorado (*Cerdá-Reverter et al., 2003b*), pero solo en la parte ventral en lubina (*Sánchez et al., 2009b*); y MC4R se expresa la parte dorsal del tegumento de pez dorado, pero no en la ventral (*Cerdá-Reverter et al., 2003b*). Respecto de AGRP, su expresión se ha detectado en la parte dorsal del pez dorado (*Cerdá-Reverter and Peter, 2003*), y sin especificar en el tegumento de peces globo (*Kurokawa et al., 2006*) y en el del salmón atlántico (*Salmo salar*) (*Murashita et al., 2009*).

3. Las melanocortinas en la regulación de la Ingesta

3.1. Regulación en mamíferos

En los mamíferos, la ingesta se regula a través de un complejo sistema neuronal del SNC que integra la información periférica, tanto corporal como ambiental, y elabora una respuesta comportamental. Dentro de este complejo sistema neuronal existen dos tipos de vías neurales: las vías catabólicas y las vías anabólicas. Las vías catabólicas inducen una respuesta anorexigénica (inhibición de la ingesta), y un aumento del gasto energético. Por el contrario, las vías anabólicas inducen una respuesta orexigénica (estimulación de la ingesta), y generan un ambiente metabólico predispuesto al ahorro energético. La regulación de estas dos vías se traduce en el nivel de ingesta diario (regulación a corto plazo) y el peso corporal del organismo (regulación a largo plazo). Los sistemas de regulación a largo plazo son capaces de superponerse a los de corto plazo en función del resultado del balance energético; en el que se integran las diferencias entre el aporte y el gasto de energía. Dicha superposición se manifiesta mediante una variación de las sensibilidades de la regulación a corto plazo que modulan el nivel de la ingesta diaria (revisado por *Schwartz et al., 2000*).

La regulación a corto plazo se realiza mediante el denominado circuito de saciedad gastrointestinal que envía información a las vías orexigénicas/anorexigénicas codificada de forma nerviosa u hormonal. La información neural viaja fundamentalmente a través del nervio vago ingresando en el SNC a través del núcleo del tracto solitario (NTS), que a su vez transmite la información a diferentes núcleos neuronales diencefálicos. La distensión estomacal producida tras la ingesta se codifica de forma neural y es capaz de inhibir la ingesta mediante la activación a corto plazo de las vías anorexigénicas. La llegada de alimento al tracto gastrointestinal también provoca la liberación de diferentes péptidos gastrointestinales que son capaces de alcanzar sus receptores neurales a través de la barrera hematoencefálica. Como inhibidores de la ingesta destacan la colecistoquinina (CCK) y el péptido tirosina-tirosina (PYY). Como estimulador destaca la grelina (GRE), un péptido estomacal que también es capaz de estimular la secreción de hormona de crecimiento (GH) (revisado *Morton 2006*).

La regulación a largo plazo es la encargada de informar al SNC sobre las reservas energéticas de las que dispone el animal para atender a otros procesos fisiológicos. En la mayoría de vertebrados, la reserva de energía a largo plazo se acumula en forma de grasa corporal, y su nivel debe estar codificado hormonalmente. El primer candidato fue la insulina, pero a mediados de los años 90 se caracterizó una nueva hormona, denominada leptina, que era liberada desde el tejido adiposo de forma correlativa a la cantidad de grasa acumulada en el organismo. La leptina fue caracterizada molecularmente mediante clonación posicional del locus *ob* responsable del fenotipo de obesidad mórbida en ratones homozigotos (*ob/ob*) (*Zhang et al., 1994*). Posteriormente, se demostró que las mutaciones que inhabilitaban la señalización del receptor de leptina (l*ep*) generaban un fenotipo similar al *ob/ob* (*Lee et al., 1996*).

Cuando algunos de estos péptidos señalizadores alcanzan las neuronas primarias hipotalámicas se aumenta o disminuye la secreción de péptidos hipotalámicos relacionados con la función de la ingesta según sea el tipo de péptido señalizador.

Uno de estos péptidos hipotalámicos es la α-MSH, cuyos índices de expresión se pueden medir en función de la expresión del POMC. En los mamíferos, α-MSH se sintetiza principalmente en el núcleo arqueado, y es uno de los péptidos utilizados por las vías anorexigénicas centrales. La administración intracerebroventricular de α-MSH o de agonistas sintéticos reduce la ingesta de manera dosis-dependiente en ratones (*Cone, 2006*). La actividad reducida o ausente de los receptores cerebrales estimulados por la α-MSH, MC3R y/o MC4R, induce obesidad. Ambos receptores participan en la regulación del balance energético activando mecanismos alternativos, como demuestra el hecho de que el índice de obesidad de los ratones deficientes en MC3R es menor en que los deficientes en MC4R (*Huszar et al., 1997; Butler et al., 2000; Chen et al., 2000*).

Otro de estos péptidos hipotalámicos es la AGRP, que se expresa exclusivamente en las neuronas orexigénicas del núcleo arqueado, y tienen un marcado carácter orexigénico (*Hahn et al., 1998*). Su administración y sobreexpresión en modelos de transgénesis induce hiperfagia y aumento de peso (*Ollmann et al., 1999, Korner et al., 2003*). Estos efectos son debidos a que AGRP antagoniza la actividad constitutiva de MC4R en el núcleo paraventricular (PVN). La actividad constitutiva de MC4R inhibe de manera continua la necesidad de ingesta, y es necesaria la liberación de AGRP para producir la sensación de hambre. Acorde a su función, la expresión de AGRP aumenta muy significativamente durante periodos de ayuno. La expresión ubicua de ASIP en las cepas de ratón mutantes (a/Ay) emula la actividad de AGRP en el cerebro aumentando la tasa de ingesta e induciendo obesidad (*Lu et al., 1994; Cone, 2006*).

3.2. Regulación en los teleósteos

Los péptidos señalizadores y los hipotalámicos de los teleósteos son homólogos a los de los mamíferos tanto en estructura como en función.

En los teleósteos, el POMC (*Cerdá-Reverter et al., 2003a*) y la AGRP (*Cerda-Reverter and Peter, 2003*) se expresan en el núcleo lateral tuberal, homólogo al núcleo arqueado hipotalámico de los mamíferos (*Cerdá-Reverter and Canosa, 2009*). Ambas poblaciones neuronales se proyectan de forma profusa al área preóptica, zona propuesta como la homologa del PVN de los mamíferos (*Cerdá-Reverter and Canosa, 2009*). De forma similar a su función en los mamíferos, la administración central de α-MSH (*Cerdá-Reverter et al., 2003a*) o agonistas químicos (*Cerdá-Reverter et al., 2003b*) inhiben la ingesta de forma dependiente de la dosis. El ayuno tampoco induce en teleósteos una disminución de la expresión del POMC hipotalámico (*Cerdá-Reverter et al., 2003a*), pero al igual que en los mamíferos sí que induce una elevación

muy significativa de los niveles de expresión tuberal de AGRP (*Cerdá-Reverter and Peter, 2003*). De forma similar al modelo de los mamíferos, AGRP actúa como un agonista inverso sobre el MC4R que se expresa de forma profusa y constitutiva en el diencéfalo de los teleósteos (*Cerdá-Reverter et al., 2003b; Sánchez et al., 2009a*). La sobreexpresión de AGRP en modelos de transgénesis en el pez cebra provoca un aumento del crecimiento lineal y en peso de los peces con hipertrofia de los adipocitos y mayor nivel de triglicéridos plasmáticos, sugiriendo la inducción de obesidad en peces (*Song and Cone, 2007*).

4. Las melanocortinas y el estrés

4.1. Regulación en mamíferos

En mamíferos, la respuesta hormonal al estrés está mediada principalmente por la actividad de los ejes hipotálamo-hipófisis-adrenal y hipotalámo-simpático-cromafín.

En respuesta a diferentes estímulos ciertas neuronas hipotalámicas producen la hormona liberadora de la corticotropina (CRH). La CRH estimula las células hipofisarias corticotropas productoras de la hormona adenocorticotropa (ACTH). La ACTH pasa al torrente sanguíneo y alcanza la glándula adrenal, donde estimula la producción de mineralo-corticiodes y glucocorticoides vía activación del MC2R. Los glucocorticoides liberados al plasma sanguíneo actúan sobre el hipotálamo y la hipófisis inhibiendo la producción de CRH y ACTH, en un ciclo de retroalimentación negativo.

Algunos autores han señalado a la α-MSH como inductora de la secreción de aldosterona en rata (*Szalay an Stark, 1982*). Esta afirmación estaría apoyada por la presencia de MC5R en el tejido suprarrenal (*Griffon et al., 1994*).

4.2. Regulación en teleósteos

En teleósteos, el control hormonal del estrés esta conservado. Las neuronas del hipotálamo producen CRH que induce en la síntesis y liberación de ACTH desde las células corticotropas de la *pars distalis*. Esta hormona, también vía MC2R, induce la síntesis y liberación del cortisol (principal glucocorticoide de peces) por parte de las células del tejido interrenal, que es el tejido equivalente al tejido suprarrenal de los mamíferos.

Pese a que algunas especies de peces teleósteos se han constatado una alta presencia de MC5R en el tejido interrenal, todos los resultados parecen indicar que a diferencia de lo que se sugiere para los mamíferos, en los teleósteos α-MSH no está implicada en la producción de esteroides (*Haitina et al., 2004; Aluru and Vijayan, 2008*).

4.3. Las MRAPs

Durante cierto tiempo el estudio farmacológico del MC2R *in vitro* estuvo limitado por la falta de un sistema de expresión funcional. El gen del MC2R se transfectaba correctamente en las líneas celulares convencionales (HEK, CHO, COS), pero su expresión no era funcional. La caracterización de la resistencia a ACTH de las líneas celulares derivadas de la corteza adrenal de ratón conocidas como Y6, con una mutación de MC2R (*Schimmer et al., 1995*), permitió el primer sistema celular capaz de expresar funcionalmente el MC2R (*Noon et al., 2002*). En este sistema plenamente funcional, el receptor se localizaba en la membrana celular, lo que hizo suponer que era necesaria la participación de un factor producido por las células adrenales que asistiera al receptor en su tránsito hacia la membrana.

Este factor pudo ser identificado gracias al estudio del síndrome hereditario de deficiencia de glucorticoidies (FGD). El FGD es un desorden hormonal caracterizado por una baja concentración de cortisol en plasma en presencia de altas concentraciones de ACTH. Tan solo un 25% de los casos de FGD se deben a una mutación en el MC2R (FGD de tipo I). Mediante el uso de micoarrays en muestras de pacientes con FGD tipo II (no asociados a mutaciones del MC2R) pudo identificarse un gen expresado en las células corticales de ratón que daba lugar a una proteína transmembrana que denominaron proteína accesoria del receptor de melanocortinas (MRAP) (*Metherell et al., 2005*).

Las MRAPs no solo resultan necesarias para el tránsito del receptor hasta la membrana, también participan en la regulación de la capacidad de respuesta de MC2R (*Roy et al., 2007: Cooray et al., 2008; Sebag and Hinkle, 2009a*).

Posteriormente, se identificó una segunda MRAP (MRAP2) (*Chan et al., 2009*), que, si bien puede asistir en el tráfico del MC2R hasta la membrana celular, carece de la estructura asociada para conferir funcionalidad al MC2R (*Sebag and Hinkel, 2009*).

En la mayoría de los genomas de los teleósteos estudiados se han identificado ortólogos de las dos MRAPs, pero en el genoma del pez cebra se han identificado dos copias de MRAP2, (a y b, *Agulleiro et al., 2010*). Según los resultados obtenidos en pez cebra, las funciones de asistencia y mejora de la capacidad de respuesta del receptor en membrana a la ACTH por parte de la MRAP1 parecen estar conservadas, pero a diferencia de lo que ocurre en mamíferos, en los teleósteos, la presencia de MRAP2 no es suficiente para que MC2R alcance la membrana (*Agulleiro et al., 2010*). En teleósteos, las MRAP2 interactúan con MC4R. La MRAP2a convierte a MC4R en un receptor de ACTH estableciendo un claro vínculo molecular entre la regulación del estrés (ACTH) y el control de la ingesta (MC4R). LA MRAP2b disminuye la actividad constitutiva del MC4R implicando así su expresión central en el control de la ingesta (*Agulleiro et al., 2013*).

Objetivos

El objetivo principal de esta tesis es el estudio de los mecanismos moleculares que subyacen en la participación del sistema de melanocortinas en la regulación de la pigmentación y el crecimiento de los peces.

Para alcanzar este objetivo general se asumieron una serie de objetivos concretos:

El primer objetivo fue caracterizar la presencia de agonistas inversos y su potencial implicación en el establecimiento del patrón dorsoventral de pigmentación en los peces planos que exhiben una pronunciada polaridad pigmentaria.

El segundo objetivo fue establecer una relación causal entre la sobreexpresión de ASIP y el patrón dorsoventral de pigmentación en el pez cebra utilizando técnicas de transgénesis.

El tercer objetivo fue identificar los efectos de la sobreexpresión de ASIP sobre la ingesta y el crecimiento, asi como los posibles mecanismos/sistemas neuronales implicados en el fenotipo energético diferencial.

El cuarto y último objetivo fue caracterizar la intervención de otros sistemas hormonales en la regulación de la pigmentación en los peces.

CAPÍTULO I

En el capítulo se establece una relación causal entre ASIP y el mecanismo de regulación del patrón pigmentario en los peces teleósteos.

Los peces planos presentan un marcado patrón dorsoventral que se caracteriza por una región dorsal melanizada (cara ocular) en contraposición a una región ventral despigmentada (cara ciega). Esta característica hace que sea un grupo de especial interés para el estudio de los efectos de la sobrexpresión de ASIP sobre la polaridad pigmentaria dorsoventral.

Mediante la inyección de RNA mensajero, se consiguió la producción ectópica de la proteína ASIP en la región dorsal, lo que conlleva una inhibición de la melanogenesis en la región de inyección, demostrando una relación directa de la proteína ASIP con el control de la pigmentación de los peces planos y su posible implicación en el establecimiento del patrón de pigmentación dorsoventral.

La caracterización de ASIP en lenguado y rodaballo permite introducir estas nuevas secuencias en los análisis evolutivos de esta familia de péptidos. La evolución de esta familia puede explicarse actualmente mediante dos modelos. En este capítulo se exponen ambas hipótesis, y se analiza el encaje de las nuevas secuencias en ellas.

Transient Ectopic Overexpression of Agouti-Signaling Protein 1 (Asip1) Induces Pigment Anomalies in Flatfish

**Raúl Guillot[1], Rosa Maria Ceinos[2], Rosa Cal[3],
Josep Rotllant[2], José Miguel Cerdá-Reverter[1]**

1. Department of Fish Physiology and Biotechnology, Instituto de Acuicultura de Torre de la Sal (IATS), Consejo Superior de Investigaciones Científicas (CSIC), Castellón, Spain.
2. Aquatic Molecular Pathobiology Group, Instituto de Investigaciones Marinas (IIM), CSIC, Vigo, Spain.
3. Instituto Español de Oceanografía de Vigo (IEO), Vigo, Spain.

Abstract

While flatfish in the wild exhibit a pronounced countershading of the dorso-ventral pigment pattern, malpigmentation is commonly observed in reared animals. In fish, the dorso-ventral pigment polarity is achieved because a melanization inhibition factor (MIF) inhibits melanoblast differentiation and encourages iridophore proliferation in the ventrum. A previous work of our group suggested that asip1 is the uncharacterized MIF concerned. In order to further support this hypothesis, we have characterized asip1 mRNAs in both turbot and sole and used deduced peptide alignments to analyze the evolutionary history of the agouti-family of peptides. The putative asip precursors have the characteristics of a secreted protein, displaying a putative hydrophobic signal. Processing of the potential signal peptide produces mature proteins that include an N-terminal region, a basic central domain with a high proportion of lysine residues as well as a proline-rich region that immediately precedes the C-terminal poly-cysteine domain.The expression of asip1 mRNA in the ventral area was significantly higher than in the dorsal region. Similarly, the expression of asip1 within the unpigmented patches in the dorsal skin of pseudoalbino fish was higher than in the pigmented dorsal regions but similar to those levels observed in the ventral skin. In addition, the injection/electroporation of asip1 capped mRNA in both species induced long term dorsal skin paling, suggesting the inhibition of the melanogenic pathways. The data suggest that fish asip1 is involved in the dorsal-ventral pigment patterning in adult fish, where it induces the regulatory asymmetry involved in precursor differentiation into mature chromatophore. Adult dorsal pseudoalbinism seems to be the consequence of the expression of normal developmental pathways in an inaccurate position that results in unbalanced asip1 production levels. This, in turn, generates a ventral-like differentiation environment in dorsal regions.

1. Introduction

In teleosts fish, pigment cells are commonly found in the dermis and can be divided into light-absorbing (melanophores, xantophores, erythrophores and cyanophores) and light-reflecting (leucophores and iridophores) chromatophores. Fish melanophores contain eumelanins (black-brown pigments), whereas xantophores and erytrophores synthesize carotenoids and/or pteridines that contribute to the reddish and yellowish components of the skin coloration. Iridophores are commonly localized in whitish and silvery areas of the skin, predominantly on the belly surface. They contain

crystalline platelets composed of purines, mainly of guanine, which are responsible for the reflection of light (*Fujii, 1993*). Fish countershading is achieved by a patterned distribution of the pigment cells, with the light-absorbing and light-reflecting chromatophores mostly distributed in the dorsal and ventral areas, respectively (*Fukuzawa and Ide, 1998, Zuasti et al., 1992*). Although the pigment pattern is most evident in the adult animal, its cellular basis is established during embryogenesis (*Kelsh et al., 2000a*). Experimental data in fish and amphibian species suggest that this dorso-ventral pigment pattern is achieved because a putative diffusible melanization inhibition factor (MIF), locally produced by cells in the ventral skin, inhibits melanoblast differentiation and stimulates iridophore proliferation in the ventrum (*Fukuzawa and Ide, 1998, Bagnara and Fukuzawa, 1990, Zuasti, 2002*). Our recent studies support agouti-signalling protein 1 (asip1) as the fish MIF (*Cerdá-Reverter et al., 2005*). *Asip1* encodes a 131 amino acid protein with structural characteristics of a secreted protein, which has a hydrophobic signal sequence and lacks a transmembrane domain. A highly basic domain with a high proportion of arginine and lysine residues forms the N-terminal region of the agouti protein. The latter region heads a proline-rich area that immediately precedes the cysteine-rich C-terminal domain. This cysteine domain resembles the conotoxins and plectoxins of snails and spiders, respectively (*Manne et al., 1995*).

In goldfish (*Carassius auratus*), *asip1* is expressed in the ventral skin but not in the dorsal skin. It inhibits melanocortin-induced melanin dispersion in melanocytes and selectively binds melanocortin receptor 1 (MC1R) (*Cerdá-Reverter et al., 2005*). This receptor shows high sensitivity to the melanocyte-stimulating hormone (α-MSH) and is profusely expressed within both dorsal and ventral skin (*Cerdá-Reverter et al., 2005, Sánchez et al., 2010*). Interestingly, frameshift mutations introducing a premature stop codon in melanocortin MC1R or inactivating mutations in blind Mexican cave tetra (*Astyanax mexicanus*) are responsible for a decrease in the number of melanocytes and of the melanin content. This phenotype is recapitulated by MC1R knockdown in zebrafish (*Gross et al., 2009*). Taken together, the data support that interaction between α-MSH/asip1 and MC1R is involved in the establishment of the dorsal-ventral pigment pattern, controlling chromatoblast survival, differentiation and/or proliferation as well as melanin synthesis.

Flatfish exhibit a pronounced countershading and are an excellent model to study the establishment of the dorso-ventral pigment pattern. These fish species undergo a metamorphosis from symmetrical free-swimming larvae to asymmetrical bottom-dwelling animals with both eyes on the same side. The dorsal-ocular side becomes dark pigmented whereas the ventral-blind side is white in color (*Hamre et al., 2007*). This pigment asymmetry appears in the adult stage and is hypothesized to depend upon the asymmetry of organizational environments that potentially regulate latent chromatophore precursor survival, proliferation and differentiation (*Hamre et al., 2007, Bolker and Hill, 2000*). Such regulatory asymmetry may be due to differences in the expression and distribution of secretory proteins involved in the precursor differentiation into mature chromatophore (*Yamada et al., 2010*). Accordingly, the common malpigmentation observed in reared flatfish, including pseudoalbinism (partial or total unpigmented ocular side) and hypermelanism (partial or total pigmented blind side), could be due to abnormalities in the asymmetry of the regulatory system (*Bolker and Hill, 2000, Bolker et al., 2005, Barton, 2009*). The aim of this paper was to gain evidence supporting the view that *asip1* is able to generate a regulatory asymmetry that leads to dorsal-ventral pigment asymmetry. To this aim, we characterized sole (*Solea senegalensis*) and turbot (*Scophtalmus maximus*) *asip1* gene and analyzed tissue and developmental expression. We demonstrate that *asip1* is significantly more expressed in the ventral skin than in the dorsal skin. Moreover, when *asip1* is ectopically overexpressed in the ocular side it induces skin paling probably via inhibition of the melanogenic processes, whereas pseudoalbino animals exhibit increased *asip1* expression within the anomalous pigment areas.

2. Results

Cloning flatfish *asip1* gene

Reverse transcription-polymerase chain reaction (RT-PCR) using degenerate primers designed by alignments of available fish *asip1* sequences; produced a partial cDNA fragment of 135 and 159 bp for sole and turbot, respectively. The putative translations exhibited high identity with the C-terminal cysteine domain of the published *asip1* sequences. To obtain the sequence of the complete peptide precursor RACE-PCR was performed in the 3' and 5' directions with specific primers. 3' RACE generated unique bands of 422 and 499 bp for sole and turbot, respectively and provided information about the coding region of the exon 4 and the 3' untranslated region. 5' RACE experiments generated unique bands of 379 and 498 bp and provided information about the first *asip1* exons as well as the 5 'untranslated region.

The peptide precursors have the same organization as other species. The first 22 amino acids are estimated to constitute the signal peptide, which is followed by the 101 (turbot) or 110 (sole) amino acids of the mature peptide. One putative glycosylation sites were found within the highly basic N-terminal region of the sole but no glycosylation consensus sites were found in the turbot mature peptide. A proline-rich region and a poly-cysteine C-terminal domain followed the basic N-terminal region in both sequences. The poly-cysteine domain contains 10 cysteine residues with identical spatial pattern to that of agouti-like proteins, and similar to mammalian asip molecules it does not exhibit a short amino acid extension following the tenth cysteine residue (Fig. 1). Sole and turbot asip1 precursors were 73% identical. Flatfish amino-acid asip1 sequences are only 15-19 % identical to asip2 of fish tetradontiform but they share 57-67% identical amino acids with asip1 precursor of the same species. The identity level of flatfish sequences with fish asip1 or asip2 was 18-20% and 15-19%, respectively. Phylogenetic analysis grouped flatfish asip1 sequences with the asip1 precursors of fish and tetrapod species. A different branch of the same cluster grouped asip2 and agrp2 sequences, whereas agrp precursors were grouped in a different cluster (Fig. 2)
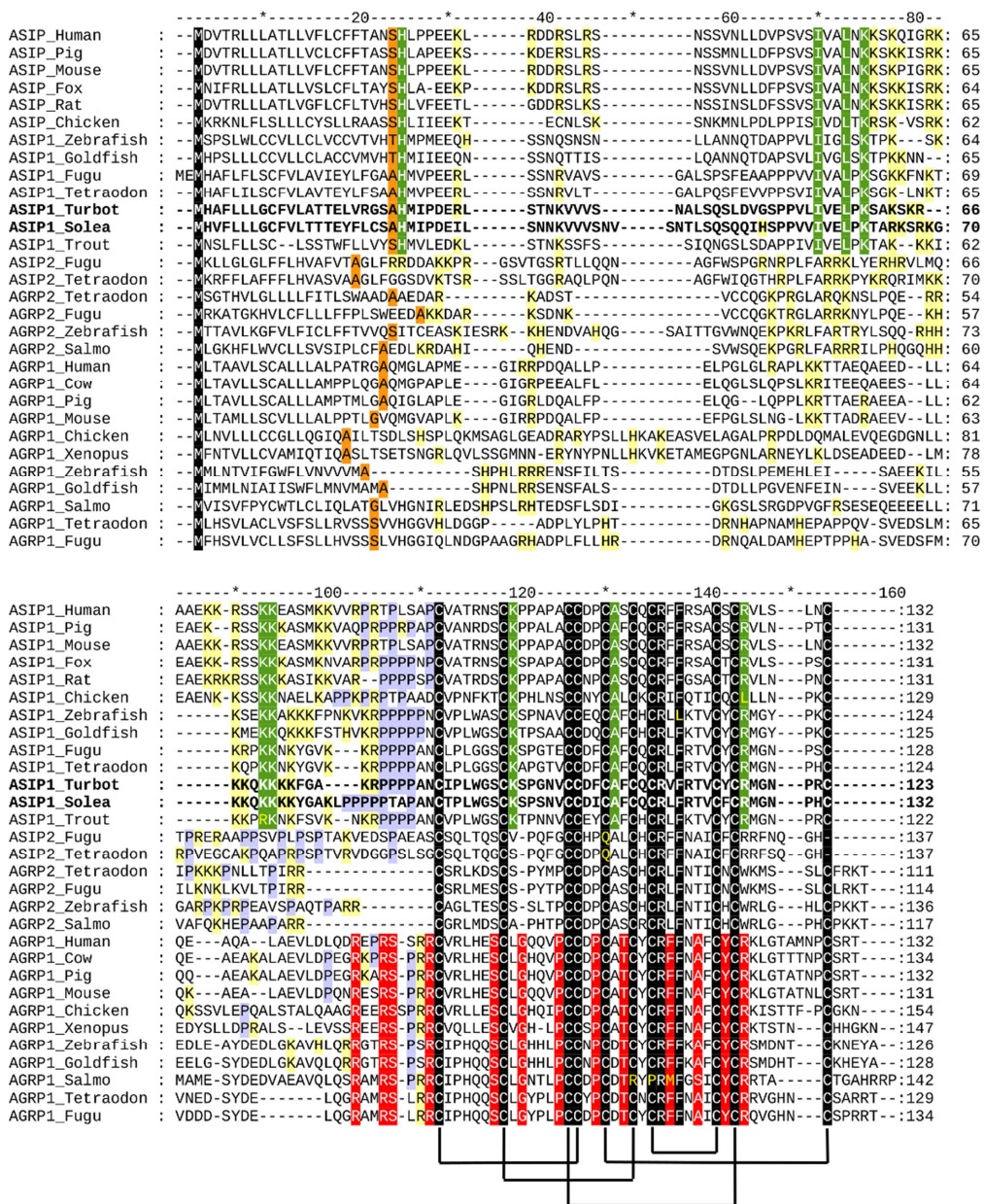
```
          ---------*---------20--------*---------40-------*---------60-------*---------80--
ASIP_Human       : --MDVTRLLLATLLVFLCFFTANSHLPPEEKL------RDDRSLRS----------NSSVNLLDVPSVSIVALNKKSKQIGRK: 65
ASIP_Pig         : --MDVTRLLLATLLVCLCFFTASSHLAPEEKS------KDERSLRS----------NSSMNLLDFPSVSIVALNKKSKKISRK: 65
ASIP_Mouse       : --MDVTRLLLATLLVFLCFFTANSHLPPEEKL------RDDRSLRS----------NSSVNLLDVPSVSIVALNKKSKPIGRK: 65
ASIP_Fox         : --MNIFRLLLATLLVSLCFLTAYSHLA-EEKP------KDDRSLRS----------NSSVNLLDFPSVSIVALNKKSKKISRK: 64
ASIP_Rat         : --MDVTRLLLATLVGFLCFLTVHSHLVFEETL------GDDRSLKS----------NSSINSLDFSSVSIVALNKKSKKISRK: 65
ASIP_Chicken     : --MKRKNLFLSLLLCYSLLRAASSHLIIEEKT--------ECNLSK----------SNKMNLPDLPPISIVDLTRSK-VSRK: 62
ASIP1_Zebrafish  : --MSPSLWLCCVLLCLVCCVTVHTHMPMEEQH------SSNQSNSN----------LLANNQTDAPPVLIIGLSKTPK---SK: 64
ASIP1_Goldfish   : --MHPSLLLCCVLLCLACCVMVHTHMIIEEQN------SSNQTTIS----------LQANNQTDAPSVLIVGLSKTPKKNN--: 65
ASIP1_Fugu       : MEWHAFLFLSCFVLAVIEYLFGAAIMVPEERL------SSNRVAVS--------GALSPSFEAAPPVVIVALPKSGKFFNKT: 69
ASIP1_Tetraodon  : --MHAFLILSCFVLAVTEYLFSAAIMVPEERL------SSNRVLT----------GALPQSFEVVPPSVILVALPKSGK-LNKT: 65
ASIP1_Turbot     : --WHAFLLLGCFVLATTELVRGSAIMIPDERL------STNKVVVS--------NALSQSLDVGSPPVLIVELPKSAKSKR--: 66
ASIP1_Solea      : --MHVFLLLGCFVLTTTEYFLCSAIMIPDEIL------SNNKVVVSNV-----SNTLSQSQQIHSPPVVIVELPKTARKSRKG: 70
ASIP1_Trout      : --MNSLFLLSC--LSSTWFLLVYSHMVLEDKL------STNKSSFS----------SIQNGSLSDAPPIVLPKTAK--KKI: 62
ASIP2_Fugu       : --MKLLGLGLFFLHVAFVTAGLFRRDDAKKPR---GSVTGSRTLLQQN--------AGFWSPGRNRPLFARRKLYERHRVLMQ: 66
ASIP2_Tetraodon  : --MKRFFLAFFFLHVASVAAGLFGGSDVKTSR---SSLTGGRAQLPQN--------AGFWIQGTHRPLFARRKPKRQRIMKK: 70
AGRP2_Tetraodon  : --MSGTHVLGLLLLFITLSWAADAAEDAR---------KADST---------------VCCQGKTRGLARRKNSLPQE--RR: 54
AGRP2_Fugu       : --MRKATGKHVLCFLLLFFPLSWEEDAKKDAR------KSDNK---------------VCCQGKTRGLARRKNYLPQE--KH: 57
AGRP2_Zebrafish  : --MTTAVLKGFVLFICLFFTVVQSITCEASKIESRK--KHENDVAHQG-----SAITTGVWNQEKPKRLFARTRYLSQQ-RHH: 73
AGRP2_Salmo      : --MLGKHFLWVCLLSVSIPLCFAEDLKRDAHI------QHEND---------------SVWSQEKPGRLFARRRILPHQGQHH: 60
AGRP1_Human      : --MLTAAVLSCALLLALPATRGAQMGLAPME----GIRRPDQALLP-----------ELPGLGLRAPLKKTTAEQAEED--LL: 64
AGRP1_Cow        : --MLTAVLLSCALLLAMPPLQGAQMGPAPLE----GIGRPEEALFL-----------ELQGLSLQPSLKRITEEQAEES--LL: 64
AGRP1_Pig        : --MLTAVLLSCALLLAMPTMLGAQIGLAPLE----GIGRLDQALFP-----------ELQG--LQPPLKRTTAERAEEA--LL: 62
AGRP1_Mouse      : --MLTAMLLSCVLLLALPPTLGVQMGVAPLK----GIRRPDQALFP-----------EFPGLSLNG-LKKTTADRAEEV--LL: 63
AGRP1_Chicken    : --MLNVLLLCCGLLQGIQAILTSDLSHSPLQKMSAGLGEADRARYPSLLHKAKEASVELAGALPRPDLDQMALEVQEGDGNLL: 81
AGRP1_Xenopus    : --MFNTVLLCVAMIQTIQASLTSETSNGRLQVLSSGMNN-ERYNYPNLLHKVKETAMEGPGNLARNEYLKLDSEADEED--LM: 78
AGRP1_Zebrafish  : --MMLNTVIFGWFLVNVVVMA-----------SHPHLRRRENSFILTS----------DTDSLPEMEHLEI-----SAEEKIL: 55
AGRP1_Goldfish   : --MIMMLNIAIISWFLMNVMAMA---------SHPNLRRSENFEIN----DTDLLPGVENFEIN----SVEEKLL: 57
AGRP1_Salmo      : --MVISVFPYCWTLCLIQLATGLVHGNIRLEDSHPSLRHTEDSFLSDI----------GKGSLSRGDPVGFRSESEQEEEELL: 71
AGRP1_Tetraodon  : --MLHSVLACLVSFSLLRVSSSVVHGGVHLDGGP-----ADPLYLPHT----------DRNHAPNAMHEPAPPQV-SVEDSLM: 65
AGRP1_Fugu       : --MFHSVLVCLLSFSLLHVSSSLVHGGIQLNDGPAAGRHADPLFLLHR----------DRNQALDAMHEPTPPHA-SVEDSFM: 70


          ------*---------100-------*---------120------*---------140------*---------160
ASIP1_Human      : AAEKK-RSSKKEASMKKVVRPRTPLSAPCVATRNSCKPPAPACCDPCASCQCRFFRSACSCRVLS---LNC-------:132
ASIP1_Pig        : EAEK--RSSKKASMKKVAQPRPPPRPAPCVANRDSCKPPALACCDPCAFCQCRFFRSACSCRVLS---PTC-------:131
ASIP1_Mouse      : AAEKK-RSSKKEASMKKVVRPRTPLSAPCVATRNSCKPPAPACCDPCASCQCRFFRSACSCRVLS---LNC-------:132
ASIP1_Fox        : EAEKK-RSSKKASMKNVARPRPPPPNPCVATRDSCKSPAPACCDPCASCQCRFFRSACTCRVLS---PSC-------:131
ASIP1_Rat        : EAEKRKRSSKKASIKKVAR--PPPPSPCVATRDSCKPPAPACCDPCASCQCRFFRSACTCRVLN---PNC-------:131
ASIP1_Chicken    : EAENK-KSSKKNAELKAPPKPRPTPAADCVPNFKTCKPHLNSCCNYCALCKCRIFQTICQCLLLN---PKC-------:129
ASIP1_Zebrafish  : ------KSEKKAKKKFPNKVKRPPPPPNCVPLWASCKSPNAVCCEQCAFCHCRLLKTVCYCRMGY---PKC-------:124
ASIP1_Goldfish   : ------KMEKQKKKFSTHVKRPPPPPNCVPLWGSCKTPSAACCDQCAFCHCRLLKTVCYCRMGY---PKC-------:125
ASIP1_Fugu       : ------KRPKNKYGVK---KRPPPPANCLPLGGSCKSPGTECCDFCACCQCRLFRTVCYCRMGN---PSC-------:128
ASIP1_Tetraodon  : ------KQPKKNKYGVK---KRPPPPANCIPLGGSCKAPGTVCCDFCACCQCRLFRTVCYCRMGN---PHC-------:124
ASIP1_Turbot     : ------KKQKKKFGA----KRPPPPANCIPLWGSCKSPGNVCCDFCACCQCRLFRTVCYCFCRMGN---PRC-------:123
ASIP1_Solea      : ------KKQKKKYGAKLPPPPPTAPANCTPLWGSCKSPSNVCCDICACCQCRLFRTVCFCRMGN---PHC-------:132
ASIP1_Trout      : ------KKPRKNKFSVK--NKRPPPPANCVPLWGSCKTPNNVCCEYCAFCHCRLLKTVCYCRMGN---PRC-------:122
ASIP2_Fugu       : TPRERAAPPSVPLPSPTAKVEDSPAEASCSQLTQSCV-PQFGCCHPQALCHCRFFNAICFCRRFNQ---GHC-------:137
ASIP2_Tetraodon  : RPVEGCAKPQAPRPSPTVRVDGGPSLSGCSQLTQGCS-PQFGCCDPQALCHCRFFNAICFCRRFSQ---GHC-------:137
AGRP2_Tetraodon  : IPKKKPNLLTPIRR-------------CSRLKDSCS-PYMPCCDPCASCHCRLFNTICNCWKMS---SLCFRKT---:111
AGRP2_Fugu       : ILKNKLKVLTPIRR-------------CSRLMESCS-PYTPCCDPCASCHCRLFNTICNCWKMS---SLCRLKT---:114
AGRP2_Zebrafish  : GARPKPRPEAVSPAQTPARR-------CAGLTESCS-SLTPCCDPCASCRCRLFNTICHCWRLG---HLCPKKT---:136
AGRP2_Salmo      : VAFQKHEPAAPARR-------------CGRLMDSCA-PHTPCCDPCASCRCRLFNTICHCWRLG---PHCPKKT---:117
AGRP1_Human      : QE---AQA--LAEVLDLQDREPRS-SRRCVRLHESCLGQQVPCCDPCATCYCRFFNAFCYCRKLGTAMNPCSRT----:132
AGRP1_Cow        : QE---AEAKALAEVLDPEGRKPRS-PRRCVRLHESCLGHQVPCCDPCATCYCRFFNAFCYCRKLGTTTNPCSRT----:134
AGRP1_Pig        : QQ---AEAKALAEVLDPEGRKARS-PRRCVRLHESCLGHQVPCCDPCATCYCRFFNAFCYCRKLGTATNPCSRT----:132
AGRP1_Mouse      : QK---AEA--LAEVLDPQNRESRS-PRRCVRLHESCLGQQVPCCDPCATCYCRFFNAFCYCRKLGTATNLCSRT----:131
AGRP1_Chicken    : QKSSVLEPQALSTALQAAGREERSSPRRCVRLLESCLGHQIPCCDPCATCYCRFFNAFCYCRKISTTF-PCGKN----:154
AGRP1_Xenopus    : EDYSLLDPRALS--LEVSSREERS-PRRCVQLLESCVGH-LPCCSPCATCYCRFFKAFCYCRKTSTN--CHHGKN--:147
AGRP1_Zebrafish  : EDLE-AYDEDLGKAVHLQRRGTRS-PSRCIPHQQSCLGHHLPCCNPCDICYCRFFKAFCYCRSMDNT---CKNEYA--:126
AGRP1_Goldfish   : EELG-SYDEDLGKAVQLQRRGTRS-PSRCIPHQQSCLGNTLPCCDPCDTRYPRMFGSICYCRRTA-----CTGAHRRP:142
AGRP1_Salmo      : MAME-SYDEDVAEAVQLQSRAMRS-PRRCIPHQQSCLGNTLPCCDPCDTRYPRMFGSICYCRRTA-----CTGAHRRP:142
AGRP1_Tetraodon  : VNED-SYDE-------LQGRAMRS-LRRCIPHQQSCLGYPLPCCDPCDICYCRFFNAICYCRRVGHN---CSARRT--:129
AGRP1_Fugu       : VDDD-SYDE-------LQGRAMRS-LRRCIPHQQSCLGYPLPCCDPCDICYCRFFNAICYCRQVGHN---CSPRRT--:134
```

Figure 1. *Alignment of agouti-signaling protein (asip) and agouti-related protein (agrp) amino acid sequences. Dashes were introduced to improve alignment. Orange boxes indicate the last residue of the predicted signal peptide. Black boxes show amino acid residues conserved in all sequences. Green boxes show residues only conserved in asip1 sequences. Red boxes indicate residues only conserved in agrp1 sequences. Yellow boxes indicate basic residues before cysteine domain. Blue boxes show residues of the short tail present in all agrp sequences. Purple boxes indicate putative glycosilation sites. Lines joining cysteine residues indicate putative disulfide bonds forming the cysteine domain. Arrow shows conserved motif for agrp post-transcriptional processing.*
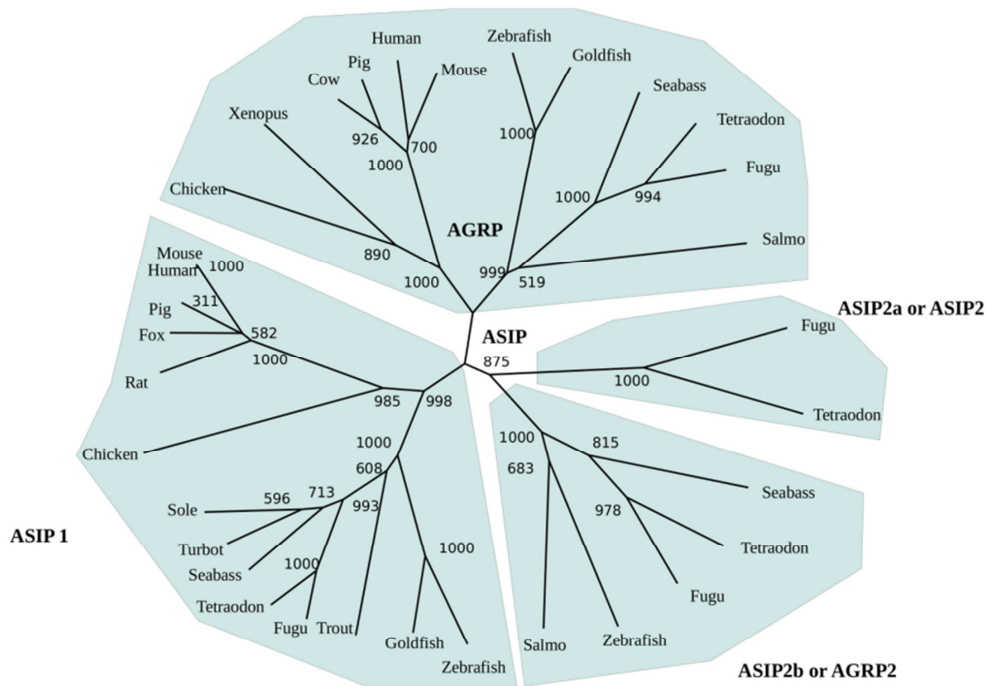
Figure 2. *Phylogenetic tree of asip and agrp amino acid sequences built using CulstalX, which uses the Neighbor-Joining method on a matrix of distances. Numbers at branch nodes represent the confidence level of 1000 bootstrap replications. Phylogenetic analysis were done also by maximum likelihood using Seaview free software and no considerable differences were found.*

Temporal and spatial expression of *asip1*

The RT-PCR analysis (Fig.3 A,B) showed that *asip1* transcripts existed maternally at a relatively low level, whereas zygotic expression persisted at relatively constant levels until the end of the sampling period (45 days post-fertilization, dpf) for turbot (Fig.3A) and (29 dpf) sole (Fig.3B).

At tissue level, *asip1* was highly expressed in the brain eye, heart, muscle, gonads and pineal organ of turbot. Very low expression levels were found in the hypophysis and liver. Residual levels were found in the remaining tested tissues including skin (Fig.4A). Similar to turbot, sole *asip1* was expressed in the brain, hypophysis, eye, liver muscle and gonads but not in the heart. Additionally, high expression levels were detected in the gill, dorsal and ventral skin and adipose tissue (Fig.4B).
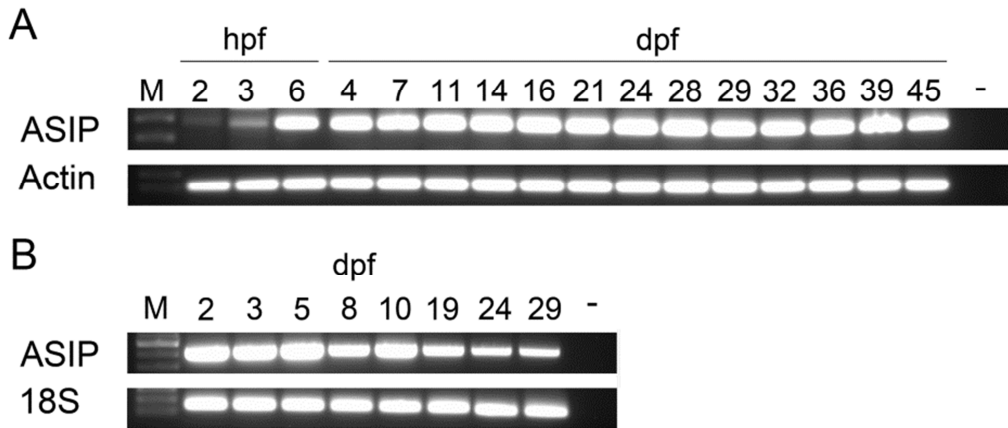
Figure 3. *Expression of asip 1 gene during early development. RT-PCR analysis of the temporal expression pattern of asip1 in turbot (A) and sole (B). Hours post-fertilization, hpf; days post-fertilization, dpf.*
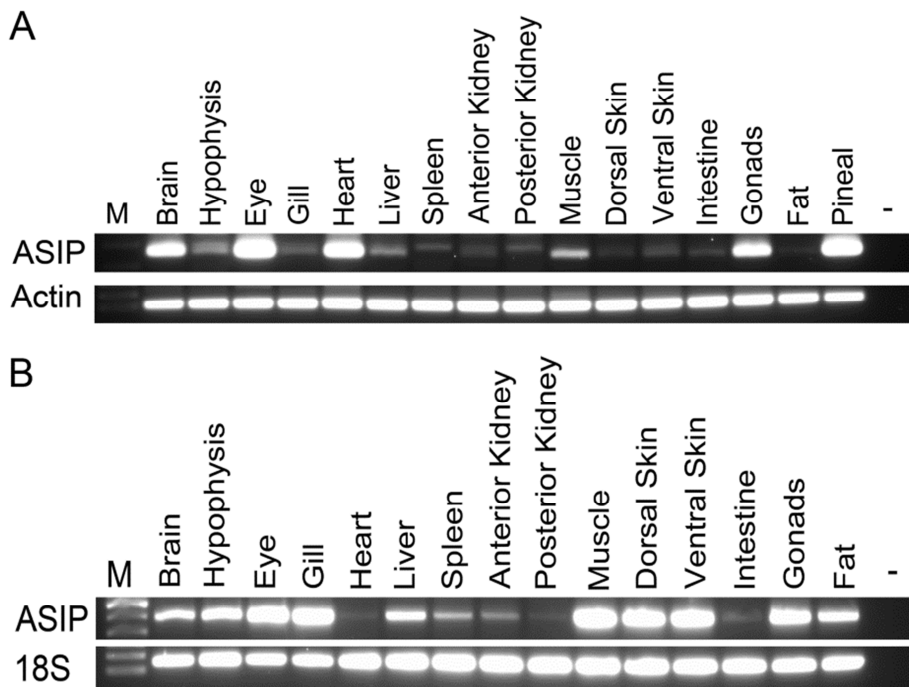
Figure 4. *RT-PCR analysis of the tissue specific expression pattern of asip1. (A) Turbot and (B) sole.*

Spatially controlled expression of *asip1* gene

To examine whether the expression of *asip1* gene is spatially regulated in turbot and sole skin, samples of dorsal and ventral skin were taken and *asip1* gene expression evaluated by absolute qRT-PCR. Consistent with the dorso-ventral expression pattern of *asip1* gene described in other fish species (*Cerdá-Reverter et al., 2005*), the *asip1* transcripts were significantly more expressed in the ventral non-pigmented skin than in the dorsal pigmented skin of both fish species (Fig. 5A,B).
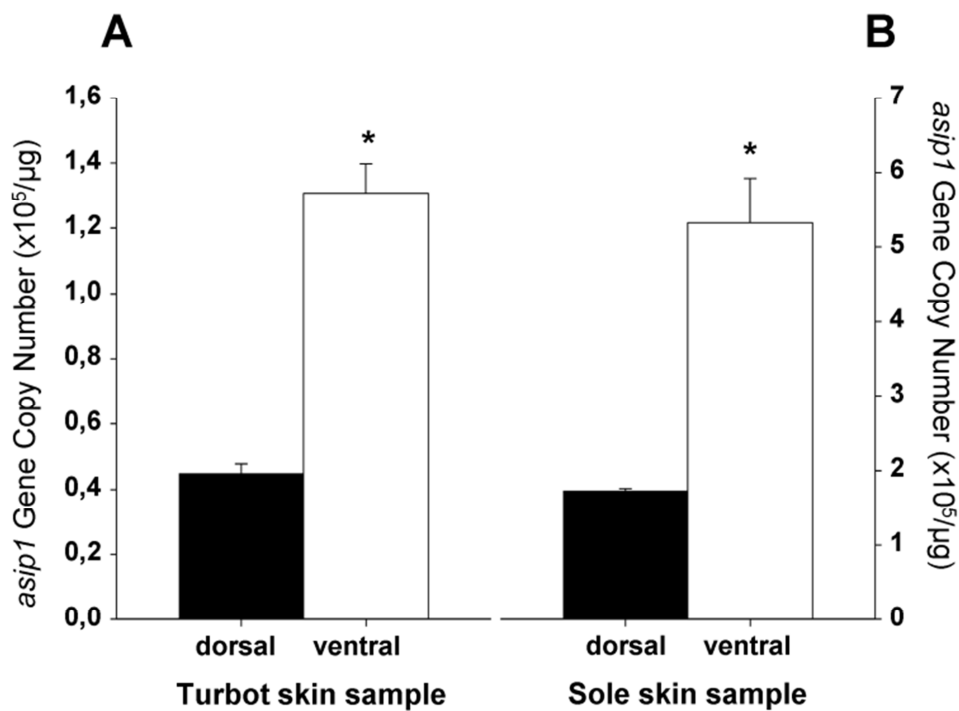
Figure 5. *Analysis of differential dorsal-ventral* asip1 *gene expression. Asip1 was differentially expressed in ventral non-pigmented skin or dorsal pigmented skin in turbot (A) and sole (B).* Asip1 *gene expression was quantified by absolute qRT-PCR. The average* asip1 *gene copy number per μg of primed cDNA was calculated from 5 individuals analyzed each time in triplicate. Data are expressed as mean ± SEM. Comparisons of numerical data were made by paired Student t-tests. *P<0.05.*

In pseudo-albino turbot (Fig. 6A) and sole (Fig. 6C), *asip1* gene expression was upregulated in dorsal non-pigmented regions compared with the dorsal pigmented regions in both turbot (Fig. 6B) and sole (Fig. 6D), suggesting a relationship of *asip1* gene expression levels and changes in skin pigmentation.
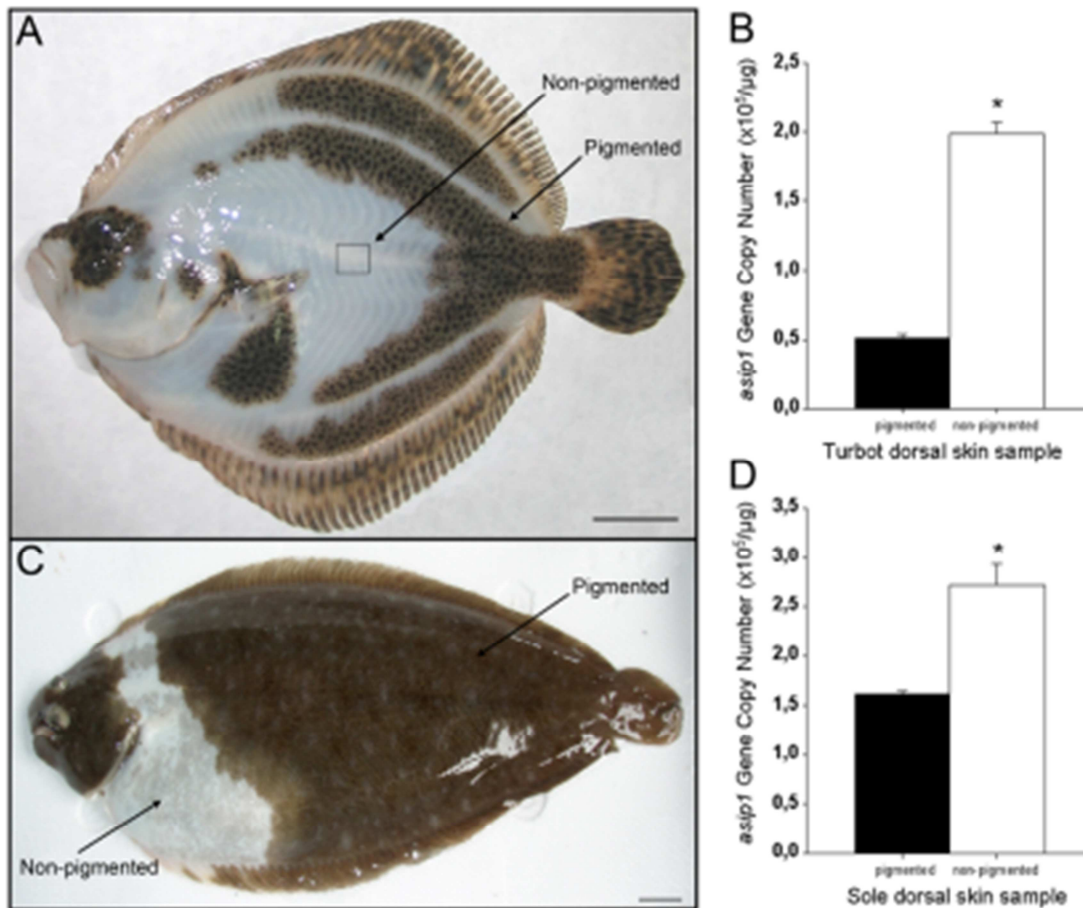
Figure 6. Analysis of asip1 *gene expression in pseudoalbino flatfish. Pseudo-albinism phenotype present in cultured turbot (A) and sole (C).* Asip1 *was differentially expressed in non-pigmented white or pigmented brown dorsal skin areas in turbot (B) and sole (D).* Asip1 *gene expression was quantified by absolute qRT-PCR. The average* asip1 *gene copy number per µg of primed cDNA was calculated from 5 individuals analyzed each time in triplicate. Data are expressed as mean ± SEM. Comparisons of numerical data were made by paired Student t-tests. *P<0.05. Scale bars: 1 cm.*

Transient ectopic overexpression of *asip1* gene

To investigate whether ectopic *asip1* expression could lead to pigment alteration on flatfish dorsal skin, we transiently overexpressed the *asip1* gene in turbot and sole dorsal skin area by *asip1*-capped mRNA injection and electroporation. The transient ectopic overexpression of *asip1* in the dorsal skin of turbot and sole induced a powerful paling of the skin 4 days after *asip1* gene overexpression (Fig. 7B; 8B). No skin pigmentation alteration was found in the antisense asip1-capped mRNA injected and electroporated fish (Fig. 7D; 8D) or *e*GFP (Fig. 7H; 8H) using brightfiled ilumination but increased fluorescence was evident in animals injected with sense *e*GFP (Fig.7F; 8F). It means that sense *e*GFP injection and electroporation caused the expected effect without alteration of skin pigmentation.

To confirm the effects of asip1 injection on melanogenic synthesis pathways, we studied tyrosinase-like protein 1 (Tyrp1) expression in intact, eGFP- and sense capped mRNA asip1-injected turbot skin. As expected Tyrp1 expression levels were lower in the ventral skin when compared to dorsal skin (Fig 9A). Similarly the injection of sense asip1-capped mRNA, but no eGFP mRNA, induced a severe decrease in the Tyrp1 expression levels (Fig 9B).
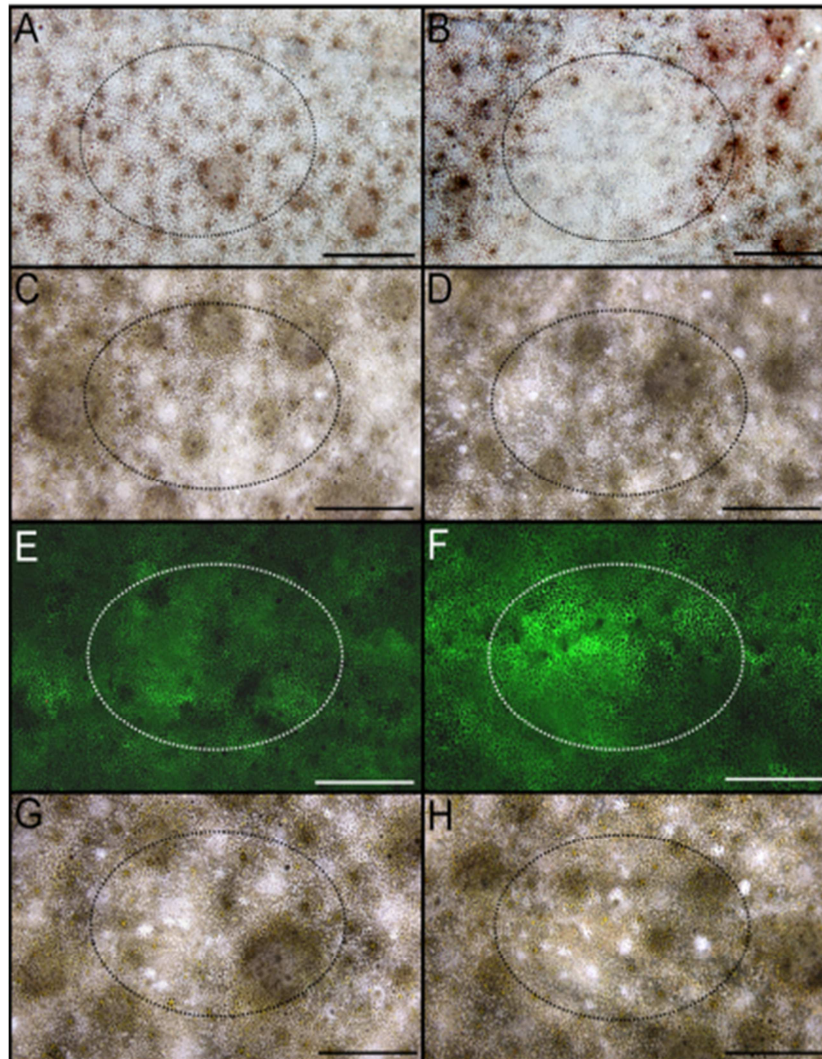
Figure 7. *Views of dorsal skin of turbot injected and eletroporated in vivo to evaluate the effect of asip 1 overexpression on skin paling. Animals were injected with about 10 μg of capped sense (B) or antisense (D) mRNA per cm2 of dorsal skin and the effect was evaluated 4 days post injection/electroporation. Dorsal skin of control non-treated turbots are shown in A, C, E, and G. E and F show dorsal skin of control (E) and injected/electroporated animals with capped sense eGFP-mRNA (F) animals under fluorescent incident light w. G and H display animals shown in E and F under brilliant incident light. . Fluorescence was determined with a binocular Leica Stereoscope M165FC with digital camera (Leica Microsystem). Images were processed with Photoshop 7.0 (Adobe Systems) programs. Dorsal views, anterior to the right. Scale bars: 0.6 cm.*
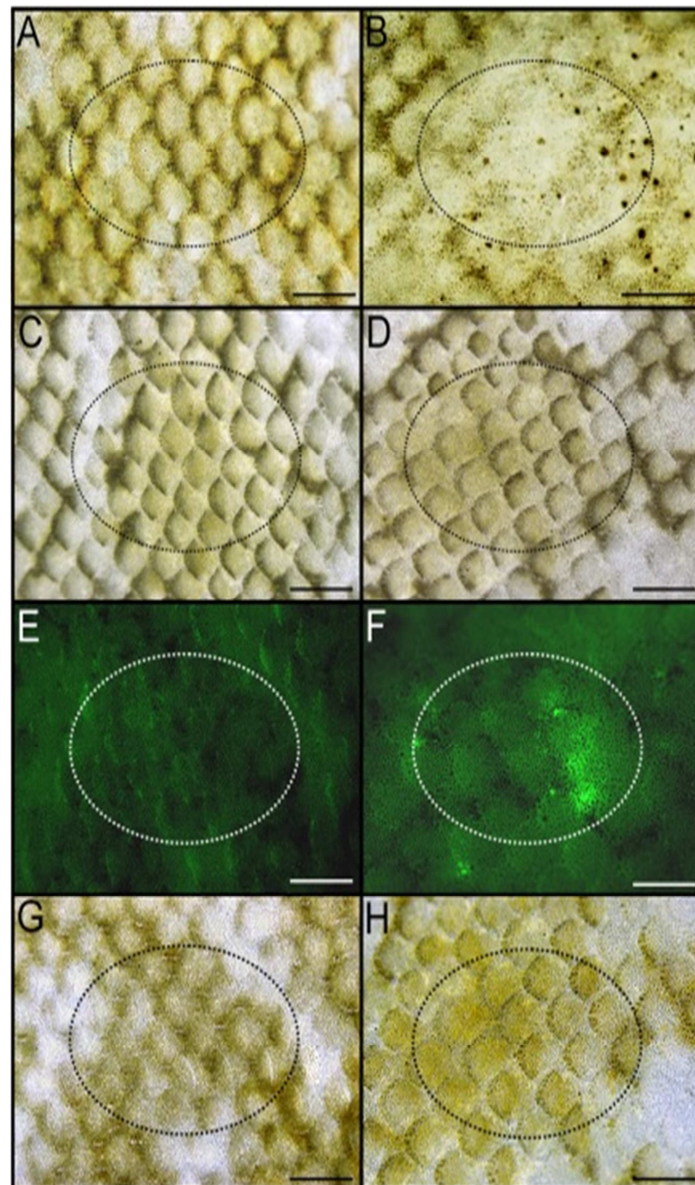
Figure 8. *Views of dorsal skin of sole injected and eletroporated in vivo to evaluate the effect of asip 1 overexpression on skin paling. Animals were injected with about 10 μg of capped sense (B) or antisense (D) mRNA per cm2 of dorsal skin and the effect was evaluated 4 days post injection/electroporation. Dorsal skin of control non-treated turbots are shown in A, C, E, and G. E and F show dorsal skin of control (E) and injected/electroporated animals with capped sense eGFP-mRNA (F) animals under fluorescent incident light. G and H display animals shown in E and F under brilliant incident light. See Figure 7 for more details. Dorsal views, anterior to the right. Scale bars: 0.2 cm.*
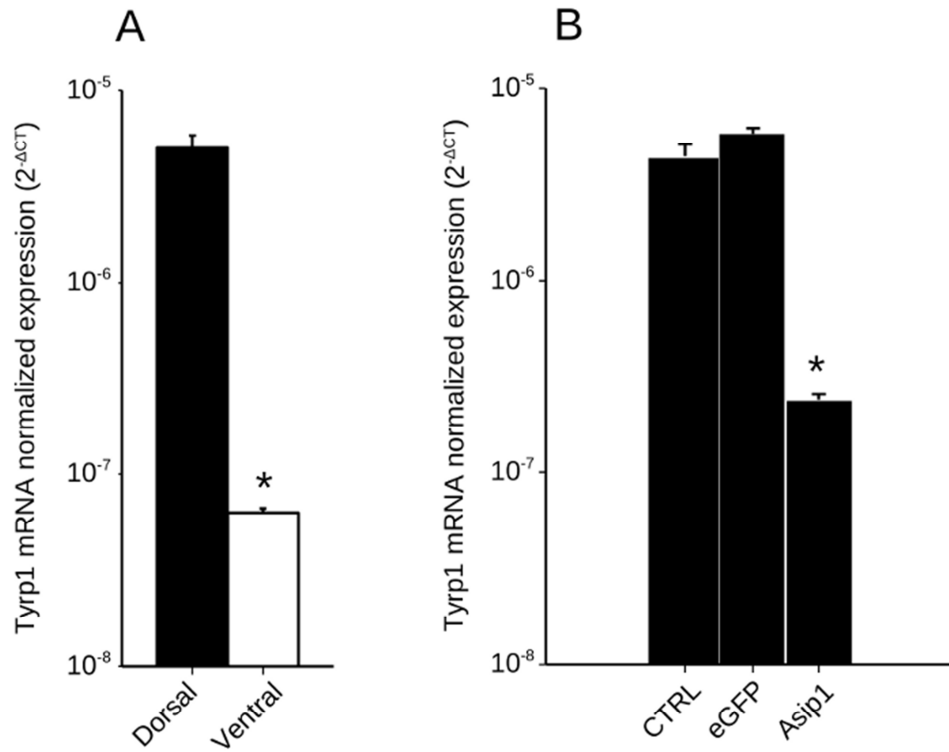
Figure. 9. *Normalized gene expression levels of tyrosinase-related protein 1 (Tyrp1) in turbot skin. (A) Analysis of differential dorsal-ventral Tyrp1 gene expression in turbot. (B) Effect of the in vivo injection of capped mRNA on Tyrp1 expression. Shown are log10 transformed ΔCt values of Tyrp1 relative to β-actin. Data are the mean ± SD from four samples after triplicate PCR analysis. Comparisons of numerical data were made by paired Student t-tests. Asterisk indicate significant differences (P<0.05) between dorsal and ventral Tyrp1 expression (A) and between control non-treated (CTRL) and eGFP capped mRNA injected skin Tyrp1 expression (B).*

3. Discussion

In this paper, we characterize *asip1* mRNA sequences for sole and turbot. *Asip1* is expressed in the main pigment tissues, i.e. eye and skin, but also in the central nervous system, including the pineal complex of turbot. Transitory overexpression of *asip1* mRNA in the melanic-dorsal side induces skin paling in both studied species and reduces the expression of key enzymes of the melanogenic pathway in turbot. Quantitative experiments demonstrated that *asip1* mRNA is overexpressed in non-pigmented regions of the dorsal skin in pseudoalbino turbot compared with melanic regions. The results demonstrate *asip1* participation in fish melanophore physiology and suggest its involvement in the organization of the dorsal-ventral pigment pattern.

Flatfish asip1 peptides keep the same structure exhibited by all agouti family of peptides. The putative asip precursors have the characteristics of a secreted protein, displaying a putative hydrophobic signal. Processing of the potential signal peptide produces 101 and 110-amino acid mature proteins in turbot and sole, respectively, including an N-terminal region, a basic central domain with a high proportion of lysine residues as well as a proline-rich region that immediately precedes the C-terminal poly-cysteine domain. Sole asip1 exhibited one potential N-glycosylation site within the N-terminal region asip but no consensus glycosylation sites were found in the turbot sequence. In mice, glycosylation of asip is an important factor for protein functionality as disruption partially reduces peptide activity in transgenic mice (*Perry et al., 1996*). Similar to mammalian species, the basic domain of the sole and turbot peptides exhibit 10 lysine (K) and 2 and 3 arginine (R) residues, respectively. The integrity of this basic domain is also key for the full activity of the asip protein (*Miltenberger et al., 1999 and 2002*). The N-terminal region of mouse agouti has been shown to down-regulate melanocortin receptor signaling in *Xenopus* melanophore (*Ollmann and Barsh, 1999*) and is also thought to mediate low affinity interactions with the product of the mahogany locus, i.e atracttin (*He et all., 2001*). Spacing of the 10 cysteines within the C-terminal poly-cysteine domain is totally conserved in asip1 orthologues and the flatfish sequences are not an exception. This cysteine pattern resembles that of the conotoxins and agatoxins, suggesting that agouti-like proteins adopt an inhibitory cysteine knot (ICK) fold (*Jackson et al., 2002*). Structural studies have demonstrated that five disulfide bridges between cysteine residues, C87-C102, C94-C108, C101-119, C105-129 and C110-C117 stabilize the human agrp molecule (*Bures et al., 1998, Bolin et al., 1999, McNulty et al., 2001, Jackson et al., 2002*). Interestingly, Asip2 proteins lack the 5th and 10th cysteine residues which form the last disulfide bridge of agouti-like

molecules. How these structural differences affect the dimensional conformation and receptor binding is unknown but we do know that the C-terminal loop in asip1 is required for MC1R binding (*Patel et al., 2010*).

Studies on the evolutionary history of the agouti family of peptides are controversial. Tetrapod species have two different melanocortin antagonists, i.e. *asip* and *agrp*, but teleost fish have four endogenous antagonists. *asip1*, *asip2*, *agrp1* and *agrp2*. Studies have suggested that *asip2* and *agrp2* are ohnologue genes of *asip1* and *agrp1*, respectively, which are generated during teleost-specific genome duplication (TSGD) (*Kurokawa et al., 2006*). Recent synteny data support the view that the *agrp2* chromosomal region does not share a synteny relationship with the fish *agrp1* or with the tetrapod *agrp*. The *agrp2* and *asip2* regions show conserved synteny with a region of human chromosome 8 that, in turns, shares paralogies with the *asip* region on chromosome 20. The model proposes that the *agrp/asip* precursor was duplicated twice during the two rounds of vertebrate genome duplication (R1, R2). *Agrp2* and *asip2* were missed in the tetrapod genome but *asip2* was retained in the teleost genome. After TSGD, the additional copy of *agrp* gene was missed again from the teleost genome but both copies of the *asip2* gene were retained. These copies are named *asip2* and *agrp2* (*Kurokawa et al., 2006*) but the new model proposes naming them *asip2a* and *asip2b*, respectively (*Brash and Postlethwait, 2011*). Schiöth and collaborators rebuilt the phylogeny by introducing a sequence from elephant shark (*Schiöth et al., 2011*). If *agrp* is used to root the tree, the results support Braasch and Postlehwait's hypothesis but if the tree is rooted by the ancient sequence, the *agrp2* and *asip2* clusters group with the *agrp* cluster, supporting the previous nomenclature (*Kurokawa et al., 2006*). Flatfish sequences were grouped with asip1 sequences, suggesting their orthology. The incorporation of flatfish asip1 sequences does not modify the phylogeny reported by Braasch and Postlehwait's (*Brash and Postlethwait, 2011*).

Structural and/or functional data could discern between both hypotheses. Human agrp is processed after the motif Arg^{79}-Glu^{80}-Pro^{81}-Arg^{82} to release the active peptide agrp 83-132 (*Creemers et al., 2006*). Both arginine (R) residues are fully conserved in all agrp sequences but not in asip1, asip2 and agrp2 sequences, which suggests that, unlike argp1 but similar to asip-like peptides, agrp2 peptides are not processed. The N-terminal region of asip peptides is rich in basic residues, particularly lysine (K). Similar to asip peptides, agrp2 peptides also exhibit a high number of basic residues before the cysteine domain. Asip1 sequences also present a proline domain immediately prior to the C-terminal cysteine domain. This domain is not present in

agrp1 peptides and is not clearly defined in agrp2 or asip2 peptides. Also noteworthy is the fact that all asip2 and agrp2 sequences exhibit 5 residues between the second and third cysteine residue of the C-terminal domain, whereas asip1 and agrp1 peptides exhibit 6 residues. Therefore, structural data seem to support Braasch and Postlehwait's hypothesis defending the asip2/agrp2 ohnology and, by extension, the new nomenclature, asip2a/asip2b, respectively. However, one intriguing item of structural evidence disproves this reflexion. The alignment of peptide sequences show that all agrp sequences exhibit a short tail after the last cysteine residue and agrp2 sequences are not an exception. This short tail does not seem to confer any binding property to the molecule since the last twelve amino acids of the human agrp peptide can be eliminated without affecting MC3R or MC4R binding (*Jackson et al., 2002*). Therefore, the function of this conserved short C-terminal extension in all agrp1 and agrp2 sequences remains unknown. It is known that agouti peptides can interact with other molecules other than melanocortin receptors (*He et all., 2001*) suggesting a still undiscovered intermolecular interaction mediated by segments outside the cysteine-rich domain.

From the functional point of view, in mammalian species, *agrp* is expressed mainly in the hypothalamus where it regulates the energy balance. *Asip* is produced by dermal papillae cells in which it governs the switch between production of eumelanin and pheomelanin (*Cerdá-Reverter et al., 2011*). In fish all three *agrp*, i.e. *agrp1*, *agrp2* and *asip1* are expressed in the brain and skin (*Cerdá-Reverter et al., 2011, Kurokawa et al., 2006, Cerdá-Reverter and Peter, 2003*). In the brain, *agrp1* is exclusively expressed within the lateral tuberal nucleus, the fish homologue of the arcuate nucleus (*Cerdá-Reverter and Peter, 2003*), whereas *agrp2* is only expressed in the pineal complex of zebrafish (*Zhang et al., 2010*). Our results demonstrate that, similar to *agrp2*, *asip1* is expressed in the turbot pineal complex. Coincident expression in the pineal complex can be expected if both genes derive from a common ancestral pineal-expressed gene, once again supporting a relationship between *argp2* and *asip* genes. As in other fish species, *asip1* was also expressed in the brain of flatfish. Specific *asip1*-expressing brain areas or projections, as well as the asip function in the brain, are unknown. We have previously shown that both MC4R (*Cerdá-Reverter et al., 2003b, Sánchez et al., 2009a*) and MC1R (*Sánchez et al., 2010*) are expressed in the fish brain. In addition, goldfish asip1 can bind both receptors (*Cerdá-Reverter et al., 2005*), as agrp1 does (*Sánchez et al., 2009a and 2010*) thus significantly increasing the complexity of the central melanocortin signaling in fish.

In our previous studies, we proposed that asip could be the uncharacterized MIF in fish. We suggested that the ventral expression of asip induces an inhibitory effect on melanophore differentiation and/or proliferation but stimulates iridophore differentiation and/or proliferation via MC1R antagonism. Accordingly, the absence of asip expression in the dorsal skin allows melanoblasts to differentiate and/or proliferate, leading to dark coloration in the dorsal region (*Cerdá-Reverter et al., 2005*). In both sole and turbot, the expression of *asip1* in ventral skin was higher than in melanic dorsal skin. These findings are not so striking as those reported in goldfish, in which *asip1* expression in the dorsal skin was essentially absent. A possible reason for this discrepancy in dorsal/ventral relative expression levels could be the pigmental structure of the ocular side of flatfish. This side is normally patterned with dark patches and spots, as well as white and colored spots with a high number of iridophores, of all which are morphological entities (reviewed in *Barton, 2009*). Therefore, it is possible that *asip1* expression might also contribute to the dorsal heterogeneous pigment pattern in flatfish. In contrast, dorsal skin in goldfish is un-patched and much more homogeneous in dark pigmentation. We are currently testing the possibility that *asip1* might contribute to the pigment patterning outside the dorsal and ventral regions by comparing *asip1* expression in the lateral white and dark stripes of zebrafish.

We further demonstrated that transient *asip1* overexpression, following the injection of homologous capped mRNA, can induce skin paling in the dorsal melanic side of flatfish, *in vivo*. This result supports our hypothesis defending the involvement of asip1 protein in the patterning of dorsal-ventral pigmentation in fish. Our experimental design cannot elucidate whether the observed paling in turbot and sole skin was induced by a transient melanosome reorganization, similar to that observed during short-term background adaption or physiological color change, by a decrease in melanin synthesis or by a reduction in melanophore number, similar to that observed after long-term background adaptation or morphological color changes (*Barton, 2009, Sugiomoto, 2002*). All three scenarios are possible and could concur concomitantly. Experiments using recombinant goldfish asip1 demonstrated that this protein can inhibit melanin dispersion stimulated by melanocyte-stimulating hormone (MSH) in the melanophores of medaka scales in a reversible way (*Cerdá-Reverter et al., 2005*). However, our results show that treatment-induced effects persist even after 4 days post-administration, suggesting the presence of morphological color changes. Asip 1 overexpression induced a significant reduction in the Tyrp1 expression to reach similar levels to those exhibited in the ventral skin. Tyrp1 promotes final steps of eumelanin synthesis supporting that asip1 overexpression inhibits melanogenesis and/or

melanophore differentiation. Accordingly, asip1 has been shown to inhibit MSH-induced *mitf* expression, melanogenic gene promoters including tyrosinase, Tyrp1 and Tyrp2, melanoblast differentiation into melanocytes and induce melanocyte de-differentiation in mammals (*Aberdam et al., 1998, Sviderskaya et al., 2001, Le Pape et al., 2009*).

Capped mRNA administration experiments suggest a role for *asip1* in the adult pigment pattern of flatfish. Similar to *Danio* species, flatfish melanophores can be divided into larval, early or embryonic and adult or metamorphic-type melanophores (*Matsumoto and Seikai, 1992*). During larval stages, pigment cell latent precursors are symmetrically located mainly along the dorsal and ventral margins of the flank and migrate continuously from these regions to the lateral sides. After late metamorphic stages, these precursors differentiate into adult-type chromatophore on the lateral asymmetrical sides. Pigment asymmetry in flatfish seems to depend upon an asymmetric organizational environment that may regulate survival, proliferation, distribution and differentiation of latent precursors into adult-type pigment cells since an asymmetric body plan, including eye migration, precedes adult pigment pattern formation (*Yamada et al., 2010, Watanabe et al., 2008*). Recent studies in zebrafish have demonstrated that proliferative pigment cell precursors are associated with the peripheral nerve and ganglia and migrate to the hypodermis during pigment pattern metamorphosis, when they differentiate into melano-phores or iridophores (*Budi et al., 2011*). These precursors seem to be bipotential and thus capable of differentiating into melanophores or iridophores, depending on the interplay between forkhead transcription factor, *foxd3*, and microphthalmia subtype a, *mitfa*. Nacre zebrafish, a mutant for *mitfa*, exhibit an increased number of ectopic iridophores (*Lister et al., 1999*), while the loss of *foxd3*, a *mitfa* repressor, resulted in fewer iridophores (*Curran et al., 2009 and 2010*). We hypothesized that, after migration, these bipotent precursors reach different developmental environments patterned by *asip1* expression, which finally governs the differentiation into melanophores or iridophores. There is no information about whether asip1 affects *foxd3* activity but we anticipate that asip1 could stimulate the expression of this *mitf* repressor. This model would not be only true for the tandem melanophore/iridophore since xantic goldfish lack dermic melanophore but display striking differences in the dorsal-ventral expression of *asip1* mRNA (*Cerdá-Reverter et al., 2005*). Therefore, a more plausible scenario is that asip1 could induce iridophore differentiation from bipotential melanophore/iridophore precursors which subsequently inhibit the differentiation of any type of chromatophore.

Pigment anomalies are common in reared flatfish including albinism of the ocular side and hypermelanism of the blind side. We demonstrated that asip expression in the albino regions of the ocular side in pseudoalbino turbots is similar to that observed in the ventral region but significantly higher than that seen in the dark areas of the ocular side. This suggests that ectopic expression of asip 1 could be involved in flatfish pseudoalbinism. It has been reported that albino flatfish, including turbot, are able to feed more efficiently and grow faster than controls (reviewed in *Bolker and Hill, 2000*). This phenotype is recurrent to that observed in agouti mice carrying the unusual allele A^y. The associated phenotype is characterized by yellow fur and the ubiquitous expression of agouti gene, resulting in hyperphagia, hyperinsulinemia, increased linear growth, increased propensity for developing tumors, premature infertility and maturity-onset obesity (*Michaud et al., 1993, Miller et al., 1993*). This metabolic syndrome is mediated by antagonizing α-MSH signaling at central MC4R that arbitrates the negative effects of melanocortin peptides on the energy balance (*Lu et al., 1994*). We have previously demonstrated that central melanocortin system is involved in the regulation of the energy balance in fish via MC4R (*Cerdá-Reverter and Peter, 2003, Cerdá-Reverter et al., 2003a and 2003b*) and that asip1 can antagonize MSH effects on the latter receptors (*Cerdá-Reverter et al., 2005*). However, we cannot discriminate whether the increased expression levels of asip in the anomalous dorsal pigmental regions are the consequence of the expression of a normal developmental pathway in an incorrect position as result of a patterning error. It means, albino areas expressing higher asip1 mRNA levels within the melanic ocular side are indeed a portion of wrong-patterned ventral skin in dorsal position or, in other words, dorsal skin following the ventral skin developmental pathway. Asip1 expression levels in ventral skin and albino areas of the dorsal skin of turbot were similar. In addition, preliminary experiments further demonstrated that injection of cappep Asip1 mRNA into the hypermelanic regions of the ventral skin of sole inhibited melanogenesis (unpublished data; Guillot R, Ceinos, R, Rotllant, J and Cerdá-Reverter, JM).

In summary, we have characterized asip1 mRNAs in both turbot and sole and used deduced peptide alignments to study the evolutionary history of the agouti-family of peptides. Structural and functional data suggest that agrp2 is more closely related to asip than agrp1 sequences. Data suggest that fish asip is involved in the dorsal-ventral pigment patterning in adult fish, where it induces the regulatory asymmetry involved in precursor differentiation into mature chromatophores. Adult dorsal pseudoalbinism seems to be the consequence of the expression of normal developmental pathways in

an erroneous position, resulting in unbalanced asip production levels. These, in turn, generate a ventral-like differentiation environment in dorsal regions.

4. Materials and Medthods

Experimental animals

Turbot (*Scophtalmus maximus*) and sole *(Solea senegalensis)* larvae reared under standard commercial conditions were provided by the Instituto Español de Oceanografia (IEO), Vigo, Spain. Control and pseudoalbino adult fish were also obtained from stocks of the IEO. Animals were anesthetized in 0.02% tricaine methasulfonate (MS-222) before any manipulation and sacrificed by rapid decapitation when required. All experiments were carried out in accordance with the principles published in the European animal directive (86/609/EEC) for the protection of experimental animals and approved by the Consejo Superior de Investigaciones Científicas (CSIC) ethics committee (project numbers AGL2010-22247-C03-01 to JMC-R and ALG2011-23581 to JR). Unless otherwise indicated, all reagents were purchased from Sigma (St Louis MO, USA).

Molecular cloning of flatfish asip1 gene

Total RNA from ventral skin of sole and turbot was extracted with Tri-reargent and treated with RQ1-DNAse I (Promega). Subsequently, mRNA was isolated with polyATrack mRNA isolation system III (Promega) following the manufacturer's manual. Synthesis of cDNA was primed with random hexameres (Invitrogen) and was used as template for PCR reactions with degenerate primers. These primers were designed based on *asip1* sequences from different species. The primers used to amplify sole *asip1* were Multi_Agouti_Fw 5' CCKCCTCCBSCBAACTGY 3' and Multi_Agouti_Rv 5' CCCATKCGRCARTARCASAC 3'. These primers did not work with turbot cDNA and new primers called Flatfish_Agouti were designed based on cloned fish *asip1* sequences. The latter primers had the sequence: Flatfish_Agouti_Fw 5' CTCCTGCYAACTGCMYTYCCTT 3' and Flatfish_Agouti_Rv: 5' GGGTTGCCC-ATTCGR-CAGWAACA 3'. Fragments of 135 bp and 159 bp for sole and turbot asip, respectively, were cloned into pGEM-T easy vector (Promega), sequenced and found to show a high similarity with fish *asip1* sequences. To resolve 5' and 3' ends of sole and turbot cDNAs, 5' and 3' rapid amplification of cDNA ends (RACE) were performed

using the Smart-RACE PCR cDNA amplification system (Clontech) following the manufacturer's manual and specific primers designed according to the previously obtained sequences. Purified fragments were treated as above. To corroborate that 5' and 3' ends correspond to the same transcript, full *asip1* sequences were amplified using specific primers targeting the cDNA extremes. Full cDNAs were cloned and sequenced as before. The nucleotide sequences of turbot and sole asip1 have been deposited with EMBL Nucleotide Sequence Database under accession numbers HE598752 and HE598753, respectively.

Tissue and larvae RNA isolation and RT-PCR

Total RNA was purified as before. Superscript II reverse transcriptase (Invitrogen) was used for cDNA synthesis by priming total RNA from brain, hypophysis, pineal, eye, gill, spleen, anterior and posterior kidney, heart, liver, muscle, dorsal skin, ventral skin, intestine, gonads and fat with random hexameres (Invitrogen). PCR amplification was carried out with the primers specific primers amplifying the full coding region. As internal control of the reverse transcription step, PCR for β-actin (turbot) or 18S (sole) cDNA amplification was carried out. The following primer sequences were used; for sole, 18S forward primer had the sequence 5'-GAATTGACGG-AAGGGCACCACCCAG-3' and 18S-reverse primer had the sequence 5'-ACTAAGAA-CGGCCATGCACCACCAC-3'. Turbot β-actin primers were β-actin-forward 5'-TGAA-CCCCAAAGCCAACAGG-3' and β-actin-reverse 5'-CAGAGGCATACAGGG-ACAGCAC-3'. Similarly, RNA from embryos collected at 2, 3 and 6 hours post fertilization (hpf) and 4, 7, 11, 14, 16, 21, 24, 28, 29, 32, 36, 39 and 45 days post hatching (dph) for turbot and 2, 3, 5, 8, 10, 19, 24 and 29 dph for sole were extracted and cDNA was primed as before.

Skin RNA isolation and absolute-quantitative real time PCR (qRT-PCR)

Dorsal and ventral skin samples from control and pseudoalbino turbot and sole were collected and total RNA was extracted as before. cDNA was synthesized from total RNA using superscript III (Invitrogen) according to manufacturer's recommendations.

Absolute quantification was used as a method to analyse the skin spatially specific expression of asip 1 genes. Sole and turbot asip1 cDNAs cloned into pGEM-T easy were used as standards. 10-fold serial dilutions of asip1 into pGEM-T, ranging

from 1×10^5 to 1×10^{10} copies/µL, were used to construct standard curves for both asip1 genes. The concentration of the dsDNA standards was measured using a fluorometer and the corresponding copy number was calculated following the Whelan method (*Whelan et al., 2003*). Real time PCR quantification (qRT-PCR) was performed in 96-well optical plates in triplicate on an Applied Biosystems 7500 analyzer with Maxima SYBR Green qPCR master mix (Fermentas, Life Science). The total reaction volume was 25 µl with 12.5 µL of SYBR green, 0.5 µL of each primer, 9.5 µL of nuclease free water and 1 µL of cDNA template. After denaturation at 95 °C for 10 min, 40 cycles of amplification were carried out with denaturation at 95°C for 15 s, annealing and elongation at 60°C for 1 min, followed by the melting curve analysis. The following primer sequences were used for qRT-PCR: for turbot *asip1* (5'primer/3'primer) 5' CTGCGAACTGCATTCCCTTGT 3' and 5' TCAGCAGCGAGGGTTGCC 3', for sole *asip1* (5'primer/ 3'primer) 5' GCACTCCCTTGTGGGGAAG 3' and 5' TCAGC-AGTGTGGGTTGCC 3'. A standard curve was drawn by plotting the natural logarithms of the threshold cycle (C_T) against the number of molecules, respectively. C_T was calculated under default settings for the real-time sequence detection software (Applied Biosystems). The equation drawn from the graph was used to calculate the precise number of specific *Asip1* cDNA molecules present per microgram of total primed cDNA, tested in the same reaction plate as the standard.

Turbot Tyrp1 gene expression was quantified by relative qRT-PCR. The level of β-actin mRNA was used as an internal reference for sample normalization. Two pairs of primers were used for amplification: Tyrp1 forward (5′ CCAGG-TTCAGCAATGTATCC 3′) and Tyrp1 reverse (5′ GCCATT-CGGCTTCATAAGAG 3′). Data were analyzed using the comparative cycle threshold method (CT method). Characteristics of the real time PCR (qRT-PCR) system was the same as used above.

Capped mRNA synthesis, injection and electroporation

To generate capped mRNA, DNA fragments containing the Kozak sequence followed by entire ORF of turbot and sole *asip1* were generated by PCR. These DNA fragments were subcloned into the pCS2+ vector to generate the *asip1* overexpression plasmid DNAs (pCS2+*asip1*-Turbot and pCS2+*asip1*-Sole). The purified plasmids were dissolved in DNase free water and stored at –20°C until use. The pCS2+*asip1* plasmids were linearized by restriction with NotI and used for capped sense or antisense *asip1* mRNA synthesis using mMessage Machine kit (Ambion). Five and seven month-old turbot and sole, respectively were anesthetized and asip1 capped

mRNA was injected into the dorsal skin area using a 1ml Omnifix®-F syringes. Approximately 10 µg of capped-mRNA was injected per cm^2 of dorsal skin. Immediately following injection, both dorsal and ventral halves were electroporated using a ECM 830 BTX electroporator (Harvard apparatus, Inc.). Electric pulses were applied by a pair of electrode disks (7 mm diameter) rigged on the tips of tweezers (pinsettes-Type electrode 524, BTX instrument). The following parameters were used: 5-msec pulses of 10V with a 200 msec pause between pulses. Fish were then rapidly returned to their tanks for skin coloration analysis at 4 days post-electroporation (dpe). The mRNA for green fluorescent protein (eGFP), which was synthesized from pCS2+-eGFP, was injected-electroporated into the skin as control.

At 4 dpe, fluorescein uptake was monitored. Five fish were tested in all experiments.

Data analysis and statistics

Specimens were observed and photographed under a Leica M165FC fluorescence stereoscope (Leica Microsystems, Germany) equipped Leica DFC 500 digital camera. Adobe Photoshop™ software was used to adjust contrast levels in all images.

Flatfish sequences were compiled with Generunner free software and compared with known *asip1* and agouti-related protein (*agrp*) sequences from the National Center for Biotechnology Information (NCBI) and ENSEMBL databases. Sequence alignments were performed using public domain ClustalX 2.1 and edited with GeneDoc software. Phylogenetic tree was derived using CulstalX and SeaView that uses the Neighbor-Joining method on a matrix of distances and maximum likelihood, respectively. The cleavage site for removal of the hydrophobic signal peptide was predicted using SignalP 3.0 (http://www.cbs.dtu.dk/services/SignalP/). Differences in gene expression were assayed by Student t-test and statistical significance was considered at $p<0.05$. Results are given as mean ± SEM.

5. Acknowledgements

CAPÍTULO II

En este capítulo se llega a la conclusión de que el patrón de coloración observable en los peces cebra adultos es el resultado de dos patrones conjugados que tienen procesos de regulación diferentes. Un patrón dorsoventral basal, ancestral, que es común a todos los grupos de vertebrados, sobre el que se superpone un patrón bandeado característico de la especie, evolutivamente más reciente.

El establecimiento de una línea transgénica de peces cebra que sobrexpresan el gen ASIP de pez dorado permite estudiar los efectos que tiene la sobrexpresión ubicua de esta proteína en el patrón de pigmentación.

Los peces pertenecientes a esta línea transgénica apenas presentan alteraciones en el patrón bandeado. En cambio, el patrón dorsoventral está fuertemente alterado. En la parte dorsal una el número de melanocitos sufre una drástica reducción. Esa alteración se interpreta como un proceso de ventralización de la región dorsal inducido por la expresión ectópica de ASIP.

Pigment patterns in adult fish result from superimposition of two largely independent pigmentation mechanisms

Rosa M Ceinos[1], Raúl Guillot[2], Robert N. Kelsh[3],
José Miguel Cerdá-Reverter[2], Josep Rotllant[1]

1. Aquatic Molecular Pathobiology Group, Instituto de Investigaciones Marinas (IIM), Consejo Superior de Investigaciones Científicas (CSIC),Vigo, Spain.
2. Control of Food Intake Group, Department of Fish Physiology and Biotechnology, Instituto de Acuicultura de Torre de la Sal (IATS), Consejo Superior de Investigaciones Científicas (CSIC), Castellón, Spain.
3. Centre of Regenerative Medicine and Developmental Biology Programme, Department of Biology and Biochemistry, University of Bath, Bath, England

Sumary

Dorso-ventral pigment pattern differences are the most widespread pigmentary adaptations in vertebrates. In mammals, this pattern is controlled by regulating melanin chemistry in melanocytes using a protein (ASIP). In fish, studies of pigment patterning have focused on stripe formation, identifying a core striping mechanism dependent upon interactions between different pigment cell types. In contrast, mechanisms driving the dorso-ventral countershading pattern have been overlooked. Here, we demonstrate that, in fact, zebrafish utilize two distinct adult pigment patterning mechanisms - an ancient dorso-ventral patterning mechanism, and a more recent striping mechanism based on cell-cell interactions; remarkably, the dorso-ventral patterning mechanism also utilizes ASIP. These two mechanisms function largely independently, with resultant patterns superimposed to give the full pattern.

1. Introduction

Pigment patterns allow animals to distinguish among individuals, groups and species and are an essential characteristic for the survival of most animals in wild populations. These patterns allow appropriate adaptation to the environment, often having crucial roles as components of courtship behaviors, or making hunting easier, or providing camouflage against potential predators. A prime example of an evolutionarily conserved pigment pattern is dorso-ventral countershading - a dark dorsal region contrasting with a pale ventrum - a pattern that is easily recognizable in most vertebrate taxa. These patterns are dependent upon pigment cells, or chromatophores, that synthesize or accumulate pigments or crystalline compounds (*Kelsh, 2004*). All vertebrate integumentary chromatophores arise from neural crest cells (NCCs), multipotent embryonic cells that also give rise to other cell types, such as neurons and glia of the peripheral nervous system and elements of the craniofacial skeleton (*Le Douarin and Kalcheim, 1999; Moury and Jacobson, 1989*). Mammalian species have only one type of chromatophore, the melanocyte, which synthesizes eumelanin (black/brown pigment) or pheomelanin (yellow/red pigment) under the control of two main loci, *extension* and *agouti*. The *extension* locus encodes the receptor for α-Melanocyte Stimulating Hormone (α-MSH), melanocortin 1 receptor (MC1R), which promotes eumelanin synthesis when stimulated (*Robbins et al., 1993*). The agouti protein, termed agouti-signalling protein (ASIP) in species other than mouse, is encoded by the *Agouti* locus and antagonizes MSH effects at MC1R, resulting in

58

inhibition of eumelanin synthesis coupled to a switch to pheomelanin synthesis (*Bultman et al., 1992; Michaud et al., 1993; Miller et al., 1993*).

In mammals, dorso-ventral countershading is driven by regulation of agouti expression and consequent modification of the melanin type in differentiated melanocytes. The differential usage of alternative promoters regulates the spatial and temporal expression of the *ASIP* gene that, in turn, controls positional and temporal synthesis of eumelanin versus pheomelanin. The sustained expression of ASIP protein in the ventral region is responsible for the dorso-ventral pigment pattern in which the ventrum is light (pheomelanin) while the dorsum is more darkly colored (eumelanin) (*Millar et al., 1995; Vrieling et al., 1994*). Similarly, a temporal pulse of *agouti* expression during a window of the hair growth cycle results in the classical black-yellow-black banded ('agouti') pattern in the dorsal fur of many mammalian species (*Vrieling et al., 1994*). Studies in rodents indicate that the local production of agouti protein also appears to contribute to changes in pigment pattern evolution through developmental modifications (*Manceau et al., 2011*).

In poikilotherms, including fish, dorso-ventral countershading is achieved by means of a mechanism distinct from the differential differentiation of melanocytes in mammals. In fish, the mechanism involves a patterned distribution of different types of pigment cells or chromatophores, with the light-absorbing (melanocytes, often known as melanophores) and light-reflecting (iridophores) chromatophores mostly distributed in the dorsal and ventral areas, respectively (*Bagnara and Matsumoto, 2006*). Experimental data in amphibian and fish species support the hypothesis that the dorso-ventral pigment pattern results from interaction between two factors, melanization inhibition factor (MIF) and α-MSH. Although so far MIF has never been purified, it has been suggested thar MIF is a factor present in tissue extracts from the ventral skin thar reduces the melanocyte number and increase the number of iridophores in the ventrum (*Bagnara and Fukuzawa, 1990; Fukuzawa and Ide, 1988; Zuasti, 2002*). Amphibian MIF blocks the stimulation of melanization provoked by α-MSH in neural explants of Xenopus (*Fukuzawa and Bagnara, 1989*). Similarly, amphibian MIF has been shown to block α-MSH-induced tyrosine hydroxylase and dopa oxidase activity, both key enzymes in the melanogenic pathway, in malignant mouse melanocytes (*López-Contreras et al., 1996*). Our previous studies have lead us to propose that Asip1 corresponds to the uncharacterized non-mammalian MIF (*Cerdá-Reverter et al., 2005; Darias et al., 2013; Guillot et al., 2012*). Thus, *asip1* is predominantly expressed in the ventral skin with residual levels in the dorsal skin (*Cerdá-Reverter et al., 2005; Guillot et al., 2012*). Secondly, the injection of capped *asip1* mRNA induces lightening of

dorsal skin in flatfish whereas white skin patches in the dorsal area of pseudoalbino flatfish overexpress *asip1* mRNA. Thirdly, *asip1* mRNA injection results in lowered expression of transcripts for tyrosinase-related protein-1 (*tyrp1*), a key enzyme of melanin synthesis, and *tyrp1* gene expression is downregulated also in dorsal white patches (*Guillot et al., 2012*). Finally, goldfish Asip1 is able to block the α-MSH-induced melanosome movement in the medaka scales via MC1R (*Cerdá-Reverter et al., 2005*). If our proposal that MIF is in fact Asip1 is true, this suggests the exciting hypothesis that ASIP has a conserved function, but that it acts through a different cellular mechanism in mammals and in fish.

Zebrafish is widely used as a model organism for developmental studies and there are now a number of studies reporting gene regulatory networks underlying the development of pigment cells, both in the embryo (*Greenhill et al., 2011*) and in the adult (*Kelsh et al., 2009; Parichy et al., 2009*). Adult pigment patterns derive from adult pigment stem cells, including melanocyte stem cells (MSCs), set aside from the neural crest in the embryo but differentiating during metamorphosis (*Budi et al., 2011; Dooley et al., 2013*). In adult zebrafish, most of these studies have focused on determining the mechanism underlying the intrinsically interesting, but evolutionarily labile, formation of stripes (*Quigley and Parichy, 2002*). These studies have identified a core striping mechanism dependent upon interactions between different pigment cell-types (*Frohnhöfer et al., 2013; Inaba et al., 2012; Krauss et al., 2013; Maderspacher and Nüsslein-Volhard, 2003; Patterson and Parichy, 2013; Yamaguchi et al., 2007*). These studies overlook the fact that zebrafish also display a dorso-ventral countershading pattern, conserved across the vertebrates. We hypothesized that zebrafish utilizes two distinct adult pigment patterning mechanisms: an ancient dorso-ventral patterning mechanism, and a more recent striping mechanism based on cell-cell interactions; these mechanisms function largely independently and the resultant patterns are then superimposed to give the full pattern. We hypothesized that the dorso-ventral pattern might result from a dorso-ventrally graded expression of *asip1* that regulates the balance of the different types of pigment cells derived from adult pigment stem cells. To test this hypothesis, we first show that *asip1* expression in wild-type (WT) zebrafish shows a dorso-ventral gradient, high ventrally; we show too that this gradient is established at a time coincident with the onset of metamorphosis and that expression in adults is predominantly restricted to iriodophores. Then, we assess the effects of disruption of this gradient, by generating transgenic lines overexpressing *asip1* under the control of a constitutive promoter. These fish exhibit lightening of the dorsal skin; melanocyte counts and quantitation of molecular markers show that this results from

inhibition of melanocyte differentiation, but also from a partial reduction of melanocyte numbers. Concomitantly, extensive iridophores becomes visible in the dorsal area of *asip1* transgenic zebrafish that together with the lack of dorsal melanophores gives a ventralised appearance to the dorsal region. In contrast, we see only relatively modest effects on the core striped pattern, with most stripes still visible. We conclude that adult zebrafish utilize two superimposed pigment patterning mechanisms to generate their characteristic pattern.

2. Results

Temporal and spatial characterization of asip1 expression

To investigate the role of *asip1* in zebrafish pigment pattern formation, we first examined the temporal and tissue distribution of *asip1* expression by RT-PCR (see Figure S1). *Asip1* was detected at all stages examined (Figure S1A). In adult fish, *asip1* mRNA was widespread: we found expression primarily in the eye, dorsal and ventral skin, heart, fat and muscle and was present at lower levels in the intestine, liver, brain, gill and kidney, and at extremely low levels in the gonads (Figure S1B). Because RT-PCR has inherent limitations, particularly those that result in biases in the template-to-product ratios of target sequences, we used quantitative real-time PCR (qRT-PCR) to characterize further the transcriptional regulation of *asip1* during zebrafish development (Figure 1A). qRT-PCR showed that a high level of *asip1* mRNA was associated with larval to adult metamorphosis (2–4 weeks post-fertilization; *Johnson et al., 1995*) (Figure 1A), the time when the larval pigment pattern established during the first few days of development is gradually replaced by the adult pigment pattern.
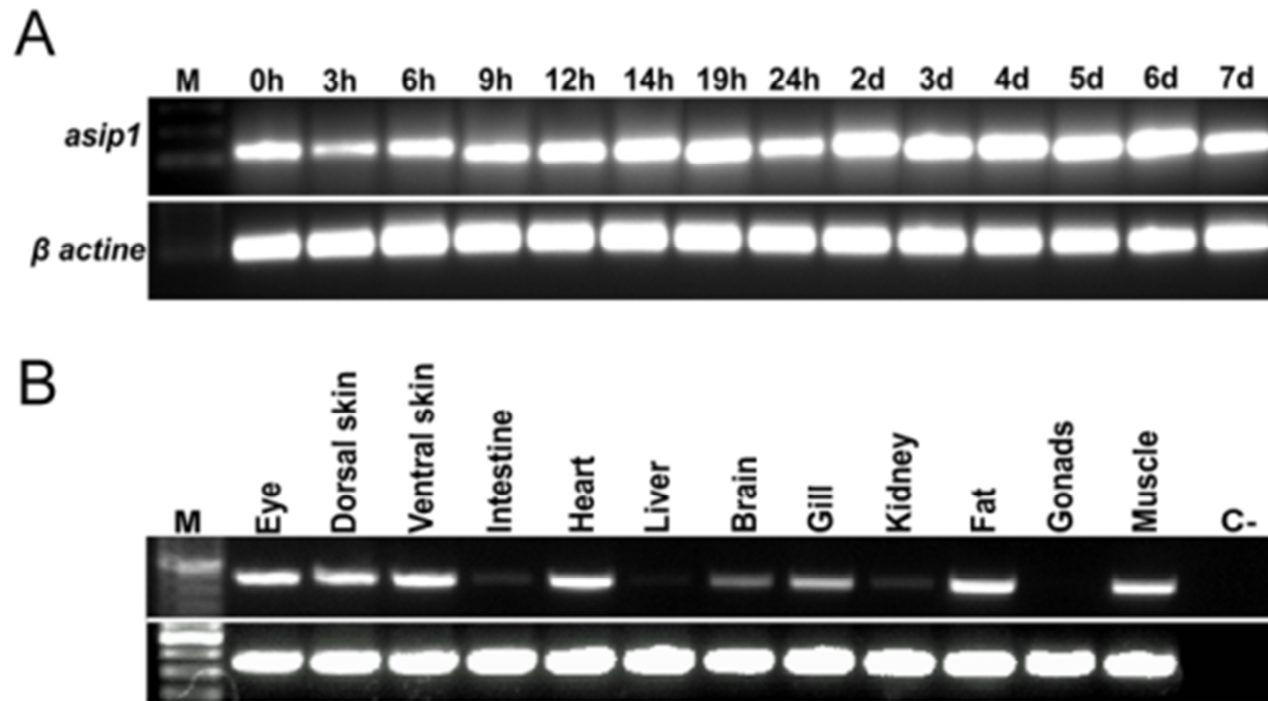
Supplementary Figure. 1. *Temporal and spatial expression of asip1 gene in zebrafish. (A) RT-PCR analyses of asip1 gene during early development. Hours post-fertilization, hpf; days post-fertilization, dpf. (B) RT-PCR analysis of the tissue specific expression pattern of asip1 in adults.*
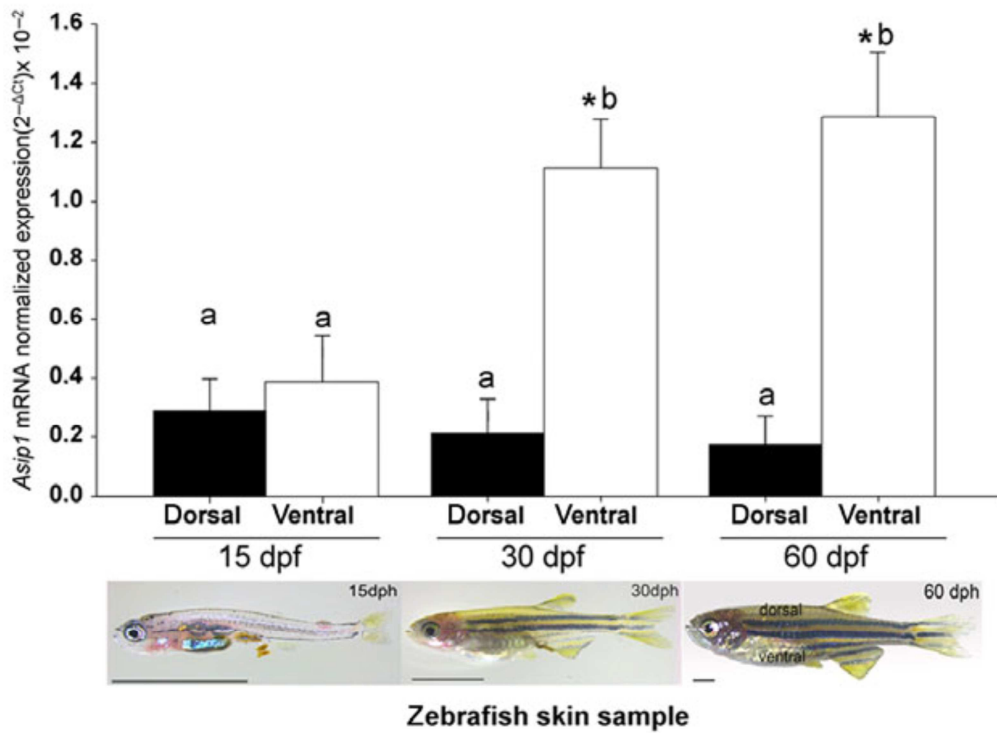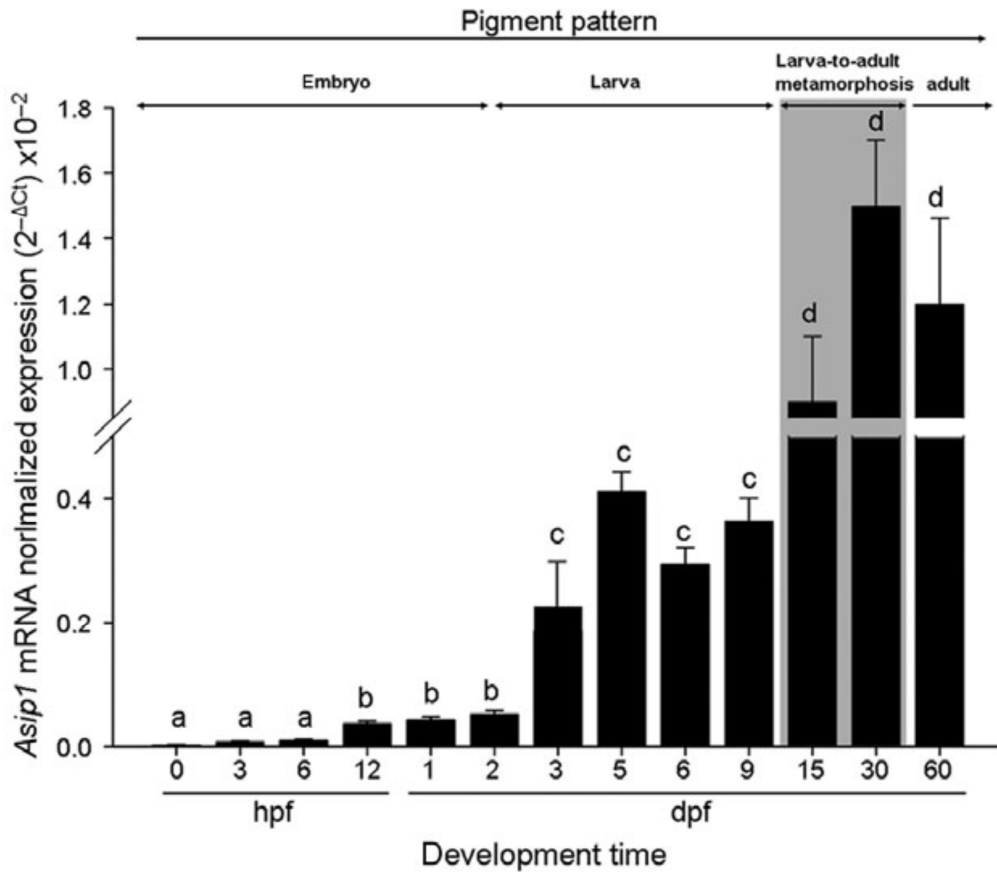
Figure 1. (previous page) The asip1 gene is dynamically expressed during zebrafish development. (A) Normalized gene expression levels of zebrafish asip1 throughout embryonic, larval and adult zebrafish development. (B) Analysis of differential dorsal–ventral asip1 gene expression in 15, 30 and 60 dpf wild-type (WT) zebrafish. Asip1 starts to be differentially expressed in ventral non-pigmented skin or dorsal pigmented skin at 30 dpf WT zebrafish. The relative expression of total asip1 mRNA was determined by real-time qRT-PCR. Shown are log 10-transformed ΔCt values of asip1 relative to Ef-1 alpha. Data are the mean ± SEM from eight samples after triplicate qRT-PCR analysis. Data are the mean ± SEM from eight samples after triplicate qRT-PCR analysis. Superscripts a, b and c indicate statistical differences (P < 0.05) in gene expression levels among developmental stages (A, B). Superscripts * indicate statistical differences (P < 0.05) in gene expression among skin region (B) at the same developmental stage (statistics data are similar if share at least one letter).

We then used whole-mount mRNA *in situ* hybridization to examine where *asip1* mRNA was expressed at different stages. In the embryo, we saw no detectable expression at 30 h post-fertilization (hpf), and expression was first detectable by this method in 3-day postfertilization (dpf) embryos, when the developing opercle was the initial site of expression (Figure 2A–C). At 6 dpf, *asip1* transcripts were still present in the opercle, but not seen elsewhere. In contrast, in adult (210 dpf) zebrafish, *asip1* messenger RNA was detectable in the dermal iridophores located in the most ventral interstripe (interstripe X1V) (Figure 2G) and stripe (stripe 2V) (Figure 2H) but not in the dermal iridophores located in the most dorsal stripes and interstripes (data not shown). Additonally, *asip1* transcripts were also expressed in the intraperitoneal membrane region where a reflecting iridophore layer was located (Figure 2F), but otherwise were not seen in tissues other than the skin.
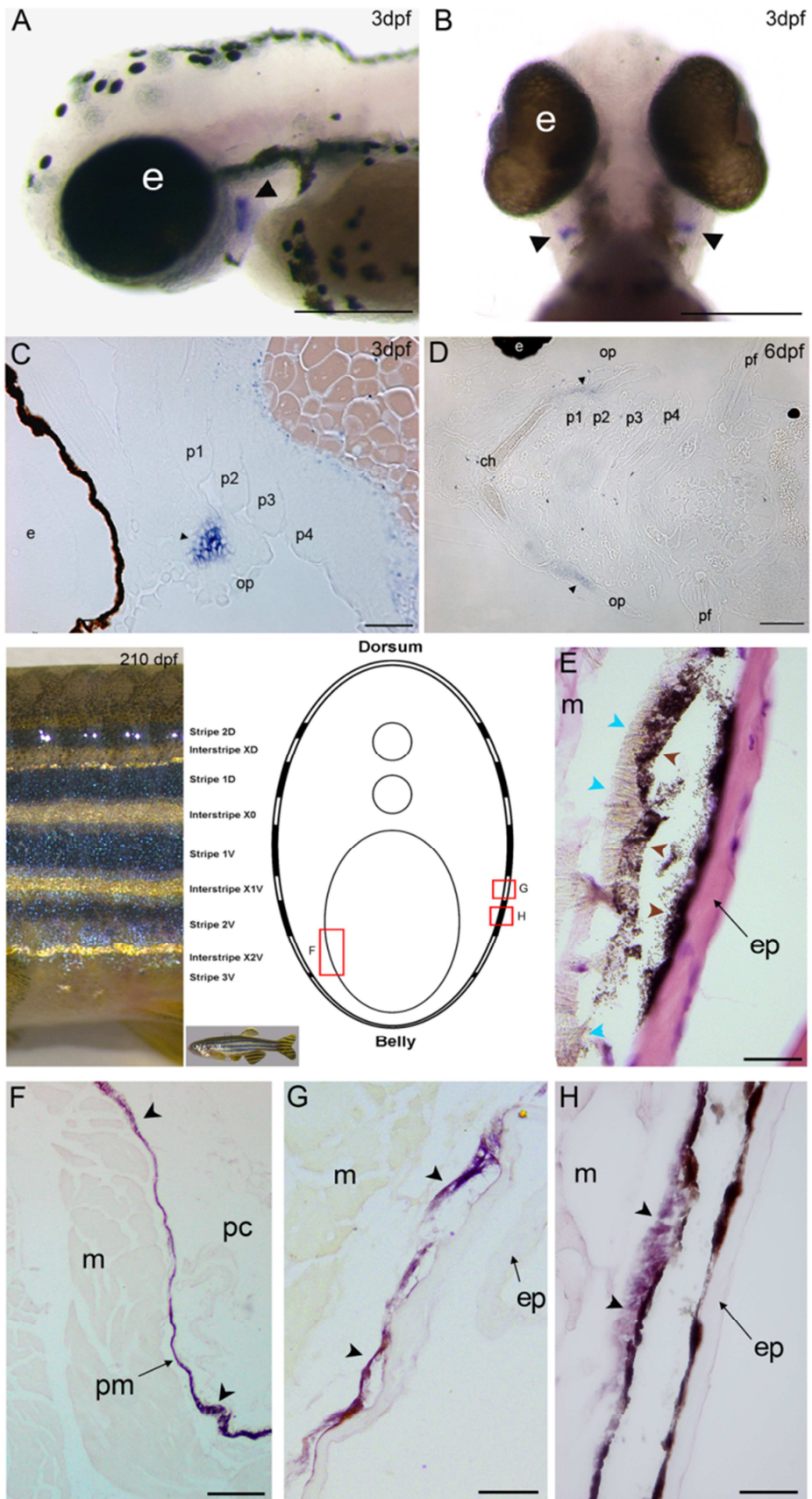
Figure 2. (previous page) Spatial expression of asip1 transcripts in larvae and adult zebrafish. (A) Lateral and (B) ventral view of whole-mount in situ hybridization of asip1 expression of 3 dpf wild-type zebrafish larvae. Staining with the asip1 antisense probe shows expression in bilaterally symmetric regions posterior to the eye (arrow heads). (C–D) Ventral longitudinal sections (4 µm thick) of epon-embedded, whole-mount asip1 in situ hybridizations in 3 dpf (C) and 6 dpf (D) zebrafish identify asip1 expression as being in the developing opercle. Anterior to the left. (E–H) Rostro-caudal transverse sections (10 µm thick) of paraffinembedded, in situ hybridization of asip1 expression in 210 dpf (360 mm total body length) zebrafish. The section in E has been stained with hematoxilyn–eosin and shows the typical location of dermal melanophores (brown arrows) and iridophores (blue arrows) in the zebrafish dermis. G and H are sequential sections of the fish shown in E. Asip1 transcripts are expressed in the dermal iridophores located in the most ventral interstripe (interstripe X1V) (G) and stripe (stripe 2V) (H). The section in (F) shows the expression of asip1 transcripts in the intraperitoneal membrane region where a reflecting iridophore layer is located. Abbreviations: ch, ceratohyal; e, eye; ep, epidermis; m, muscle; op, opercle; p, pharyngeal arches; pc, peritoneal cavity; pm, peritoneal membrane; pf, pectoral fin; scale bars: (A, B) 0,25 mm; (C) 25 µm; (D) 50 µm; (E, H) 20 µm; (F) 80 µm; (G) 60 µm.

Dorso-ventral gradient of agouti expression

Our detection of *asip1* expression in the skin of adult fish (Figures 2 and S1B) was consistent with *asip1* having a possible role in adult pigment pattern formation, and the whole-mount *in situ* hybridization studies indicated that expression might vary spatially. To test this quantitatively, we investigated whether and when there were dorso-ventral differences in expression levels by qRT-PCR. We measured *asip1* transcript levels in skin from dorsal and belly regions of 15, 30 and 60 dpf zebrafish (Figure 1B). Dorso-ventral differences in *asip1* expression levels were found at 30 and 60 dpf, but were not significantly different at 15 dpf. The highest *asip1* transcript levels were found in the belly (Figure 1B). To precisely characterize the dorsal–ventral differences in *asip1* expression levels, we determined *asip1* transcript levels in adult skin from different dorso-ventral positions, specifically, dorsal, all body stripes (2D, 1D, 1V and 2V) and belly skin regions (Figure 3A,I). Figure 3K shows the expression levels of *asip1* in skin samples obtained along the dorso-ventral axis in wild-type adult zebrafish. The highest levels of expression of *asip1* were found in the belly (P < 0.001); however, *asip1* transcripts showed a gradual decrease from the belly to the dorsal

midline of the fish. This striking observation leads us to hypothesize that *asip1* activity might contribute to dorso-ventral differences in zebrafish pigment pattern formation.

Conversely, although *asip1* mRNA expression was also detected in WT zebrafish fins, no dorso-ventral gradient expression was detected in all these tissues (see Figure S2).

Overexpression of *asip1* modifies the zebrafish pigment pattern

To investigate whether dorso-ventral *asip1* expression levels regulate pigment pattern, we studied whether changes in the concentration and distribution of *asip1* expression were accompanied by phenotypic changes in the pigment pattern. Specifically, we predicted that overexpression of *asip1* in dorsal regions of the skin would result in a ventralization (i.e. a lightening due to an increased ratio of iridophores to melanocytes) of the pigment pattern. We generated three independent transgenic zebrafish lines [*Tg(Xla.Eef1a1:Cau. Asip1)iim03*, *Tg (Xla.Eef1a1:Cau.Asip1)iim04*, *Tg(Xla.Eef1a1: Cau.Asip1)iim05*] that overexpress goldfish *asip1* using the constitutive EF1-alpha promoter (see Figure S2). All of these fish showed a distinct pigment pattern phenotype as adults (Figure 3B). In the following analyses, we focus on line *Tg (Xla.Eef1a1:Cau.Asip1)iim05*. To test whether this correlated with an expected homogenization of the *asip1* gradient due to the transgene, *asip1* transgene expression levels were determined in six skin samples from the most dorsal to the most ventral regions in adult fish (Figure 3J) by qRT-PCR (Figure 3L). The domain of transgene expression extended throughout the dorsoventral axis, and no significant differences were found in the levels of expression between these positions. We conclude that the transgene generates an essentially homogeneous distribution of *asip1* gene expression in the skin, eliminating the striking gradient seen in WT siblings. Furthermore, comparing the normalized expression levels in each genotype, we note that the levels of *asip1* expression throughout the skin of transgenic fish are equivalent to those in the ventral regions of a WT fish (Figure 3K,L). Compared with WT siblings (Figure 3C,G), the transgenics had reduced pigmentation over the entire dorsal region (Figure 3D), including the head (Figure 3H). This dramatic hypomelanization results from an almost complete absence of melanin from the dorsal scale melanophores, and was also prominent in the body stripes, with 2D absent and the others showing reduced melanin (Figure 3B,F). In place of stripe 2D, the transgenics show an extensive dorsal extension of the dorsal most band of iridophores (interstripe) dorsal to the remaining stripe 1D (Figure 3B,F). Nevertheless, other aspects of the pigment pattern are

unchanged, with fin pigment pattern, opercula iridophores and pigmentation of the eye (both choroidal and retinal pigmented epithelium) occurring in a manner indistinguishable from WT fish. The pattern seen can reasonably be described as a ventralization, consistent with the qRT-PCR results showing that transgenic fish attain a level of *asip1* expression typical of WT ventral levels.

Embryonic, metamorphic and adult pigment patterns can be distinguished at different stages of the zebrafish life cycle, mainly by an increase in the number of melanophores and changes in their distribution (*Kelsh, 2004; Parichy et al., 2009*). To identify which of these patterns were affected in transgenic fish, melanophores were counted during larval (5 dpf, SL 3 mm), metamorphic (15 dpf, SL 6.3 mm) and two adult stages (60 dpf, SL 13 mm and 210 dpf, SL 25 mm) (Figures 4 and S4). No differences was observed in the number of dorsal stripe melanophores in fish at 5 and 15 dpf, nor in lateral stripe melanophores in the horizontal myoseptum at 15 dpf (see Figure S4). Whole-mount *in situ* hybridization was performed to determine whether *asip1* overexpression affected the expression pattern of *microphthalmiarelated transcription factor a* (*mitfa*), *xanthine dehydrogenase* (*xdh*) and *leucocyte tyrosine kinase* (*ltk*), early markers for melanophores, xanthophores and iridophores, respectively (*Lopes et al., 2008; Parichy et al., 2000*). Although *asip1* overexpression is widespread in the transgenic line even as early as embryonic stages (Figure S3), we saw no differences in the expression pattern of any of these markers at 24–30 hpf, consistent with the normal embryonic pigment pattern of the transgenic fish (data not shown). In contrast, transgenic fish at 60 and 210 dpf showed pronounced pigment defects. Figure 4 shows the melanophore distribution in representative WT (A) and transgenic (B) fish at 210 days of life. To enable accurate quantitation of melanophore numbers, fish were treated with epinephrine and fixed in 4% paraformaldehyde, which removes the pigments of xanthophores and iridophores but does not affect melanin. At 60 dpf, the number of skin melanophores in transgenic fish was decreased by 61% in the head, 66% in the dorsum and 35% in stripe 1D on the trunk compared to the control group ($P < 0.001$); we saw no differences in the melanophore number in the anterior and posterior regions of stripe 1V nor belly (Figure 4C). At 210 days of life, a similar pattern of decreased number of melanophores in the dorsum and stripe 1D persisted, and the transgenic fish lacked the additional 2D melanophore stripe, having only a few scattered melanophores (Figure 4B,D). Control individuals of the same SL and age as transgenic fish showed the normal 2D band (Figure 4A,C). Thus, the increase in *asip1* expression consistently reduced the number of melanophores, but this effect was restricted to dorsal regions of metamorphic transgenic fish.
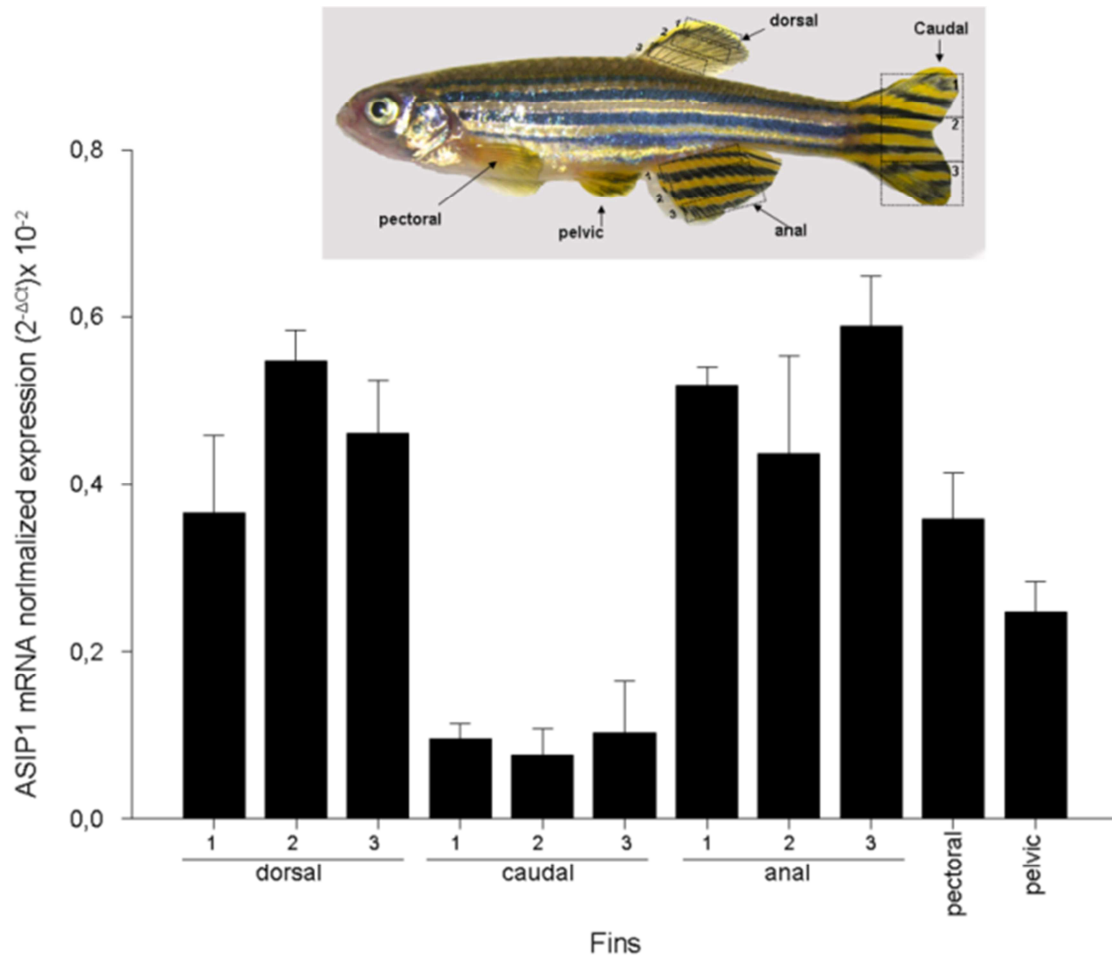
Supplementary Figure 2. *Normalized gene expression levels of zebrafish asip in anal, caudal, dorsal, pectoral and pelvic fin samples from 210 dpf adult WT zebrafish. Shown are log 10 transformed ΔCt values of asip1 relative to EF1-alpha. Data are the mean ± SEM from eight samples after triplicate qRT-PCR analysis.*
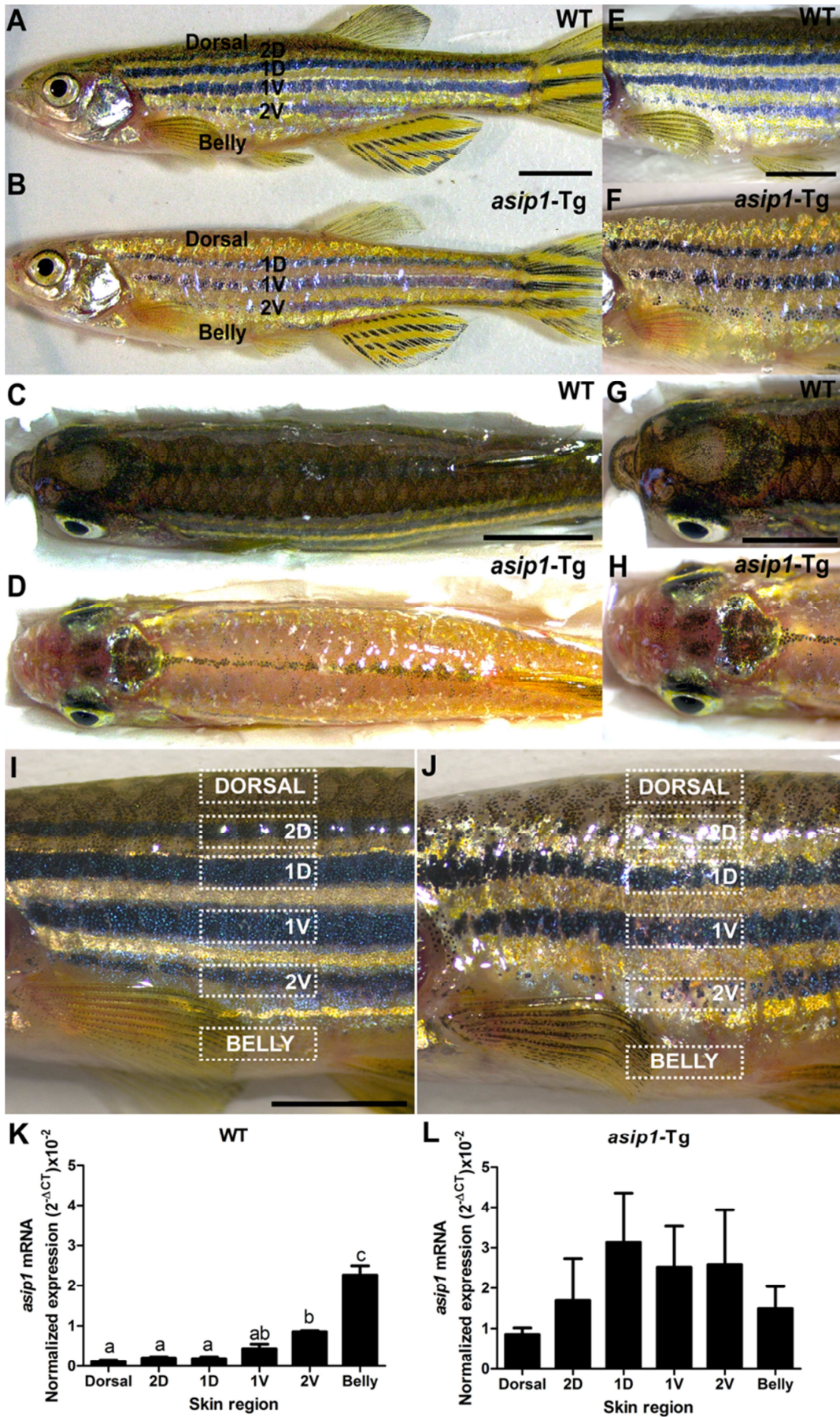
Figure 3. (previous page) *Adult pigment pattern of wildtype (WT) and transgenic agouti fish [asip1-Tg; line Tg(Xla.Eef1a1:Cau.Asip1)iim05]. Lateral (A, B), dorsal (C, D), anterior-lateral (E, F, J, I) and dorsal head close-up views (G, H) of 210 dpf zebrafish. (A, B) WT fish have a pattern with dark stripes and light interstripes. Letters indicate the name of each dark stripe rich in mature melanophores: the two primary stripes are designated 1D and 1V, and the two secondary stripes 2D and 2V. Asip1 overexpression resulted in a lighter pigment pattern. In asip1-Tg fish, the 2D stripe is absent, and there are fewer melanophores in the 1D stripe. In areas lacking melanophores, xanthophores become more evident, and the fish looks much paler and yellower (B, D). Asip1-Tg fish show a dramatic reduction in melanophore number over the flank (E, F). In WT, melanophores are distributed at the end of scales and over the head; in asip1-Tg, the head is clearly hypopigmented, xanthophores and iridophores are more evident and the scales largely lack melanophores (G, H). (I, J) location of skin sample points (white boxes) of 210 dpf adult WT (I) and asip1-Tg (J) fish. (K, L) normalized gene expression levels of zebrafish asip1 in skin samples from dorsum, primary stripes (1D and 1V), secondary stripes, (2D and 2V) and belly of 210 dpf adult WT (I) and asip1-Tg (J) fish. Shown are log 10-transformed ΔCt values of Asip1 relative to ef1-alpha. Data are the mean ± SEM from eight samples after triplicate qRT-PCR analysis. Superscripts a, b and c indicate statistical differences (P < 0.05) in gene expression levels among skin region (statistics data are similar if share at least one letter). Scale bar: 0.5 cm.*
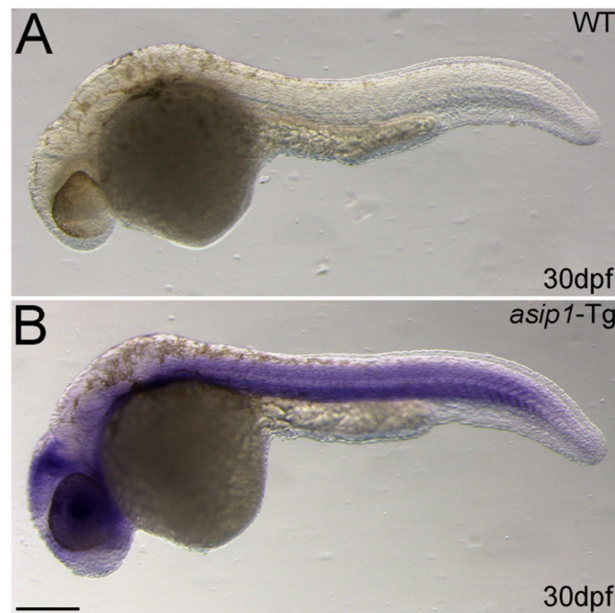
Supplementary Figure 3. *Widespread expression of asip1 transgene. In situ hybridization on 30hpf WT (A) and asip1-Tg (B) zebrafish embryos showing the spatial expression pattern of asip1 transgene mRNA; as expected the transcript is very widely expressed using this constitutive promoter. Scale Bars: 1 mm.*

Figure 4. *(next page) Distribution (A–B) and number (C, D) of melanophores in wild-type (WT) and asip1-Tg in 60 dpf (C) and 210 dpf zebrafish (A, B, D). Lateral views of 210 dpf WT (A) and asip1-Tg (B) showing the fish body regions selected for melanophore count are displayed (A, B). At 60 dpf (C), black melanophores are organized in a longitudinal stripe pigment pattern scattered over the flank, head and ventral areas. At this stage, wild-type fish show the first two primary dark stripes, 1D and 1V (C, inset); stage-matched asip1-Tg fish showed significantly lower numbers of melanophores in the head, dorsal area and 1D stripe region but not in ventral areas (1V stripe and belly) than their WT siblings (P < 0.001). At 210 dpf (D), additional melanophore stripes are formed (D, inset). Asip1-Tg fish showed significantly reduced numbers of melanophores in the head, dorsal area, 1D and 2D stripe region but not in ventral areas (1V and 2V stripe and belly) than WT siblings (P < 0.001). Melanophores within a 1-mm2 area were counted in the in the dorsal head (head), dorsal lateral back (dorsal), anterior and posterior 1D and 1V stripes and in the lateral belly of 60 dpf WT and asip1-Tg fish and in the dorsal head (head), dorsal lateral back (dorsal), anterior 2D and 2V stripes, anterior and posterior 1D and 1V stripes and in the lateral belly of 210 dpf WT and asip1-Tg fish. Data are the mean _ SEM, n = 8. Asterisks indicate significant differences (P < 0.05) between WT and Asip1-Tg fish. Scale Bars: 1 mm.*
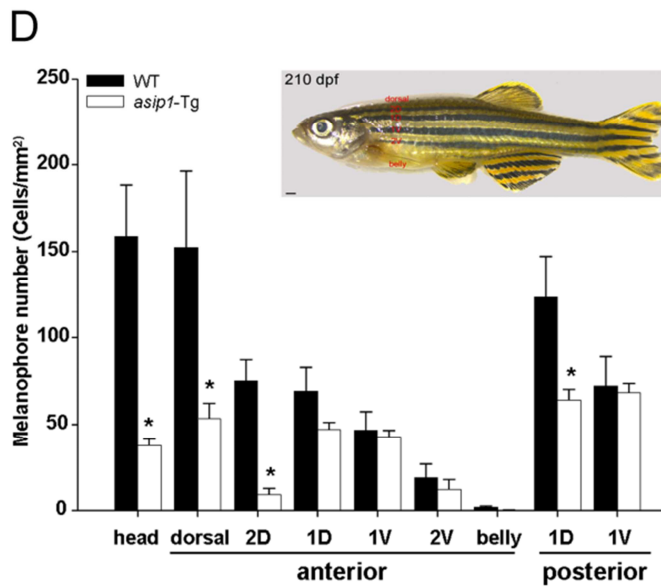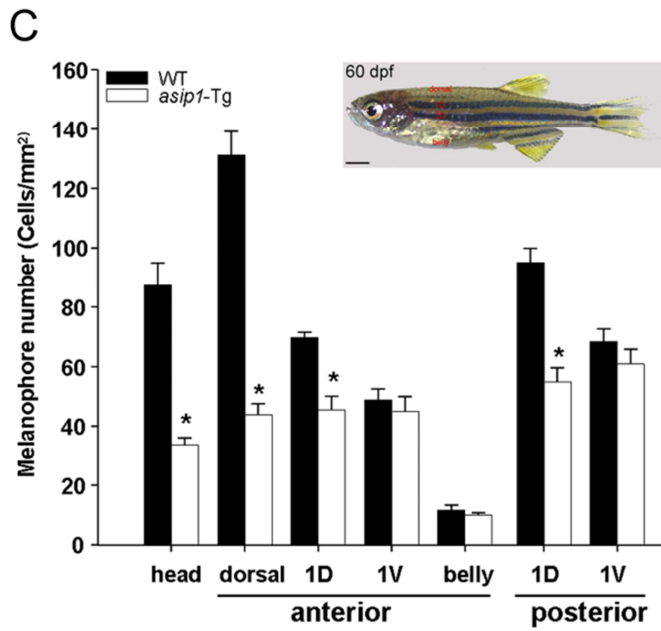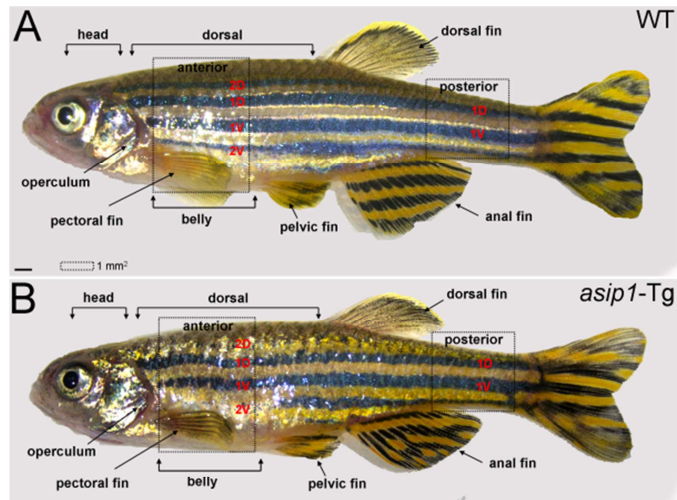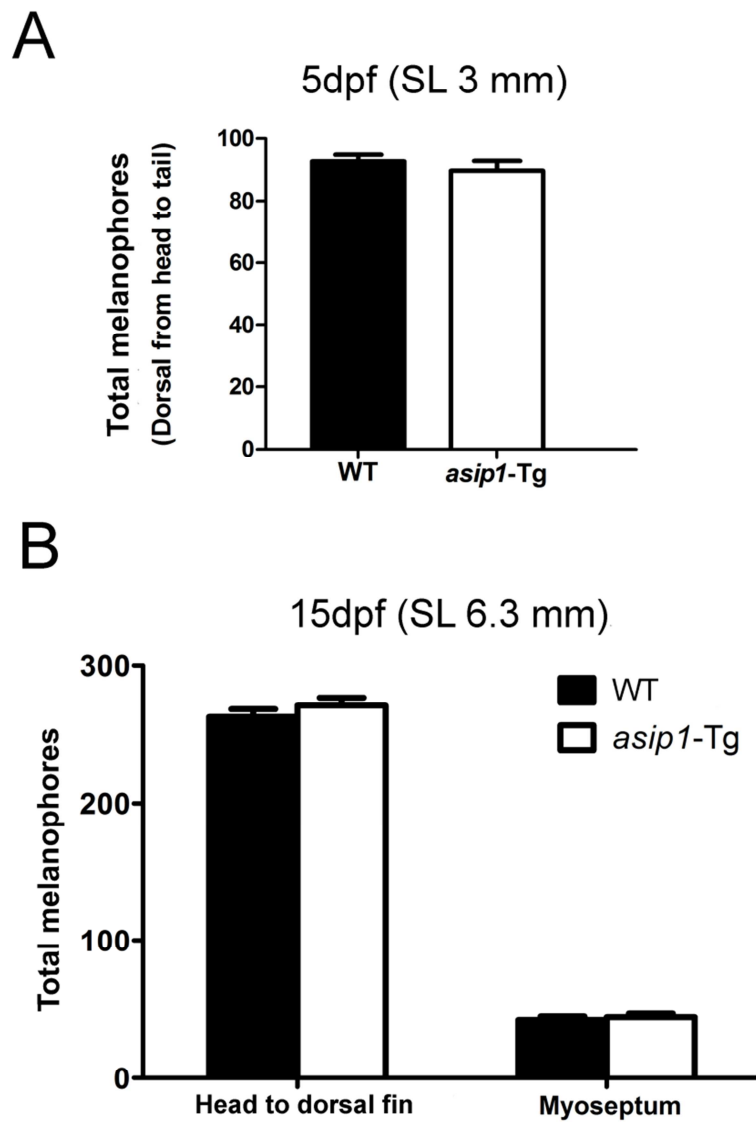
Supplementary Figure 4. *Total melanophore number in 5 and 15 dpf WT and asip1-Tg zebrafish. Total dorsal stripe melanophores from head to tail were counted at 5 dpf (SL 3 mm) (A) and at 15 dpf (SL 6.3 mm) (B). In this latter group, total melanophores in the lateral stripe within the horizontal myoseptum were also scored. Data are the mean ± SEM, n=8.*

Pattern changes results from decreased melanocyte numbers, as well as decreased melanization

Next, we asked whether the modified pigment patterns observed in transgenic fish were due to changes in melanoblast differentiation, especially inhibition of the melanin synthesis pathway, or due to absence of melanophores. *mitfa* is a critical regulator of melanophore fate specification and encodes a transcription factor required for the expression of melanin synthesis-involved genes such as *dct* and *tyrp1b*, but also for ongoing maintenance of the melanocyte phenotype (*Johnson et al., 2011; Lister et al., 1999*). We analysed the levels of expression of *mitfa*, *dct* and *tyrp1b* in the skin from the dorsum and from dorsal (2D, 1D) and ventral (1V, 1D) dark stripes and belly in control and *asip1* transgenic fish by qRT-PCR (Figure 5). Both *tyrp1b* and *dct* (*tyrp2*) code for enzymes that participate in the melanogenic pathway, but *dct* in particular is also an early marker of melanoblast differentiation (*Kelsh and Eisen, 2000; Lister et al., 1999*). Figure 5B shows the levels of expression of *dct* along the dorso-ventral axis in the skin of control and transgenic fish. In transgenic fish, *dct* expression was decreased by 93.4% in the dorsum and by 84.2% in 2D stripes in comparison with the same regions in WT fish. *Dct* expression in 1D, 1V and 2V stripes and belly did not differ significantly between transgenic and WT fish. The expression pattern of *tyrp1b* (Figure 5C) was similar to that of *dct*. Thus, in the transgenic group, the expression of *tyrp1b* was 2.63 times less in dorsum and 3.7 times less in the 'virtual' 2D stripe than in the control group. In dark stripes 1D, 1V and 2V, *tyrp1b* expression was similar in the two groups. Thus, consistent with the dorsal reduction in melanization, we see a dramatic reduction in the expression of melanophore differentiation genes in the dorsal, but not ventral, regions of transgenic fish. Figure 5A shows the expression levels of *mitfa* in skin samples obtained along the dorso-ventral axis in zebrafish adults. In wild-type control fish, the highest levels of expression of *mitfa* were found in the dorsum ($P < 0.001$), but *mitfa* transcripts showed a gradual decrease from the dorsum to the belly of the fish, thus showing an evident dorso-ventral gradient expression in adult WT zebrafish. In transgenic fish, *mitfa* expression was decreased by 50% in the dorsum with no significant difference in the other skin regions in comparison with the same regions in WT fish. Therefore, comparing the normalized expression levels of *mitfa* in each genotype, we conclude that the disruption of the *asip1* dorso-ventral expression gradient found in the transgenic fish produces a disruption of the striking *mitfa* gradient expression seen also in WT siblings. Furthermore, we note the good correlation between *mitfa* expression levels (Figure 5A) and melanophore numbers (Figure 4D),

suggesting that most, if not all, melanophores in the transgenics are pigmented and that their number is indeed decreased in dorsal regions of the transgenic lines. Comparing the data for *dct* and *tyrp1b*, we note that in stripe 2D, *mitfa* is not significantly changed, whereas the melanocyte differentiation genes are dramatically reduced in good correlation with the counts of melanized melanophores; we interpret these data as indicating that in this region, elevated *asip1* levels result in partial inhibition of melanocyte differentiation. In contrast, in the dorsal most region, where dct, *tyrpb1b* and *mitfa* are all at least very substantially reduced, we suggest that *asip1* overexpression results in a decrease in the number, as well as the differentiation, of melanophores in transgenic fish.

Early markers of xanthophores and iridophores are unaffected by asip1 overexpression

The pigment pattern of zebrafish is composed not only of melanophores but also of xanthophores and iridophores. Unlike melanophores, it is particularly difficult to distinguish individual xanthophores and iridophores, so that it is difficult to count them in post-embryonic stages. Therefore, to determine whether xanthophores and iridophores in transgenic fish were affected, we analysed the levels of expression of *xdh*, a gene encoding an enzyme required for the synthesis of yellow–orange pteridine pigments (*Parichy et al., 2000*), and *ltk*, an early and persistent marker of the iridophore lineage (*Lopes et al., 2008*) by qRT-PCR in the skin of control and transgenic adult fish. Both *xdh* and *ltk* were detected in dorsum and belly and also in dark stripes in control and transgenic fish (Figure 5D,E), with no significant difference in their expression levels at this stage. We conclude that numbers of each of these cell types are likely to be largely unchanged in transgenic fish.
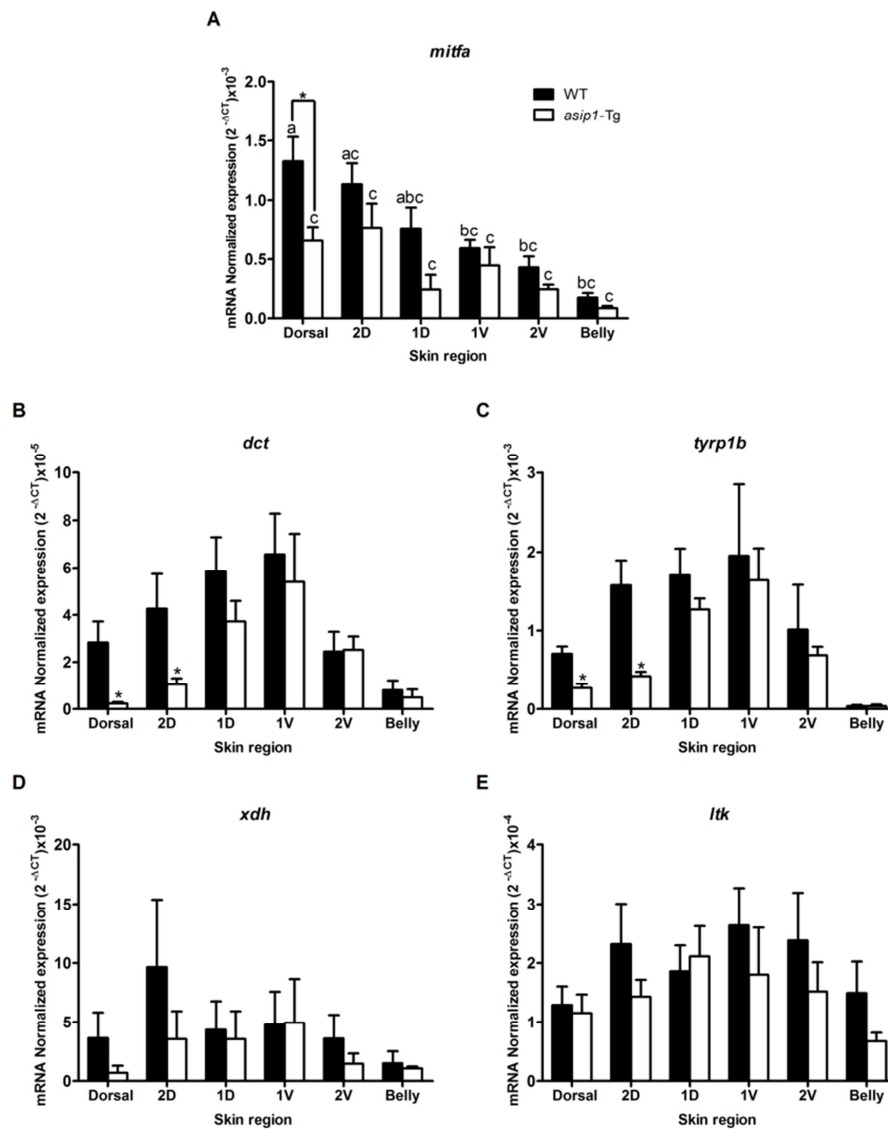
Figure 5. *qRT-PCR analysis of pigment cell markers in the skin of wild-type (WT) and asip1-Tg zebrafish. mRNA expression levels of microphthalmia-associated transcription factor a (mitfa) (A), dopachrome tautomerase (dct) (B), tyrosinase-related protein 1 (tryp1b) (C), xanthine dehydrogenase (xdh) (D) and leucocyte tyrosinase kinase (ltk) (E) were determined in skin samples from dorsum, primary stripes (1D and 1V), secondary stripes, (2D and 2V) and belly of 210 dpf adult fish. Shown are log 10-transformed ΔCt values of mitfa, dct, tryp1b, xdh and ltk relative to ef1-alpha. Data are the mean ± SEM from eight samples after triplicate qRT-PCR analysis. Asterisks indicate significant differences (P < 0.05) between WT and asip1-Tg fish. Superscripts a, b and c indicate statistical differences (P < 0.05) in gene expression levels among skin region (statistics data are similar if share at least one letter).*

3. Discussion

In this study, we show a dorso-ventral gradient of *asip1* expression in the skin of adult zebrafish, with lower levels in the dorsum, remaining constant until the horizontal myoseptum, and increasing gradually to reach a maximum in the belly. This expression pattern correlates with the dorso-ventral pigment pattern showing darkly coloured skin in the dorsal area and light ventrum. Disruption of the dorso-ventral expression gradient in transgenic zebrafish overexpressing *asip1* results in a modification of the dorso-ventral pigment pattern. Transgenic fish exhibit a drastic reduction in the number of differentiated melanocytes in the dorsal region, due to the absence of most scale-associated melanophores as well as most of the melanophores in the dorsal stripes (1D and 2D) and the dorsal head of adult zebrafish. The lack of melanized cells in the dorsal region enhances the visibility of the underlying iridophores, thus giving a ventral-like aspect to the dorsal skin of transgenic zebrafish. Careful quantitation of transcripts for two key melanogenic enzymes, *dct* and *tyrp1b*, and of the transcription factor *mitfa*, which is crucial for specification and maintenance of melanocytes, clearly indicates that this reduction in the number of differentiated melanophores results both from a reduction in the number of dorsal melanocytes and from a reduction in the differentiation (melanization) of the remaining cells.

Our data thus shows that *asip1* function is crucial for development of the dorso-ventral countershaded pattern in adult zebrafish. Our data suggest that zebrafish adult pigment pattern formation involves two processes. To date, previous work has focused on a stripe-forming mechanism, which is dependent upon interactions between xanthophores and melanophores (*Kelsh et al., 2009; Parichy, 2009*), but with recent work beginning to uncover a key role for iridophores in this mechanism too (*Frohnhöfer et al., 2013; Patterson and Parichy, 2013; Singh et al., 2014*). Here, we have identified a role for *asip1* in generating an underlying dorso-ventral (countershading) mechanism. *Asip1* overexpression affects adult melanophores in a position-dependent manner. Thus, *asip1* overexpression induces a drastic reduction in the number of differentiated melanophore, but has no effect on those localized ventral to the horizontal myoseptum, despite the fact that *asip1* levels in ventral stripe regions 1V and 2V of transgenic fish were as high as those recorded in the dorsal regions of transgenic fish. This dorso-ventral pattern, although the second to be recognized in zebrafish, is likely to be an ancestral one, given the ubiquitous nature of countershading in vertebrates. It seems that the zebrafish exhibits an ancestral dorso-ventral pigment pattern on which the striped pattern is superimposed. The graded expression of *asip1* seems to induce an

inversely correlated expression pattern of *mitfa*, showing minimal expression levels in the ventrum and maximal in the dorsal region. In contrast, the pattern of *dct* and *tyrp1b* is more complex, being lowest in the belly, but otherwise not tightly correlated to the *mitfa* pattern. When the *asip1* expression gradient is disrupted in transgenic zebrafish so as to generate dorsal *asip1* levels comparable to those observed in the belly of transgenic or WT zebrafish, the expression pattern of both melanogenic enzymes and the transcription factor *mitfa* is also disrupted. These observations are consistent with our previous study, which showed that local injection of *asip1*-capped mRNA on dorsal dark skin of turbot decreased the expression of tyrp1b (*Guillot et al., 2012*). Furthermore, the effects were only detectable during metamorphosis and then maintained throughout adulthood, as transgenic zebrafish never developed the 2D dark stripe on the dorsum that usually develops with growing size.

Our observations indicate that the pattern change derives from both an inhibition of melanization, directly comparable to the mechanism of countershading documented in mammals, but importantly also from a novel mechanism regulating the number of melanocytes, and thus the ratio of melanocytes and other pigment cells. Thus, we have shown in zebrafish that *asip1*'s role in the regulation of melanocyte melanisation is conserved. In rodents, ASIP function is generally stated to act via repression of melanocyte differentiation, specifically expression of melanogenic enzymes such as Dct and Tyrp1 (*Candille et al., 2004; Manceau et al., 2011; Millar et al., 1995*). Likewise, in rodent cell culture, ASIP inhibits α-MSH-induced eumelanization of melanoblasts (*Aberdam et al., 1998; Le Pape et al., 2008; Sviderskaya et al., 2001*) showed that melanocortin agonists stimulated differentiation of immortal cell lines of murine melanoblasts but inhibited growth; however, when these cells were cultured with agouti, melanoblast differentiation was inhibited and growth-stimulated.

The mechanism by which *asip1* decreases *dct* and *tyrp1b* expression and inhibits melanophore differentiation is likely to be similar to that described in mammalian species. In mammals, ASIP antagonism of MC1R signalling induces the eumelanin–pheomelanin switch by lowering cAMP response element-binding protein (CREB)-dependent expression of *MITF* that stimulates transcription of *TYR*, *TYRP1* and *DCT* (*Bertolotto et al., 1998a, 1998b*). In fish, MC1R signalling is also involved in the control of pigmentation as nonsense mutations in MC1R have been reported to result in albinism (*Gross et al., 2011*). Consistent with the antagonistic role in mammals, Asip1 blocks α-MSH-induced melanin dispersion in medaka scale melanophores by acting as a competitive antagonist at MC1R (*Cerdá-Reverter et al., 2005*). In the sea bass (*Dicentrarchus labrax*), MC1R is constitutively activated, and the

endogenous melanocortin antagonists work as inverse agonists, thus decreasing the constitutive activity of the receptor (*Sánchez et al., 2010*). It is, therefore, plausible that the constitutive activation of MC1R leads to dorsal melanogenesis, but the ventral expression of asip1 blocks the constitutive activity, thus inhibiting ventral melanogenesis. When *asip1* is overexpressed in transgenic zebrafish, Asip1/MC1R interaction in the dorsal striped region results in reduced *mitfa* expression that results in a lowering of the expression levels of melanogenic enzymes.

At least in the very dorsal most regions, our data suggest this reduction in melanization is concomitant with a diminution of the number of melanocytes, so that the ventralization of the dorsal region is partially dependent upon a reduction in the ratio of different cell types. This might also be dependent upon the levels of *mitfa* expression, as at low levels, melanocyte specification from MSCs and/or survival or proliferation of melanoblasts might be affected (*Carreira et al., 2006; Lister et al., 1999*).

In contrast to a clear role in post-metamorphic (adult) melanocyte development and pattern formation, our data give no evidence for a role for *asip1* in embryonic melanocyte development nor in larval (pre-metamorphic) pigment pattern formation, as we saw no differences in the number of melanophores at 5 and 15 dpf, and as the embryonic WT expression pattern is totally uncorrelated with pigment pattern.

Our results lead us to propose also a differential regulation of adult melanophore differentiation, proliferation and/or survival depending on their position. The number of ventral melanophores (1V and 2V) was unaffected by *asip1* overexpression. In addition, pigmentation of fin stripes of *asip1* transgenic fish was indistinguishable from that observed in WT fish. The independence of some mechanisms underlying the control of body and fin pigment patterns has been also reported in some zebrafish mutants like *shady/ltk* (*Lopes et al., 2008*). Similar to *asip1* transgenic fish, *shady/ltk* zebrafish exhibit a severe disruption of the body stripe pattern but keep intact the fin stripes. It seems likely that some subpopulations of melanophores or their latent precursors are not susceptible to the effects of *asip1*; our expression data indicated that, although expressed in all fin tissue, *asip1* expression levels did not show a graded expression pattern in any thatweexamined, and furthermore, there was no correlation between *asip1* expression levels and the location of the fin. Thus, fin pigment pattern formation appears to be largely independent of *asip1*.

Cell culture studies exploring the actions of MIF have reported stimulation of iridophore proliferation, in addition to the inhibition of melanocyte development (*Bagnara and Fukuzawa, 1990; Zuasti et al., 1992*). Suggestively, a common origin of both post-embryonic iridophore and melanophore has been recently proposed from the socalled MSCs (*Budi et al., 2011*). The dorsal most band of iridophores appears expanded in the dorsal area of *asip1* transgenic zebrafish, strongly contributing to the ventralized appearance of their dorsal skin. However, our studies of sectioned adult fish indicate that these cells are present in WTs, but lie underneath, and are obscured by the dorsal melanophores. This is consistent with the extensive distribution of these cells throughout stripe and interstripe regions as demonstrated by electron microscopy (*Hirata et al., 2003, 2005*). We analysed the distribution in adult skin of xanthophores and iridophores using the molecular markers *xdh* (*Parichy et al., 2000*) and *ltk* (Lopes et al., 2008), respectively. Although expression of both *xdh* and *ltk* genes was widespread throughout the skin, we saw no correlation of either to the expression levels of *asip1*. Thus, our data do not support an agoutiinduced switch of MSCs to iridophores. Taken together, we conclude that the development of xanthophores and iridophores may be largely independent on *asip1* levels; although as we were unable to count the number of xanthophores or iridophores in adult fish, we cannot rule out a more subtle effect on their patterning. We suggest that the more pronounced band of iridophores in the transgenics results at least largely from the underlying cells becoming more visible in the absence of stripe 2D melanocytes.

From an evolutionary point of view, we note both the conserved and novel aspects of the mechanisms of *asip1* function in establishing the dorso-ventral pigment pattern in these divergent vertebrates. In mammals, ASIP regulates the differentiation of their only chromatophore type, the melanocyte.

In contrast, in fish, a similar dorso-ventral pigment patterning process comes about by regulating the ratio of different pigment cell types in different dorsoventral zones, as well as by regulating melanocyte differentiation. Nevertheless, a further role for ASIP in mice in regulating specification, proliferation or survival of melanoblasts has not been ruled out experimentally (*Hirobe, 1982, 1992; Tamate et al., 1986*). In the light of our data, we suggest that a rigorous examination of this issue of pigment cell numbers (melanocytes, but in fish also iridophores) using transgenic markers in both mouse and zebrafish will be important to clarify the degree to which a conserved mechanism of ASIP-dependent control of melanoblast numbers may contribute to dorso-ventral pigment pattern differences throughout the vertebrates. In the evolution of mammals, the loss of pale-coloured chromatophores appears to have allowed

selection for biochemical mechanisms to produce pale versions of melanin to replace the function of light-reflecting chromatophores. Concomitantly, the function of ASIP/MC1R interaction evolved to control the spatial–temporal switch in the synthesis of melanins. In conclusion, we demonstrate for the first time the existence of a graded expression of *asip1* along the dorso-ventral axis in adult fish, with the highest levels in the belly. This gradient functions to establish a dorso-ventral pigmentation pattern, because the disruption of the dorso-ventral expression gradient in transgenic fish overexpressing *asip1* leads to phenotypic changes including the elimination of dorsal melanin pigmentation. *Asip1* seems to affect both melanocyte numbers and their differentiation in adult fish, but has no effect on embryonic pigment pattern. Thus, ASIP's role in establishing dorso-ventral pigment pattern is not unique to mammalian species, and it is likely that its function is conserved among vertebrates. However, *asip1* overexpression had only modest effects on the general striped pattern of the body, demonstrating that zebrafish has two largely independent pigment patterning mechanisms, an ancestral dorsoventral pigment patterning process, onto which the striping mechanism is superimposed. Our study opens new ways for investigating the factors that control regional *asip1* expression and which may have a role in generating natural variations in pigment pattern formation in fish. Transgenic zebrafish overexpressing *asip1* will be a key tool for the study of adult pigmentation in fish.

4. Methods

Zebrafish strains and husbandry

Zebrafish were cultured as previously described (*Westerfield, 2007*). Experiments were performed with a TU-WT strain (Tübingen (TU), Nüsslein-Volhard Lab). Post-embryonic stages were estimated by both standardized length (SL) measurements according to (*Parichy et al. 2009*) and time post-fertilization in hours or days (hpf or dpf).

Transgenic zebrafish lines

Three independent transgenic zebrafish lines [Tg(Xla.Eef1a1:Cau.Asip1)iim03, *Tg(Xla.Eef1a1:Cau.Asip1) iim04* and *Tg(Xla.Eef1a1:Cau.Asip1*) iim05] were generated with the *Tol2* transposon system. The *Tol2* vector was kindly provided by Dr. Kochi Kawakami (2007). The goldfish *asip1* gene sequence was published by Cerdá-Reverter et al. (2005) (NCBI reference sequence: XM_001334910.3). To obtain a full-

length cDNA sequence of asip1 from goldfish skin, we used the asip1 5'-ATGCATCCGTCATTGTTG-3' and 5'-TCAGCATTT CGGGTAAC-3' primers (*Cerdá-Reverter et al., 2005*). The *asip1* PCR product was subcloned into pGEMT easy vector with BamH I and Not I restriction sites. PGEMT-*asip1* goldfish was digested with BamH I and Not I and subcloned into pT2AL200R1506 cut with the same restriction sites. The Tol2-transposon-based vector pT2AL200R150G contains the *eGFP* gene under the control of elongation factor *1-alpha* (*ef1-alpha*), a constitutive promoter. We replaced the *eGFP* gene with *asip1* gene. A total of 250 pg of construct and synthetic 5'-capped mRNA (150 pg) encoding a transposase were co-injected into WT embryos at the one- or two-cell stage, with 1% of phenol red as tracer.

The pigment pattern of all adult mosaic fish (F0) showed a pronounced phenotype, with paler head and body than WT fish (Figure S5). Positively identified F1 siblings were mated. The F2 embryos were grown to sexual maturity, and individuals F2 were mated to wild-type fish. The F3 progeny were analyzed for the transgene. Identified homozygous F2 were mated to each other to produce a large stable homozygous (F3) population.
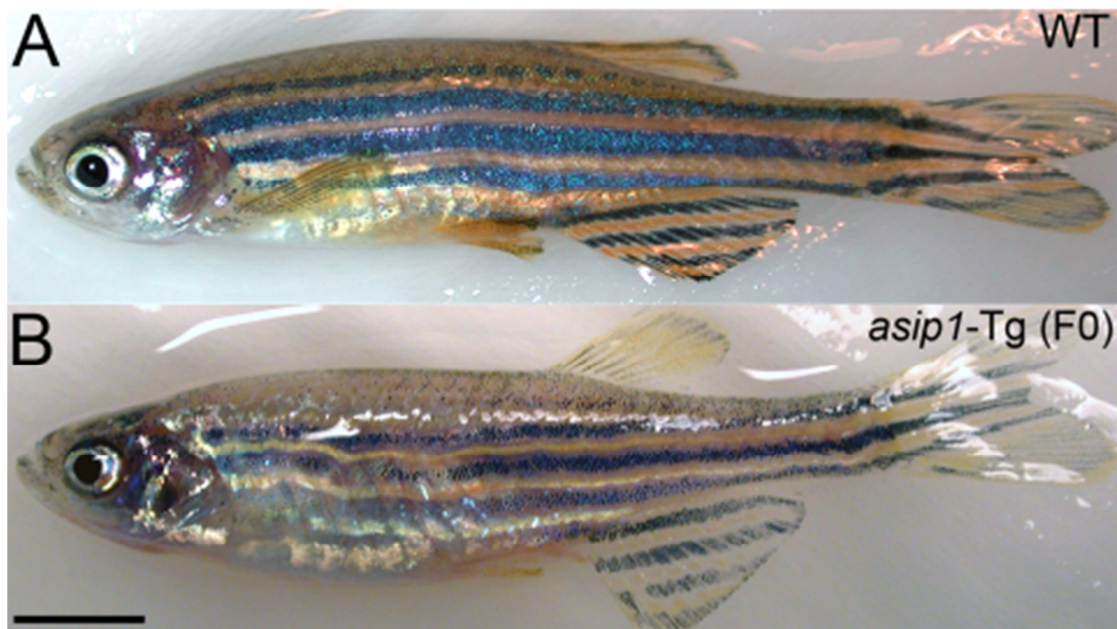
Supplementary Figure 5. *Adult pigment pattern of wild-type (WT) (A) and asip1 mosaic fish (F0) (B). Lateral view of 210 dpf zebrafish. Asip1 mosaic fish (F0) showed a pronounced phenotype, with paler head and body than WT fish. Scale bar: 0.5 cm.*

Ethics statement

All zebrafish experiments were approved by the National Advisory Committee for Laboratory Animal Research Guidelines licensed by the Spanish Authority (1201/2005) and conformed to the European Convention for the Protection of Animals used for Experimental and Scientific Purposes (ETS No 123, 01/01/91).

Zebrafish tissues

Eggs and larvae from fish aged 0–24 hpf and 2–7 dpf and adult tissues from the eye, dorsal and ventral skin, intestine, heart, liver, brain, gill, kidney, fat, gonads and muscle were sampled for RT-PCR. Two groups of eight fish were established, a WT group and a group of transgenic fish that overexpress the asip1 gene, Tg(Xla.Eef1a1: Cau.Asip1)iim05, see below. For each group, dorsal, primary and secondary stripes (1D, 1V and 2D, 2V, respectively) and belly skin samples were excised with a scalpel for qRT-PCR (see Figure 1I,J for location of skin sample points). Animals were anaesthetized with 0.02% tricaine, adults were rapidly decapitated, and all samples were frozen at _80°C until analysis. RNA was extracted for comparison of expression levels. Larvae from 30 hpf were anaesthetized and fixed in 4% paraformaldehyde for in situ hybridization. Individual larvae, metamorphic and adult stages (SL 3.6, 6.3, 13 and 25 mm or 5, 15, 60 and 210 dpf, respectively) were obtained for melanophore counts.

RNA isolation, RT-PCR and qRT-PCR

Total RNA was isolated from zebrafish tissues using Trizol reagent (Invitrogen) according to the manufacturer's instructions and concentration determined by absorbance at 260 nm using NanoDrop 2000 (Thermo scientific). A total of 100 ng of messenger RNA (mRNA) was reverse-transcribed using a first-strand complementary DNA (cDNA) synthesis kit (Fermentas).

The ontogenic and tissue expression pattern of *asip1* mRNA was determined by RT-PCR. Quantification of *asip1*, *microphthalmiaassociated transcription factor* (*mitfa*), *dopa-chrome tautomerase* (*dct*), *tyrosinase-related protein 1b* (*tyrp1b*), *leucocyte tyrosine kinase* (*ltk*) and *xanthine dehydrogenase* (xdh) mRNA expression was determined by quantitative real-time PCR (qRT-PCR) in the skin of WT and *Tg (Xla.Eef1a1:Cau.Asip1)iim05*, *asip1* transgenic fish line and for temporal expression *asip1* pattern in wt zebrafish. The sequencespecific primer sets are listed in Table S1. *Asip1* primer sets for zebrafish were designed from the mRNA sequence published in

the Genbank database (NM_001128801.1, (*Klovins and Schiöth, 2005*). β-actin (actb) was used as the internal reference to test the quality of the cDNA. A negative control was incorporated by replacing the cDNA template with molecular biology-grade water. The qRT-PCR reaction was set up in triplicate, containing 2 µl of first-strand cDNA, 10 pmol of each forward and reverse primer and SYBR PCR mix (Fermentas) to a final volume of 20 µl.

PCR was performed with an AB 7300 Real-Time PCR System. The thermal cycle protocol for SYBR Green-based qRT-PCR for all primer sets was as follows: denaturation at 95°C for 10 min, followed by 40 cycles of 95°C for 15 s and 60 °C for 1 min. Each set of skin samples from each group was tested five or seven times. The housekeeping gene elongation *factor-1 alpha* (*ef-1 alpha*) was used as an internal reference to normalize the cDNA template between tissue and development stage samples. Normalized relative quantities of mRNA expression were calculated with the mathematical method of ΔCt (*Livak and Schmittgen, 2001*). The melting curves of the products were verified to confirm the specificity of PCR products.

In situ hybridization

For whole-mount in situ hybridization, samples at 1, 3 and 6 dpf were fixed in 4% paraformaldehide (PFA) containing 1% DMSO in 19 PBS overnight at 4°C and stored in 100% methanol at -20°C. Wholemount *in situ* hybridization was performed using digoxigenin-labelled antisense probes as previously described (*Rotllant et al., 2008*). Antisense and sense riboprobes were made from linearized fulllength zebrafish and/or goldfish *asip1* cDNA. For plastic sections, embryos with ISH staining were fixed, dehydrated and eponembedded, and cut into 4-µm ventral longitudinal sections and mounted with EUKIT as previously described (*Westerfield, 2007*) and imaged.

In situ hybridization of adult (210 dpf) zebrafish followed Cerdá-Reverter et al. (2000). Samples were fixed in 4% paraformaldehyde and 0.1 M phosphate buffer, for 2 days at 4°C, dehydrated and embedded in Paraplast (Sherwood, St Louis, MO, USA). Serial 10-µm rostro-caudal transverse sections were cut using a rotary microtome. Sections were mounted on 3-aminopropyltriethoxylane (TESPA)-treated slides, air-dried at room temperature (RT) overnight and stored at 4°C under dry conditions and used for hybridization within one month. Adjacent sections were stained with haematoxylin–eosin (HE) to identify physiological structures.

Primer set	Forward 5'-3'	Reverse 5'-3'
qRT-PCR		
EF1-alpha	CTTCTCAGGCTGACTGTGC	CCGCTAGCATTACCCTCC
β-actin	AGCACGGTATTGTGACTAACTG	TCGAACATGATCTGTGTCATC
tyrp1b	CGACAACCTGGGATACACCT	AACCAGCACCACTGCAACTC
mitfa	TGAACGAAGAAGGCGGTTTA	TTCTGCTGCTCTTTCTGCAA
dct	ACCTGTGACCAATGAGGAGATT	TACAACACCAACACGATCAACA
ltk	AGAACATTGTCCGCT GCATT	GTAAATATCTCGGGCCATCC
xdh	TCAAAGGCTGTGGGTGAACCT	GCACTGCCCATGGAATAAAGG
asip1 Dre	CTGCGATCAGTGCGCTTTCT	TCAGCATTTGGGGTATC
asip1 Cau	ATGCATCCGTCATTGTTG	CGGCGGAGGTCTCTTCACAT
RT-PCR		
*asip1*full Dre	ATGAGTCCGTCATTGTG	TCAGCATTTGGGGTATC
*asip1*full Cau	ATGCATCCGTCATTGTTG	TCAGCATTTCGGGTAAC

Table 1. *Gene-specific primer sequences used for RT-PCR and qRT- PCR analysis. Dre (Danio rerio), Cau (Carassius aurata).*

Melanophore counts

To test whether the melanophore pattern of transgenic fish is different from that of control fish, we quantified melanized melanophores in both groups. The region selected for counting melanophores depended on the stage of development. In early and metamorphic stages (5 and 15 dpf, respectively), we counted total melanophores from head to tail in a dorsal view. For the metamorphic stages, the melanophores visible in the horizontal myoseptum were also included. For adult fish (60 and 210 dpf), melanophores within a 1-mm^2 area were counted in multiple defined positions: from a dorsal view, on the head (head areas) and on the dorsal areas (edge of the head to the dorsal fin); from a lateral view, on the 2D, 1D, 1V and 2V areas (anterior areas (pectoral to pelvic fin) and posterior areas (end anal fin); and from a ventral view on belly area (pectoral to pelvic fin) (see Figure 2A,B). To analyse the number of melanophores, fish were immersed in fish water solution containing 10 mg/ml epinephrine (Sigma) for approximately 30 min to contract melanosomes. Afterwards, fish were anesthetized and imaged. Melanophores were counted manually utilizing ADOBE PHOTOSHOP CS2 software (Adobe Systems Software Adobe Systems Ib_erica SL, Barcelona, Spain). The number of melanophores was plotted against the area in mm^2.

Statistics

Data are expressed as mean ± standard error of the mean (SEM). Comparisons between numerical data were evaluated by one- or two-way ANOVA with the Tukey's or Dunnett's post hoc test. A P value <0.05 (asterisks and letters) was considered statistically significant. Statistics data are similar if share at least one letter. Statistical analyses and figures were performed with GraphPad Prism 5.0. (GraphPad Software, La Jolla, CA, USA).

5. Acknowledgements

CAPÍTULO III

En este capítulo se demuestra que la expresión ubicua de ASIP induce mayores niveles de ingesta en el pez cebra

La proteína ASIP es el antagonista competitivo natural de MC1R, pero su estructura también le permite ser antagonista competitivo de MC4R. En condiciones normales la proteína ASIP, expresada a nivel tegumentario, no se relaciona con el MC4R expresado en el sistema nervioso central. En la cepa de peces transgénicos ASIP, la expresión ubicua de esta proteína permite su interacción con el MC4R, donde emulando las funciones de AGRP desensibiliza los mecanismos de la saciedad.

Los peces ASIP ingieren mayor cantidad de alimento creciendo un 15% más en longitud. El crecimiento mejorado se mantiene al limitar la ingesta, lo que sugiere que los peces ASIP exhiben tasas de conversión alimenticia superiores a sus congéneres salvajes.

El estudio comparativo de los transcriptomas cerebrales e hipofisarios sugiere diferentes rutas centrales que podrían estar implicadas en señalización neuronal "downstream" de los efectos de los antagonistas endógenos de melanocortinas en vertebrados.

Behind melanocortin antagonist overexpression in the zebrafish brain: A behavioral and transcriptomic approach

Raúl Guillot[1], Raúl Cortés[1], Sandra Navarro[1],
Morena Mischitelli[1], Víctor García-Herranz[1],
Elisa Sánchez[1], Laura Cal[2], Juan Carlos Navarro[3],
Jesús Míguez[4], Sergey Afanasyev[5], Aleksei Krasnov[6], Roger D Cone[7],
Josep Rotllant[2*],
Jose Miguel Cerdá-Reverter[1*]

1. Control of Food Intake Group, Department of Fish Physiology and Biotechnology, Instituto de Acuicultura de Torre de la Sal (IATS), Consejo Superior de Investigaciones Científicas (CSIC), Castellón, Spain.
2. Aquatic Molecular Pathobiology Group, Instituto de Investigaciones Marinas (IIM), Consejo Superior de Investigaciones Científicas (CSIC),Vigo, Spain.
3. Lipid Group, Department of Biology, Culture and Pathology of Marine Species, Instituto de Acuicultura de Torre de la Sal (IATS), Consejo Superior de Investigaciones Científicas (CSIC), Castellón, Spain.
4. Laboratorio de Fisioloxía Animal, Departamento de Bioloxía Funcional e Ciencias da Saúde, Facultade de Bioloxía, Universidade de Vigo, Vigo, Spain.
5. Sechenov institute of Evolutionary Physiology and Biochemistry, M. Toreza Av. 44, saint Petersburg 194223, Russia.
6. Nofima Marine, Norwegian Institutes of Food, Fisheries and aquaculture Research, 5010 1432 Å, Norway.
7. Deparment of Molecular Physiology and Biophysics, Vanderbilt University School of Medicine, 702 Light Hall (0165), Nashville, TN 37232-0165, United States

Abstract

Melanocortin signaling is regulated by the binding of naturally occurring antagonists, agouti-signaling protein (ASIP) and agouti-related protein (AGRP) that compete with melanocortin peptides by binding to melanocortin receptors to regulate energy balance and growth. Using a transgenic model overexpressing ASIP, we studied the involvement of melanocortin system in the feeding behaviour, growth and stress response of zebrafish. Our data demonstrate that ASIP overexpression results in enhanced growth but not obesity. The differential growth is explained by increased food intake and feeding efficiency mediated by a differential sensitivity of the satiety system that seems to involve the cocaine- and amphetamine- related transcript (CART). Stress response was similar in both genotypes. Brain transcriptome of transgenic (ASIP) vs wild type (WT) fish was compared using microarrays. WT females and males exhibited 255 genes differentially expressed (DEG) but this difference was reduced to 31 after ASIP overexpression. Statistical analysis revealed 1122 DEG when considering only fish genotype but 1066 and 981 DEG when comparing ASIP males or females with their WT counterparts, respectively. Interaction between genotype and sex significantly affected the expression of 97 genes. Several neuronal systems involved in the control of food intake were identified which displayed a differential expression according to the genotype of the fish that unravelling the flow of melanocortinergic information through the central pathways that controls the energy balance. The information provided herein will help to elucidate new central systems involved in control of obesity and should be of invaluable use for sustaining fish production systems.

1. Introduction

The melanocyte-stimulating hormones (MSHs) and adrenocorticotropic hormone (ACTH) are the main melanocortin peptides. All of them are encoded in a common precursor called proopiomelanocortin (POMC), which is expressed mainly in the pituitary (*Castro and Morrison 1997*). In the rat brain, POMC is also expressed in two discrete neuronal groups, the arcuate nucleus (Ac) of the hypothalamus, and the caudal region of the nucleus of the tractus solitarius (NTS) of the medulla (*Bangol et al., 1999*). Melanocortin signaling is mediated by binding to a family of specific G protein-coupled receptors that positively couple to adenylyl cyclase. Five melanocortin receptors (MC1R-MC5R) have been characterized in tetrapods but only *mc3r* and *mc4r* are abundantly expressed within the mammalian central nervous system (CNS).

Subtype 2 receptor binds ACTH, whereas the other four MCRs distinctively recognize MSHs (*Schiöth et al., 2005; Cortes et al., 2014*). Atypically, melanocortin signaling is not exclusively regulated by the binding of endogenous agonists, as naturally occurring antagonists, agouti, designed as agouti-signaling protein (ASIP) in species different form mouse, and agouti-related protein (AGRP) compete with melanocortin peptides by binding to MCRs. ASIP is a potent melanocortin antagonist at MC1R and MC4R (*Cone, 2005; 2006*). In mice, ASIP is exclusively produced within the hair follicle, where it locally regulates the production of pigment in follicular melanocytes by antagonizing the effects of α-MSH on MC1R (*Lu et al., 1994*). In contrast, AGRP is mainly produced within the hypothalamic arcuate nucleus and the adrenal gland, and it is potent in inhibiting melanocortin signaling at MC3R and MC4R, but inactive at MC1R (*Ollmann et al., 1997*). Strong evidence has demonstrated that the central melanocortin system is a nodal point in controlling the energy balance in mammals (*Girardet and Butler, 2014*). Central activation of MC3R and MC4R is thought to mediate melanocortin effects on the energy balance (*Cone, 2005; 2006*) since both *mc3r* knockout rats (*Chen et al., 2000*) and *mc4r* knockout mice (*Huszar et al., 1997*) display severe alterations in energy homeostasis. The interruption of α-MSH central signaling by ubiquitous constitutive expression of agouti gene in obese yellow mice (*Ay*) results in hyperphagia, hyperinsulinemia, increased linear growth, maturity-onset obesity and yellow fur (Lu et al., 1994). A similar metabolic syndrome is also observed in transgenic mice ubiquitously overexpressing *agouti* or *agrp* genes (*Klebig et al, 1995; Ollmann et al., 1997*), and in *mc4r* knockout mice (*Huszar et al., 1997*). However, mice with multiple copies of *agouti* gene expressed under the control of a skin-specific promoter do not exhibit the obesity-related phenotype but manifest yellow fur (*Klebig et al., 1995*). This suggests that the central antagonism α-MSH signaling by agouti protein in obese yellow mice is responsible for this metabolic syndrome. Accordingly, the central administration of the C-terminal fragment of AGRP (*Rossi et al., 1998*) or chemical antagonists for MC3R and MC4R increase food intake in rodents (*Fan et al., 1997; Kask et al., 1998*), and intracerebroventricular (icv) injections of the melanocortin receptor agonist MTII (melanotan-II) produce a dose-dependent reduction in food intake in mice (*Fan et al., 1997*). However, *mc4r* deficient mice do not respond to the anorectic effects of MTII, suggesting that endogenous melanocortins inhibit feeding primarily by activating MC4R (*Marsh et al., 1999*). In several species including sea bass (*Sánchez et al., 2009a*), mice (*Nijenhuis et al., 2001*) and humans (*Tolle and Low, 2008*), *in vivo* and *in vitro* experiments have demonstrated that MC4R signalling does not require binding agonist but it is constitutively activated. AGRP binding reduces the

constitutive activity of the receptor as an inverse agonist does. It suggests that hunger is constitutively inhibited by MC4R signalling and AGRP binding to the receptor overcomes the MC4R-induced inhibition to promote feeding (*Tolle and Low, 2008*).The structure of the melanocortin system in fish diverges from that reported in tetrapods as the genome of the teleost antecessor doubled once more (3R), resulting in an expansion of the receptor/peptide systems (*Cerdá-Reverter et al., 2011; Cortés et al., 2014*). Therefore, the zebrafish genome has two *pomc* (*González-Nunez et al., 2003*), *agrp* paralogue genes, a single copy of *asip* gene (*Klovins and Schiöth, 2005*) and six different *mcrs* since *mc5r* duplicated (*Logan et al., 2003*). In contrast, neuronal pathways expressing *pomc* (*Cerdá-Reverter et al., 2003a; Forlano and Cone, 2007*), AGRP (*Cerdá-Reverter and Peter 2003; Forlano and Cone, 2007*) and mc4r (Cerdá-Reverter et al., 2003b) are well conserved, as is the involvement of the melanocortin system in the energy balance regulation (*Cerdá-Reverter et al., 2011*). The central administration of melanocortin agonist severely inhibits food intake in fasted goldfish (*Cerdá-Reverter et al., 2003a, 2003b*), whereas MC4R antagonists stimulate food intake in fed animals (*Cerdá-Reverter et al., 2003b*). Fasting increases *agrp* expression in the lateral tuberal nucleus, the homologue of the mammalian arcuate nucleus of goldfish (*Cerdá-Reverter and Peter, 2003*) and zebrafish (*Song et al., 2003*). Overexpression of *agrp* in transgenic models resulted in increased linear growth and adipocyte hypertrophy, suggesting that zebrafish could serve as a model for obesity research (*Song and Cone, 2007*). The AGRP-mediated suppression of MC4R activity seems critical for early larval growth (*Zhang et al., 2012*). In addition, non-functional Y-linked *mc4r* copies are associated with the larger males of *Xhiphophorus* and act as dominant-negative mutations, delaying the onset of puberty (*Lampert et al., 2010*).

In recent experiments, we generated a transgenic zebrafish strain over-expressing goldfish *asip* (*Ceinos et la., 2015*). Because ASIP is an antagonist (*Cerdá-Reverter et al., 2005*) of the constitutively activated MC4R (*Sánchez et al., 2009a*), *asip* overexpression could reduce the activation of the central MC4R resulting in enhanced growth. This model offers an excellent scenario to analyze the phenotype induced by decreased activity of the central melanocortin system, and to study the neuronal pathways downstream of the melanocortin system. Here, we demonstrate that *asip*-overexpressing zebrafish exhibit an enhanced linear growth that could be mediated by increased food intake because of a decreased satiety but also as a result of increased food efficiency.

Transcriptomic analysis reveals several candidate neuronal pathways that could mediate the melanocortin effect on food intake. Total lipid levels and profiles remained unaltered, suggesting that enhanced food intake does not result in an obese phenotype.

2. Material and methods

Animals and reagents

Wild type (WT) TU and ASIP [Tg(Xla.Eef1a1:Cau.Asip1) iim04, overexpresing asip1 (*Ceinos et al., 2015*) zebrafish strains were raised at 24-28ºC, with 14h light/10h dark cycle. *mc4r*$^{-/-}$ mutant strain *sa122* generated on Tupfel long fin background were obtained from the Sanger Institute Zebrafish Mutation Project and genotyped as previously described (*Zhang et al., 2012*). Prior any manipulation, animals were netted and anaesthetized for 1 minute in 2-phenoxy-ethanol (0.05%) in the sampling tank. When required, animals were sacrificed by rapid decapitation after anaesthesia or cold exposition. All experiments were carried out in accordance with the principles published in the European animal directive (86/609/EEC) for the protection of experimental animals and approved by the Consejo Superior de Investigaciones Científicas (CSIC) ethics committee (project number AGL2013-46448-C3-3-R). Unless otherwise indicated, all reagents were purchased from Sigma (St Louis MO, USA). Primers used in the experiments are summarized in supplementary Table 1.

Cell culture and transfection

HEK cells were maintained in DMEM media (Gibco) supplemented with 10% FBS (Gibco) and 1% penicillin/streptomycin mixture (Gibco) in a humidified atmosphere of 5% CO_2 at 37ºC. Transient transfections were carried out using Lipofectamine LTX (Invitrogen) according to the manufacturer's instructions with 25ng of each construct, and total amounts of DNA were kept constant in 2µg with pBSSK plasmid.

Pharmacological experiments

A HEK-293 cell clone (clone Q), stably expressing β-galactosidase under the control of a vasoactive intestinal peptide promoter placed downstream of tandem repetitions of cAMP responsive elements (CRE) was used to evaluate receptor activation (CRE-GAL) (*Sánchez et al., 2009a*). MCR constructs alone or in combination were transiently transfected in the clon Q. A construct carrying luciferase gene under the control of a constitutive promoter was also transfected to standardize transfection levels. The following day, cells were split up into 96-well plates and stimulated with human α-MSH (Bachem) ranging from 10^{-6} to 10^{-12} M or forskolin 10-6 in assay medium at 48h post-transfection. After 6h, the medium was removed, cells were lysed and galactosidase activity measured as previously described (*Sánchez et al., 2009a*). The effect of human ASIP (Phoenix Pharmaceuticals Inc, USA) 10-7 M on MTII-stimulated MCRs (Bachem, Switzerland) activity was studied also. Measurements were normalized for the protein content, the luciferase activity and forskolin-induced galactosidase activity. Protein content was determined using the BCA protein assay kit (Pierce). Luciferase activity was determined using the luciferase assay kit (Promega) following provider instructions. Receptor activation assays were performed in quadruplicate wells and repeated at least three times independently (n=3). EC_{50} levels after MTII or MTII + hASIP stimulation were calculated using SigmaPlot software and comparisons for each receptor were performed by t-test ($p<0.05$). Available human ASIP peptide exhibits 39% identity to zebrafish ASIP1 (*Guillot et al., 2012*).

Growth experiments

Three males and three females of ASIP or TU strain WT fish were inbred to obtain sufficient embryos for the experiment. Six hundred embryos of each group were initially reared in 15-liter tanks and fed three times a day (9.00, 13.00, 17.00 h) with rotifer and *Artemia* nauplii for 15 days. At 30 days post fertilization (dpf) animals of each group were split up into two 45-liter tanks (n=150/tank) and were fed twice a day (9.00, 17.00 h) with *Artemia* nauplii and commercial flakes (SeraVipan, GmbH), which were suspended in fresh water and administered with plastic Pasteur pipettes. The same volume of *Artemia* and/or flakes was administered to each experimental tank. Animals (n=50) were then sampled for standard length (L) and body weight (BW) and visually sexed at 90, 120 and 150 dpf. Sampled animals were not placed back into the home tanks, so that the rearing density did not increase with time. In every sampling,

six animals (3 males and 3 females) of each group (n=6) were euthanized by cold exposure for lipid determination. This experiment was carried out twice using different parental fish in order to discriminate parent-related effects. Special care was taken to maintain rearing density similar in both groups throughout the experiment as well as supported feeding amount.

Analysis of total lipids and fatty acids

Total lipids from lyophilized individuals were extracted according to Monroig et al. (2006). After evaporation of the solvent mixture under nitrogen, the lipids were dried overnight in a vacuum desiccator and quantified gravimetrically (0.01 mg, Mettler Toledo XS 105, Barcelona, Spain). Total lipids were stored at 10mg/ml in chloroform:methanol (2:1, *v/v*) which also contained 0.01% of butylated hydroxytoluene (BHT) as an antioxidant. Total lipid samples were stored at -30°C, in sealed vials, under nitrogen. Fatty acid methyl esters (FAMEs) from total lipids were prepared by direct acid transmethylation and subsequently purified by thin layer chromatography (Silca gel G 60, Merck) using a mix of hexane:diethylether:acetic acid (85:15:1.5, *v/v/v*) as the solvent phase. FAMEs were analysed with a Thermo gas chromatograph (Thermo Trace GC Ultra, Thermo Electron Corporation, Waltham, MA, USA) fitted with an on-column injection system, a FID detector, and a silica capillary column (30 m × 0.25 mm × 0.25 µm film thickness, TR-WAX, Teknokroma, Spain), using helium as a carrier gas. The analytical temperature was programmed from 50°C to 220°C. Chromatograms were integrated and analysed with Azur Datlys (St Martin d'Heres, France) software. FAMEs were identified by comparison of retention times of each peak with those of a well characterised sardine oil named Marinol (Fishing Industry Researh Institute, Rosebank, South Africa) and the FAME 37 mix from Supelco®.

Feeding experiments

For these experiments, ASIP1 (n=5, BW=0.42 g ±0.009 g) or WT (n=5, BW=0.42±0.018 g) males were individually placed into 6-liter tanks and fed with granulated diet for tropical fish [Supervit, Tropical]. Animals were supplied with 10 pellets (0.0114±0.0002 between 2-3 % body weight) at 10.00 h, and 4 hours later the uneaten pellets were siphoned and counted. The water level was made up to the original level. Food intake was calculated as the difference between the initial weight and the uneaten food weight. The reduction in weight of food in water for 4 h was <

2%. This feeding protocol was followed for 15 consecutive days (acclimatisation period). Once the feeding base line was stable, feeding levels were recorded for 5 additional consecutive days for comparison. Subsequently, the same feeding protocol was used but animals were fed twice a day at 10.00 and 15.00 h.

Stress experiments

Two experiments were made to evaluate the effects of stress on the feeding behavior of ASIP1 fish. In the first experiment, animals were subjected to acute stress induced by netting, and in the second animals were subjected to chronic stress by confinement. For the first experiment, 10 ASIP and WT adult males (n=5/group) were placed individually in 6-liter tanks and acclimated as before for 17 days. On the stress day, animals were netted, air-exposed for 3 minutes and then released back into the home tank for an additional three minutes. This protocol was repeated 3 consecutive times before placing the fish definitively in the home tanks. Subsequently, food intake was evaluated as before for 10 consecutive days. For the chronic stress experiment, 10 ASIP and WT adult males (n=5/group) were placed individually in 6-liter tanks and acclimated as before for 8 days. Fish were then placed in cylindric tanks with a cross-section of 5 cm (total volume ~ 0.2 l). Tanks were perforated to allow water circulation. These confinement tanks were placed in 40-liter tank on a platform to reach a volume of 50 ml. These conditions were maintained for two weeks and, subsequently, fish were put back into the home 6-liter tanks for an additional two weeks. Feeding levels were recorded as before.

In situ hybridization

Animals were anaesthetized and sacrificed and the tissues were carefully dissected. Muscle and brain tissues were fixed with paraformaldehyde (PAF, 4%) in phosphate buffer (PB, 0.1 M pH 7.4) overnight, dehydrated, and embedded in Paraplast (Sherwood, St Louis, MO). Serial 7 µm transverse sections were cut using a rotary microtome. Sections were mounted on 3-aminopropyltriethoxylane (TESPA)-treated slides and then air-dried at room temperature (RT) overnight. Sections were stored at 4 ºC under dry conditions and used for hybridization within one month. The in situ hybridization with sense and antisene probes were performed according to Cerdá-Reverter et al. (2003b). Brain anatomical localizations were confirmed by reference to the zebrafish atlas (*Wulliman et al., 1996*).

Central melatonin and neurotransmitters

To measure central melatonin and neurotransmitter levels forty WT (n=20) or ASIP (n=20) adult zebrafish were placed separately in two 20-liter tanks under a 14h light/10h dark cycle and fed twice a day (9.00 and 13.00 h) for 15 days. After the acclimation period, 5 females and 5 males from each genotype were sampled at 2.00 h (n=10) and 14.00 h (n=10). Brains were dissected and immediately placed at -80ºC. Brain melatonin levels were assayed by HPLC according to Muñoz et al. (2009) with modifications. Each brain was homogenized in 200 µl of 0.2 M phosphate buffer (pH 6.7) and centrifuged at 16,000 g for 10 min. A 100 µL aliquot of supernatant was mixed with 1 ml chloroform for 1 min, then centrifuged and the aqueous phase was removed. After washing with 200 µl 0.2M NaOH, the aqueous phase was aspirated and the organic volume was dried under vacuum. The residual was dissolved in 100 µl of mobile phase, filtered and injected into the HPLC. Melatonin was separated on a 5 µm C18 analytical column (Phenomenex Inc, Torrance, CA, USA). The mobile phase consisted of a solution of 85 mmol^{-1} acetic acetate, 0.1 mmol^{-1} Na2-EDTA and acetonitrile (14% of final volume), with the pH was adjusted with acetic acid to 4.7. Brain levels of noradrenaline (NA), dopamine (DA), serotonin (5HT) and the respective DA and 5HT acidic main metabolites 5-hydroxyphenylacetic acid (DOPAC), and 5-hydroxyindoleacetic acid (5HIAA) were analyzed by HPLC with electrochemical detection, as previously described (*Gesto et al., 2013*). Briefly, 20 µL of a 1:5 dilution from the brain supernatant was used to inject into the HPLC system. The mobile phase was composed of 63.9 mmol l^{-1} NaH2PO4, 0.1 mmol l^{-1} Na2EDTA, 0.80mmol l^{-1} sodium 1-octanesulfonate and 15.3% (*v/v*) methanol; pH was adjusted to 2.95 with ortho-phosphoric acid. For the acquisition and integration of chromatograms ChromNAV version 1.12 software (Jasco Corp., Tokyo, Japan) was used.

Data were normalized according to the protein content of the tissues, which was measured with the bicinchoninic acid method.

Microarray

Twenty ASIP1 (5 males + 5 females) and WT (5 males + 5 females) zebrafish were placed in 6-liter tanks and acclimated for 30 days prior to sampling to minimize physiological differences. On the sampling day, animals were sacrificed and the brain + pituitary dissected under a stereo microscope, placed in trizol and stored at -80ºC until RNA extraction. After RNA extraction (following the manufacturer's protocol), samples

were treated with DNAse (Promega). Subsequently total, RNA was quantified by spectrometry (NanoDrop ND1000) and quality was confirmed by an RNA 6000 Nano Bioanalyzer (Agilent Technologies) assay. 150 ng of total RNA were used to produce cyanine 3-CTP-labeled cRNA using the Low Input Quick Amp Labelling Kit, One-Color (Agilent p/n 5190-2305) according to the manufacturer's instructions. Following One-Color Microarray-Based Gene Expression Analysis protocol Version 6.6 (Agilent p/n G4140-90040), 1650 ng of labeled cRNA was hybridized with the Zeno Custom Gene Expression Microarray (Agilent p/n G2514F-044138). Arrays were scanned in an Agilent Microarray Scanner (Agilent G2565C) according to the manufacturer's protocol and data extracted using Agilent Feature Extraction Software 11.5.1.1 following the Agilent protocol GE1_1050_Oct12, grid template 044138_D_F_20121017 and the QC Metric Set GE1_QCMT_ Oct12. Six biological replicates (3 females and 3 males) of each group (ASIP1 and control) were analyzed in a total of 3 slides containing 4 microarrays in the 4 × 44 k format. Microarrays included 60-mer probes to the unique transcripts from Ensembl and Unigene, which were annotated by functional categories of gene ontology (GO) and pathways of Kyoto encyclopedia of genes and genomes (KEGG) with bioinformatics package STARS, which was also used for processing the data. Spot intensities were filtered by the criterion (I/B)>8, where I is the median signal and B the background intensity. The arrays were equalized according to the mean intensities. For each gene, the individual values were divided by the mean value of all samples. The log2-ER (Expression Ratios) were normalized by locally weighted non-linear regression (Lowess). The differentially expressed genes (DEG) were selected according to the criteria p<0.05 after t-test and log2ER ≥ |0.7| (1.6-fold), and analyzed using the newly developed Gene-Hub software (Afanasyev and Krasnov, unpublished data). Interactions between genotype and sex were analyzed by Two-Way ANOVA (p<0.05). Hierarchical clustering analysis of the samples followed Ward's method. Enrichment analysis was performed by comparison of counts per pathway in the lists of DEG and all microarray features that passed the quality control. Difference was assessed with Yates' corrected chi square test (p<0.05). Complete microarray results were submitted to GEO (GSE72908).

qPCR validation and expression levels

Up to 13 differentially expressed genes were validated by real-time qPCR on the same individual RNA samples used for cDNA labeling for microarray analysis. One microgram of total RNA was used for cDNA synthesis with Superscript III reverse

transcriptase (Invitrogen) primed with random hexamers and oligo(dT)$_{12\text{-}18}$ (Invitrogen). Subsequently, one microlitre of pure or diluted cDNA was added to 10 µl of 2X Taqman PCR master mix (ABgene, Thermo Scientific, Spain). Reactions were carried out in triplicate in a Realplex Mastercycler (Eppendorf). Primer and cDNA concentrations were tested for each gene and reaction efficiencies below 90% were not accepted. The housekeeping genes β-actin and elongation factor-1α (EF-1α) were used as internal reference to normalize the cDNA template between samples. The melting curves of the products were verified to confirm the specificity of PCR products. *Cart2b* expression levels in the brain of sa122 (+/+ and MC4R$^{-/-}$) were determined by qPCR as above but only β-actin was used as housekeeping gene for normalization. RNA extraction, DNAse treatment, cDNA synthesis and calculations were carried out as above.

Fasting experiments

WT (+/+, n=40) or MC4R knockout (MC4R$^{-/-}$, n=40) zebrafish were placed in two tanks and fed ad libitum for 15 days. After this acclimation period, the whole brain of ten animals (time 0) was dissected, placed in Trizol (Sigma) and frozen in liquid N$_2$ until RNA extraction. Subsequently, the whole brain of 10 WT or mutant animals was sampled after 4, 6 and 12 days of progressive fasting and samples were treated as before. Animals were always sampled at 10.00 h.

Data analysis and statistics

Receptor activation data were fitted to logistic curves using SigmaPlot software. For a graphic representation, the response average for each dose from 3 independent experiments was calculated and data were fitted to logistic and ED50 values were resumed in supplementary Table 2. For qPCRs, normalized relative quantities of mRNA expression were calculated with the mathematical method of ΔΔCt (cycle threshold). Statistical analysis comparing biometrical parameters, food intake and gene expression levels was conducted by one-way ANOVA followed by Tukey´s multiple range test or t-test but interaction between variables (sex vs genotype) when comparing biometrical parameters or lipid content was analyzed using two-way ANOVA. Differences were considered statistically significant at $P < 0.05$.

3. Results

Human ASIP is a competitive antagonist of zebrafish melanocortin receptors

In previous studies, we demonstrated that a conditioned medium of HEK-293 cells overexpressing goldfish *asip1* is able to antagonize NDP-MSH binding as well as NDP-MSH-induced cAMP production at goldfish MC1R and MC4R (*Cerdá-Reverter et al., 2005*). Since ASIP1 molecules are moderately conserved (*Cortés et al., 2014*), we explore the ability of human ASIP1 (the only ASIP1 commercially available) to act as a functional melanocortin antagonist in zebrafish receptors. We subcloned zebrafish *mc1r*, *mc3r*, *mc4r*, *mc5ra*, and *mc5rb* into expression vectors that were transiently transfected into HEK-293 cells. As expected MTII, a potent universal agonist of melanocortin receptors was able to promote cAMP-induced galactosidase activity (Fig. 1). The EC_{50} of all the receptors increased when the transfected cells were stimulated with graded concentrations of MTII in media containing ASIP1 (10^{-7} M) (supplementary Table 2) in the same way as a competitive antagonsist does. The order of potency was MC4R~MC5Ra>MC1R~MC5Rb~MC3R.

Transgenic zebrafish grow faster than WT fish

Transgenic zebrafish were longer and heavier than WT animals (Fig. 2). Differences were evident throughout the experimental period. After 6 months, transgenic males were 4.6% longer and 15.6% heavier than WT fish, while transgenic females were 14.4% longer and 62.9% heavier than their WT counterparts. Similarly, ASIP1 fish exhibited higher levels of condition factor $[BW(g)/L(cm)^{3}]$ although the difference gradually decreased as the experiment progressed. This reduction in condition factor level was also observed in WT animals. Total fat levels, as well as the fatty acid profile, were statistically similar in both ASIP1 and WT fish, confirming that ASIP1 fish were not obese. Independently of the treatment, sex differences in both total fat levels and fatty acid profiles were found (data not shown).

Under our experimental conditions WT males were significantly longer (2.5%), but not heavier, than females. This condition was reversed in ASIP1 animals, where females were significant longer (7.4%) and heavier (29%) than males. The weight of WT animals was independent of sex, whereas the condition factor was always higher in females independently of the genotype. However, ASIP1 exhibited significantly higher levels when the sex of the animals was taken in consideration except in 6-month old ASIP1 males, which showed similar condition factor levels to WT fish (Fig. 2).

Food intake levels increase in transgenic fish

To compare food intake levels of ASIP1 and WT fish, an experiment was set up in which animals were housed individually and fed once a day for 5 consecutive days after an acclimatization period. Subsequently, the same animals were fed twice a day in order to evaluate the satiation effect of the first meal (Fig. 3). When fed once or twice a day, transgenic fish ate more than WT animals during the entire experimental period. Accordingly, mean daily food intake was significantly higher in ASIP1 fish thant in WT fish. No differences in food intake levels were observed when WT fish were fed once or twice, whereas ASIP1 fish fed twice a day ate significantly more than when fed only once a day.

Transgenic zebrafish cope with stressful conditions similarly to WT fish

Two experiments were undertaken to evaluate how transgenic fish cope with stressful conditions using food intake level as a stress marker (Leal et al., 2011). In the first experiment, animals were subjected to acute stress induced by netting/air exposition whereas in the second animals were subjected to chronic stress by confinement. Acute stress induced a severe decrease in food intake levels in both WT and transgenic fish although both groups recovered during the third experimental day (Fig 4A). As mentioned above, transgenic fish exhibited higher food intake levels both before and after application of the acute stressor. Similarly, chronic stress induced a reduction in food intake levels, which gradually recovered after cessation of the stress (Fig 4B). Again, transgenic fish exhibited higher food intake levels before and after the chronic stressor, while during the stressful period and the first recovery week, levels were statistically identical
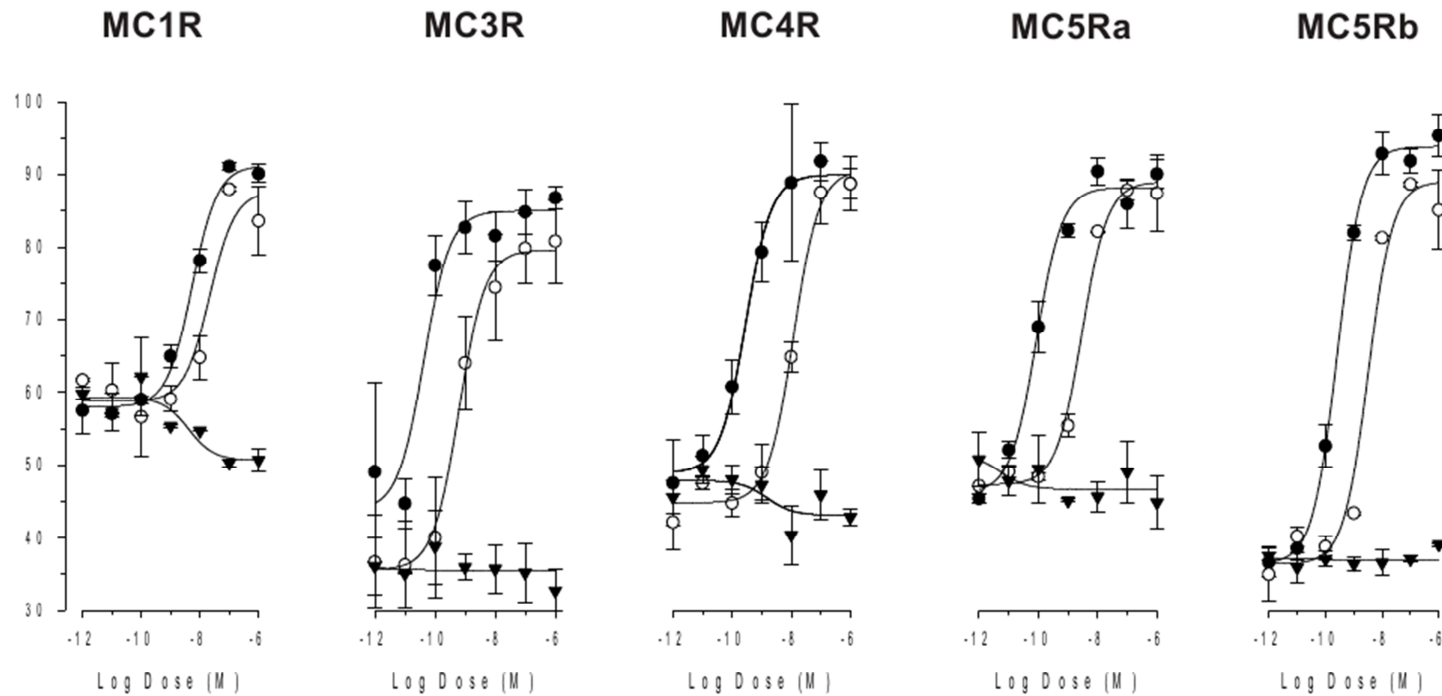
Figure 1. Effects of pig agouti-signaling protein (ASIP) on MTII-stimulated galactosidase activity in HEK-293 cells transiently expressing the different zebrafish melanocortin receptors but stably cAMP-responsive β-galactosidase reporter gene. ○ (MTII), ● (MTII + ASIP 10-7M), ▼(ASIP). Data were normalized to protein levels and expressed as percentage of the basal levels. Experiments were performed using quadruplicate data points and repeated at least three independent times. Data were normalized to protein levels and expressed as percentage of the basal levels. A construct carrying luciferase gene under the control of a constitutive promoter was also transfected to standardize the transfection levels. Experiments were performed using quadruplicate data points and repeated at least three times independently. Data are mean ± SEM of the tree independent experiments.
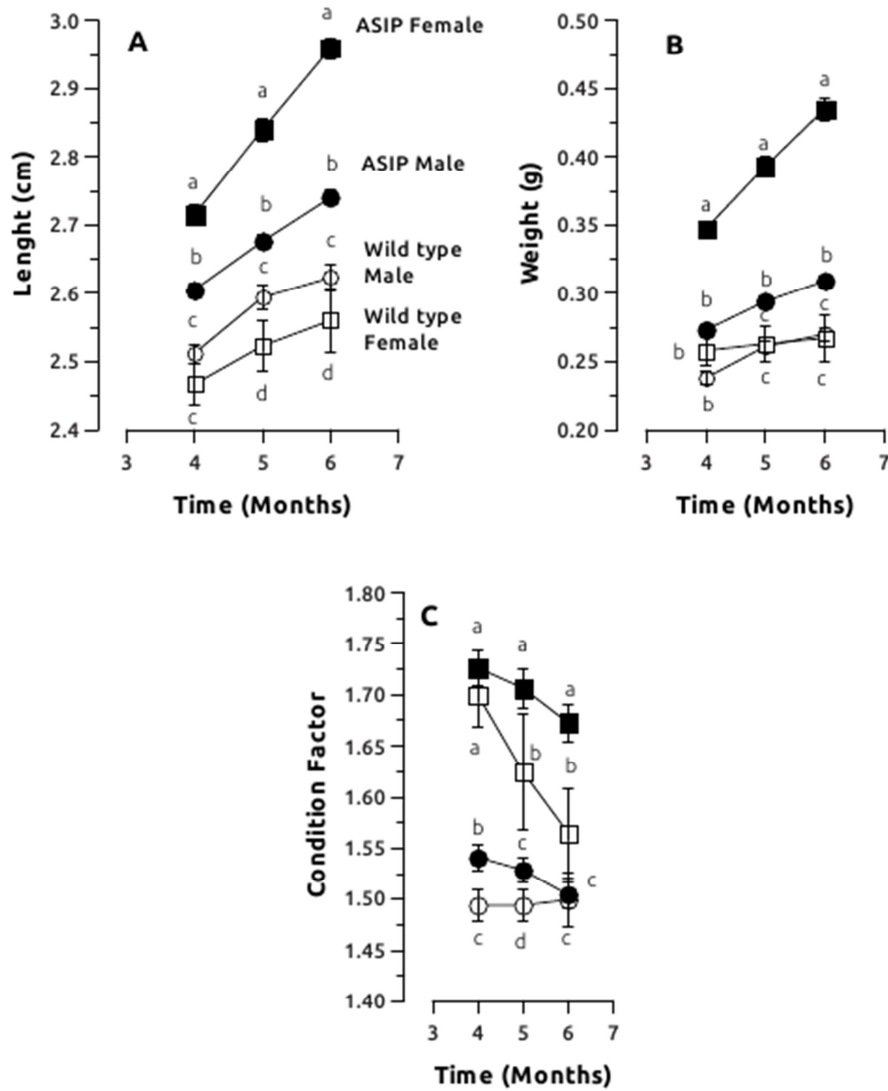
Figure 2. Overexpression of ASIP causes an increased rate of length (A), weight (B) and condition factor (CF) in the zebrafish. Animals were sampled and visually sexed at 90 (n=50), 120 (n=50) and 150 (n=50) days post fertilization (dpf). Sampled animals were not placed back in the home tanks, and so rearing density did not increase with time. This experiment was carried out twice, using different parental fish in order to discriminate parental-related effects. Different letters indicates significant differences for each sampling time after one-way ANOVA followed by Tukey´s multiple range test (p<0.05)
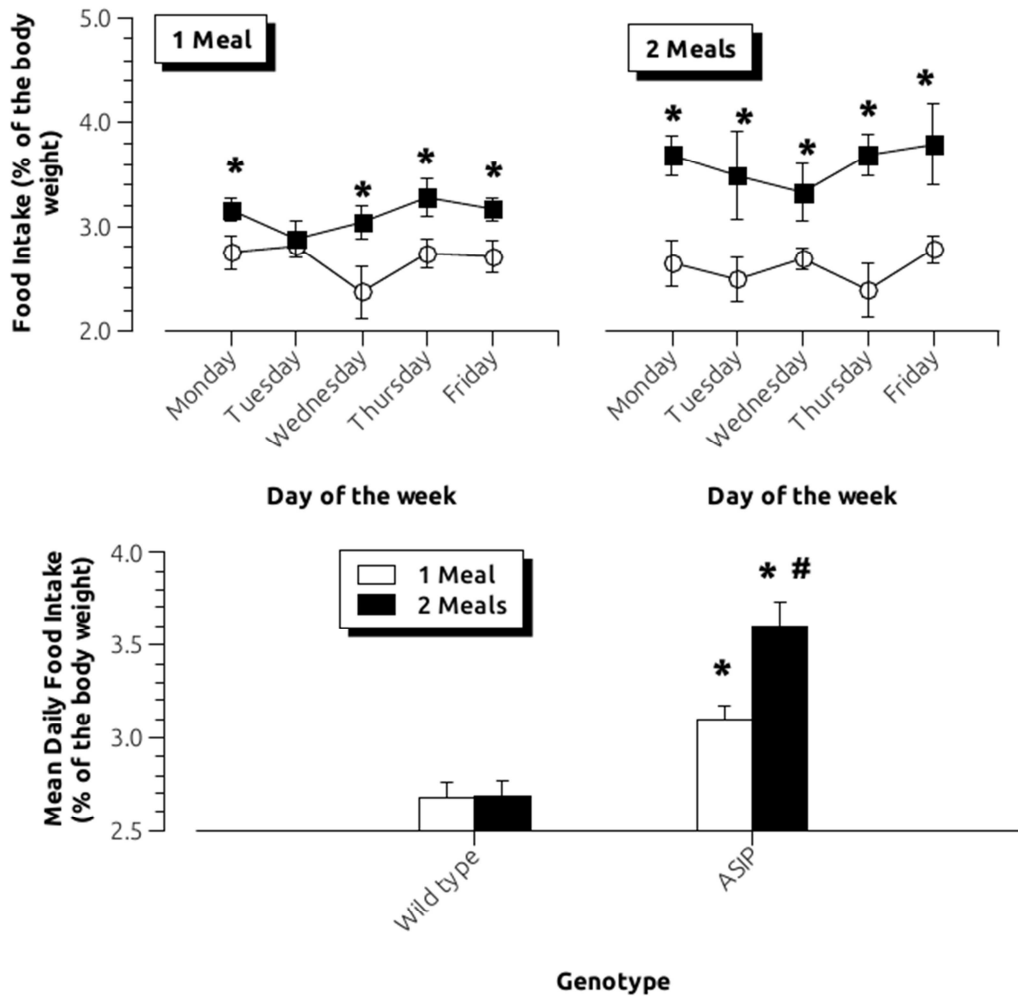
Figure 3. ASIP1 (■, n=5) or WT (○, n=5) males were placed individually into 6-liter tanks and supplied with 10 pellets of dry food at 10.00 h. Four hours later the uneaten pellets were siphoned and counted. Food intake was calculated as the difference between the initial weight and the uneaten food weight. Once the feeding base line was stable, feeding levels were recorded for 5 additional consecutive days for comparison (upper left panel). Subsequently, the same feeding protocol was used but animals were fed twice a day at 10.00 and 15.00 h (upper right panel). Bottom panel shows daily mean food intake using data from upper panels. Data were expressed as percentage of body weight. * indicates significant differences between ASIP and WT fish after one-way ANOVA followed by Tukey´s multiple range test, upper panels of t-test bottom panel (p<0.05). # indicates significant differences between 1 and 2 meals of the same genotype fish after t-test (p<0.05).
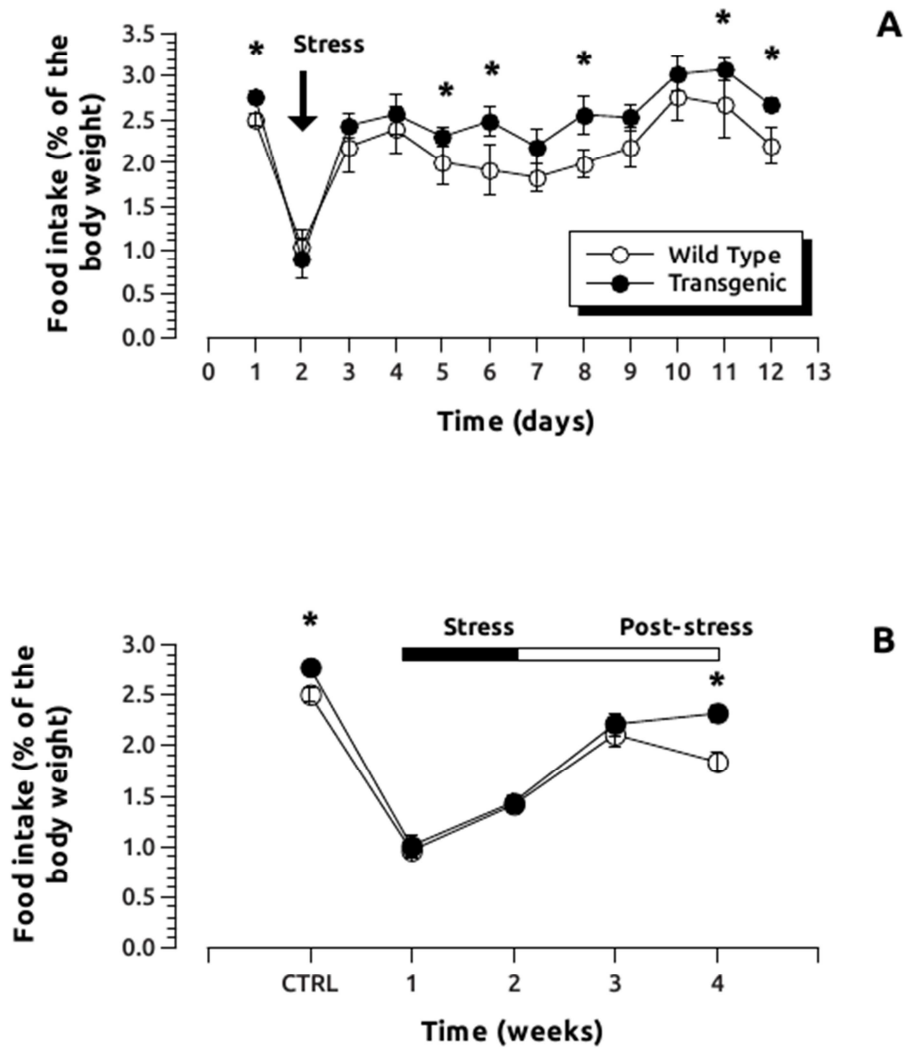
Figure 4. Effects of acute (A) or chronic stress (B) on feeding levels of ASIP (●) and WT (○) zebrafish. For acute stress experiments, ASIP and WT adult males (n=5/group) were placed individually in 6-liter tanks and acclimated for 17 days (see Fig. 3 for details). After physical stress, food intake was evaluated as before 10 consecutive days. For the chronic stress experiment, ten ASIP and WT adult males (n=5/group) were placed into cylindric tanks with a section of 5 cm (total volume ~0.2 l). Tanks were perforated to allow water circulation and placed into 40-liters tank on a platform to reach a volume of 50 ml. These conditions were kept for two weeks and subsequently, fish were put back into the home 6-liter tanks for two additional weeks. Feeding levels were recorded as before.

MC4R is profusely expressed in the zebrafish muscle and brain

In situ hybridization experiments demonstrated that MC4R is profusely expressed in zebrafish muscle (Fig. 5A) but also throughout the rostro-caudal extension of the brain, including the fore-, mid- and hindbrain (data not shown). We also observed high expression levels within the ventral and dorsal epithalamic habenula (Fig 5B). The in situ hybridization with the sense probe never generated specific signals (data not shown).
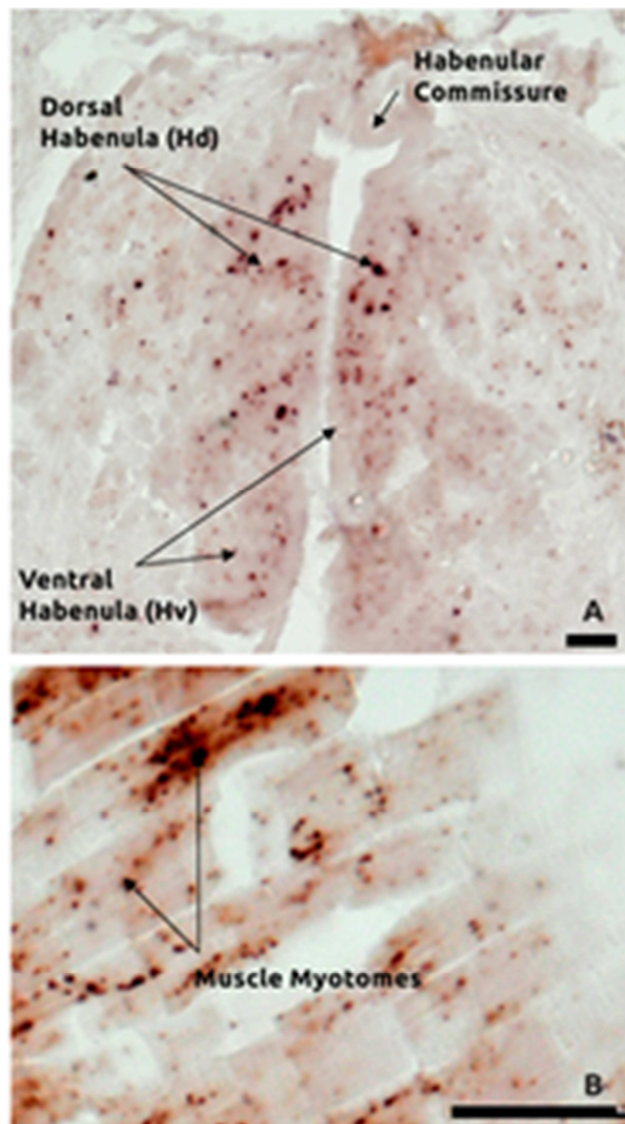

Figure 5. *In situ hybridization of MC4R the level of preoptic*
area (A) or muscle (B). Scale bar = 20 μm.

Central melatonin and neurotransmitters

As expected, WT zebrafish exhibited higher melatonin levels at night than during the photophase. Surprisingly, no statistical differences were found when comparing diurnal and nocturnal melatonin levels in ASIP zebrafish (Fig. 6A). Both male and female WT exhibited higher dopamine levels than ASIP zebrafish during the photophase (Fig. 6B). Similarly no daily differences were found in 5-HT central levels. WT females exhibited significantly higher levels than those measured in ASIP females. In addition, diurnal 5-HT levels in WT females were significantly higher than those in WT males but these diurnal differences in 5-HT central levels were not detected in transgenic zebrafish (Fig 6C). Higher levels of noradrenaline were measured in WT females during both sampling periods. Noradrenaline levels in WT females were significantly higher than those recorded in the brain of WT males during the photophase, although, again, this difference was mitigated by asip overexpression (Fig 6D).

Validation of microarray results

To confirm the reliability of microarray results, the abundance of selected transcripts was quantified using qPCR. The genes selected were those of potential interest for understanding key physiological functions such as circadian rhythms (*hiomt*), steroid biosynthesis (*srd5a1*, *hsd11b2*), the control of food intake (*adipor2*, *cart2b*, *kiss1*, *tacr3b*, *tgfbr1a*, *mboat1*), and neurotransmitter signaling (*comtb*, *dd3r*, *gabra6*). The results of the qPCR analysis were in close agreement with the microarray findings, all the genes showing significant changes in the same direction (Fig. 7).
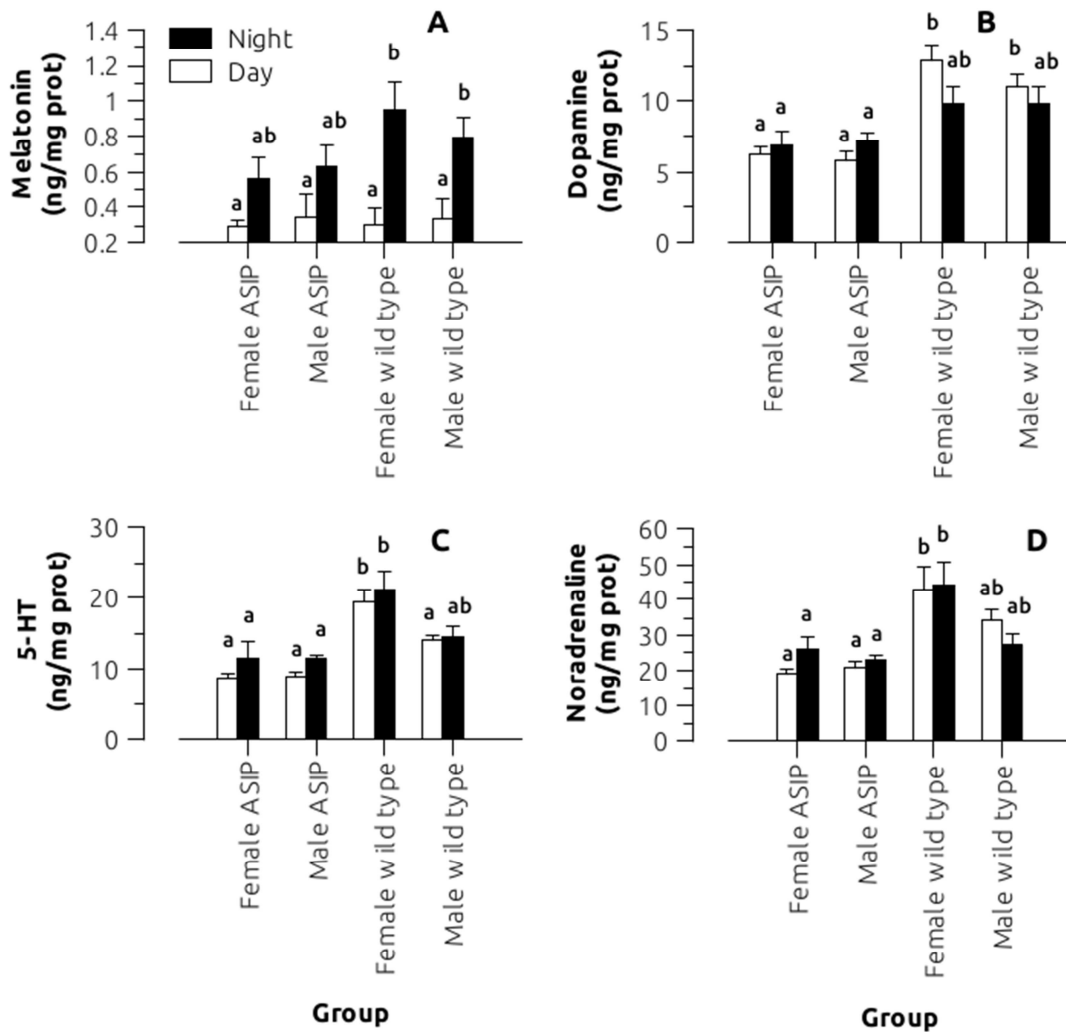
Figure 6. *Melatonin (A), dopamine (B), serotonine, 5-HT, (C) and noradrenaline (D) brain levels in ASIP. Forty WT (n=20) or ASIP (n=20) adult zebrafish were placed separately in two 20-liter tanks under 14h light/10h dark cycle and fed twice a day (9.00 and 13.00 h) for 15 days. After the acclimation period, 5 females and 5 males from each genotype were sampled at 2.00 h (n=10) and 14.00 h (n=10). Different letters indicate significant differences after two-way ANOVA (p<0.05).*
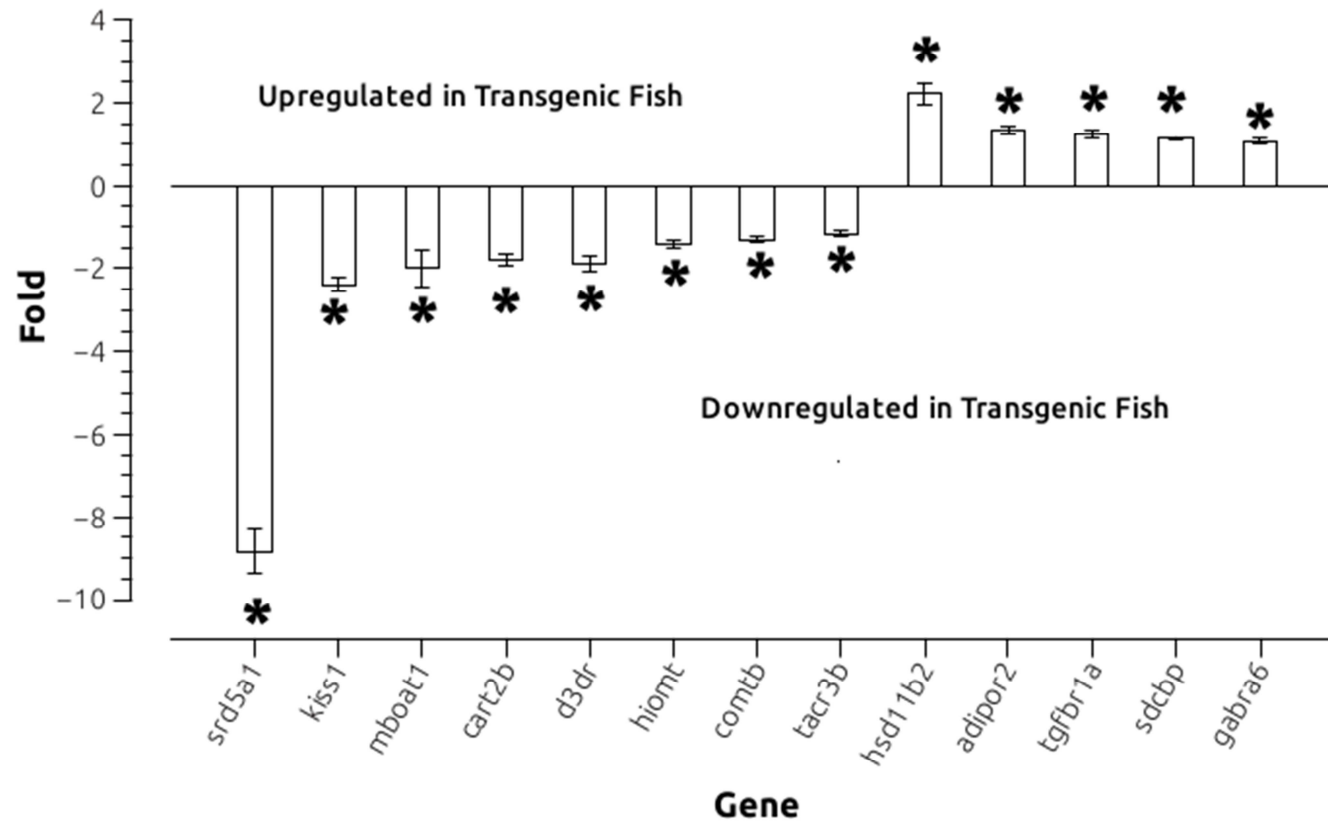
Figure 7. Genes of potential interest in the understanding of key physiological functions were selected to confirm the reliability of the microarray results. The qPCR analysis of gene expression was in good agreement with the microarray findings, all genes showing significant changes in the same direction (Fig. 7).

Characteristics of the microarray and pathways analysis

To gain new insight into the neuronal pathways involved in the melanocortin response, the central transcriptomic response was compared with the melanocortin pathway blockade mediated by *asip1* overexpression in transgenic zebrafish. The aim of this experiment was to identify functional classes of genes and individual candidates underlying susceptibility to melanocortin signalling, elucidating the functional significance of sets of DEG in some neuronal functions. Hierarchical clustering analysis successfully grouped both WT and transgenic fish. The sex of WT fish was accordingly grouped but, surprisingly, one transgenic female grouped with ASIP1 males (data not shown). As a result, the transcriptome of WT females and males was compared, detecting 255 genes to be differentially expressed (113 upregulated in females and 142 in males; see Figs. 8 and 9, and complete list in additional file 1). Initial classification of DEG by gene ontology (GO) revealed a significant degree of enrichment in functional categories related to neurotransmitter secretion (e.g. *slc6s6a*, *slc6s6*b, *nrxn1a*), synapse assembly (e.g. *pou4f1*, *nrxn1a*, *cdk5*), and steroid hormone receptor activity (e.g. *nr1d1*, *rorca*, *nr1i2*). Circadian rhythm category was also significantly affected by sex (e.g. *nr1d1*, *atoh7*, *cry2b*, *nfil3-5*, *per*3, *ciartb*) (Table 3). By contrast, statistical analysis revealed no sex-dependent KEGG pathways. When comparing ASIP1 in males and females, the number of DEG decreased to 31 (18 and 13 upregulated in females and males, respectively) and no significant enrichment in GO categories or KEGG pathways was detected (see complete list in additional file 2). Only three genes were regulated by sex independently of ASIP overexpression (*igf1*, *dio2a* and *perc*). All three genes were downregulated in the brain-pituitary complex of female zebrafish. Therefore, ASIP1 overexpression was able to abolish the differential expression of 252 sex-induced DEG (Fig. 8, additional file 1) but also to induce the differential expression of 28 additional genes (Fig. 9, additional file 2). Two-way ANOVA showed that the interaction between genotype and sex significantly affected the expression of 97 genes, meaning that genes are differentially affected by the genotype depending on the sex of the animal (see complete list in additional file 3).
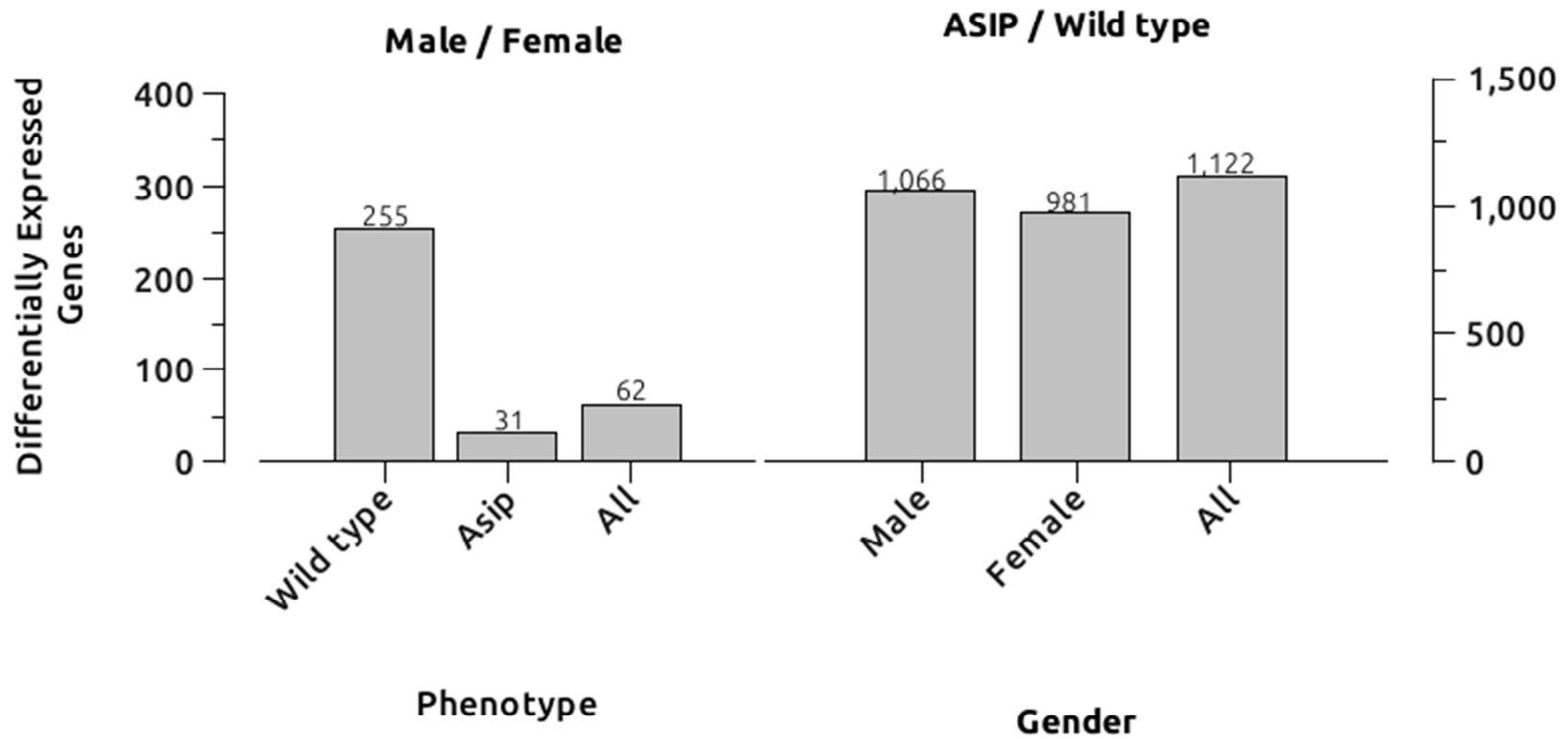
Figure 8. Differentially expressed genes (DEG) between males and females (left panel) or ASIP and WT fish after microarray analysis (see Material and Methods for details). See additional files 1, 2, 4, 5, 6 for complete listing of DEG.

Statistical analysis revealed 1122 DEG when considering only fish genotype (ASIP1 vs WT) independently of the sex of the animals (Fig. 8, see additional file 4). The KEGG pathways and GO terms significantly affected are shown in Table 4a and 4b, respectively. Analysis also revealed 1066 (543 and 523 up- and downregulated in ASIP1 zebrafish) and 981 (482 and 499 up- and downregulated in ASIP1 zebrafish) DEG when comparing ASIP males (see complete list in additional file 5) or females (see complete list in additional file 6) with their WT counterparts, respectively (Fig. 8). Tables 5 and 6 show significantly enriched KEGG pathways (5a, 5a) and GO terms (6b, 6b) in a comparison of ASIP1 males or females vs their WT counterparts, respectively. Significantly, analysis of the KEGG pathways showed that steroid hormone synthesis in the brain-pituitary complex was affected by the melanocortin system in both males (e.g. cyp1c, hsd17b8, srd5a2b, sult2st3, udpgt2b10, Table 5a) and females (e.g. cyp1c, hsd17b8, srd5a2b, sult2st3, udpgt2b10, Table 6a). This was further corroborated when the shared genes between both lists were analyzed (see below). Enrichment analysis showed that functions related to steroid metabolism, such as terpenoid backbone biosynthesis (e.g. acat, pdss2, idi1, fdps, hmgcra, hmgcs1, mvda), were also affected by ASIP overexpression in females (Table 6a). Similarly, mitochondrial function, go terms mitochondrion, mitochondrial inner membrane and mitochondrial matrix (e.g. abca12, cds2, cox5b2, cratb, cyp27a1.2, eci1, efhd1, fahd1, fpgs , ghitm, hccsa, hspd1, metaxin 1b, prkar2abas, prodha, slc25a32b, timm8b), as well as lipid transport and metabolism (acat2, apol1, gst3, plpt, sdc, stard4) were severally affected in both sexes (Table 5b and 6b). Circadian rhythms seemed to be affected only in males, as indicated by significant enrichment of the tryptophan metabolism (aanat1, acat2, aldh2, cyp1a, ddc; Table 5a) and the proper circadian rhythm GO term (aanat1, clock3, ddc, homer1b, nr1d2a, per3, 5ht-7; Table 5b). Lists of DEG in ASIP1 vs WT males and ASIP vs WT females shared 323 common DEG (Fig. 10, see additional file 7). Again, both steroid hormone (e.g. hsd17b8, srd5a2b, cyp27a1.4, cyp27a7, udpgt2b10) and terpenoid backbone biosynthesis (acat2, idi1, hmgcs1) were significantly enriched (Table 7a).

This means further that 743 (see additional file 8) and 658 (see additional file 9) genes were differentially expressed exclusively in males and females, respectively. Only, the KEGG pathway "arginine and proline metabolism" (e.g. aldh4a1, nos1, nos2a, ckba, gamt, p4ha1b, sat2b for male and agmat, aldh9a1b, ass1, ckba, dao.2, nos2a, nos2b, gatm, lap3, prodha, p4ha1b for female) was commonly affected in both males and females, suggesting that the nitric oxide pathway is involved in melanocortin signaling (Tables 8a and 9a). All GO terms enriched in males (Table 8b) were included in the enriched GO terms of females (Table 9b).
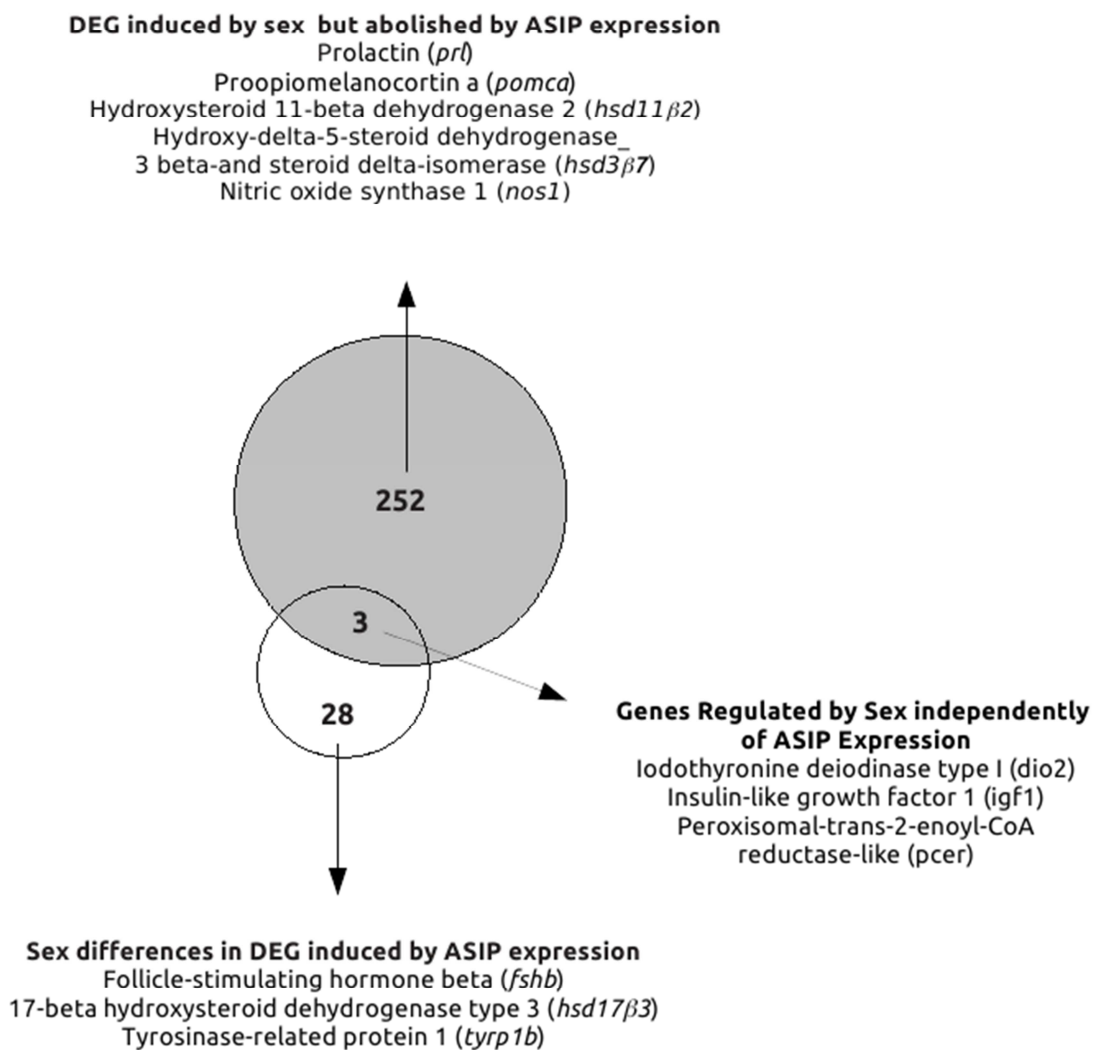

Figure 9. Comparison of differentially expressed genes (DEG) between ASIP males and females or WT males and females. Some physiologically important and common DEGs are highlighted. Complete list of DEG can be obtained in additional files 1 and 2.
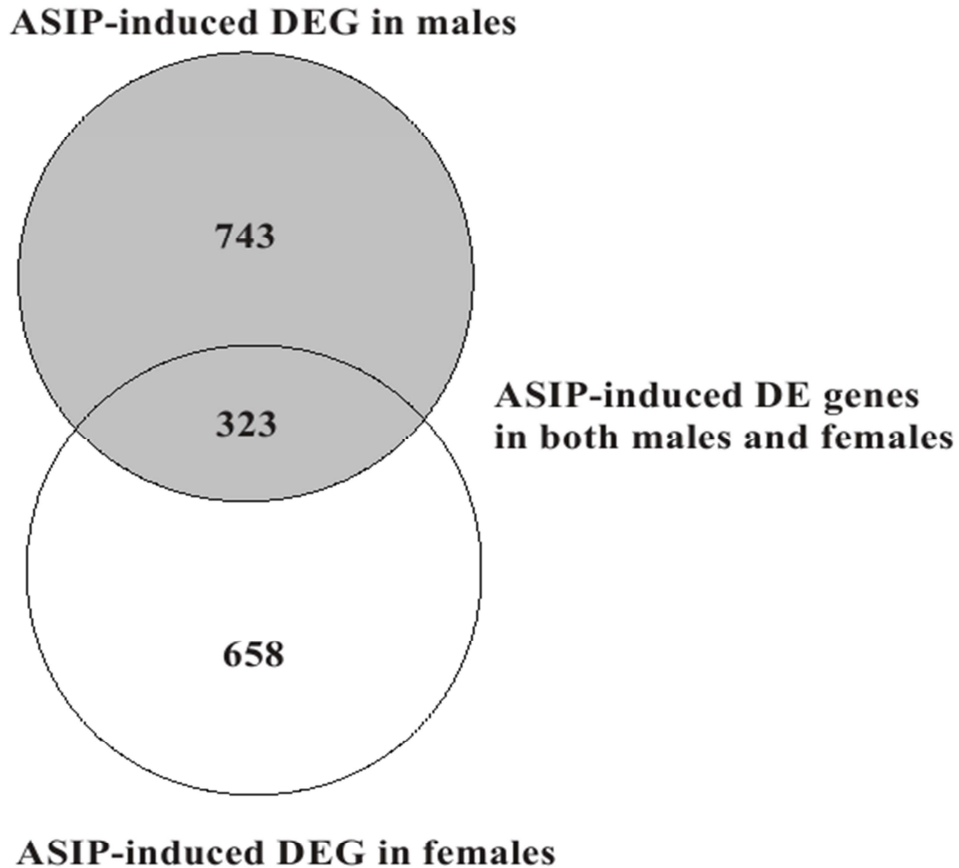
Figure 10. ASIP-induced DEG genes in both females and males. Complete lists of DEG can be obtained in additional files 5-9.

Candidate genes involved in the control of food intake

Our results demonstrate that *asip1* overexpression in a transgenic model results in enhanced growth and food intake levels as well as a differential regulation of the satiety system. Analysis of the transcriptomic results allowed us to explore individual candidates that could mediate downstream melanocortin effects on food intake. As a result, several neuronal systems involved in the control of food intake were identified which displayed a differential expression according to the genotype of the fish. For example, *neuromedin U* (*nm*u), *kisspeptin 1* (*kiss1*) and *cocaine-*and *amphetamine-regulated transcript 2b* (*cart2b*) transcripts were downregulated in both male and female transgenic fish. The *cart2b* and *kiss1* results were corroborated by qPCR. All

three neuropeptides have been demonstrated to inhibit food intake in mammals (*Howard et al., 2000, Stengel et al., 2011, Kristensen et al., 1998*). By contrast, *nitric oxide synthase 2a* (*nos2a*) was upregulated in transgenic fish. The number of *histamine N-methyltransferase* (*hnmt*) transcripts was downregulated in transgenic fish. HNMT is known to participate in the degradation of histamine, which, when administered centrally, decreases cumulative food intake and body weight in agouti yellow mice (*Ay/a*) (*Masaki et al., 2003*). Similarly, the expression of *dopa decarboxylase* (*ddc*) was upregulated in the brain-pituitary axis of ASIP1 zebrafish. DDC participates in the last step of the central synthesis of dopamine and serotonine, both of which are known to regulate food intake in vertebrates, including fish (*Leal et al., 2013*).

Asip1 overexpression also modified the sensitivity of the brain-pituitary axis to different neurotransmitter, neuroendocrine or endocrine systems by regulating receptor expression. Some of these systems are known to be involved in the control of food intake. Therefore, *tachykinin* (*tacr3l*), *dopamine* (*drd3*), and *apelin* (*aplnra*) receptor transcripts are dowregulated after *asip1* overexpression in both the male and female brain-pituitary complex. Both *tacr3l* and *drd3* were also tested by qPCR. In contrast, the expression of *adiponectin* (*adipor2a*), *cannabinoid* (*cnr1*) and *gamma-aminobutyric acid* (*GABA*) *A* (*gabra6b*) receptors are upregulated in transgenic fish. The results on *adipor2a* and *gabra6* gene expression were also corroborated by qPCR.

In addition, the expression of other receptors, including orphan receptors, was seen to be regulated by ASIP overexpression. Therefore, transcripts for *adrenergic alpha-1Ab receptor* (*adra1ab*), *tumor necrosis factor receptor superfamily member 14* (*tnfrsf14*), *cytokine receptor family member b1* (*crfb1*), *prolactin receptor a* (*prlra*), *G protein-coupled receptor 22* (*gpr22*) *G protein-coupled receptor 144* (*gpr144*), and *G protein-coupled receptor 176* (*gpr176*) were downregulated. However, the expression of *nuclear receptor subfamily 1, group D, member 2a* (*nr1d2a*), *cholinergic receptor nicotinic alpha 10a* (*chrna10a*), *transforming growth factor beta receptor 1 a* (*tgfbr1a*) and *transferrin receptor 1b* (*trf1b*) was upregulated, indicating alteration of brain-pituitay axis sensitivity.

A possible role for the central CART system in melanocortin-induced feeding

In order to evaluate the involvement of MC4R in the central expression of *cart2b*, WT (+/+) and MC4R knockout (-/-) fish were fasted and the central *cart2b* expression measured by qPCR. Progressive fasting induced a reduction in the central expression of *cart2b* in WT fish but not in MC4R knockout fish (Fig 11), suggesting that a functional MC4R is required for the fasting response of *cart2b*. Basal expression levels (time 0) were significantly lower in ASIP than in WT fish (data not shown).
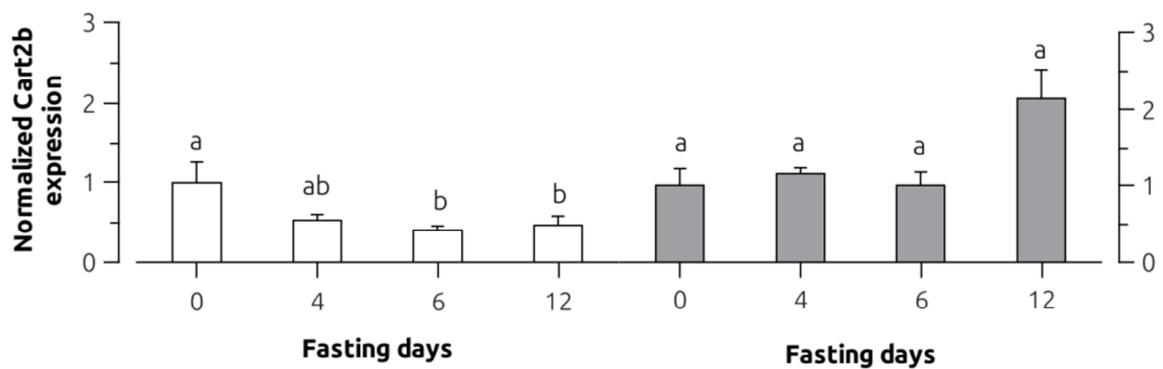

Figure 11. Effects of fasting on brain Cart2b expression of WT (+/+, n=40) or mutant strain sa122 (MC4R -/-, n=40) Animals were fed ad libitum for 15 days. Brains were dissected after 0, 4, 6 and 12 days of progressive fasting. The animals were always sampled at 10.00 h. Different letters indicate significant differences for each genotype after one-way ANOVA followed by Tukey´s multiple range test (p<0.05).

4. Discussion

In this paper, we demonstrate that *asip1* overexpression results in increased growth but not in obesity in zebrafish. Increased food intake levels mediated by a differential sensitivity of the satiety system, together with improved food efficiency, could explain the observed differences. Transcriptomic studies revealed expression differences in several central circuits involved in the control of food intake as well as modifications in the central responsiveness to neurotranstmitter, neuropeptides and

peripheral hormones known to be involved in control of the energy balance. Our data in transgenic models demonstrate that *asip* overexpression results in both increased linear growth and body weight. However, the total content and lipid profile were similar in WT and ASIP fish, suggesting that asip overexpression does not result in obesity. *Agrp* overexpression in transgenic founder zebrafish (±) produced similar results although the authors reported adipocyte hypertrophy and increased total triglyceride levels, suggesting an obese phenotype in zebrafish overexpressing *agrp* (*Song and Cone 2007*). A possible explanation for the observed discrepancy could be the different feeding rates of the experimental animals. Because fish were fed with live prey and commercial flakes, it is difficult to calculate feeding rates and so compare both experimental designs. It is plausible that restricted feeding rates result in increased growth rates but not in obesity.

Increased linear growth and obesity as a result of disruption of MC4R signaling has been reported in several rodent models including lethal (*Ay*/+) or viable agouti-yellow mice (*Avy*/+) (*Klebig et al., 1995*), AGRP transgenic mice (*Ollmann, 1997*) and MC4R knockout mice (*Huszar et al., 1997*) but also in humans (*Martinelli et al., 2011*). In zebrafish, AGRP morpholino blockage reduces larval growth but not in the absence of a functional MC4R, which, in turn, is responsible for the increased growth rate in adult zebrafish (*Zhang et al., 2012*). In addition, natural mutations affecting MC4R signaling have been shown to modify swordtail fish (*Xiphophorus nigrensis* and *X. multilineatus*) growth. Large males in this species result from multiple copies of mutant MC4R at the P locus that seem to work as a negative domain version involved in downregulating the signal transmitted by the WT receptor (*Lampert et al., 2010*). Pharmacological studies show that ASIP is a competitive antagonist at MC4R in several vertebrate species (*Lu et al., 1994*) including goldfish (*Cerdá-Reverter et al., 2005*) and zebrafish (present work). ASIP antagonism on central MC4R provides an explanation for the increased growth and obesity of dominant alleles of agouti locus (*Fan et al., 1997*). It is therefore plausible that the increased growth observed in ASIP zebrafish could be mediated by ASIP binding to central MC4R. The expression of central *mc4r* is well conserved in mammalian species when compared to fish models (*Cerdá-Reverter et al., 2003b, Sánchez et al., 2009a*). We have previously demonstrated that selective antagonism of MC4R by HS024 is able to stimulate food intake in fed goldfish, whereas MTII inhibits food intake in 24 h fasted animals (*Cerdá-Reverter et al., 2003a, 2003b*). Accordingly, ASIP fish fed once a day exhibited increased food intake levels. When fish were fed twice a day, WT animals split the amount of ingested food between both meals but ASIP fish ate more than those fed

once a day, suggesting that the satiety system of ASIP fish exhibits reduced sensitivity that allows them to increase food intake levels upon food availability. Melanocortin has been proposed as an essential substrate for the integration of long-term and short-term satiety signals. Therefore, MC4R is necessary for the cholecystokinin-induced suppression of feeding that may explain, in part, the hyperphagia and increased meal size seen in obese subjects with dampened MCR4 signaling (*Fan et al., 2004*). Our transcriptomic studies revealed ASIP-induced downregulated expression of some neuropeptides involved in the control of food intake, including the CART system. Zebrafish exhibit four different cart genes. Although the central expression of all four is downregulated by fasting in zebrafish (*Nishio et al., 2012*), only *cart2b* expression was depressed in transgenic fish. Our fasting experiments using *Sa122* allele demonstrate that a functional MC4R seemed to be necessary for the CART2b response to energy depletion. Because MC4R signaling is expected to be reduced in ASIP fish, CART2b levels may be expected to be depressed in fish lacking functional MC4R, as demonstrated by expression experiments. Interestingly, experiments in zebrafish have demonstrated that cannabinoid receptor 1 (CNBR1) lies upstream of the CART system and signals the appetite through the downregulation of cart expression (*Nishio et al., 2012*). Accordingly, anandamide, an endogenous cannabinoid, has been shown to increase food intake via CNBR1 in goldfish (*Valenti et al., 2005*). ASIP fish show upregulated cnbr1 expression and it is known that the activation of *cnr1* increases feeding by selective β-endorphin release from POMC neurons of rat hypothalamus (*Koch et al., 2015*). Taken together, the data suggest that CNBR1 neurons upstream of CART/POMC neurons express *mc4r*. Depressed MC4R signaling in ASIP fish results in dampened cart expression, probably increasing β-endorphin release, leading to the attenuation of satiety and, by extension, increasing food intake levels. However, more experiments are required to explore this hypothesis.

Other central neuropeptide systems could also participate in ASIP-induced feeding as *neuromedin U* and *kiss 1* expression have been shown to be downregulated in transgenic fish. Central administration of neuromedin U inhibits food intake in goldfish (*Maruyama et al., 2009*). Although it is known that KISS1 inhibits food intake in rats (*Stengel et al., 2011*), no studies have been reported in fish. Kiss1 is exclusively expressed in the ventral habenula and is downregulated after induction of the fear response in zebrafish (*Ogawa et al., 2014*). AGRP projections in the ventral habenula of zebrafish are scarce but α-MSH innervation is profuse (*Forlano and Cone, 2007*). The abundant expression of *mc4r* in the ventral habenula reported here suggests the involvement of hypothalamic α-MSH projections in the KISS1-mediated habenular

functions that are antagonized in ASIP fish. We propose that habenular MC4R signaling, via α-MSH binding or MC4R constitutive activity (*Sánchez et al., 2009a*), could be involved in feeding anxiety in zebrafish via caudal serotoninergic pathways (*Oiwaga et al., 2014*). In this respect, we found increased serotonin central levels in ASIP fish but differences were only statistically significant in females. Similarly, diurnal dopaminergic levels were significantly elevated in the brain of both ASIP males and females. Accordingly, *dopa decarboxilase* (*ddc*), which is involved in dopamine synthesis, and *catechol-O-methyltransferase b* (*comtb*), which is involved in the dopamine degradation, were up- and downregulated, respectively. In addition, *dopamine receptor D3* (*drd3*) was severely downregulated in transgenic zebrafish. The presence of MC4R in dopamine receptor-expressing neurons has been reported in the brain rat (*Roseberry et al., 2015*). Dopamine effects on food intake are controversial, for example, mice unable to synthesize central dopamine are hypoactive, hypophagic and die of starvation, but L-dopa restores feeding behavior (*Szczypka et al., 1999; Zhou and Palmiter, 1995*). However, earlier studies showed that the hypothalamic injection of dopamine inhibits food intake in rats (*Leibowitz and Rossakis, 1979*). Our previous studies in the sea bass demonstrated that oral L-dopa inhibits growth by reducing both food intake and feed conversion efficiency (FCE) without altering daily feeding rhythms (*Leal et al., 2013*). It is difficult to conclude that there is any dopamine-mediated effect of melanocortin-induced feeding, although it is clear that ASIP overexpression profoundly alters central dopamine metabolism and sensitivity. Interestingly, ASIP overexpression induced upregulation of inducible nitric *oxide synthase* (*nos2a*) but downregulation of the *neuronal isoform* (*nos1*). Accordingly, KEGG pathway analysis revealed an alteration of the arginine/proline metabolism. Nitric oxide seems to be among the principal components in the neuropeptide regulation of food intake (*Morley et al., 2011*) and NOS1 activation in the paraventricular nucleus suppresses feeding in mice (*Sutton et al., 2014*).

Sensitivity to central neuropeptide and neurotransmitter by modulation of receptor abundance could also account for the variations in food intake levels observed in ASIP fish. Therefore, *apelin receptor a* (*aplnra*) is downregulated but *gamma-aminobutyric acid A receptors* (*gabra6b*) are upregulated in ASIP fish. The central administration of apelin has been shown to stimulate food intake in goldfish (*Volkoff and Wyatt, 2009*). Studies focusing gamma-aminobutyric acid (GABA) involvement in the control of food intake in fish are absent, it is well know that this neurotransmitter regulates food intake in mammals via a GABA A receptor (*Wu et al., 2015*). Finally, transcriptomic data also revealed the overexpression of *adiponectin receptor 2*

(*adipor2*). Adiponectin plays important roles in the inflammation, glucose and lipid metabolism and oxidative stress in rat (*Yamauchi et al., 2007*). It is mainly produced in the adipose tissue, reaches the cerebrospinal fluid from the circulation and stimulates food intake via the activation of adipoR1/AMPK in the arcuate nucleus. Accordingly, adipo(-/-) mice fed a high fat diet exhibited decreased food intake levels (*Kubota el al., 2007*). There is little information about adiponectin in fish but it is known that adipor1/2 are insensitive to fasting in the brain of orange-spotted grouper (*Qin et al., 2014*). Therefore, increased adipoR1 expression could mean enhanced sensitivity to the orexigenic adiponectin.

Increased food intake levels provide only partial explanation for the enhanced growth rates in ASIP fish, although in the growth experiments, animals were fed with the same quantity of food, pointing to an improved conversion rate in ASIP zebrafish. The long-term administration of MC4R antagonist HS024, or agonist MTII has been shown to increase and decrease food conversion rate in rats, respectively (*Jonsson et al., 2002*). In addition, genetic analysis has demonstrated the association of MC4R polymorphisms with food efficiency in several species (*Houston et al., 2004, Davoli et al., 2012*). Therefore, ASIP fish grow more and faster not only because of the increased food intake levels but also because feed conversion efficiency is improved. The molecular basis of increased growth associated with MC4R signaling is unclear, but studies in the early stages of zebrafish development have reported a dense projection of AGRP and POMC neurons to the pituitary (*Zhang et al., 2012*). Morpholino blockage of *agrp* expression results in depressed *growth hormone* (*gh*) expression, in accordance with the increased expression of *GH-releasing hormone* (*ghrh*) and decreased expression of central *somatostatins* (*sst*) (*Zhang et al., 2012*). The present study points to the profuse expression of mc4r in zebrafish muscle fibers, suggesting that the peripheral melanocortin system could be involved in muscle energy metabolism and/or development. Therefore, MC4R signaling in the muscle could involve a physiological restrain in muscle development that could be bypassed by ASIP antagonism in transgenic fish. Ongoing experiments will elucidate the role of MC4R in muscle hypertrophy and/or hyperplasia.

Most vertebrate species, including fish, exhibit sex dimorphic growth. In our experiment, WT male were longer than WT females despite their similar weights. However, this sex dimorphism pattern was reversed in ASIP fish since ASIP females were much longer and heavier than males. Our data suggest that the melanocortin system could be involved in sexual dimorphic growth in fish. To the best of our knowledge, no data are available concerning the dimorphic effect of melanocortin on

vertebrate growth, although polymorphism analysis revealed that MC4R was associated with enhanced body weight in female broilers (*Sharma et al., 2008*). The fact that MC4R was found to be expressed in muscle fibers suggests that dimorphic effects could be peripherally or centrally mediated. Gender specific roles of melanocortin receptors in the CNS of mice have been described previously. Particularly, MC3R deletion increases dopamine levels in the ventral tegmental area (VTA) and decreases sucrose intake and preference only in females, suggesting a sexually dimorphic function of MC3R in the regulation of the dopaminergic system and reward (*Lippert et al., 2014*). Overexpression of ASIP in transgenic fish increased diurnal dopamine levels in both males and females but selectively increased nocturnal and diurnal levels of 5-HT in transgenic females, suggesting dimorphic regulation of the serotoninergic pathways. The sex dimorphic regulation of central pathways becomes more evident with an analysis of transcriptomic data. A comparison between WT males and females reveals that ~0.7% of DEG enriches GO terms related to neurotransmitter secretion, circadian rhythms and sex steroid activity. Surprisingly, when ASIP is overexpressed, the number of DEG is reduced by ~90% and no GO terms are enriched. The results show that ASIP overexpression makes more uniform the gender-induced differences in the brain-pituitary transcriptome. This is further supported by clustering analysis, which displays ASIP females grouping together with ASIP males, which, in turn, suggests that ASIP overexpression induces a masculinization of the female central transcriptome by removing differential expression ~99% of DEG but inducing 28 new DEG. Two-way ANOVA revealed a sex-genotype interaction in 97 DEG. Interestingly, *hydroxysteroid 11-beta dehydrogenase 2* (*hsd11b2*) expression was downregulated in WT females compared with WT males. This enzyme regulates the bioavailability of cortisol by catalyzing its conversion to inactive forms (*Alderman and Vijayan, 2012*). It is tempting to speculate that the cortisol metabolism and, by extension, the central response to stress can be sexually regulated; however; ASIP overexpression masked any sex dimorphic expression. Whether this possible increase in central cortisol degradation in females is related to the reversion of dimorphic growth remains to be explored. When transgene effects were analyzed according to gender, the sex-dependent response to ASIP overexpression was more evident as the list of DEG in ASIP1 vs WT males and ASIP vs WT females shared only ~30% of DEG. However, when GO enrichment of non-shared genes was compared between both lists, 100% of GO terms enriched in males were included in the list of GO terms enriched in females, which suggests that the female brain-pituitary complex is more severely affected by ASIP1 overexpression than male axis.

A common term/pathway that is noticeably affected by ASIP overexpression in both the male and female brain-pituitary axis is steroid metabolism/biosynthesis. Phenotype implications of the melanocortin-induced effects on the central steroid metabolism could cover a wide range of physiological processes as steroids exhibit pleiotropic effects. At the reproductive level, melanocortins are not critical since knockout (MC3R, MC4R), transgenic (AGRP) or genetic (lethal and viable agouti yellow) models reproduce naturally. However, it is known that the melanocortin system is involved in the regulation of sexual function and behavior (*Schioth and Watanobe, 2002; Roulin and Ducrest, 2011*). In fish, particularly in *Xiphophorus*, *mc4r* fills locus P that regulates both growth and puberty timing. Body size differences are linked to behavioral differences. Larger males court females whereas small males perform sneak mattings (*Lampert et al., 2010*). While we have no behavioral data to compare reproductive patterns in ASIP and WT fish, preliminary data support modifications in the puberty timing of ASIP zebrafish (Navarro S, Guillot R, Schultz R, Wei G, Cerdá-Reverter JM, unpublished data). Ongoing experiments will focus on the reproductive behavior of transgenic fish.

5. Conclusion

Results provide direct evidence on the involvement of melanocortin systems in fish feeding behavior and growth. We demonstrate that ASIP overexpression results in increased growth but not obesity. Increased food efficiency and food intake levels, mediated by a differential sensitivity of the central satiety system, can explain the observed differences. Female and male transcriptome is different and ASIP overexpression induces both sex-dependent and independent differences in the central/pituitary transcriptome that help to unravel the flow of melanocortinergic information through the central pathways that controls the energy balance.

6. Acknowledgements

7. Competing interest

The authors declare they have no competing interests.

8. Supplentary data

Supplementary data to this article can be found online at http://dx.doi.org/10.1016/j.yhbeh.2016.04.011.

CAPÍTULO IV

En este capítulo se constata que, en los peces cebra adultos, la administración oral de hormonas tiroideas induce un aclaramiento reversible de la pigmentación.

Los experimentos llevados a cabo con el fin de caracterizar el mecanismo molecular responsable de este aclaramiento mostraron que las hormonas tiroideas provocan una reducción del número melanocitos en las diferentes bandas (dorsales y ventrales) del pez cebra, así como una inhibición de los principales enzimas de la ruta melanogénica (Tyr y Tyrp1b). Dicha inhibición no se produce por igual en machos y hembras, revelando una regulación de la expresión de genes melanogénicos dependiente del sexo. La inhibición en ambos sexos de FoxD3, un factor de trascripción necesario para mantener la pluripotencia de las células de la cresta neural, sugiere que las hormonas tiroideas podrían afectar a la diferenciación de melanocitos adultos en el pez cebra.

Thyroid Hormones Regulate Zebrafish Melanogenesis in a Gender-Specific Manner

Raúl Guillot[1], Borja Muriaxh[2], Ana Rocha[1],
Josep Rotllant[2], Robert N. Kelsh[4],
José Miguel Cerdá-Reverter[1]

1. Department of Fish Physiology and Biotechnology, Instituto de Acuicultura de Torre de la Sal (IATS), Consejo Superior de Investigaciones Científicas (CSIC), Castellón, Spain. 12595.
2. Facultad Ciencias de la Salud, Universidad CEU Cardenal Herrera, Castellón, Spain, 12006.
3. Aquatic Molecular Pathobiology Group, Instituto de Investigaciones Marinas, Consejo Superior de Investigaciones Científicas (IIM-CSIC), Vigo, Spain. 36208.
4. Centre for Regenerative Medicine and Developmental Biology Programme, Department of Biology and Biochemistry, University of Bath, Bath, England, BA2 7AY.

Abstract

Zebrafish embryos are treated with anti-thyroidal compounds, such as phenylthiourea, to inhibit melanogenesis. However, the mechanism whereby the thyroidal system controls melanin synthesis has not been assessed in detail. In this work, we tested the effect of the administration of diets supplemented with T3 (500µg/g food) on the pigment pattern of adult zebrafish. Oral T3 induced a pronounced skin paling in both adult female and male zebrafish that was reversible upon cessation of treatment. The number of visible melanophores was significantly reduced in treated fish. Accordingly, treatment down-regulated expression of tyrosinase-related protein 1 in both sexes. We also found sexually dimorphic regulation of some melanogenic genes, such as *Dct/Tyrp2* that was dramatically up-regulated in females after T3 treatment. Thus, we demonstrated that melanogenesis is reversibly inhibited by thyroid hormones in adult zebrafish and make the discovery of gender-specific differences in the response of melanogenic gene expression. Thus, fish gender is now shown to be an important variable that should be controlled in future studies of fish melanogenesis.

1. Introduction

Fish exhibits a wide chromatic diversity that is obtained by the patterned distribution of different types of chromatophores that can be divided mainly into light-absorbing (melanophores, xantophores, erythrophores and cyanophores) and light-reflecting (leucophores and iridophores) chromatophores (*Sugimoto, 2002*). The pigment pattern of zebrafish is obtained by the patterned distribution of three different chromatophore types, i.e. melanophore, xanthophore and iridophore. In the dark stripes xanthophores occupy the most superficial hypodermal layer which is underlaid by type S iridophores. Just beneath these, a layer of melanophores is found on a deepest layer of type L iridophore, immediately above the skeletal muscle. In the interstripe region, type S iridophores lay just above the muscular layer while xhantophores are found between the tractum compactum of the dermis and the iridophore layer (*Hirata et al., 2003*) Pigment pattern in adult zebrafish is sexually dimorphic. Adult males exhibit a yellow shade that is less intense in females, while females are brighter than males. No sex differences in the patterned distribution of chromatophore have been reported (*Hirata et al., 2003, 2005*) Therefore, gender differences in zebrafish pigmentation might be expected to result from differences in the ratio of chromatophore types and/or the quantity of pigments. It is thus conceivable

that genes involved in pigment synthesis exhibit gender-specific regulation but this assumption is obviated in many experimental designs.

The synthesis of melanin is limited by the hydroxylation of tyrosine to dopaquinone mediated by tyrosinase (Tyr) activity. Dopaquinone is converted into dopachrome that serves as a substrate for tyrosinase-related protein 2 (Tyrp2) to catalyze the formation of 5,6 dihydroxyindole-2-carboxilic acid (DHICA). Tyrosinase-related protein 1 (Tyrp1) mediates the last step of melanogenesis by oxidizing DHICA to melanin (*Ito and Wakamatsu, 2008*). Anti-thyroidal compounds, such as phenylthiourea (PTU), are used commonly to prevent melanisation during embryogenesis by blocking all tyrosinase-dependent steps in the melanin pathway (*Karlsson et al., 2001*). Recent investigations have related the thyroidal system to the regulation of melanin synthesis in fish (*Walpita et al., 2007, 2009*).*Tyr* gene expression is down-regulated in zebrafish embryos showing low intracellular 3,3',5-triiodo-L-thyronine (T3) availability but exogenous T3 causes increased pigmentation thus suggesting that the activation of the thyroidal system is necessary for the regulation of the melanisation in early larvae (*Walpita et al., 2007, 2009*). On the contrary, T3 exposition or endocrine disruptors that mimic thyroid hormone activity decreased melanin pigmentation and increased apoptosis in the retina of zebrafish embryos (*Dong et al., 2014*). Accordingly, McMennamin and collaborators (*McMennamin et al., 2014*) have shown that treatment with thyroxine (T4), as well as an activating mutation in the *thyroid-stimulating hormone receptor* (*tshr/opallus*) gene, results in a paling phenomenon. Recently, we have demonstrated the presence of thyrogenic activity in commercially available fish diets that are widely used in aquaculture (*Quesada et al., 2012*). It is therefore plausible that the presence of thyrogenic activity in fish feeds could produce pigmentation anomalies in reared fish. In fact, dietary-induced pigment anomalies are common in reared flatfish including albinism or pseudoalbinism of the ocular side and hypermelanism of the blind side (*Darias et al., 2013*).

In a different study focusing the thyroidal regulation of melanocortin accessory proteins (MRAPs), we observed that adult zebrafish treated with oral T3 undergo a profound skin paling (*Agulleiro et al., 2013*), opposite to that reported in embryos (*Walpita et al., 2007, 2009*). Therefore, we design a new experiment to quantify the effect of thyroid hormones on different genes involved in the control of melanogenic pathway but also involved in the melanophore differentiation. Here, we demonstrated that melanogenesis is reversibly inhibited by thyroid hormones in adult zebrafish. We found the existence of both gender-specific patterns and response to thyroidal treatments of the melanogenic gene expression.

Thus, our results demonstrate that fish gender is a critical variable that should be controlled in studies of fish melanogenesis.

2. Material and Methods

Animals and reagents

Wild-type TU strain one year old zebrafish were raised at 24–28°C, with 14h light/10h dark cycle. All experiments were carried out in accordance with the principles published in the European animal directive (86/609/EEC) and approved by Consejo Superior de Investigaciones Científicas (CSIC) ethics committee (Project Number AGL2013-46448-C3-3-R) as well as the local ethics committee at the Instituto de Acuicultura de Torre de la Sal. Unless otherwise indicated, all reagents were purchased from Sigma (St Louis MO, USA).

Diets and feeding protocol

Animals were fed with control diet (CTRL), a granulated commercial diet [Supervit (Tropical, DE)]. To prepare the experimental diet, the amount of T3 to reach the experimental dose (500µg/g food) was dissolved in 2 ml 100% ethanol and sprayed onto 10 g of control diet, mixed, dried at room temperature and stored at 4° C. Animals were fed 4% of body weight (BW) with control or T3-containing diet. The total amount of food was divided into two meals provided at 10.00h and 14.00h. Tank water was renovated every three days.

Hormonal levels

After euthanization by overdose of anesthetic (MS-222) at 10 am, zebrafish blood from 15 CTRL (7 females and 7 males) and T3-treated (7 females and 7 males) zebrafish was collected by sectioning the caudal fin at peduncular level. Serum T3 levels were measured by ELISA (Abcam, UK) according to the manufacturer's instructions.

Sex effects on pigmentation-related genes

The whole skin of twenty adult zebrafish (10 males and 10 females) was sampled for total RNA extraction and gene expression experiments. After euthanization at 10 am by overdose of anesthetic (MS-222) and skin sampling, gonads were dissected to confirm the fish gender. Skin samples were kept at -80°C until processing for RNA extraction.

Effects of T3 on pigmentation-related genes

Ninety adult zebrafish (BW = 0.33 ± 0.05 g) were reared in four 40-liter tanks. Two tanks (n = 20 each) were fed with CTRL diet whereas the other two tanks (n = 25 each) were fed with T3-containing diet. After 7 days, animals were euthanized at 10 am as before and the whole skin was removed from 37 (19 CTRL and 18 T3-treated fish) animals and processed for total RNA extraction (see below). The same protocol was followed for 8 further days (15 day treatment in total) and skin samples were dissected from 27 animals (13 CTRL and 14 T3-treated fish) with the same aim following the previous protocol. Gonads were extracted for sexing. To study the reversibility of the T3 effect, 18 fish that had been hormone-treated for 15 days were subsequently fed with CTRL diet for a further 15 days. The experiment was done independently three times to corroborate the morphological effects, but tissue samples were only obtained in the first experiment.

Melanophore counts

To enable accurate quantification of melanophore numbers, twenty fish (10 males and 10 females from each treatment) were treated with epinephrine (10 mg/ml) for approximately 30 min. Afterwards, fish were sacrificed by anesthetic overdose, fixed in 4% paraformaldehyde (PFA) in phosphate buffer 0.1M, pH = 7.4 and imaged using an Olympus SZX16 stereo microscope. Fixation with PFA removes the pigments of xanthophores and iridophores but does not affect melanin. Melanophores within a 1 mm^2 area on the rostral portion of the second (D2) dorsal stripe as well as the first (V1) and second (V2) ventral stripe (Fig 1) were counted manually, from a lateral view, utilizing Adobe Photoshop CS2 software. The number of melanophores was plotted against the area in mm^2.
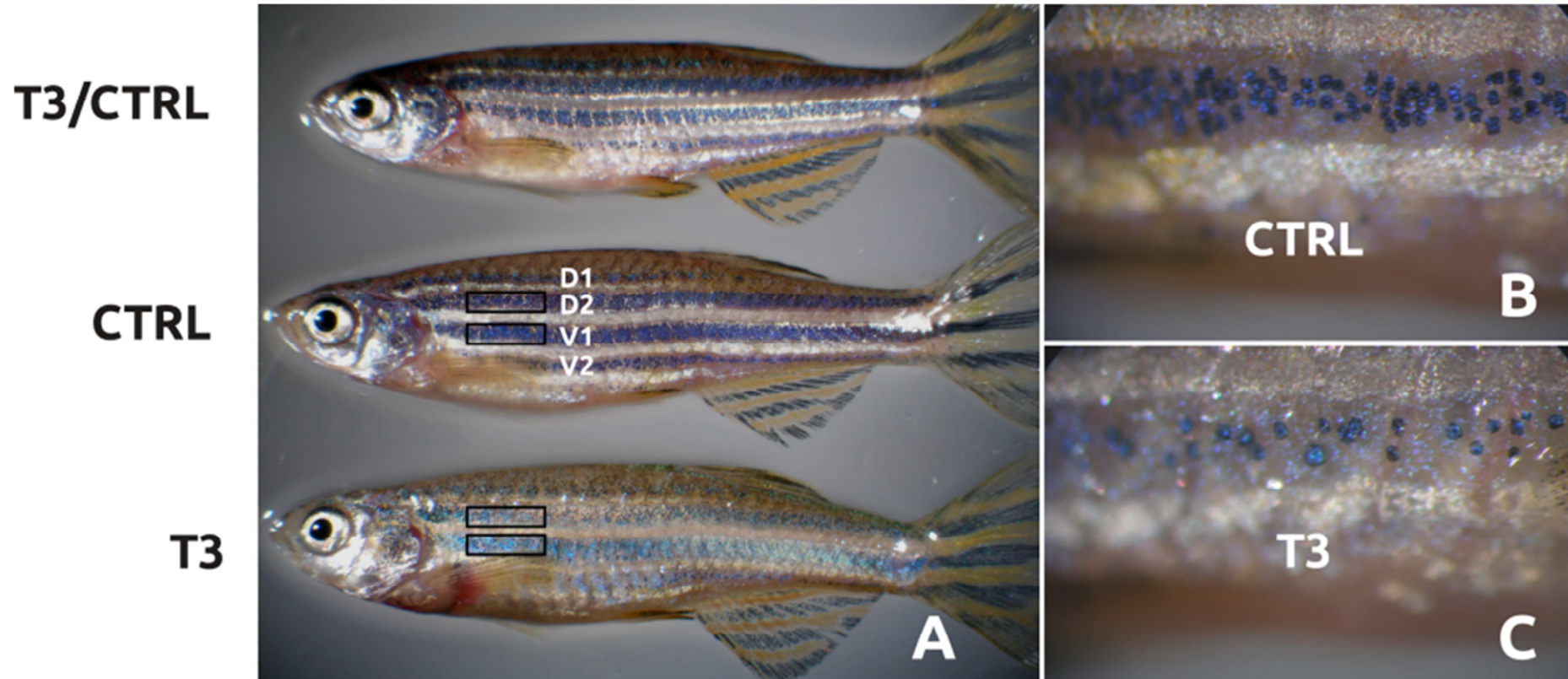
Fig 1. *Panel A shows the effects of oral T3 (500 µg/g of food) on zebrafish pigment phenotype. Fish were feed with control (CTRL) or T3-supplemented (T3) diet during 15 days and then fed with CTRL diet for 15 additional days (T3/CTRL). Higher magnification of melanic stripes in CTRL (B) and T3 (C) fish. D1 and D2, dorsal stripes 1 and 2. V1 and V2, ventral stripes 1 and 2, respectively. Boxes represent melanophore counting areas in D2 and V1.*

RNA isolation, RT-PCR and qRT-PCR

Total skin RNA was purified with Tri-Reagent and 1μg was used for cDNA synthesis with Superscript III reverse transcriptase (Invitrogen) primed with random hexamers and oligo(dT)12-18 (Invitrogen). The cDNA was subsequently used as template for quantitative real-time PCR (qPCR). The expression of genes encoding melanogenic enzymes [Tyrosinase (*Tyr*), Tyrosinase-related protein 1a (*Tyrp1a*), Tyrosinase-related protein 1b (*Tyrp1b*), Dopachrome tauromerase (*Dct* or *Tyrp2*), transcription factors [Microphthalmia-associated transcription factor a (*Mitfa* or *nacre*), Sox10 (*sox10* or *colourless*), Forkhead transcription factor 3 (*Foxd3*)], receptors [Kit receptor tyrosine kinase a (*Kita*, *sparse*), Kitb (*kitb*), Melanocortin 1 receptor (*Mc1r*)], ligands [(Agouti-signaling protein 1 (*Asip1*)] and carriers [Solute carrier family 24 member 5 (*Slc24a5*)] was evaluated by qRT-PCR. Primer and cDNA concentrations were tested for each gene and conditions with reaction efficiencies below 90% were not accepted. One microlitre of pure or diluted cDNA was added to 10 μl of 2X Taqman PCR master mix (ABgene, Thermo Scientific, Spain). Reactions were carried out in triplicate in a Realplex Mastercycler (Eppendorf, Spain). The housekeeping genes *β-actin* and *elongation factor-1alpha* (*EF-1α*) were used as internal reference to normalize the cDNA template between samples. Normalized relative quantities of mRNA expression were calculated with the mathematical method of ΔΔCt. The melting curves of the products were verified to confirm the specificity of PCR products. Primer sequences are shown in S1 Table.

Data analysis and statistics

Statistical analysis was conducted by t-test, one -way ANOVA followed by Tukey-HSD's multiple range test and two-way ANOVA. Differences considered significant when $p < 0.05$ for serum hormone levels, $p < 0.004$ for gene expression and $p < 0.01$ for melanocyte counts after Bonferroni's correction of P value for multiple tests performed simultaneously on a single data set. Data were tested previously for normality (Kolmogorov–Smirnov's test) and variance homogeneity (Bartlett's test).

3. Results

Sex-dependent expression of genes involved in Melanogenesis.

Prior to studying the gender-specific effects of T3 treatment on adult zebrafish, we set up a preliminary experiment to evaluate the differences in the expression of genes involved in melanophore development and melanin synthesis inherent to gender *per se*. The expression of *asip1*, *dct/tyrp2* and *kita/sparse* was significantly higher in males compared with females, whereas expression of *mitfa/nacre* was significantly higher in females when compared to males (Fig 2).
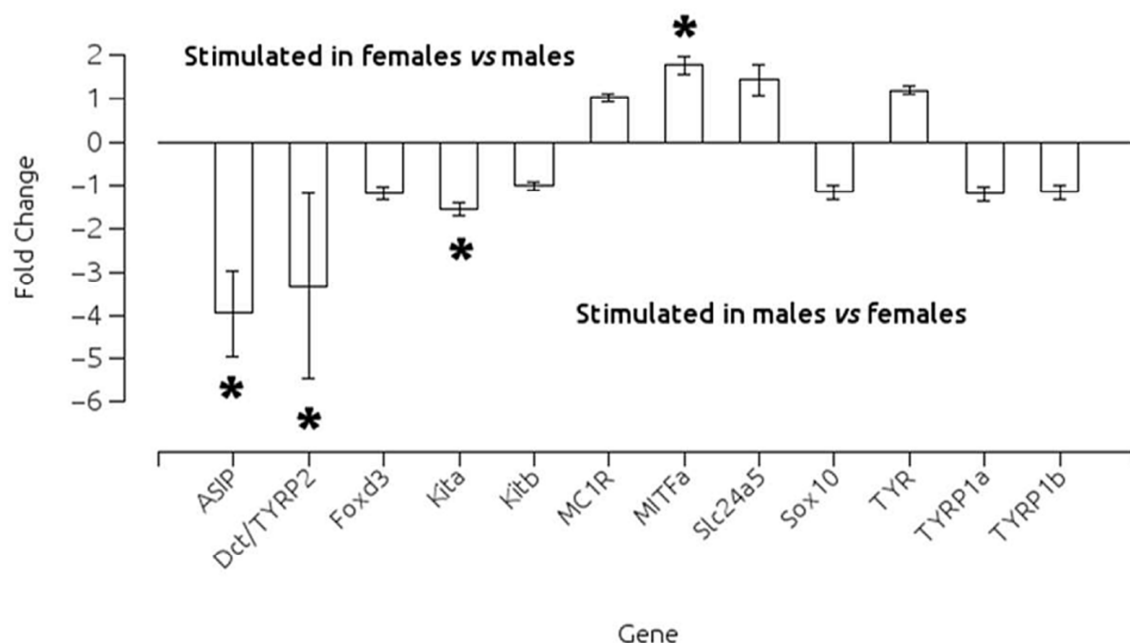

Fig 2. *Effects of gender on gene expression levels of some genes associated with the melanogenic pathways in zebrafish as measured by qPCR.Tyrosinase (tyr), tyrosinase-related protein 1a (tyrp1a), tyrosinase-related protein 1b (tyrp1b), dopachrome tautomerase (dct/tyrp2), microphthalmia-associated transcription factor a (mitfa/nacre), sox10 (colourless), forkhead transcription factor 3 (foxd3), kit receptor tyrosine kinase (kita, sparse), kitb, melanocortin 1 receptor (mc1r), agouti-signaling protein 1 (asip1) and solute carrier family 24 member 5 (slc24a5). Asterisks indicate significant differences after t-test (p<0.01) between sexes after Bonferroni's correction.*

T3 plasma levels

Oral hormone administration resulted into increased T3 serum levels in both males and females whne compared to control animals. No differences in serum levels were detected between treated males and females (Fig 3).
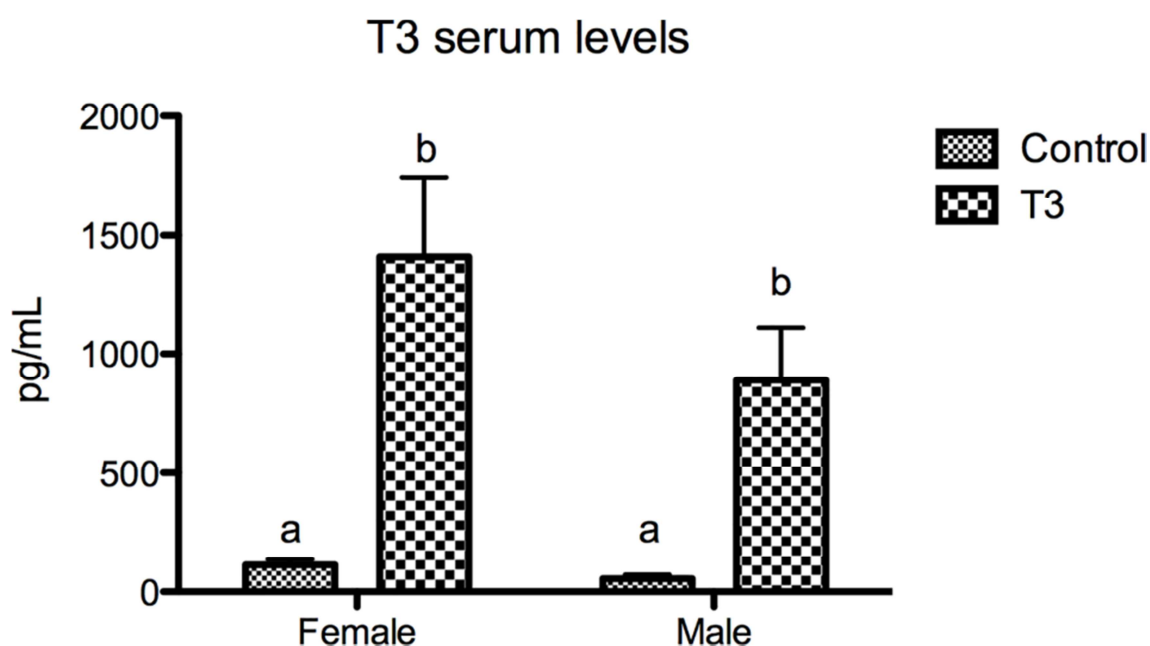

Fig 3. Serum T3 levels after hormone oral administration for 15 days. Different letters indicate significant differences after one way-ANOVA followed by Tukey's multiple range test (p<0.05). No significant interactions gender/treatement were detected after two way-ANOVA (p<0.05).

T3-induced pigment pattern is gender-specific

Previous studies demonstrated that oral T3 induced skin paling in zebrafish. Here, we wished to refine and extend these studies by assessing them for gender specific effects on melanogenic gene expression. One-way ANOVA showed that females always have more melanocytes in the ventral stripes than males and the same is true when stripes were considered altogether (Fig 4). Oral administration of T3 severely inhibited melanogenesis in zebrafish males and females. Skin paling was observed visually at 7 days (data not shown) and notably evident after 15 days of

treatment (Fig 1). When T3 treatment ceased the phenotype recovered to a normal pigmentation level within 15 days (Fig 1). Two-way ANOVA revealed both sex and treatment effects on the number of visible melanophores/mm^2 in V1, V2 and D2+V1+V2 (S2 Table) but interactions sex-treatment only reached significant values in V2. However, sex did not induce differences in D2 (p = 0.039) as T3 treatment did (p<0.001).
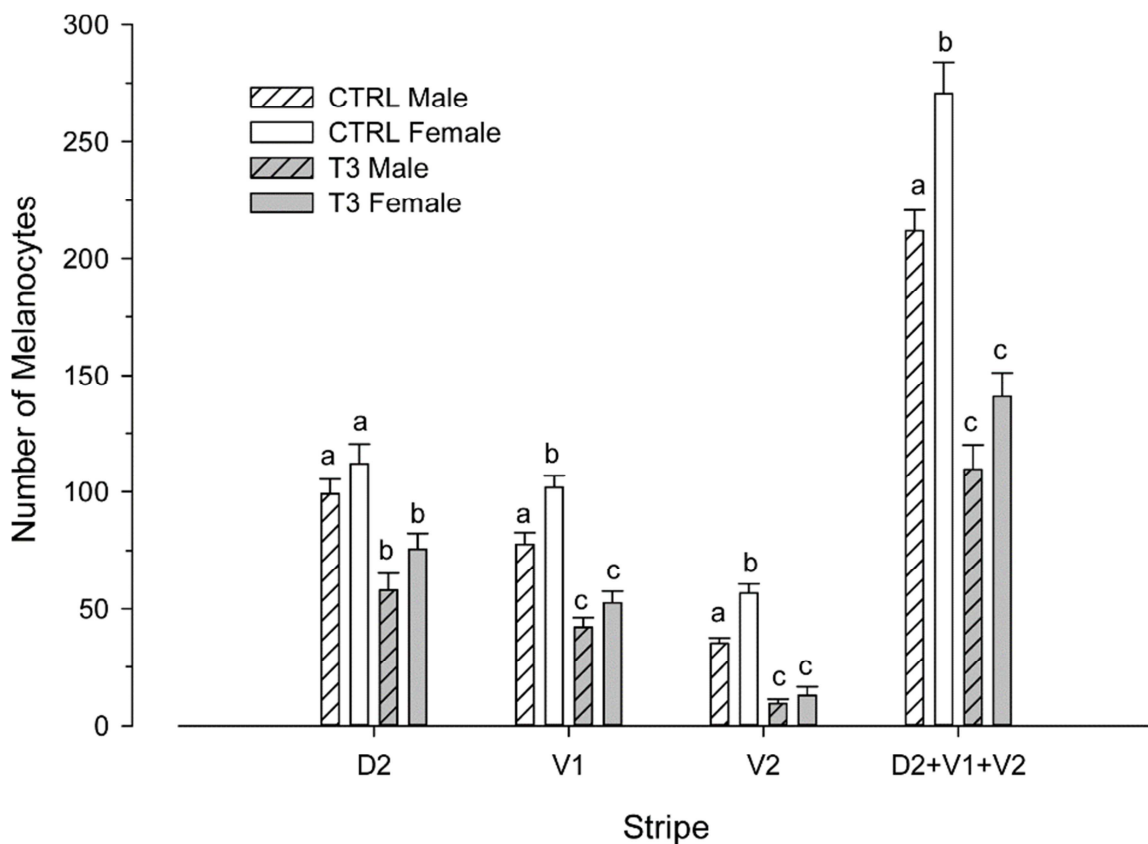

Fig 4. *Number of visible melanised melanocytes after oral supplementation of control (CTRL) diet with T3.Melanophore counts within a 1 mm2 area on the rostral portion of the second dorsal (D2) and first ventral (V1) stripes were counted manually, from a lateral view. Different letters indicate significant differences in the number of melanophores for each stripe after one-way ANOVA followed by Tukey-HSD test (p<0.05).*

Gender-specific effects of T3 on genes involved in melanogenesis

To look for subtler effects and to begin to explore possible mechanisms of paling, we turned to qRT-PCR and asked whether T3 treatment affected melanophore gene expression in a gender-specific way. First, we compared the expression of the pigmentation-related genes between both sexes of control animals and found similar results to those reported above (data not shown). We then assessed whether T3 treatment differentially affected melanophore gene expression in a gender-specific way at 7 and 14 days (Fig 5). We found both sex-dependent and sex-independent effects of T3-treatment on the expression of pigmentation-related genes. The pattern of sex-dependent effects was complex. Thus, after 7 days, T3 treatment *tyr* and *tyrp1b* expression was down-regulated in treated males (but not females) (Fig 5). After 15 days, *dct/tyrp2* was, respectively, -upregulated in females, but not significantly changed in males; in contrast, *kitb* and *tyr* were, respectively, up- and down-regulated in males, but unchanged in females (Fig 5). Two-way ANOVA revealed significant interactions treatment/gender in the expression levels of *Dct*, and *Tyr* genes after 15 days treatment (S3 Table). Gender-independent effects were also seen. Thus, at 15 days, T3-treatment inhibited *tyrp1b* and *foxd3* expression in the skin of both males and females (Fig 5).
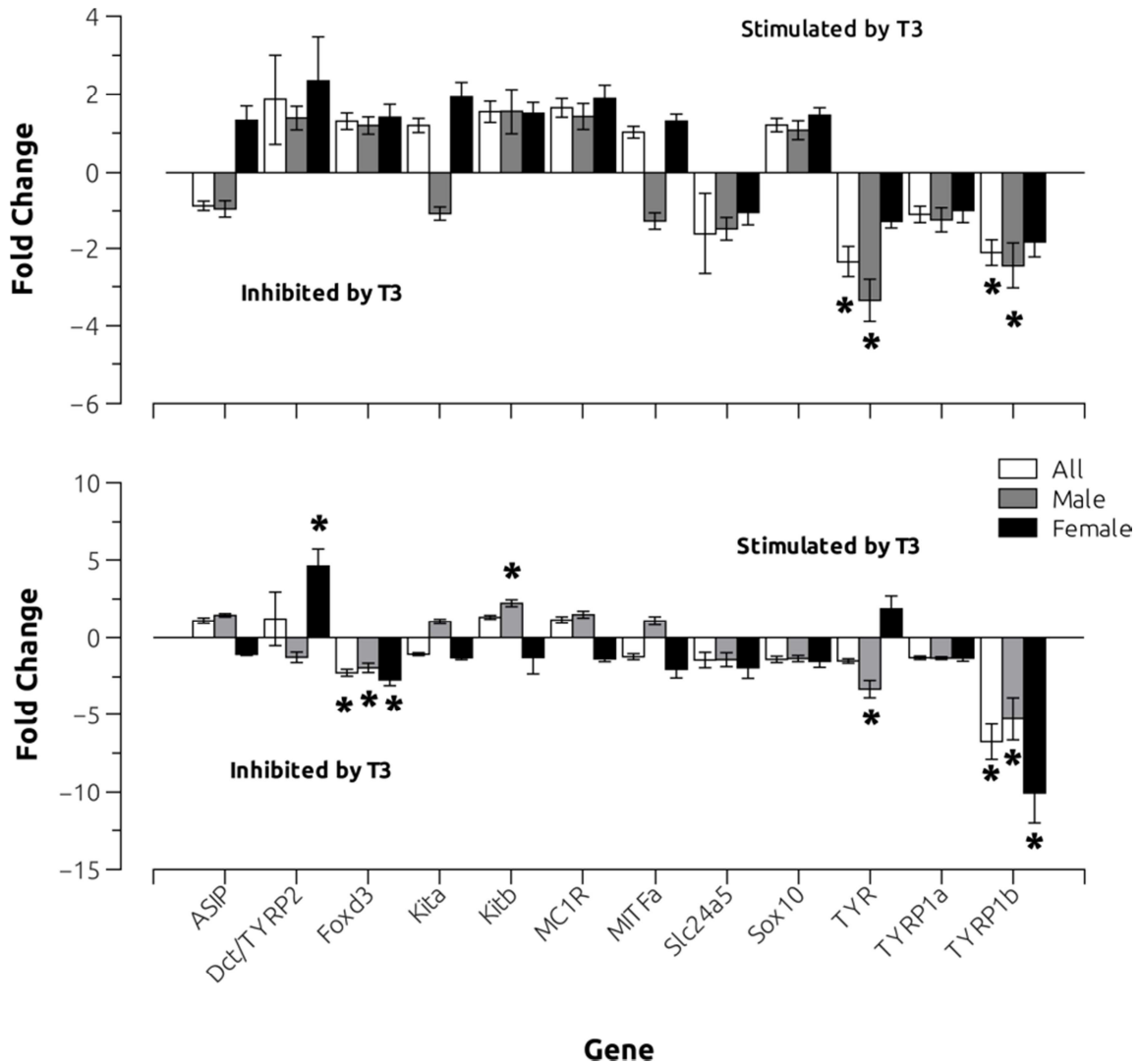
Fig 5. *Effects of oral T3 (500 µg/g of food, B) on gene expression levels of genes associated with the melanogenic pathways in zebrafish as measured by qPCR after 7 days (upper panel) and 15 days (lower panel). After 7 days post-treatment, we found 10 and 9 control females and males, respectively and 10 and 8 T3-treated females and males, respectively. After 15 days post-treatment, we found 6 and 7 control males and females, respectively and 8 and 6 T3-treated males and females, respectively. Asterisks indicate significant T3-induced differences after t-test (p<0.004) after Bonferroni's correction.*

4. Discussion

In this study, our most striking conclusion is that there are previously overlooked gender-specific differences in pigmentation, and in melanogenic gene expression patterns, in adult zebrafish. Although many zebrafish workers use body pigmentation as a guide to sexing, the emphasis is usually on the more intense yellow (xanthophore) colouration of males; the somewhat less contrasting pattern of the stripes in females is known, but whether this reflects differences in melanophore biology, or is somehow an optical illusion resulting from the xanthophore colouration has not been widely considered. Our data clearly show differences in melanophore biology in male and female zebrafish. This has important implications for studies of adult zebrafish pigmentation, since gender now becomes an important factor to control during such studies.

We demonstrate that oral administration of T3 induces skin paling by reducing the number of melanised melanophores in the zebrafish stripes. Recently, McMennamin (*McMennamin et al., 2014*) have shown that treatment with thyroid hormones result in a paling phenomenon as described here; in agreement with our study, they also show that the paling results from a decreased number of melanophores, correlating with increased melanophore death in hyperthyroid animals. A full explanation will require a more comprehensive characterization of gene expression in the skin, but our data suggest the hypothesis that inhibition of Tyrp1b expression in the skin may well contribute to this paling, since this is one effect that is consistent in fish of both genders. A dominant Tyrp1a mutation leads to melanophore death in zebrafish, perhaps through disrupting melanosome integrity (*Krauss et al., 2014*), but unfortunately the zebrafish *tyrp1b* mutant phenotype remains to be characterized. It will be important to test whether simple loss of function mutations result in decreased intensity of melanin pigment, similar to the effect seen in mouse (*Sarangarajan and Boissy, 2001*). The expression of *foxd3* was also consistently downregulated in both males and females. Foxd3 is a robust marker of pre-migratory neural crest throughout vertebrates (*Curran et al., 2009*). This transcription factor acts as a transcriptional repressor in the neural crest that is associated with the maintenance of pluripotency and pluripotent cells. In zebrafish embryos, it prevents melanophore fate by inhibiting *mitfa* expression (*Curran et al., 2009, 2010*). *Foxd3* is also expressed in putative glial cells of the peripheral nervous system (*Kelsh et al., 2000b*). Pigment cells in adult fish derive from post-embryonic stem cells of neural crest origin (*Nishimura et al., 2002; Robinson and Fisher, 2011*), associated with the

peripheral nerves and glia (*Budi et al., 2011; Dooley et al., 2013*). During post-embryonic development, a proliferative population of Erbb3b-dependent *foxd3*- and *sox10*-expressing cells associated with the peripheral nervous system differentiates into adult melanophores (*Budi et al., 2011; Dooley et al., 2013*). It is conceivable that the T3-induced *foxd3* inhibition may reflect changes in the balance of melanocyte stem cell proliferation/differentiation, but detailed investigation will be necessary to explore this idea. *Foxd3* inhibition could result from a feedback mechanism uncovered by the hormonally-induced inhibition of the melanogenesis pathway.

The effects of T3 treatment appear to vary with age. T3 treatment promotes melanisation in zebrafish embryos (*Walpita et al., 2007*), whereas morpholino-mediated knockdown of type 2 iodothyronine deiodinase (D2), delays embryonic pigmentation (*Walpita et al., 2009*). *Tyr* expression is inhibited in D2 morphants suggesting that T3 is required for the normal expression of the melanogenic enzyme in early developmental stages. T3 treatment of D2 morphants rescues the pigment phenotype as well as normalizing *tyr* expression (*Walpita et al., 2009*). These results are opposite to those in our experiments however careful observation of the photographic data reported after T3 treatment in zebrafish larvae (*Walpita et al., 2007*) suggests that T3 supplementation seems to stimulate pigmentation at 36 hours post fertilization (hpf). This phenotype is no longer visible at 72 hpf. Actually, it seems that the number of melanophores is reduced at 72hpf. Unfortunately, no quantitative studies were conducted in these studies (*Walpita et al., 2007*). In addition, an earlier study reported that the paling phenomenon can be reversibly induced by thyroid hormones during metamorphosis, (*Mukhi et al., 2007*). It is thus likely that the ability of thyroid hormones to induce paling appears sometime during metamorphosis.

The paling effect is more severe in females than in males as demonstrated by significant positive sex/treatment in V2 suggesting gender-specific contributions to the molecular mechanism. We observe a complex series of gender-independent and gender-specific regulatory changes in melanogenic gene expression but these changes cannot be attributed to gender differences in T3 metabolism since both treated male and females displayed similar serum levels after hormonal treatment. The differential expression of *tyr*, and *dct/tyrp2* demonstrate a sexually-dimorphic response of the melanogenic pathway to T3 treatment. Again, these data highlight the importance of sex in the study of adult melanogenesis in zebrafish. Can anything be said regarding the molecular mechanisms of paling and the sexual dimorphism in the severity? Our data suggests that this may come from gender specific effects on gene expression.

Consistent with the T3-induced phenotype, *tyr* expression was downregulated but only in males. Since Tyrp1 activity is downstream of Tyr activity a more severe phenotype is not expected in males. However, downregulation of *tyrp1b* expression was more severe in T3-treated females, despite it did not reach statistical significance after Bonferroni's correction ($p = 0.03$), matching the increased T3 effects in reducing of number of visible melanophores. Unexpectedly, *dct/tyrp2* expression was stimulated only in females. We do not have an explanation for the gender-specific stimulation of *dct/tyrp2* expression and more experiments are required to understand the role of the T3-stimulated **dct/tyrp2** expression levels.

In summary, we demonstrate that administration of thyroid hormones inhibits zebrafish melanogenesis due to a significant decrease of melanised melanophores and a robust decrease of *tyrp1* expression in both males and females. This effect is reversible, since cessation of the T3 treatment reverses the pigmentation anomalies back to the control phenotype, suggesting that maintenance of the adult pigment pattern is hormonally controlled. We demonstrated that some key genes related to melanogenesis are differentially expressed in males and females thus highlighting the importance of gender in the regulation of melanogenic pathways in zebrafish. Our demonstration that the response to T3 treatment is sexually dimorphic will only be explained by detailed characterization of the adult melanophore gene regulatory network. Meanwhile, our data highlight the importance of taking account of gender effects when studying adult zebrafish melanogenesis.

5. Acknowledgements

6. Supplentary data

Supplementary data to this article can be found online at http://dx. doi.org/10.1016/j.yhbeh.2016.04.011.

Discusión

General

1. Papel del sistema de melanocortinas y de las hormonas tiroideas en la regulación de la pigmentación en el pez cebra

1.1 ASIP y el patrón de pigmentación dorsoventral en los peces

En los animales en general y en los vertebrados en particular, el patrón de coloración es un elemento esencial para la correcta adaptación al medio. Algunos patrones son crípticos, permitiendo a los animales mimetizarse con el medio. Otros son vistosos, muestran su capacidad para defenderse ante una agresión. Con variaciones voluntarias o involuntarias en los patrones algunos animales pueden comunicar a sus congéneres una condición fisiológica, como la predisposición para la reproducción. Esta importancia de los patrones de coloración hace suponer que los mecanismos que regulan su organización estén bajo una fuerte presión selectiva.

Entre todos los patrones que se pueden describir en los vertebrados hay uno que se ha conservado en todas las líneas evolutivas: el patrón de pigmentación dorsoventral. Este patrón consiste en una marcada diferencia de color entre las regiones dorsales y ventrales; la zona dorsal es más oscura, mientras que la zona ventral es más clara, incluso blanca. La explicación para la aparición de este patrón en los vertebrados primitivos y su prevalencia hasta nuestros días es doble; por un lado, implicaría la protección frente a la radiación UV que incide desde la parte superior, y por otro la necesidad de camuflarse en espacios abiertos. Esta capacidad críptica es especialmente patente en los peces pelágicos. Cuando observamos el mar desde la superficie percibimos un color oscuro debido al fondo o al efecto de la profundidad, mientras que cuando contemplamos la superficie estando sumergidos percibimos claridad debido a la incidencia de la luz solar.

El número de tipos de células pigmentarias que constituyen un patrón pigmentario varía entre los diferentes grupos animales; en un extremo tenemos a los mamíferos, en los que los patrones de coloración están constituidos solo por melanocitos; y en el otro a los teleósteos cuyos patrones están determinados por hasta seis tipos de cromatóforos, destacando tres de ellos por ser los mayoritarios: melanocitos, xantóforos e iridóforos.

Las primeras investigaciones sobre la pigmentación en *Rana sp.* mostraban la presencia de un factor difusible capaz de inhibir la melanogénesis (MIF). Este factor se produciría en el tegumento principalmente en la región ventral y difundiría hacia la región dorsal creando un gradiente de concentración. Extractos parcialmente purificados, a partir de la piel ventral eran capaces de inhibir la melanogénesis inducida por α-MSH, inhibir la diferenciación de los melanoblastos, y estimular la proliferación de iridóforos (*Fukuzawa et al., 1995*). Trabajos simultáneos en ratón, demostraron que la polaridad pigmentaria en mamíferos era debida a la expresión diferencial del gen agoutí (ASP o ASIP, *Vrierling et al., 1994*). Este gen se expresa principalmente en las papilas dermales de la piel ventral, y es capaz de regular el cambio entre la síntesis de eumelanina (pigmento negro/marrón) a feomelanina (pigmento amarillo/rojo). El uso alternativo de 4 promotores diferentes permite que

ASIP regule la producción de las diferentes melaninas espacial y temporalmente, dando lugar al patrón dorsoventral de los ratones salvajes. Aunque la homología entre el pelaje de los mamíferos y la piel de los batracios es distante, algunos mecanismos de desarrollo del patrón pigmentario parecen estar conservados (*Lister et al., 1999*). La interacción de MIF con el sistema de melanocortinas antagonizando los efectos de α-MSH sugería que detrás del MIF de los batracios podría ser la proteína ASIP.

Estudios posteriores demostraron la presencia de ASIP en el genoma de los peces. Estos mismos estudios también mostraron su expresión diferencial en el eje dorsoventral, su capacidad de inhibición de la motilidad de los melanosomas inducida por α-MSH, y el antagonismo competitivo sobre MC1R y MC4R (*Cerdá-Reverter et al., 2005*). Estos resultados sugerían la equivalencia funcional entre MIF y ASIP.

1.1.1. ASIP en los peces planos (pleuronectiformes)

Hasta la fecha de inicio de esta tesis, los resultados publicados respecto a la relación de ASIP con la pigmentación en peces eran todos de carácter asociativo, por lo que era pertinente corroborar estos datos con experimentos de tipo causal. Para desarrollar este propósito empleamos peces planos (pleuronectiformes). La elección de este grupo de teleósteos se hizo en base a dos hechos. En primer lugar, porque no se habían caracterizado secuencias de ASIP en este grupo. Y, en segundo lugar, por el marcado contraste pigmentario dorsoventral que se da en todas las especies.

En los pleuronectiformes la región ocular está pigmentada y es responsable de los procesos de mimetismo, mientras que la región ciega ventral es de color blanco. Este patrón se organiza durante un complicado proceso de metamorfosis en el que las larvas pasan de una vida pelágica a una vida adulta bentónica. Al inicio de esta metamorfosis, el pez se tumba sobre uno de sus costados e inicia una reorganización de diversas estructuras y características corporales. Estos cambios morfológicos y fisiológicos deben de estar perfectamente orquestados, y dependen de la existencia de asimetrías en los ambientes organizativos.

Durante la metamorfosis, en la región ocular se produce la proliferación y diferenciación de precursores de cromatóforos latentes y en la región ciega los melanóforos existentes desaparecen y se inhibe la diferenciación de sus precursores (*Bolker and Hill 2000; Hamre et al., 2007*) Dicha asimetría puede ser debida a la expresión diferencial de proteínas que controlan positiva o negativamente la diferenciación de los cromatóforos, y de un factor inhibidor de la melanogénesis, que en este caso no puede ser difusible, ya que el cambio de coloración entre una región y otra es brusco. Este proceso parece ser relativamente lábil, ya que en régimen de cultivo intensivo el número de malformaciones pigmentarias es elevado. Se observan frecuentes casos de pseudoalbinismo dorsal, manchas blancas (sin pigmentación) en la región ocular (*Bolker and Hill 2000*), e hipermelanosis ventral, manchas oscuras (pigmentadas) en la región ciega, viéndose reducido el valor comercial de los individuos afectados.

El primer objetivo de esta tesis fue adquirir evidencias de que ASIP participa en la organización del patrón dorsoventral de los pleuronectiformes. Con este propósito caractericé las secuencias ASIP en rodaballo (*Scophthalmus maximus*) y lenguado senegalés (*Solea senegalensis*). Las proteínas deducidas en estas dos especies mantienen las características estructurales de la familia de proteínas agutí (ASIP): una región N-terminal rica en residuos básicos, principalmente lisina (K), y una región rica en prolinas (P) que precede el dominio de policisteínas (C). Este último dominio contiene 10 residuos de cisteína con un patrón de espaciado idéntico al resto de proteínas de la familia. Las dos proteínas ASIP caracterizadas no presentan la extensión peptídica tras la última cisteína característica de las secuencias descritas de AGRP. El análisis filogenético basado en el alineamiento de 30 secuencias aminoacídicas de péptidos de esta familia, mostró que las dos proteínas caracterizadas se agrupan con las secuencias ASIP1 de teleósteos.

Los tetrápodos solamente presentan dos péptidos de esta familia, un péptido ASIP y un péptido AGRP; los cuales tienen diferentes dominios de expresión, piel e hipotálamo respectivamente. Sin embargo, los teleósteos tienen cuatro antagonistas endógenos. Actualmente existen dos hipótesis evolutivas para la familia de péptidos agutí.

En la primera hipótesis propuesta por Kurokawa et al. (2006), basada principalmente en datos morfológicos, se identifica a los cuatro péptidos como ASIP1, ASIP2, AGRP1 y AGRP2. La secuencia de AGRP1 presenta una pequeña extensión peptídica tras la última cisteína del dominio C-terminal que también está presente en AGRP2, lo que sugiere un origen común. Si esta extensión C-terminal tiene implicaciones funcionales y/o farmacológicas es una incógnita hasta el momento. También, a favor de la teoría, se debe destacar que AGRP1 es un péptido procesado. En los residuos di-básicos que preceden el dominio de policisteínas presenta una serie de dianas sobre las que actúan peptidasas. Estas dianas de escisión no están presentes en las secuencias ASIP2, pero si en las AGRP2.

Para explicar el diferente número de copias entre tetrápodos y teleósteos Kurokawa et al. (2006) propone un modelo evolutivo simple. En la primera duplicación génica de la línea de los cordados (1R), el gen ancestral AGRP/ASIP se duplicaría, y estas copias divergirían hacia ASIP y AGRP. En la segunda (2R), estos genes ya diferenciados se duplican, pero las copias de ambos se perderían rápidamente, lo que explica la presencia de una única copia en los tetrápodos. En la tercera (3R), específica de teleósteos, las copias remanentes volverían a duplicarse y divergirían dando lugar a los cuatro componentes de esta familia génica en teleósteos.

Sin embargo, los estudios filogenéticos recientes implementados con las relaciones sinténicas defienden que AGRP2 no mantiene relaciones estructurales cromosómicas con el gen AGRP1 de teleósteos o cualquier gen AGRP de tetrápodos (*Braasch and Postlethwait, 2011*) Por el contrario, AGRP2 y ASIP2 sí que tienen relaciones posicionales con una región del cromosoma 8 de humano que, a su vez, mantiene paralogía con la región ASIP del cromosoma 20. Segúnesta segunda hipótesis, en los teleósteos habría una única copia de AGRP, una de ASIP1 y dos de

ASIP2 (a y b). Para explicar la presencia de estas variantes Braasch and Postlethwait (2011) proponen una ruta filogenética alternativa. Como en la hipótesis anterior un gen ancestral AGRP/ASIP se duplicaría en la 1R y las dos copias divergieron a AGRP y ASIP. En la 2R ambos genes se duplicaron dando lugar a AGRP1, AGRP2, ASIP1 y ASIP2. AGRP2 se perdió tempranamente, por lo que no aparece en ninguna línea evolutiva de los vertebrados. ASIP2 se perdió más tarde, en algún punto después de que divergiera la línea de los peces modernos, por lo que no aparece en las líneas de tetrápodos, pero si estaría presente en los ancestros de los teleósteos. En la 3R, los tres péptidos presentes en la línea basal de los teleósteos volvieron a duplicarse. La nueva copia de AGRP volvió a perderse. Lo mismo que ocurrió con la copia de ASIP1. Pero las dos copias de ASIP2 permanecieron. Por lo que, según esta hipótesis, la AGRP2 de Kurokawa et al. (2006) es en realidad la copia 2b de ASIP.

El análisis filogenético que realizamos introduciendo las nuevas secuencias de pleuronectiformes indicaba que el "cluster" de secuencias ASIP1 está más íntimamente relacionado con los "clusters" de secuencias ASIP2a y AGRP2, que con el "cluster" de secuencias AGRP1. Estos últimos resultados parecen apoyar el modelo sinténico de Braasch and Postlethwait (2011). Pero, las evidencias morfológicas que alinean AGRP1 con AGRP2 siguen teniendo mucho peso, por lo que la hipótesis inicial de Kurokawa et al. (2006) no puede ser todavía descartada. Es necesario seguir identificando secuencias de esta familia peptídica para poder afinar más sus relaciones filogenéticas.

Los experimentos de expresión llevados a cabo en las dos especies de pleuronectiformes demuestran claramente la existencia de una polaridad dorsoventral de la expresión de ASIP1; con máximos en la región ventral (o ciega). Estos resultados de expresión están en concordancia con los resultados publicados en carpa dorada mediante experimentos de "Northern blot" (*Cerdá-Reverter et al., 2005*).

Con el fin de establecer una relación causal diseñamos un experimento que permitiera establecer que papel podía jugar ASIP1 en la organización del patrón de coloración. Nuestros resultados experimentales demuestran que la inyección de ARN mensajero de ASIP1 específico en la región ocular es capaz de producir un aclaramiento de la piel dorsal en ambas especies. La reducción de la expresión de la proteína relacionada con la tirosinasa (Tyrp1), un enzima clave en la síntesis de melanina, en estas manchas claras demuestra que este aclaramiento se produce por inhibición de la melanogénesis. Estos resultados en su conjunto, defienden claramente el papel de ASIP1 en el establecimiento del patrón de pigmentación dorsoventral en los peces y su identidad funcional con el MIF.

1.1.2. El estudio de ASIP de ASIP en el pez cebra mediante el uso de un modelo transgénico de expresión ubicua

Las especies modelo son una excelente oportunidad para los estudios genéticos gracias a las posibilidades que ofrece el hecho de que sus genomas estén secuenciados. De entre todos los peces modelo, el pez cebra ha demostrado ser excelente para los estudios de biología evolutiva del desarrollo (EVO-DEVO). Todas estas ventajas hacen que el pez cebra sea un buen candidato para estudios de la regulación hormonal que incluyan niveles transcriptómicos.

El pez cebra presenta dos patrones de pigmentación temporales que se suceden durante el desarrollo. Las larvas desarrollan un sencillo patrón que es sustituido durante la metamorfosis por el patrón bandeado característico de los adultos. Estudios recientes han demostrado que el origen de las células pigmentarias larvarias y las que dan posteriormente lugar al patrón de pigmentación adulto son diferentes (*Kelsh et al., 2009; Budi et al., 2011; Dooley et al., 2013*).

En los mamíferos, todas las células pigmentarias tegumentarias provienen de una línea celular migrada directamente de la cresta neural e instalada en el tegumento durante el desarrollo embrionario. En el pez cebra, se ha demostrado que, si bien las células pigmentarias larvarias son también células directamente migradas de la cresta neural (*Kelsh et al., 2009*), las que organizan el patrón bandeado del adulto se originan en parte de una población de células indiferenciadas de la región subepitelial (*Budi et al., 2011*). Esta población de células precursoras también se origina a partir de células que han migrado desde la cresta neural, pero permanece en estado latente durante el crecimiento de la larva, activándose al iniciarse la metamorfosis (*Dooley et al., 2013*).

En la caracterización de cepas mutantes pigmentarias se observaban diferencias en como ciertas mutaciones afectaban de manera diferente a los patrones adulto y larvario. Las líneas mutantes de pez cebra Picasso (*erbb3b*) (*Budi, et al., 2008, 211*), puma *(tuba8l3)* (*Larson et al., 2010*), Bonaparte (*bcn2*) (*Patterson and Parichy, 2013*), rose (*ednrb1a*) (*Patterson and Parichy, 2013*), jaguar/obelix (*Kir7.1*) (*Iwashita et al., 2006*), schachbrett (*Tj1a*) (*Fadeev A. et al. 2015*), franke/leopard (*connexin41.8*) (*Maderspacher F. et al. 2003, Watanabe et al. 2006*), son algunas de las líneas mutantes que presentan alteraciones del patrón pigmentario adulto, pero con un patrón pigmentario larvario normal. Esto se debe a que todos estos genes están relacionados con procesos que afectan a la diferenciación de las células precursoras subepiteliales. El gen *erbb3b* está relacionado con la diferenciación de células de la glía a partir de las células precursoras migradas desde la cresta neural, las células indiferenciadas que organizan el patrón de coloración adulto se asientan en torno a estas células de la glía. Los genes *tuba8l3* y *bcn2* están relacionados con la diferenciación de nuevos melanóforos a partir de las células precursoras. Los genes *ednrb1a* y *Kir7.1* están relacionados con la supervivencia de los melanóforos durante la diferenciación y la migración al epitelio. Los genes *Tj1a* y *connexin41.*8 están relacionados con las interacciones que se establecen con los cromatóforos anexosrelaciones aparentemente críticas para una correcta organización del patrón de coloración bandeado durante la metamorfosis.

En contraposición a las anteriores, las líneas mutantes descritas con un patrón de pigmentación larvario alterado, también tienen alterado el patrón adulto. Esto es debido a que las mutaciones capaces de alterar el patrón larvario afectan a genes que regulan procesos basales de la pigmentación.

El gen *sox10* interviene en la organización de las células de la cresta neural (*Dutton et al., 2001*). Los genes *kita (Parichy et al., 1999)*, *pax3* y *pax7* (*Minchin and Hughes, 2008*) están relacionados con la correcta diferenciación y migración de células precursoras desde la cresta neural. En concreto *kita (Parichy et al., 1999)*, sirve de marcador de toda la línea celular de los melanocitos, independientemente de que sean primarios o secundarios, ya que además de estar relacionado con la migración de los precursores también está relacionado con su capacidad de diferenciación y/o supervivencia. Los genes *cfs1r (Parichy et al, 2000; Parichy and Turner 2003)*, *mifta (Lister et al., 1999)* y *ltk (Lopes et al., 2008)* sirven como marcadores de otros tipos de cromatóforos, al estar relacionados con la capacidad de diferenciación y/o supervivencia. Los genes *slc24a5 (Lamason et al., 2005)* y *tyr (Kelsh and Eisen, 2000)* están directamente relacionados con la síntesis de los pigmentos.

Nuestros análisis previos del patrón temporal de expresión de ASIP1 en el pez cebra mostraron que los niveles de expresión aumentan paulatinamente durante el desarrollo embrionario alcanzando los niveles máximos al inicio de la metamorfosis. Por el contrario, la expresión diferencial dorsoventral no es patente hasta la fase final de la metamorfosis (30 días tras la eclosión). Estos datos indican que ASIP1 no es determinante en la adquisición del patrón larvario, pero cobra especial relevancia al iniciarse la metamorfosis, sugiriendo que la expresión de ASIP1 es la encargada de generar el ambiente endocrino adecuado para que se pueda organizar del patrón de pigmentación dorsoventral.

Aprovechando las técnicas de transgénesis desarrolladas en esta especie y el conocimiento de su genoma nos planteamos el desarrollo de una nueva línea de peces cebra transgénicos que sobre-expresara el gen ASIP1 bajo el control de un promotor ubicuo. Esta expresión ubicua de ASIP1 nos permitiría obtener un doble fenotipo potencial; con alteraciones en la pigmentación, vía la interacción con el MC1R tegumentario, y con un comportamiento de ingesta y crecimiento alterado, vía el MC4R cerebral. La línea transgénica fue desarrollada mediante el sistema de transposición Tol2 (*Kawakami K, 2007*) colocando el gen de la carpa dorada (con una identidad proteica mayor al 90%) (*Cerdá-Reverter et al., 2005*) bajo el control del promotor del factor de elongación 1α y utilizando embriones en estado de 1-2 células para la micro-inyección de ADN. La elevada identidad proteica aseguraba la conservación de la función, pero las pequeñas diferencias en la secuencia de ADN proporcionaban un sistema más flexible para el genotipado de los animales.

En lo que respecta a la pigmentación, la hipótesis de partida fue que ASIP 1 inhibiría la melanogénesis produciendo un fenotipo albino similar al de la cepa mutante de peces cebra *nacre*. En esta cepa mutante el gen MITFa está inactivado, lo que impide la diferenciación de melanóforos (*Lister et al., 1999*). La sobreexpresión de ASIP1 reduciría notablemente, o podría llegar a anular totalmente, la estimulación MC1R con el concomitante descenso de la actividad MITFa.

La observación macroscópica de los individuos transgénicos evidencia la desestructuración del patrón de pigmentación dorsoventral sin afectar sustancialmente el patrón bandeado. Este fenotipo sólo puede apreciarse claramente en individuos que ya han completado la metamorfosis, y es especialmente visible cuando se observa a los animales desde la parte superior.

El recuento celular demuestra una drástica reducción del número de melanocitos del área más dorsal pero solo una sensible o inexistente reducción en los melanóforos de las bandas pigmentadas con melanina (bandas oscuras) situadas por debajo del mioseptum. Los experimentos de expresión cuantitativa en la cepa salvaje demuestran la existencia de un gradiente de expresión a lo largo del eje dorsoventral, con niveles máximos en la región ventral y mínimos en la dorsal. Dicho gradiente no aparece en los peces transgénicos. La sobreexpresión de ASIP1 redujo de forma significativa la expresión de MITF y de otros genes que codifican enzimas directamente relacionados con la síntesis de melanina (*dopacroma tautomerasa* ó *dct*, y *tyrp1b*) en la región más dorsal pero no en las bandas mediales o más ventrales. Estos resultados, en su conjunto, confieren una base molecular a la ruptura del mecanismo de regulación del patrón de pigmentación dorsoventral.

El análisis de la expresión de *xdh* (marcador de la síntesis de pteridinas en los xantóforos) y *ltk* (marcador de la línea celular de los iridóforos) mostró que no existían diferencias remarcables entre la cepa salvaje y la cepa transgénica sugiriendo que la sobreexpresión de ASIP1 afecta principalmente a los melanocitos.

La conclusión que se puede extraer a partir de estos resultados es que el pez cebra postmetamórfico presenta dos patrones de pigmentación simultáneos, un patrón dorsoventral ancestral, sobre el que se impone un patrón bandeado específico. Ambos patones se regulan de forma independiente ya que la sobreexpresión de ASIP1 modifica el primero, pero no altera el segundo.

1.2. Las hormonas tiroideas en la regulación hormonal de la melanogénesis.

En un experimento diseñado para el estudio del control hormonal de la expresión de las MRAPs se observó que la administración de 3,3',5-triiodo-L-tironina (T3) en la dieta de peces cebra adultos inducía un aclaramiento de las bandas oscuras en el pez cebra. Este cambio es reversible, de manera que, al dejar de suministrar la hormona, el individuo recuperaba su pigmentación original. Los resultados hacían suponer que las hormonas tiroideas eran capaces de inhibir la melanogenesis y/o la diferenciación de los melanóforos en el pez cebra.

El primer paso fue comprobar que efectivamente la hormona administrada oralmente alcanzaba el sistema circulatorio. El análisis del plasma mediante ELISA mostró diferencias significativas en los niveles plasmáticos de hormona tiroidea entre los peces alimentados con piensos tratados y los controles; no existiendo diferencias significativas entre machos y hembras. Tras comprobar que la vía de administración tenía efectos sistémicos, cuantificamos la reducción en la pigmentación mediante la estimación del número de melanóforos visibles (con presencia de melanina) en tres de las bandas oscuras, en concreto la V1, la V2 y la D1. El tratamiento indujo una fuerte reducción en el número de melanóforos visibles tanto en la banda dorsal (D1) como en las dos bandas ventrales (V1, V2) en machos y hembras. Sin embargo, las hembras no tratadas siempre exhibieron mayor número de melanóforos que los machos control en las bandas ventrales (V1, V2), una diferencia sexual que desaparece en los animales tratados. Estos resultados indican un efecto diferencial del tratamiento dependiente del sexo.

El siguiente paso fue estudiar la correlación entre la reducción del número de melanóforos inducida por T3 con la expresión génica de los principales enzimas y factores de transcripción implicados en la síntesis de melanina y/o diferenciación de melanóforos. Dadas las diferencias sexuales observadas primero estudiamos la expresión diferencial de dichos genes. El análisis mostró que los machos presentan niveles de expresión de *Asip*, *Dct* (*Tyrp2*) y *Kita* más elevados que las hembras mientras que estas muestran mayores niveles de expresión de *Mitfa*. Por tanto, el tratamiento con T3 indujo diferencias de expresión, tanto dependientes como independientes del sexo.

Tras 15 días de tratamiento con T3, la expresión de *FoxD3* y *Typr1b* fue inhibida en ambos sexos, la de *Dct* fue estimulada solamente en hembras, y las de *Kitb* y *Tyr* fueron estimuladas e inhibidas, respectivamente solamente en los machos. La inhibición de *Tyrp1b*, tanto en machos como en hembras, sugiere que este gen es el principal responsable del efecto inducido por T3. Las mutaciones dominantes con pérdida de función para *Tyrp1a* conllevan la muerte de los melanóforos en el pez cebra (*Krauss et al., 2014*), pero desafortunadamente las mutaciones para *Tyrp1b* no se han caracterizado todavía en peces. Sería interesante comprobar si la pérdida de función de *Tyrp1b* produce también una reducción en la intensidad de la pigmentación melánica como ocurre en el ratón (*Sarangarajan y Boissy, 2001*).

La expresión del factor de transcripción FoxD3 también fue inhibida en ambos sexos por el tratamiento con T3. Este factor de trascripción es un sólido indicador de las células pre-migratorias de la cresta neural, a partir de donde se desarrollan los cromatóforos y supone un freno transcripcional que mantiene las células de la cresta en estado pluripotente. En los embriones de pez cebra, inhibe la expresión de Mitfa previniendo así la diferenciación de los melanóforos (*Curran et al., 2009; 2010*). Sin embargo, *FoxD3* también se expresa en las células gliales del sistema nerviosos periférico (*Kelsh et al., 2000b*). De hecho, las células pigmentarias adultas derivan de células madre post-embrionarias acantonadas entre las células gliales y neuronas de los nervios periféricos (*Budi et al., 2011*). Una posible explicación es que la inhibición de *FoxD3* inducida por T3 refleje cambios en el balance de proliferación y

diferenciación de células madre de los melanóforos. Es decir, el tratamiento con T3 podría inducir una inhibición de la diferenciación de los melanocitos que conllevaría el aclaramiento de la pigmentación. Esto, a su vez, provocaría la consecuente inhibición de *FoxD3* y estimulación de *Mitfa*, lo que permitiría una nueva ola de diferenciación con la que contrarrestar el efecto de la T3. El tratamiento con T3, induciendo la inhibición de la maduración, habría revelado este proceso de retroalimentación. Sin embargo, se requieren más experimentos para comprobar dicha hipótesis.

Nuestros experimentos también demostraron que el efecto de las hormonas tiroideas es reversible y los animales recuperan la pigmentación normal tras 15 días, aproximadamente. Esta lentitud en el proceso de recuperación apoya la hipótesis de que el aclaramiento no solo se deba a una inhibición de la melanogénesis, sino también a un efecto sobre la diferenciación de los melanóforos.

Los resultados obtenidos concuerdan con los publicados por McMennamin y colaboradores (2014) quienes mostraron que una mutación constitutiva del receptor de la hormona estimulante del tiroides (TSH) que induce hipertiroidismo (niveles elevados de tiroxina o T4, el precursor de la T3) tiene como efecto un aclaramiento de la pigmentación resultado de una disminución en el número de melanóforos e incremento en el de xantóforos. Sin embargo, no concuerda con los resultados publicados por Walpita et al. 2009 quien demostró que la supresión de la actividad yodotirosina desyodinasa 2 (dio2), que media la conversión de T4 en T3, mediante la técnica de morfolino en embriones de pez cebra, retrasa la pigmentación del embrión mediante inhibición de *Tyr*; un fenotipo que puede rescatarse mediante el tratamiento con T3. Paralelamente el tratamiento con T3 en animales salvaje promueve la melanización, un efecto contrario al observado en mis estudios y en los de McMennamin et al. (2014). Una posible explicación de esta controversia es que las hormonas tiroideas tengan un efecto diferencial y opuesto sobre los patrones de pigmentación larvario y adulto.

Los efectos hormonales son más potentes sobre las hembras, como lo demuestran las interacciones positivas en el análisis estadístico del número de melanocitos en V2. De hecho, estas diferencias se correlacionan con complejos cambios regulatorios específicos del género que no pueden ser atribuidos a diferencias en el metabolismo de T3, ya que ambos géneros muestras niveles similares de hormonas plasmáticas.

Los resultados dimórficos desde el punto de vista sexual resaltan la importancia de tener en cuenta el factor sexo en los estudios de pigmentación. Aunque el mecanismo de una acción dependiente del género es desconocido, se debe resaltar que muchos eventos, tanto comportamentales (dominancia) como fisiológicos (reproducción, estrés), están regulados hormonal-mente y se asocian a modificaciones de la pigmentación.

2. Papel de las melanocortinas en el crecimiento e ingesta en el pez cebra

Con el fin de caracterizar el fenotipo inducido por la sobreexpresión de ASIP1 más allá de la pigmentación se diseñaron experimentos de crecimiento de juveniles e ingesta en adultos. Los cuales se complementaron con experimentos transcriptómicos de genes candidato (qPCRs), o mediante screening en masa (microarrays).

2.1. Ingesta y crecimiento

Los experimentos de crecimiento mostraron que la sobreexpresión de ASIP1 en los peces cebra transgénicos indujo un aumento muy significativo del crecimiento en peso y talla, tanto en machos como en hembras. Tras 6 meses, los machos transgénicos eran 4.6% más largos y pesaban un 15.6% más que los machos salvajes; y las hembras transgénicas eran 14.4% más largas y 62.9% más pesadas que las hembras salvajes. Sin embargo, pese a este aumento de peso, los peces transgénicos no exhibieron muestras de obesidad, siendo los niveles porcentuales de grasa corporal y los perfiles lipídicos equivalentes a los de los peces cebra salvajes del mismo sexo.

Bajo nuestras condiciones experimentales, los machos salvajes fueron significativamente más largos que las hembras salvajes. Pero esta situación se revirtió claramente en los peces transgénicos, debido al mayor crecimiento diferencial, en comparación a los peces salvajes, experimentado por las hembras transgénicas.

Estos resultados sugieren que las melanocortinas podrían estar implicadas en el crecimiento sexualmente diferencial de esta especie. Sin embargo, se requieren más experimentos para corroborar esta hipótesis.

Una explicación sencilla para el mayor crecimiento de los peces transgénicos podría ser un nivel de ingesta más elevado, como el que se observa en ratones mutantes de la cepa agoutí que sobreexpresan ASIP. Para comprobar esta hipótesis diseñamos una serie de experimentos que pusieran de manifiesto las posibles diferencias en la tasa de ingesta. Los resultados de estos experimentos muestran que los animales transgénicos son capaces de comer más que los salvajes cuando se alimentan una vez al día. Cuando se alimentan dos veces al día, los animales salvajes siguen comiendo la misma cantidad, pero reparten la tasa de ingesta entre las dos tomas. Sin embargo, los animales transgénicos son capaces de ingerir todavía una mayor cantidad de pienso que cuando se administra una única toma, lo que sugiere modificaciones en su sistema de saciedad.

Los resultados de la comparación transcriptómica del cerebro de los peces salvajes y transgénicos han revelado diferentes vías neuronales que podrían mediar tal reducción de la sensación de saciedad. Uno de los genes cuya expresión está reducida en los peces transgénicos es el transcrito inducido por la cocaína y anfetamina (CART), un péptico anorexigénico que induce saciedad tras su

administración intracerebroventricular (*Volkoff et al., 2005*); y cuyos niveles de expresión se reducen durante el ayuno (*Nishio et al., 2012*).

Los peces transgénicos que sobre-expresan ASIP1 y los peces MC4R "knockout" tienen una expresión CART menor que los salvajes. La sobreexpresión de ASIP1 inhibe de manera crónica MC4R. La ausencia de un MC4R funcional en los "knockout" se puede interpretar como una inhibición absoluta del receptor. Por tanto, un MC4R inhibido mantiene las expresiones de CART bajas, y que la regulación de CART requiere de un MC4R funcional, estableciéndose una relación de causa-efecto entre la actividad de MC4R y la expresión de CART. Uno de los posibles mecanismos de actuación de la α-MSH sobre la ingesta sería estimular la expresión de CART vía MC4R, o al menos impedir la inhibición de la expresión de CART estimulando MC4R.

La sobreexpresión de ASIP1 también afectó otros sistemas implicados en el control de la ingesta, incluyendo el sistema Kiss 1 y neuromedia U, pero la disección de las vías neuronales a partir de las cuales actúa el sistema de melanocortinas para inducir su efecto sobre la ingesta requerirá del diseño de nuevos experimentos.

Los resultados de estos experimentos de ingesta en peces adultos sugieren que los mayores niveles de ingesta podrían ser responsables del crecimiento incrementado. Sin embargo, el hecho de que no se observen indicios de obesidad en los peces transgénicos, y que las dos poblaciones de peces fueran alimentadas con la misma cantidad de pienso, alcanzando los peces transgénicos mayores tallas, sugiere que este crecimiento diferencial se deba también a una mejor tasa de conversión por parte de los peces transgénicos.

Estudios recientes han demostrado que el bloqueo de la expresión de AGRP mediante métodos morfolino induce un aumento de la tasa metabólica en larvas (*Renquist et al., 2013*). Estos resultados no se han comprobado en organismos adultos, pero podrían ayudar a explicar el mejor aprove-chamiento energético observado en nuestros peces transgénicos. La sobreexpresión de AGRP en modelo de transgénesis también induce incrementos de talla y peso en peces cebra (*Song and Cone 2007*) aunque a diferencia de nuestros experimentos con ASIP, la sobreexpresión de AGRP en estos experimentos sí que sugirieron el desarrollo de obesidad en peces adultos.

Actualmente, no hay ninguna hipótesis sólida para explicar los mayores niveles de crecimiento inducidos por la inhibición central del sistema de melanocortinas. Sin embargo, el efecto sobre el crecimiento es constante en diversos modelos murinos que carecen de un MC4R funcional (*Huszar et al., 1997*) o sobreexpresan agonistas inversos del receptor (*Ollmann et al., 1997; Miller et al., 1993*). Experimentos recientes realizados en larvas de pez cebra han demostrado que el bloqueo de la expresión de AGRP mediante técnicas de morfolino induce un retraso en el crecimiento en longitud de los peces y a su vez un descenso en la expresión de hormona de crecimiento (GH) comparado con los animales salvajes (*Zhang et al., 2012*). El efecto sobre el eje hipotálamo/hipofisiario que regula la secreción de GH podría ayudar a explicar los efectos sobre el crecimiento, sin embargo, en nuestro análisis transcriptómico no

aparecieron diferencias en ninguno de los reguladores clásicos de la expresión/secreción de GH incluyendo las diferentes somatostatinas (Sst) y el factor liberador de la hormona de crecimiento (GHRH).

Otra posible vía de explicación podría venir de una inhibición periférica. Experimentos de hibridación *in situ* han detectado una expresión elevada de MC4R en el músculo del pez cebra. Actualmente se están intentando dilucidar el papel de este receptor en la fisiología muscular. Una posibilidad es que el MC4R sirva como un freno en el desarrollo muscular hipertrófico o hiperplásico y el agonismo inverso de ASIP sea el responsable de un mayor desarrollo muscular en los peces transgénicos.

2.2. Dimorfismo sexual a nivel cerebral

El análisis comparativo del transcriptoma cerebral entre peces salvajes y transgénicos reveló que las hembras y machos salvajes expresan de forma diferencial 255 genes. Por el contrario, cuando se compara el transcriptoma del cerebro de machos y hembras transgénicos esta diferencia se reduce a, tan solo, 31 genes. De estos últimos solamente 3 son coincidentes con los 255 DEG caracterizados en animales salvajes, la yodotirosina desyodinasa 2 (*dio2*), el factor de crecimiento similar a la insulina (*igf1*) y la reductasa de coenzima A perixosomal (*pcer*). La expresión de estos tres genes es siempre diferente en el cerebro de machos y hembras, independientemente de la sobreexpresión de ASIP.

Los datos sugieren que la sobreexpresión de ASIP reduce las diferencias inducidas por el sexo sobre el transcriptoma cerebral haciendo el transcriptoma del cerebro de las hembras más similar al de los machos. El limitado tamaño muestral (n=3) no permite sacar conclusiones a partir de los resultados expuestos, pero es tentador pensar que el sistema de melanocortinas participe en la diferenciación sexual del cerebro. Cuando analizamos comparativamente el trans-criptoma de machos transgénicos y salvajes obtenemos una diferencia de 1066 DEG mientras que cuando realizamos la misma comparación entre hembras el número se eleva a 1122 DEG. Sin embargo, solamente 323 DEG coinciden entre machos y hembras. Estos resultados demuestran que el efecto de las melanocortinas sobre el transcriptoma cerebral depende del sexo del organismo, ya que hay 743 DEG en machos diferentes de los 658 DEG en hembras.

Nuestros datos sugieren que el sistema de melanocortinas podría estar implicado en el control del dimorfismo sexual observado en nuestra cepa de peces cebra. Y a su vez, estos datos podrían indicar una correlación entre el crecimiento diferencial y la inducción de un transcriptoma diferencial.

Conclusiones

1) Las formas de ASIP caracterizadas en peces planos se agrupan filogenéticamente con las formas de ASIP1 identificadas en otros teleósteos.

2) ASIP1 se corresponde funcionalmente con el factor de inhibición de la melanogénesis (MIF) descrito en poiquilotermos.

3) El gradiente de expresión dorso-ventral de ASIP1 es el responsable del establecimiento del patrón de pigmentación dorso-ventral en peces adultos mediante una reducción de la melanogénesis ventral e inhibición de la diferenciación de los melanóforos.

4) Las funciones de ASIP1 están conservadas en los vertebrados, aun cuando los patrones de pigmentación de los diferentes grupos se organizan mediante mecanismos muy diferentes.

5) ASIP1 no tiene efectos sobre el patrón de pigmentación embrionario/larvario del pez cebra.

6) El pez cebra adulto posee dos patrones de pigmentación diferentes: un patrón dorso-ventral, sobre el que se sobrepone otro patrón bandeado. Ambos patrones se regulan de forma diferencial, ya que podemos modificar el patrón dorso-ventral sin provocar cambios significativos en el patrón bandeado.

7) La administración de hormonas tiroideas provoca, en el pez cebra, una disminución reversible de la síntesis de melanina, mediante la inhibición de la proteína relacionada a la tirosinasa de tipo 1 (tyrp1).

8) Los efectos de las hormonas tiroideas sobre la pigmentación, y la expresión de enzimas y de factores de transcripción de carácter melanogénico, exhiben un dimorfismo de género.

9) La inhibición del sistema de melanocortinas, inducida por la sobreexpresión de ASIP1 en modelos de transgénesis, induce mayores tasas de ingesta, mejoras en el crecimiento en talla y en peso (característica conservada en otras líneas evolutivas) sin inducir obesidad (característica no conservada).

10) El aumento de la ingesta provocado por la sobre-expresión de ASIP1 no es el único responsable de las mejoras en crecimiento, de los peces transgénicos, ya que son capaces de alcanzar una talla comparativamente mayor bajo las mismas condiciones limitadas de alimentación que una población salvaje. Por ello, se puede concluir que los animales transgénicos exhiben una mejora en la eficiencia alimenticia.

11) El aumento del nivel de ingesta observado en los animales transgénicos se produce en función de una disminución de la sensibilidad del sistema de saciedad periférico o central.

12) La sobreexpresión de ASIP induce importantes cambios en el transcriptoma cerebral del pez cebra revelando múltiples candidatos que participan en los efectos centrales provocados por el sistema de melanocortinas.

Referencias

A

Aberdam E, Bertolotto, C, Sviderskay, EV, de Thillot V, Hemesath TJ, Fisher DE, Bennett DC, Ortonne JP, Ballotti R. (1998). Involvement of microphthalmia in the inhibition of melanocyte lineage differentiation and melanogenesis by agouti signaling protein. J. Biol. Chem. 31, 19560-19565.

Agulleiro MJ, Cortés R, Fernández-Durán B, Navarro S, Guillot R, Meimaridou E, et al. (2013). Melanocortin 4 receptor becomes an ACTH receptor by coexpression of melanocortin receptor accessory protein 2. Mol Endocrinol 27:1934–1945.

Agulleiro MJ, Roy S, Sánchez E, Puchol S, Gallo-Payet N, Cerdá-Reverter JM. (2010). Role of accessory proteins in the function of zebrafish melanocortin receptor type 2. Mol. Cell. Endocrinol. 320, 145-152.

Alderman SL and Vijayan MM. (2012). 11β-Hydroxysteroid dehydrogenase type 2 in zebrafish brain: a functional role in hypothalamus-pituitary-interrenal axis regulation. J. Endocrinol. 215, 393-402.

Aluru N and Vijayan MM. (2008). Molecular characterization, tissue-specific expression, and regulation of melanocortin 2 receptor in rainbow trout. Endocrinology 149, 4577-4588.

B

Bagnara JT and Matsumoto J. (2006). Comparative anatomy and physiology of pigment cells in nonmammalian tissues. In Nordlund JJ, ed. The Pigmentary System: Physiology and Pathophysiology. Oxford: Blackwell, pp. 11–59.

Bagnara JT and Fukuzawa T. (1990). Stimulation of cultured iridophores by amphibian ventral conditioned media. Pigment Cell Res. 3, 243-250.

Bangol D, Lu XY, Kaelin CB, Day HEW, Ollmann M, Gantz I, Akil H, Barsh GS, Watson SJJ. (1999). Anatomy of an endogenous antagonist: Relationship between agouti-related protein and proopiomelanocortin in brain. J. Neurosci. 19,1-7.

Barton D. (2009). Flatfish (Pleuronectiformes) chromatic biology Rev Fish Biol Fisheries DOI 10.1007/s11160-009-9119-0.

Bertolotto C, Abbe P, Hemesath TJ, Bille K, Fisher DE, Ortonne JP, Ballotti R. (1998a). Microphthalmia gene product as a signal transducer in cAMP-induced differentiation of melanocytes. J Cell Biol 142: 827-835.

Bertolotto C, Busca R, Abbe,P, Bille K, Aberdam E, Ortonne JP, Ballotti R. (1998b). Different cis-acting elements are involved in the regulation of TRP1 and TRP2 promoter activities by cyclic AMP: pivotal role of M boxes (GTCATGTGCT) and of microphthalmia. Mol Cell Biol 18: 694-702.

Bolin KA, Anderson DJ, Trulson JA, Thompson DA, Wilken J, et al. (1999). NMR structure of a minimized human agouti related protein prepared by total chemical synthesis. FEBS Lett 451: 125-131.

Bolker JA, Hakala TF, Quist JE. (2005). Pigmentation development, defects, and patterning in summer flounder (*Paralichthys dentatus*) Zoology 108: 183-193.

Bolker JA and Hill CR. (2000). Pigmentation development in hatchery-reared flatfishes. J Fish Biol 56: 1029-1052.

Braasch I and Postlethwait JH. (2011). The teleost agouti-related protein 2 gene is an ohnolog gone missing from the tetrapod genome. Proc Natl Acad Sci USA. 108:E47-48.

Bultman SJ, Michaud EJ, Woychik RP. (1992). Molecular characterization of the mouse agouti locus. Cell 71, 1195-1204.

Butler AA, Kesteson RA, Khong K, Cullen MJ, Pelleymounter MA, Dekoning J, Baetscher M, Cone RD. (2000). A unique metalolic sysdrone causes obesity in the melanocortin-3 receptor-deficient mouse. Endocrinology 141:9:1: 3518–3521.

Budi EH, Patterson LB, Parichy DM. (2011) Post-embryonic nerve-associated precursors to adult pigment cells: genetic requirements and dynamics of morphogenesis and differentiation. PLoS Genet. 5:e1002044.

Budi EH, Patterson LB, Parichy DM. (2008). Embryonic requirements for ErbB signaling in neural crest development and adult pigment pattern formation. Development 135:2603-2614.

Bures EJ, Hui JO, Young Y, Chow DT, Katta V, et al. (1998). Determination of disulfide structure in agouti-related protein (AGRP) by stepwise reduction and alkylation. Biochemistry 37: 12172-12177.

C

Candille SI, Van Raamsdonk CD, Chen C, Kuijper S, Chen-Tsai Y, Russ A, Meijlink F, Barsh GS. (2004). Dorsoventral patterning of the mouse coat by Tbx15. PLoS Biol. 2, E3.

Carreira S, Goodall J, Denat L, Rodriguez M, Nuciforo P, Hoek KS, Testori A, Larue. L, Goding CR. (2006). Mitf regulation of Dia1 controls melanoma proliferation and invasiveness. Genes Dev 20:3426-3439.

Castro MG and Morrison E. (1997). Post-translational processing of proopiomelanocortin in the pituitary and in the brain. Crit. Rev. Neurobiol. 11, 35-57.

Ceinos RM, Guillot R, Kelsh RN, Cerdá-Reverter JM, Rotllant J. (2015). Pigment patterns in adult fish result from superimposition of two largely independent pigmentation mechanisms. Pigment Cell Melanoma Res. 28, 196-209.

Cerdá-Reverter JM, Agulleiro MJ, Sánchez E, Guillot R. Ceinos R, Rotllant J. (2011). Fish Melanocortin System. Eur J Pharmacol 660: 53-60.

Cerdá-Reverter JM and Canosa LF. (2009). Neuroendocrine Systems of the Fish Brain. In: Bernier, N.J., Van Der Kraak, G., Farrell, A.P., Brauner, C.J. (Eds.), Fish Neuroendocrinology. Fish Physiology 28, pp. 3-74.

Cerdá-Reverter JM, Haitina T, Schiöth HB, Peter RE. (2005). Gene structure of the goldfish agouti-signaling protein: a putative role in the dorsal-ventral pigment pattern of fish. Endocrinology 146,1597-1610.

Cerdá-Reverter JM and Peter RE. (2003). Endogenous melanocortin antagonist in fish. Structure, brain mapping and regulation by fasting of the goldfish agouti-related protein gene. Endocrinology 144, 4552-4561.

Cerdá-Reverter JM, Schiöth HB, Peter RE, (2003a). The central melanocortin system regulates food intake in goldfish. Regul. Pep. 115, 101-113.

Cerdá-Reverter JM, Ringholm A, Schiöth HB, Peter RE. (2003b). Molecular cloning, pharmacological characterization and brain mapping of the melanocortin 4 receptor in the goldfish: Involvement in the control of food intake. Endocrinology 144, 2336-2349.

Cerdá-Reverter JM, Ling M, Schiöth HB, Peter RE. (2003c). Molecular cloning, pharmacological characterization and brain mapping of the melanocortin 5 receptor in the goldfish. J. Neurochem. 87, 1354-1367.

Chan LF, Webb TR, Chung TT, Meimaridou E, Cooray SN, Guasti L, Chapple JP, Egertová M, Elphick MR, Cheetham ME, Metherell LA, Clark AJ. (2009). MRAP and MRAP2 are bidirectional regulators of the melanocortin receptor family. Proc. Natl. Acad. Sci. 106, 6146-6151.

Chen AS, Marsh DJ, Trumbauer ME, Frazier EG, Guan XM, Yu H, Rosemblum CI, Vongs A, Feng Y, Cao L, Metzger JM, Strack AM, Camacho RE, Mellin TN, Nunes CN, Min W, Fisher J, Gopal-Truter S, MacIntyre DE, Chen HY, Van der Ploeg LH. (2000). Inactivation of the mouse melanocortin-3 receptor results in increased fat mass and reduced lean body mass. Nat. Genet. 26, 97-102.

Cone RD. (2006). Studies on the physiological functions of the melanocortin system. Endocr. Rev. 27, 736-749.

Cone RD. (2005). Anatomy and regulation of the central melanocortin system. Nat. Neurosci. 8, 571-578.

Cooray SN, Almiro Do Vale I, Leung KY, Webb TR, Chapple JP, Egertová M, Cheetham ME, Elphick MR, Clark AJ. (2008). The melanocortin 2 receptor accessory protein exists as a homodimer and is essential for the function of the melanocortin 2 receptor in the mouse y1 cell line. Endocrinology. 149, 1935-1941.

Cortés R, Navarro S, Agulleiro MJ, Guillot R, García-Herranz V, Sánchez E, Cerdá-Reverter JM. (2014). Evolution of the melanocortin system. Gen. Comp. Endocrinol. 209, 3-10.

Creemers JW, Pritchard LE, Gyte A, Le Rouzic P, Meulemans S, et al. (2006). Agouti-related protein is posttranslationally cleaved by proprotein convertase 1 to generate agouti-related protein (AGRP)83-132: interaction between AGRP83-132 and melanocortin receptors cannot be influenced by syndecan-3 Endocrinology. 147:1621-1631.

Cropley JE, Suter CM, Beckman KB, Martin DI. (2006). Germ-line epigenetic modification of the murine A vy allele by nutritional supplementation. Proc. Natl. Acad. Sci. USA 103,17308-17312.

Curran K, Lister JA, Kunkel GR, Prendergast A, Parichy DM, et al. (2010). Interplay between Foxd3 and Mitf regulates cell fate plasticity in the zebrafish neural crest. Dev Biol 344:107-118.

Curran K, Raible DW, Lister JA. (2009). Foxd3 controls melanophore specification in the zebrafish neural crest by regulation of Mitf. Dev Biol 332:408-417.

D

Darias MJ, Andree KB, Boglino A, Rotllant J, Cerdá-Reverter JM, Estévez A, Gisbert E. (2013). Morphological and molecular characterization of dietary-induced pseudo-albinism during post-embryonic development of Solea senegalensis (Kaup, 1858). PLoS One 8(7): e68844.

Davoli R, Braglia S, Valastro V, Annaratone C, Comella M, Zambonelli P, Nisi I, Gallo M, Buttazzoni L, Russo V. (2012). Analysis of MC4R polymorphism in Italian Large White and Italian Duroc pigs: association with carcass traits. Meat Sci. 90, 887-892.

de Souza FS, Bumaschny VF, Low MJ, Rubinstein M. (2005). Subfunctionalization of expression and peptide domains following the ancient duplication of the proopiomelanocortin gene in teleost fishes. Mol. Biol. Evol. 22, 2417-2427.

Dong W, Macaulay LJ, Kwok KWH, Hinton DE, Ferguson PL, Stapleton HM. (2014). The PBDE metabolite 6-OH-BDE 47 affects melanin pigmentation and THRb mRNA expression in the eye of zebrafish embryo Endocr Disruptors 2:1, e969072.

Dooley CM, Mongera A, Walderich B, Nüsslein-Volhard, C. (2013). On the embryonic origin of adult melanophores: the role of ErbB and Kit signalling in establishing melanophore stem cells in zebrafish. Development. 140, 1003–1013.

Dores Robert M. (2013). Observations on the Evolution of the Melanocortin Receptor Gene Family: Distinctive Features of the Melanocortin-2 Receptor. Frontiers in Neuroscience 7: 28.

Dutton KA, Pauliny A, Lopes SS, Elworthy S, Carney TJ, Rauch J, Geisler R, Haffter P, Kelsh RN. (2001). Zebrafish colourless encodes sox10 and specifies nonectomesenchymal neural crest fates. Development:128:4113–4125.

F

Fadeev A, Krauss J, Fröhnhofer HG, Irion U, Nüsslein-Volhard C. (2015). Tight junction protein 1a regulates pigment cell organisation during zebrafish colour patterning. Elife 4:e06545.

Fan W, Ellacott KL, Halatchev IG, Takahashi K, Yu P, Cone RD. (2004) Cholecystokinin-mediated suppression of feeding involves the brainstem melanocortin system. Nat. Neurosci. 7, 335-336.

Fan W, Bosto, BA, Kesterson RA, Hruby VJ, Cone RD. (1997). Role of melanocortinergic neurons in feeding and the agouti obesity syndrome. Nature 385,165-168.

Forlano PM and Cone RD. (2007). Conserved neurochemical pathways involved in hypothalamic control of energy homeostasis. J. Comp. Neurol. 505, 235-248.

Frohnhöfer HG, Krauss J, Maischein HM, Nüsslein-Volhard C. (2013). Iridophores and their interactions with other chromatophores are required for stripe formation in zebrafish. Development 140: 2997-3007.

Fujii R. (1993). Coloration and Chromatophores. In: Evans, D.H. (Ed.), The Physiology of Fishes. CRC press, Boca Raton, pp. 535-562.

Fukuzawa T, Samaraweera P, Mangano FT, Law JH, Bagnara JT. (1995). Evidence that MIF plays a role in the development of pigment patterns in the frog. Dev. Biol. 167: 148-158.

Fukuzawa T and Bagnara JT. (1989). Control of melanoblast differentiation in amphibia by α-MSH, a serum melanization factor and a melanization inhibition factor. Pigment Cell Res. 2, 171-181.

Fukuzawa T and Ide H. (1988). A ventrally localized inhibitor of melanization in *Xenopus laevis* skin. Dev. Biol. 129, 25-36.

G

Gerets HHJ, Peeters K, Arckens L, Vandesande R, Berghman LR. (2000). Sequence and distribution of proopiomelanocortin in the pituitary and brain of the chicken (Gallus gallus). J. Comp. Neurol. 417, 250-262.

Gesto M, López-Patiño MA, Hernández J, Soengas JL, Míguez JM. The response of brain serotonergic and dopaminergic systems to an acute stressor in rainbow trout: a time course study.J Exp Biol. 2013; 216:4435-4442.

Girardet C, Butler AA. (2014). Neural melanocortin receptors in obesity and related metabolic disorders. Biochim. Biophys. Acta. 1842, 482-94.

González-Nunez V, González-Sarmiento R, Rodríguez RE. (2003). Identification of two proopiomelanocortin genes in zebrafish (Danio rerio). Mol Brain Res. 120, 1-8.

Greenhill ER, Rocco A, Vibert L, Nikaido M, Kelsh RN. (2011). An iterative genetic and dynamical modelling approach identifies novel features of the gene regulatory network underlying melanocyte development. PLoS Genet 7(9): e1002265.

Griffon N, Mignon V, Facchinetti P, Diaz J, Schwartz JC, Sokoloff P. (1994). Molecular cloning and characterization of the rat fifth melanocortin receptor. Biochem Biophys Res Commun. 200(2):1007-1014.

Gross JB, Borowsky R, Tabin CJ. (2009). A novel role for Mc1r in the parallel evolution of depigmentation in independent populations of the cavefish Astyanax mexicanus. PLoS Genet. 5, e1000326.

Guillot R, Ceinos RM, Cal R, Rotllant J, Cerdá-Reverter JM. (2012). Transient ectopic overexpression of agouti-signalling protein 1 (Asip1) induces pigment anomalies in flatfish. PLoS One 7(12): e48526.

H

Hahn TM, Breininger JF, Baskin DG, Schwartz MW. (1998). Coexpression of Agrp and NPY in fasting-activated hypothalamic neurons. Nature Neuroscience 1:271–272.

Haitina T, Klovins J, Andersson J, Fredriksson R, Lagerström MC, Larhammar D, Larson ET, Schiöth HB. (2004). Cloning, tissue distribution, pharmacology and three-dimensional modelling of melanocortin receptors 4 and 5 in rainbow trout suggest close evolutionary relationship of these subtypes. Biochem. J. 380, 475-486.

Hamre K, Holen E, Moren M (2007) Pigmentation and eye migration in Atlantic halibut (Hippoglossus hippoglossus L) larvae: new findings and hypothesis Aqucult Nutr 13: 65-80.

He L, Gunn TM, Bouley DM, Lu X-Y, Watson SJ, 16. et al. (2001). A biochemical function for attractin in agouti-induced pigmentation and obesity. Nat Genet 27: 40-47.

Hirata M, Nakamura KI, Kondo S. (2005). Pigment cell distributions in different tissues of the zebrafish, with special reference to the striped pigment pattern. Dev Dyn 234: 293–300.

Hirata M, Nakamura KI, Kanemaru T, Shibata Y, Kondo S. (2003). Pigment cell organization in the hypodermis of zebrafish. Dev Dyn 227: 497–503.

Hirobe T. (1992). Control of melanocyte proliferation and differen-tiation in the mouse epidermis. Pigment Cell Res. 5, 1–11.

Hirobe T. (1982). Genes involved in regulating the melanocyte and melanoblast-melanocyte populations in the epidermis of newborn mouse skin. J. Exp. Zool. 223, 257–264.

Houston RD, Cameron ND, Rance KA. (2004). A melanocortin-4 receptor (MC4R) polymorphism is associated with performance traits in divergently selected Large White pig populations. Anim. Genet. 35, 386-390.

Howard AD, Wang R, Pong SS, Mellin TN, Strack A, Guan XM, Zeng Z, Williams DL Jr, Feighner SD, Nunes CN, Murphy B, Stair JN, Yu H, Jiang Q, Clements MK, Tan CP, McKee KK, Hreniuk DL, McDonald TP, Lynch KR, Evans JF, Austin CP, Caskey CT, Van der Ploeg LH, Liu Q. (2000). Identification of receptors for neuromedin U and its role in feeding. Nature 406, 70-74.

Huszar D, Lynch CA, Fairchild-Huntress V, Dunmore JH, Fang Q, Berkemeier LR, Gu W, Kesterson RA, Boston BA, Cone RD, Smith FJ, Campfield LA, Burn P, Lee F. (1997). Targeted disruption of melanocortin-4 receptor results in obesity in mice. Cell 88, 131-141

I

Inaba M, Yamanaka H, Kondo S. (2012). Pigment pattern formation by contact-dependent depolarization. Science 335: 677.

Ito S and Wakamatsu K. (2008). Chemistry of mixed melanogenesis—pivotal roles of dopaquinone. Photochem Photobiol 84:582–92.

Iwashita M, Watanabe M, Ishii M, Chen T, Johnson SL, Kurachi Y, Okada N, Kondo S. (2006). Pigment pattern in jaguar/obelix zebrafish is caused by a Kir7.1 mutation: implications for the regulation of melanosome movement. PLoS Genet. 2:e197.

J

Jackson PJ, McNulty JC, Yang Y-K, Thompson DA, Chai B, et al. (2002). Design, pharmacology, and NMR structure of a minimized cysteine knot with agouti-related protein activity. Biochemistry 41: 7565-7572.

Johnson SL, Nguyen AN, Lister JA. (2011). Mitfa is required at multiple stages of melanocyte differentiation but not to establish the melanocyte stem cell. Dev. Biol. 350, 405–413.

Johnson SL, Africa D, Walker C, Weston JA. (1995). Genetic control of adult pigment stripe development in zebrafish. Dev. Biol. 167, 27–33.

Jonsson L, Skarphedinsson JO, Skuladottir GV, Watanobe H, Schiöth, HB. (2002). Food conversion is transiently affected during 4-week chronic administration of melanocortin agonist and antagonist in rats. J. Endocrinol. 173, 517-523.

K

Karlsson J, von Hofsten J Olsson PE. (2001). Generating transparent zebrafish: a refined method to improve detection of gene expression during embryonic development. Mar Biotechnol 3:522–527.

Kask A, Mutulis R, Muceniece R, Pahkla R, Mutule I, Wikberg JE, Rago L, Schioth HB. (1998). Discovery of a novel superpotent and selective melanocortin-4 receptor antagonist (HS024): evaluation in vitro and in vivo. Endocrinology 139, 5006-5014.

Kawakami K. (2007). Tol2: a versatile gene transfer vector in vertebrates. Review Genome Biol 8(Suppl 1): S7.

Kelsh RN, Harris ML, Colanesi S, Erickson CA. (2009). Stripes and belly-spots -- a review of pigment cell morphogenesis in vertebrates. Semin Cell Dev Biol 20(1): 90-104.

Kelsh, RN. (2004). Genetics and Evolution of Pigment Patterns in Fish. Pigment Cell Res 17: 326-336.

Kelsh RN and Eisen JS. (2000) The zebrafish colourless gene regulates development of non-ectomesenchymal neural crest derivatives. Development 127: 515–525.

Kelsh, RN, Schmid, B, Eisen, JS. (2000a). Genetic analysis of melanophore development in zebrafish embryo. Dev Biol 225: 277-293.

Kelsh RN, Dutton K, Medlin J, Eisen JS. (2000b). Expression of zebrafish fkd6 in neural crest-derived glia. Mech Dev 93:161–164.

Klebig ML, Wilkinson JE, Geisler JG, Woychik RP. (1995). Ectopic expression of the agouti gene causes obesity, features of type II diabetes, and yellow fur. Proc. Natl. Acad. Sci. USA. 92, 4728-4732.

Klovins J and Schiöth, H.B. (2005). Agouti-related proteins (AGRPs) and agouti-signaling peptide (ASIP) in fish and chicken. Ann N Y Acad Sci 1040: 363-7.

Koch M, Varela L, Kim JG, Kim JD, Hernández-Nuño F, Simonds SE, Castorena CM, Vianna CR, Elmquist JK, Morozov YM, Rakic P, Bechmann I, Cowley MA, Szigeti-Buck K, Dietrich MO, Gao XB, Diano S, Horvath TL. (2015). Hypothalamic POMC neurons promote cannabinoid-induced feeding Nature. 519, 45-50.

Korner J, Wissig S, Kim A, Conwell IM, Wardlaw SL. (2003). Effects of agouti-related protein on metabolism and hypothalamic neuropeptide gene expression. J Neuroendocrinol. 15(12):1116-1121.

Krauss J, Geiger-Rudolph S, Koch I, Nüsslein-Volhard C Irion U. (2014). A dominant mutation in tyrp1A leads to melanophore death in zebrafish. Pigment Cell Melanoma Res 27:827–830.

Krauss J, Astrinidis P, Frohnhöfer HG, Walderich B, Nüsslein-Volhard C. (2013). Transparent, a gene affecting stripe formation in Zebrafish, encodes the mitochondrial protein Mpv17 that is required for iridophore survival. Biol Open 2: 703-710.

Kristensen P, Judge ME, Thim L, Ribel U, Christjansen KN, Wulff BS, Clausen JT, Jensen PB, Madsen OD, Vrang N, Larsen PJ, Hastrup S. (1998). Hypothalamic CART is a new anorectic peptide regulated by leptin. Nature 393:72-76.

Kubota N, Yano W, Kubota T, Yamauchi T, Ito S, Kumagai H, Kozono, H, Takamoto I, Okamoto S, Shiuchi T, Suzuki R, Satoh H, Tsuchida A, Moroi M, Sugi K, Noda T, Ebinuma H, Ueta Y, Kondo T, Araki E, Ezaki O, Nagai R, Tobe K, Terauchi Y, Ueki, K, Minokoshi Y, Kadowaki T. (2007). Adiponectin stimulates AMP-activated protein kinase in the hypothalamus and increases food intake. Cell Metab. 6, 55-68.

Kurokawa T, Murashita K, Uji S. (2006). Characterization and tissue distribution of multiple agouti-family genes in pufferfish, *Takifugu rubripes*. Peptides 27, 3165-3175.

L

Lamason RL, Mohideen MA, Mest J R, Wong AC, Norton HL, Aros MC, et al. (2005). SLC24A5, a putative cation exchanger, affects pigmentation in zebrafish and humans. Science 310:1782–1786.

Lampert KP, Schmidt C, Fischer P, Volff JN, Hoffmann C, Muck J, Lohse MJ, Ryan MJ, Schartl M. (2010). Determination of onset of sexual maturation and mating behavior by melanocortin receptor 4 polymorphisms. Curr. Biol. 20, 1729-1734.

Larson TA, Gordon TN, Lau HE, Parichy DM. (2010): Defective adult oligodendrocyte and Schwann cell development, pigment pattern, and craniofacial morphology in puma mutant zebrafish having an alpha tubulin mutation. Dev. Biol. 346:296–309.

Leal E, Fernández-Durán B, Agulleiro MJ, Conde-Siera M, Míguez JM, Cerdá-Reverter JM. (2013). Effects of dopaminergic system activation on feeding behavior and growth performance of the sea bass (*Dicentrarchus labrax*): a self-feeding approach. Horm. Behav. 64, 113-121.

Leal E, Fernández-Durán B, Guillot R, Ríos D, Cerdá-Reverter JM. (2011). Stress-induced effects on feeding behavior and growth performance of the sea bass (Dicentrarchus labrax): a self-feeding approach. J. Comp. Physiol. B. 181, 1035-1044.

Le Douarin NM and Kalcheim C. (1999). The Neural Crest. Vol. 2. Cambridge: Cambridge University Press.

Le Pape E, Passeron T, Giubellino A, Valencia JC, Wolber R, Hearing VJ. (2009). Microarray analysis sheds light on the dedifferentiating role of agouti signal protein in murine melanocytes via the Mc1r. Proc. Natl. Acad. Sci. USA. 106, 1802-1807.

Le Pape E, Wakamatsu K, Ito S, Wolber R, Hearing VJ. (2008). Regulation of eumelanin/pheomelanin synthesis and visible pigmentation in melanocytes by ligands of the melanocortin 1 receptor. Pigment Cell Melanoma Res 21: 477–486.

Lee GH, Proenca R, Montez JM, Carroll KM, Darvishzadeh JG, Lee JI, Friedman JM. (1996). Abnormal splicing of the leptin receptor in diabetic mice. Nature. Feb 15;379(6566):632-5.

Leibowitz SF and Rossakis C. (1979). Mapping study of brain dopamine- and epinephrine-sensitive sites which cause feeding suppression in the rat. Brain Res. 172, 101-113.

Lin JY and Fisher DE. (2007). Melanocyte biology and skin pigmentation. Nature 445: 843-850.

Lippert RN, Ellacott KL, Cone RD. (2014). Gender-specific roles for the melanocortin-3 receptor in the regulation of the mesolimbic dopamine system in mice. Endocrinology. 155, 1718-1727.

Lister JA, Robertson CP, Lepage T, Johnson SL, Raible DW. (1999). Nacre encodes a zebrafish microphthalmia-related protein that regulates neural-crest-derived pigment cell fate. Development. 126, 3757-3767.

Livak KJ and Schmittgen TD. (2001). Analysis of relative gene expression data using real-time quantitative PCR and the 2_DDCT method. Methods 25, 402–408.

Logan DW, Bryson-Richardson RJ, Pagán KE, Taylor MS, Currie PD, Jackson IJ. (2003). The structure and evolution of the melanocortin and MCH receptors in fish and mammals. Genomics 81, 184-191

Lopes SS, Yang X, Müller J, Carney TJ, McAdow AR, Rauch GJ, Jacoby AS, Hurst L.D, Delfino-Machín M, Haffter P, Geisler R, Johnson SL, Ward A, Kelsh RN. (2008) Leukocyte tyrosine kinase functions in pigment cell development. PLoS Genet 4(3): e1000026.

López-Contreras AM, Martínez-Liarte JH, Solano F, Samaraweera P, Newton JM, Bagnara JT. (1996). The amphibian melanization inhibiting factor (MIF) blocks the α-MSH effect on mouse malignant melanocytes. Pigment Cell Res. 9, 311-316.

Lu D, Willard D, Patel IR, Kadwell S, Overton L, Kost T, Luther M, Chen W, Woychik RP, Wilkinson WO. (1994). Agouti protein is an antagonist of the melanocyte-stimulating-hormone receptor. Nature 371, 799-802.

M

Maderspacher F and Nüsslein-Volhard C. (2003). Formation of the adult pigment pattern in zebrafish requires leopard and obelix dependent cell interactions. Development 130: 3447–3457.

Manceau M, Domingues VS, Mallarino R, Hoekstra HE. (2011). The developmental role of agouti in color pattern evolution. Science 331: 1062–1065.

Manne J, Argeson AC, Siracusa LD. (1995). Mechanism for the pleiotropic effects of the agouti gene. Proc Natl Acad Sci USA 92: 4721-4724.

Marsh DJ, Holloper G, Huszar D, Laufer R, Yagaloff KA, Fisher SL, Burn P, Palmiter RD. (1999). Response of melanocortin-4 receptor-deficient mice to anorectic and orexigenic peptides. Nature 21,119-122.

Martinelli CE, Keogh JM, Greenfield JR, Henning E, van der Klaauw AA, Blackwood A, O'Rahilly S, Roelfsema F, Camacho-Hübner C, Pijl H, Farooqi IS. (2011). Obesity due to melanocortin 4 receptor (MC4R) deficiency is associated with increased linear growth and final height, fasting hyperinsulinemia, and incompletely suppressed growth hormone secretion. J. Clin. Endocrinol Metab. 96, E181-E188.

Maruyama K, Wada K, Ishiguro K, Shimakura S, Wakasugi T, Uchiyama M, Shioda S, Matsuda K. (2009). Neuromedin U-induced anorexigenic action is mediated by the corticotropin-releasing hormone receptor-signaling pathway in goldfish. Peptides 30, 2483-2486.

Masaki T, Chiba S, Yoshimichi G, Yasuda T, Noguchi H, Kakuma T, Sakata T, Yoshimatsu H. (2003). Neuronal histamine regulates food intake, adiposity, and uncoupling protein expression in agouti yellow (A(y)/a) obese mice. Endocrinology 144, 2741-2748.

Matsumoto J, Seikai T. (1992). Asymmetric pigmentation and pigment disorders in pleuronectiformes (flounders). Pigment Cell Res 2:275-282.

Matsunaga N, Virador V, Santis C, Vieira WD, Furumura M, Matsunaga J, Kobayashi N, Hearing VJ. (2000). In situ localization of agouti signal protein in murine skin using immunohistochemistry with an ASP-specific antibody. Biochem. Biophys. Res. Commun. 270, 176-182.

McMenamin SK, Bain EJ, McCann AE, Patterson LB, Eom DS, Waller ZP, et al. (2014). Thyroid hormone-dependent adult pigment cell lineage and pattern in zebrafish. Science 345: 1358–1361.

McNulty JC, Thompson DA, Bolin KA, Wilken J, Barsh GS, et al. (2001). High-resolution NMR structure of the chemically-synthesized melanocortin receptor binding domain AGRP(87-132) of the agouti-related protein. Biochemistry 40: 15520-15527.

Metherell LA, Chapple JP, Cooray S, David A, Becker C, Rüschendorf F, Naville D, Begeot M, Khoo B, Nürnberg P, Huebner A, Cheetham ME, Clark AJ. (2005). Mutations in MRAP, encoding a new interacting partner of the ACTH receptor, cause familial glucocorticoid deficiency type 2. Nat. Genet. 37, 166-170.

Michaud EJ, Bultman SC, Stubss LJ, Woychick RP. (1993). The embryonic lethally of homozygous lethal yellow mice (Ay/Ay) is associated with the disruption of a novel RNA-binding protein. Genes Dev. 7, 1203-1213.

Millar SE, Miller MW, Stevens ME, Barsh GS. (1995). Expression and transgenic studies of the mouse agouti gene provide insight into the mechanisms by which mammalian coat color patterns are generated. Development 121, 3223–3232.

Miller MW, Duhl DMJ, Vrieling H, Cordes SP, Ollmann MM, Winkes BM, Barsh GS. (1993). Cloning of the mouse agouti gene predicts a secreted protein ubiquitously expressed in mice carrying a lethal yellow mutation. Genes Dev. 7, 454-467.

Miltenberger RJ, Mynatt RL, Bruce BD, Wilkinson WO, Woychik RP et al. (1999). An agouti mutation lacking the basic domain induces yellow pigmentation but not obesity in transgenic mice. Proc Natl Acad Sci USA 96: 8579-8584.

Miltenberger RJ, Wakamatsu K, Ito S, Woychik RP, Russell LB, Michaud EJ. (2002). Molecular and phenotypic analysis of 25 recessive, homozygous-viable alleles at the mouse agouti locus. Genetics. 160, 659-674.

Minchin JE and Hughes SM. (2008). Sequential actions of Pax3 and Pax7 drive xanthophore development in zebrafish neural crest. Dev. Biol. 317:508–522.

Monroig Ó, Navarro JC, Amat F, González P, Bermejo A, Hontoria F. (2006). Enrichment of Artemia nauplii in essential fatty acids with different types of liposomes and their use in the rearing of gilthead sea bream (Sparus aurata) larvae. Aquaculture 251, 491-508.

Morley JE, Farr SA, Sell RL, Hileman SM, Banks WA. (2011). Nitric oxide is a central component in neuropeptide regulation of appetite. Peptides 32, 776-780.

Morton GJ, Cummings DE, Baskin DG, Barsh GS, Schwartz MW. (2006). Central nervous system control of food intake and body weight. Nature. Sep 21;443(7109):289-95.

Moury JD and Jacobson AG (1989). Neural fold formation at newly created boundaries between neural plate and epidermis in the axolotl. Dev Biol 133(1): 44–57.

Muñoz JL, Ceinos RM, Soengas JL, Míguez JM. (2009). A simple and sensitive method for determination of melatonin in plasma, bile and intestinal tissues by high performance liquid chromatography with fluorescence detection. J. Chromatogr. B Analyt. Technol. Biomed. 877, 2173-2177.

Mukhi S, Torres L, Patiño R. (2007). Effects of larval–juvenile treatment with perchlorate and co-treatment with thyroxine on zebrafish sex ratios. Gen Comp Endocrinol 150: 486–494.

Murashita K, Kurokawa T, Ebbesson LO, Stefansson SO, Rønnestad I. (2009). Characterization, tissue distribution, and regulation of agouti-related protein (AgRP), cocaine- and amphetamine-regulated transcript (CART) and neuropeptide Y (NPY) in Atlantic salmon (*Salmo salar*). Gen. Comp. Endocrinol. 162, 160-171.

N

Nakanishi S, Inoue A, Kita T, Nakamura M, Chang ACY, Cohen SN, Numa S. (1979). Nucleotide sequence of cloned cDNA for bovine corticotropin-β-lipotropin precursor. Nature. 288, 610-613.

Nijenhuis WA, Oosterom J, Adan RA. (2001). AgRP(83-132) acts as an inverse agonist on the human-melanocortin-4 receptor. Mol. Endocrinol. 15, 164-171.

Nishimura EK, Jordan SA, Oshima H, Yoshida H, Osawa M, Moriyama M, et al. (2002). Dominant role of the niche in melanocyte stem-cell fate determination. Nature 416:854–860.

Nishio S, Gibert Y, Berekelya L, Bernard L, Brunet F, Guillot E, Le Bail JC, Sánchez JA, Galzin AM, Triqueneaux G, Laudet V. (2012). Fasting induces CART down-regulation in the zebrafish nervous system in a cannabinoid receptor 1-dependent manner. Mol. Endocrinol. 26, 1316-1326.

Noon LA, Franklin JM, King PJ, Goulding NJ, Hunyady L, Clark AJ. (2002). Failed export of the adrenocorticotrophin receptor from the endoplasmic reticulum in non-adrenal cells: evidence in support of a requirement for a specific adrenal accessory factor. J. Endocrinol. 174, 17-25.

O

Ogawa S, Nathan FM, Parhar IS. (2014). Habenular kisspeptin modulates fear in the zebrafish. Proc. Natl. Acad. Sci. USA. 111, 3841-3846.

Ollmann MM, Barsh GS. (1999). Down regulation of melanocortin receptor signaling mediated by the amino terminus of agouti protein in *Xenopus* melanophores. J Biol Chem 28: 15837-15846.

Ollmann MM, Wilson BD, Yang YK, Kerns JA, Chen I, Gantz I. Barsh GS. (1997). Antagonism of central melanocortin receptors in vitro and in vivo by agouti-related protein. Science. 278,135-138.

P

Parichy DM. (2009). Animal pigment pattern: an integrative model system for studying the development, evolution, and regeneration of form. Semin Cell Dev Biol 20(1): 63-4.

Parichy D, Elizondo MR, Mills MG, Gordon TN, Engeszer RE. (2009). Normal table of postembryonic zebrafish development: staging by externally visible anatomy of the living fish. Dev Dyn 238: 2975–3015.

Parichy DM and Turner JM. (2003). Temporal and cellular requirements for Fms signaling during zebrafish adult pigment pattern development. Development 130:817–833.

Parichy DM, Ransom DG, Paw B, Zon LI, Johnson SL. (2000). An orthologue of the kit-related gene fms is required for development of neural crest-derived xanthophores and a subpopulation of adult melanocytes in the zebrafish, Danio rerio. Development 127(14): 3031–3044.

Parichy DM, Rawls JF, Pratt SJ, Whitfield TT, Johnson SL. (1999). Zebrafish sparse corresponds to an orthologue of c-kit and is required for the morphogenesis of a subpopulation of melanocytes, but is not essential for hematopoiesis or primordial germ cell development. Development 126:3425–3436.

Patterson LB and Parichy D.M. (2013). Interactions with iridophores and the tissue environment required for patterning melanophores and xanthophores during zebrafish adult pigment stripe formation. PLoS Genet 9(5): e1003561.

Patel MP, Cribb Fabersunne CS, Yang YK, Kaelin CB, Barsh GS, et al. (2010). Loop-swapped chimeras of the agouti-related protein and the agouti signaling protein identify contacts required for melanocortin 1 receptor selectivity and antagonism. J Mol Biol 404:45-55.

Perry WL, Nakamura T, Swing DA, Secrest L, Eagleson B, et al. (1996) Coupled site-directed mutagenesis/transgenesis identifies important functional domains of the mouse agouti protein. Genetics 144: 255-264.

Q

Qin C, Wang B, Sun C, Jia J, Li W. (2014). Orange-spotted grouper (*Epinephelus coioides*) adiponectin receptors: molecular characterization, mRNA expression, and subcellular location. Gen. Comp. Endocrinol. 198, 47-58.

Quesada A; Valdehita A, Fernández-Cruz ML, Leal E; Sánchez E; Martín-Belinchón M Cerdá-Reverter MM. Navas J. (2012). Assessment of estrogenic and thyrogenic activities in fish feeds. Aquaculture 338-341: 172-180.

Quigley IK and Parichy DM. (2002). Pigment pattern formation in zebrafish: a model for developmental genetics and the evolution of form. Microsci Res Tech 58: 442–455.

R

Renquist BJ, Zhang C, Williams SY, Cone RD. (2013). Development of an assay for high-throughput energy expenditure monitoring in the zebrafish. Zebrafish.10(3):343-52.

Robbins LS, Nadeau JH, Johnson KR, Kelly MA, Roselli-Rehfuss L, Baack E, Mountjoy KG, Cone RD. (1993). Pigmentation phenotypes of variant extension locus alleles result from point mutations that alter MSH receptor function. Cell 72, 827-834.

Robinson KC and Fisher DE. (2011). Specification and loss of melanocyte stem cells. Semin Cell Dev Biol 20:111–6.

Roseberry AG, Stuhrman K, Dunigan AI. (2015). Regulation of the mesocorticolimbic and mesostriatal dopamine systems by α-melanocyte stimulating hormone and agouti-related protein. Neurosci Biobehav Rev. 56, 15-25.

Rossi M, Kim MS, Morgan DGA, Small CJ, Edwards CMB, Sunter D, Abusnana S, Goldstone AP, Russel SH, Stanley SA, Smith DM, Yagaloff K, Ghatei MA, Bloom SR. (1998). A C-terminal fragment of Agouti-related protein increases feeding and antagonizes the effect of alpha-melanocyte stimulating hormone in vivo. Endocrinology. 139, 4428-4431.

Rotllant J, Liu D, Yan YL, Postlethwait JH, Westerfield M, Du SJ. (2008). Sparc (osteonectin) functions in morphogenesis of the pharyngeal skeleton and inner ear. Matrix Biol 27(6): 561–572.

Roulin A and Ducrest AL. (2011). Association between melanism, physiology and behaviour: a role for the melanocortin system. Eur. J. Pharmacol. 660, 226-233.

Roy, S., Rached, M., Gallo-Payet, N., 2007. Differential regulation of the human adrenocorticotropin receptor [melanocortin-2 receptor (MC2R)] by human MC2R accessory protein isoforms alpha and beta in isogenic human embryonic kidney 293 cells. Mol. Endocrinol. 21, 1656-1669.

S

Sakai C. Ollmann M, Kobayashi T, Abdel-Malek Z, Muller J, Vieira WD, Imokawa G, Barsh GS, Hearing VJ. (1997). Modulation of murine melanocyte function in vitro by agouti signal protein. EMBO J. 16, 3544-3552.

Sánchez E, Rubio VC, Cerdá-Reverter JM. (2010). Molecular and pharmacological characterization of the melanocortin receptor subtype 1 in the sea bass. Gen. Comp. Endocrinol. 65, 163-169.

Sánchez E, Rubio VC, Thompson D, Metz J, Flik G, Millhauser GL, Cerdá-Reverter JM. (2009a). Phosphodiesterase inhibitor-dependent inverse agonism of agouti-related protein (AGRP) on melanocortin 4 receptor in sea bass (*Dicentrarchus labrax*). Am. J. Physiol. 296, R1293-R1306.

Sánchez E, Rubio VC, Cerdá-Reverter JM. (2009b). Characterization of the sea bass melanocortin 5 receptor: a putative role in hepatic lipid metabolism. J. Exp. Biol. 212, 3901-3910.

Sarangarajan R and Boissy RE. (2001). Tyrp1 and oculocutaneous albinism type 3. Pigment Cell Res 14:437–444.

Schimmer BP, Kwan WK, Tsao J, Qiu R. (1995). Adrenocorticotropin-resistant mutants of the Y1 adrenal cell line fail to express the adrenocorticotropin receptor. J. Cell Physiol. 163, 164-171.

Schiöth HB, Västermark Å, Cone RD (2011) Reply to Braasch and Postlethwait: Evolutionary origin of the teleost A2 agouti genes (agouti signaling protein 2 and agouti-related protein 2) remains unclear. Proc Natl Acad Sci USA.108:E49-50.

Schiöth HB, Haitina T, Ling MK, Ringholm A, Fredriksson R, Cerdá-Reverter JM, Klovins J. (2005). Evolutionary conservation of the structural, pharmacological and genomic characteristics of the melanocortin receptors subtypes. Peptides 26, 1886-1900.

Schiöth HB and Watanobe H. (2002). Melanocortins and reproduction. Brain Res. Brain Res. Rev. 3, 340-350.

Schwartz MW, Woods SC, Porte D Jr, Seeley RJ, Baskin DG. (2000). Central nervous system control of food intake. Nature. Apr 6;404(6778):661-71.

Sebag JA and Hinkle PM. (2009). Regions of melanocortin 2 (MC2) receptor accessory protein necessary for dual topology and MC2 receptor trafficking and signalling. J. Biol. Chem. 284, 610-618.

Sharma P, Bottje W, Okimoto R. (2008). Polymorphisms in uncoupling protein, melanocortin 3 receptor, melanocortin 4 receptor, and pro-opiomelanocortin genes and association with production traits in a commercial broiler line. Poult. Sci. 87, 2073-2086.

Singh AP, Schach U, Nüsslein-Volhard C. (2014). Proliferation, dispersal and patterned aggregation of iridophores in the skin prefigure striped colouration of zebrafish. Nat. Cell Biol. 16, 607–614.

Song Y and Cone RD. (2007). Creation of a genetic model of obesity in a teleost. FASEB J. 9, 2042-2049.

Song Y, Golling G, Thacker TL, Cone RD. (2003). Agouti-related protein (AGRP) is conserved and regulated by metabolic state in the zebrafish, *Danio rerio*. Endocrine. 3, 257-65.

Stengel A, Wang L, Goebel-Stengel M, Taché Y. (2011). Centrally injected kisspeptin reduces food intake by increasing meal intervals in mice. Neuroreport. 2, 253-257.

Sugimoto M. (2002). Morphological color change in fish: Regulation of pigment cell density and morphology. Micros Res Tech 58: 496-503.

Sundström G, Dreborg S, Larhammar D. (2009). Concomitant duplications of opioid peptide and receptor genes before the origin of jawed vertebrates. PLoS One. 5, :e10512.

Sutton AK, Pei H, Burnett KH, Myers MG Jr, Rhodes CJ, Olson D. (2014). Control of food intake and energy expenditure by Nos1 neurons of the paraventricular hypothalamus. J Neurosci. 34, 15306-15318.

Sviderskaya EV, Hill SP, Balachandar D, Barsh GS, Bennet DC. (2001). Agouti signaling protein and other factors modulating differentiation and proliferation of immortal melanoblast. Dev. Dyn. 221, 373-379.

Szala KSz and Stark E. (1992). Effect of alpha-MSH on the corticosteroid production of isolated zona glomerulosa and zona fasciculata cells. Life Sciences 30:24: 2101-2108.

Szczypka MS, Mandel RJ, Donahue BA, Snyder RO, Leff SE, Palmiter RD. (1999). Viral gene delivery selectively restores feeding and prevents lethality of dopamine-deficient mice. Neuron 22, 167-178.

T

Takahashi A and Kawauchi H. (2006). Evolution of melanocortin systems in fish. Gen. Comp. Endocrinol. 148, 85-94.

Takahashi A, Kobayashi Y, Moriyama S, Hyodo S. (2008). Evaluation of posttranslational processing of proopiomelanocortin in the banded houndshark pituitary by combined cDNA cloning and mass spectrometry. Gen. Comp. Endocrinol. 157:41-48.

Takahashi A, Amano M, Itoh T, Yasuda A, Yamanome T, Amemiya Y, Sasaki K, Sakai M, Yamamori K, Kawauchi H. (2005). Nucleotide sequence and expression of three subtypes of proopiomelanocortin mRNA in barfin flounder. Gen. Comp. Endocrinol. 141, 291-303.

Tamate H, Hirobe T, Takeuchi T. (1986). Effects of the lethal yellow (Ay) and recessive yellow (e) genes on the population of epidermal melanocytes in newborn mice. J. Exp. Zool. 238, 235–240.

Tolle V and Low MJ. (2008). In vivo evidence for inverse agonism of Agouti-related peptide in the central nervous system of proopiomelanocortin-deficient mice. Diabetes 57, 86-94.

Tuinhof R, Ubink R, Tanaka S, Atzori C, van Strien FJC, Roubos EW. (1998). Distribution of proopiomelanocortin and its peptide end products in the brain and hypophysis of the aquatic toad, *Xenopus laevis*. Cell Tissue Res. 292, 251-265.

V

Valenti M, Cottone E, Martinez R, De Pedro N, Rubio M, Viveros MP, Franzoni MF, Delgado MJ, Di Marzo V. (2005). The endocannabinoid system in the brain of Carassius auratus and its possible role in the control of food intake. J Neurochem. 95, 662-672.

Volkoff H and Wyatt JL. (2009). Apelin in goldfish (*Carassius auratus*): cloning, distribution and role in appetite regulation. Peptides 30,1434-1440.

Volkoff H, Canosa LF, Unniappan S, Cerdá-Reverter JM, Bernier NJ, Kelly SP, Peter RE. (2005). Neuropeptides and the control of food intake in fish. Gen Comp Endocrinol.142(1-2):3-19.

Vrieling H, Duhl DMJ, Millar SE, Miller KA, Barsh GS. (1994). Differences in dorsal and ventral pigmentation result from regional expression of the mouse agouti gene. Proc. Natl. Acad. Sci. USA 91, 5667-5671.

W

Walpita CN, Crawford AD, Janssens ED, Van der Geyten S, VM Darras VM. (2009). Type 2 iodothyronine deiodinase is essential for thyroid hormone-dependent embryonic development and pigmentation in zebrafish. Endocrinology 150:530–539.

Walpita CN, Van der Geyten S, Rurangwa E, Darras VM. (2007). The effect of 3,5,3'-triiodothyronine supplementation on zebrafish (Danio rerio) embryonic development and expression of iodothyronine deiodinases and thyroid hormone receptors. Gen Comp Endocrinol 152:206–214.

Watanabe K, Washio Y, Fujinami Y, Aritaki M, Uji S, et al. (2008). Adult-type pigment cells, which color the ocular sides of flounders at metamorphosis, localize as precursor cells at the proximal parts of the dorsal and anal fins in early larvae. Dev Growth Differ 50:731-741.

Watanabe M, Iwashita M, Ishii M, Kurachi Y, Kawakami A, Kondo S, Okada N. (2006). Spot pattern of leopard Danio is caused by mutation in the zebrafish connexion 41.8 gene. EMBO Rep.:7:893–897.

Westerfield M. (2007). The Zebrafish Book: A Guide for the Laboratory Use of Zebrafish (Danio rerio). 5th Ed. Eugene, Oregon, University of of Oregon Press.

Wu Z, Kim ER, Sun H, Xu Y, Mangieri LR, Li DP, Pan HL, Xu Y, Arenkiel BR, Tong Q. (2015). GABAergic projections from lateral hypothalamus to paraventricular hypothalamic nucleus promote feeding. J. Neurosci. 35, 3312-3318.

Wullimann MF, Rupp B, Reichert H. (1996). Neuroanatomy of Zebrafish Brain: A Topological Atlas. Birkhaeuser Verlag, Switzerland. 144 p.

Y

Yamada Y, Okauchi M, Araki K. (2010). Origin of adult-type pigment cells forming asymetric pigment patter in Japanese flounder (*Paralichthys olivaceus*) Dev Dyn 239: 3147-3162.

Yamaguchi M, Yoshimoto E, Kondo S. (2007). Pattern regulation in the stripe of zebrafish suggests an underlying dynamic and autonomous mechanism. Proc Natl Acad Sci USA 104: 4790-4793.

Yamauchi T, Nio Y, Maki T, Kobayashi M, Takazawa T, Iwabu M, Okada-Iwabu M, Kawamoto S, Kubota N, Kubota T, Ito Y, Kamon J, Tsuchida A, Kumagai K, Kozono H, Hada Y, Ogata H, Tokuyama K, Tsunoda M, Ide T, Murakami K, Awazawa M, Takamoto I, Froguel P, Hara K, Tobe K, Nagai R, Ueki K, Kadowaki T. (2007). Targeted disruption of AdipoR1 and AdipoR2 causes abrogation of adiponectin binding and metabolic actions. Nat. Med. 13, 332-339.

Z

Zhang C, Forlano P.M, Cone RD. (2012). AgRP and POMC neurons are hypophysiotropic and coordinately regulate multiple endocrine axes in a larval teleost. Cell Metab. 15, 256-264.

Zhang C, Song Y, Thompson DA, Madonna MA, Millhauser GL, et al. (2010). Pineal-specific agouti protein regulates teleost background adaptation. Proc Natl Acad Sci USA. 107:20164-20171.

Zhang Y, Proenca R, Maffei M, Barone M, Leopold L, Friedman JM. (1994). Positional cloning of the mouse obese gene and its human homologue. Nature. Dec 1;372(6505):425-32.

Zhou QY and Palmiter RD. (1995). Dopamine-deficient mice are severely hypoactive, adipsic, and aphagic. Cell 83, 1197-1209.

Zuasti A. (2002). Melanization stimulating factor (MSF) and melanization inhibiting factor (MIF) in the integument of fish. Micros. Res. Tech. 58, 488-495.

Zuasti A, Johnson WC, Samaraweera P, Bagnara JT. (1992). Intrinsec pigment-cell stimulating activity in the catfish integument. Pigment Cell Res. 5, 253-262.